technische universität
dortmund

Endophytic fungi harbored in *Camptotheca acuminata*, *Hypericum perforatum* and *Juniperus communis* plants as promising sources of camptothecin, hypericin and deoxypodophyllotoxin

D I S S E R T A T I O N

Submitted for the degree of Dr. rer. nat. (*rerum naturalium*)

to the

Faculty of Chemistry

Technische Universität Dortmund

by

Souvik Kusari

2010

Institute of
Environmental Research
of the Faculty of Chemistry
INFU

technische universität
dortmund

Endophytic fungi harbored in *Camptotheca acuminata*, *Hypericum perforatum* and *Juniperus communis* plants as promising sources of camptothecin, hypericin and deoxypodophyllotoxin

APPROVED DISSERTATION

Doctoral Committee

Chairman: Prof. Dr. Carsten Strohmann

Reviewers:

1. Prof. Dr. Dr.h.c. Michael Spiteller
2. Prof. Dr. Oliver Kayser

Date of defense examination: October 04, 2010

Chairman of the examination: Prof. Dr. Christof M. Niemeyer

Institute of
Environmental Research
of the Faculty of Chemistry
INFU

"The grand aim of all science is to cover the greatest number of empirical facts by logical deduction from the smallest number of hypotheses or axioms"

Albert Einstein
(March 14, 1879 – April 18, 1955)

THIS THESIS IS DEDICATED TO MY PARENTS …

Declaration

I hereby declare that this thesis is a presentation of my original research work, and is provided independently without any undue assistance. Wherever contributions of others are involved, every effort is made to indicate this clearly, with due reference to the literature(s), and acknowledgement of collaborative research and discussions.

This work was done under the guidance and supervision of Professor Dr. Dr.h.c. Michael Spiteller, at the Institute of Environmental Research (INFU) of the Faculty of Chemistry, Chair of Environmental Chemistry and Analytical Chemistry, TU Dortmund, Germany.

Dated: August 10, 2010 **SOUVIK KUSARI**

Place: Dortmund, Germany

In my capacity as supervisor of the candidate's thesis, I certify that the above statements are true to the best of my knowledge.

Prof. Dr. Dr.h.c. Michael Spiteller

Dated: August 10, 2010

List of original contributions

Parts of the work reported in this thesis have already been published, presented and/or are intended for publication.

PUBLICATIONS

PUBLISHED ARTICLES

1. **Kusari, S.**; Zühlke, S.; Spiteller, M. (2010): Chemometric evaluation of the anti-cancer pro-drug podophyllotoxin and potential therapeutic analogues in *Juniperus* and *Podophyllum* species. ***Phytochemical Analysis***, in press.

2. **Kusari, S.**; Zühlke, S.; Košuth, J.; Čellárová, E.; Spiteller, M. (2009): Light-independent metabolomics of endophytic *Thielavia subthermophila* provides insight into microbial hypericin biosynthesis. ***Journal of Natural Products***, 72, 1825-1835.

3. **Kusari, S.**; Zühlke, S.; Borsch, T.; Spiteller, M. (2009): Positive correlations between hypericin and putative precursors detected in the quantitative secondary metabolite spectrum of *Hypericum*. ***Phytochemistry***, 70, 1222-1232.

4. **Kusari, S.**; Lamshöft, M.; Spiteller, M. (2009): *Aspergillus fumigatus* Fresenius, an endophytic fungus from *Juniperus communis* L. Horstmann as a novel source of the anticancer pro-drug deoxypodophyllotoxin. ***Journal of Applied Microbiology***, 107, 1019-1030.

5. **Kusari, S.**; Zühlke, S.; Spiteller, M. (2009): An endophytic fungus from *Camptotheca acuminata* that produces camptothecin and analogues. ***Journal of Natural Products***, 72, 2-7.

6. **Kusari, S.**; Lamshöft, M.; Zühlke, S.; Spiteller, M. (2008): An endophytic fungus from *Hypericum perforatum* that produces hypericin. ***Journal of Natural Products***, 71, 159-162.

PUBLISHED BOOK CHAPTERS

1. **Kusari, S.**; Spiteller, M. (2010): Lessons from endophytes: Peering under the skin of plants. In ***Biotechnology – Its Growing Dimensions***, Patro, L. R. (ed.), Sonali Publications, New Delhi, India, pp. 1-27.

2. **Kusari, S.**; Spiteller, M. (2010): Do endophyte metabolomics reflect the phytochemical diversity of the host plant? A test of the hypothesis with *Hypericum* species. In ***Biodiversity Conservation and Management***, Patro, L. R. (ed.), Discovery Publishing House Pvt. Ltd., New Delhi, India, pp. 1-28.

SUBMITTED/UNDER REVISION

1. **Kusari, S.**; Košuth, J.; Čellárová, E.; Spiteller, M. (2010): Perspectives on the survival-strategies of endophytic *Fusarium solani* against indigenous camptothecin biosynthesis. Submitted/under review.

PRESENTATIONS

INVITED TALKS

1. *An endophytic Fusarium solani as a novel source of antineoplastic camptothecin and its 9-methoxy and 10-hydroxy derivatives.* At the University of Agricultural Sciences (UAS), Bangalore, India. Within the scope of Indo-German (DBT-BMBF/DLR) collaboration. (7–15 Nov 2008).

2. *Lessons from endophytes: Peering under the skin of plants.* At the International Scientific Colloquium (ISC) and Alumni Meeting for International Summer Schools, Center of Applied Spectroscopy, Faculty of Technology, University of Novi Sad, R. Serbia. Funded by the German Academic Exchange Service (DAAD), Germany. (2–4 Oct 2008).

ORAL PRESENTATIONS

1. *Endophytes as hidden treasures within the botanical richness of nature: Camptotheca acuminata as an example.* At the European Science Foundation-European Cooperation in Science and Technology (ESF-COST) High-Level Research Conference-Natural Products Chemistry, Biology and Medicine II, Acquafredda di Maratea, Italy. (29 Aug–3 Sept 2009).

2. *An endophytic fungus as a novel source of antineoplastic camptothecin and its methoxy and hydroxy analogues.* At the International Conference on "Emerging Trends in Biological Sciences", KIIT School of Biotechnology, KIIT University, Orissa, India. (24–25 Oct 2008).**(**)**

CONTRIBUTED TALKS

1. *Bioactive compounds from endophytic fungi: Isolation, analysis and possibilities for biotechnological production*. GDCh-Colloquium, Universität Duisburg-Essen, Germany. (02 June, 2010).

2. *Endophytes as a promising source of bioactive compounds used in traditional medicine: future prospects and challenges.* In Cameroon. (30 Nov–16 Dec 2009).

3. *Endophytes, a promising source of bioactive compounds used in traditional medicine: future prospects and challenges.* At the Alexander Humboldt Colloquium, Beijing, China. (24 Sept–2 Oct 2009).

4. *Formation and structural elucidation of biologically active compounds from endophytic fungi.* At Budapest University of Technology and Economics, Department of Inorganic and Analytical Chemistry, Budapest, Hungary. (09 Feb 2009).

5. *Formation and structural elucidation of biological active compounds from endophytic fungi.* At Sofia University "St. Kl. Ohridski", Faculty of Chemistry, Sofia. (20 Jan 2009).

POSTERS

1. *Endophytic Thielavia subthermophila demonstrates light-independent metabolomics in axenic cultures: what can we say about microbial hypericin biosynthesis in planta?* At the 3rd Tag der Chemie (Chemistry Day); the Faculty of Chemistry, TU Dortmund, and the JCF Dortmund. (5 Feb 2010).

2. *Thielavia subthermophila, an endophytic fungus from Hypericum perforatum L. as a novel source of hypericin and its probable precursor emodin.* At the International Conference on "Emerging Trends in Biological Sciences", KIIT School of Biotechnology, KIIT University, Bhubaneswar, Orissa, India. (24–25 Oct 2008).**(**)**

3. *Attenuation of camptothecin and 9-methoxycamptothecin production by endophytic Fusarium solani over generations: a possible indication of a split biosynthetic pathway?* At the International Conference on "Emerging Trends in Biological Sciences", KIIT School of Biotechnology, KIIT University, Bhubaneswar, Orissa, India. (24–25 Oct 2008).**(**)**

(**) Received **'Young Researcher Award 2008'** for best scientific contribution; awarded by panel of judges headed by Prof. Dr. Richard R. Ernst (Nobel Laureate in Chemistry, 1991), the chief-guest of the conference.

ACKNOWLEDGEMENTS

A journey is easier when we travel together. This thesis embodies the results of the last couple of years' work whereby I have been accompanied and supported by many people. It is an honor and a very pleasant opportunity to be able to express my gratitude to all of them.

It has been a privilege to work under the dynamic leadership and guidance of my supervisor **Prof. Dr. Dr.h.c. Michael Spiteller** (*Institut für Umweltforschung, INFU, der Fakultät Chemie, Lehrstuhl für Umweltchemie und Analytische Chemie, Technische Universität Dortmund*). Only at his first rendezvous with me several years ago, he foresaw my amateur scientific intentions. Those fleeting moments that featured his visage would never be erased from my heart by the winds of time. His unerring support, coherence of scientific thoughts and remarkable presence of mind propelled me through my scholarly tenure to move forward during the finest moments and the darkest hours. I bow down before him with great respect for showing me the fourth dimension of life called 'Science'.

I am deeply grateful to **Prof. Dr. Oliver Kayser** (*Lehrstuhl Technische Biochemie, Fachbereich Bio- und Chemieingenieurwesen, Technische Universität Dortmund*) for giving me the golden opportunity to present my doctoral work to him. Even before I met him in person, I was always inspired, encouraged and fascinated by reading his work. His clarity of thoughts and the superlative command on science that festooned his articles and books are ever admirable. He could not even realize how much I have learned from him. His ideas and thoughts are treasure for me and will remain so for the rest of my life.

I wish to express my deep sense of appreciation and gratitude to my senior colleagues **Dr. Sebastian Zühlke** and **Dr. Marc Lamshöft** for their generous help, critical suggestions, able guidance, and for the realization and interpretation of mass spectrometric analyses. I thank them for their painstaking efforts to nourish me through their advice and pulling me whenever I drowned in the abyssal deeps of hopelessness. I am especially indebted to Dr. Zühlke for investing time and energy in critically reviewing the manuscript of this thesis and providing incisive comments and suggestions. I am deeply grateful to **Dr. Premasis Sukul** (*INFU*) for endowing his valuable time in reading the manuscript of this thesis and offering insightful comments and suggestions.

My sincere thanks to **Prof. E. Čellárová** and **Dr. J. Košuth** (*P. J. Šafárik University in Košice, Faculty of Science, Institute of Biology and Ecology, Slovakia*) for collaborating on the molecular work on *hyp-1* (*T. subthermophila*) and *top1* (*F. solani*) genes. I am especially thankful to Prof. Čellárová for reviewing some of my manuscripts and providing valuable suggestions before we formally submitted to the respective journals.

I express my heartfelt gratitude to **Dr. M. Stadler** (*InterMed Discovery GmbH, Dortmund, Germany*), **Prof. Dr. M. H. Zenk** and **Dr. T. M. Kutchan** (*Donald Danforth Plant Science Center, St. Louis, USA*), and **Dr. D. Spiteller** (*Max Planck Institute for Chemical Ecology, Jena, Germany*) for their valuable discussions and critical suggestions on various aspects of my research, and for critically reading many of my manuscripts and providing valuable comments before we formally submitted to the respective journals. I thank **Prof. S. O'Connor** and **Dr. N. Nims** (*Massachusetts Institute of Technology, Cambridge, USA*) for discussions on the enzyme strictosidine synthase. I am grateful to **Prof. Dr. T. Borsch** (*Botanischer Garten und Botanisches Museum Berlin-Dahlem, und Institut für Biologie/Botanik, Freie Universität Berlin, Germany*), for the precious discussions on *Hypericum* species. I thank **Dr. W. Föllmann** (*Leibniz-Institut für Arbeitsforschung an der TU Dortmund, IfADo, Dortmund, Germany*) for generously permitting me to visit his laboratory and guiding me on the various aspects of cytotoxicity assays. It was their unconditional support and encouragement that brightened my days and geared my research forward.

My sincere thanks to **Dr. O. Kracht** (*Thermo Fisher Scientific, Bremen, Germany*), **Dr. P. B. Kamp** (*IIT Biotech, Bielefeld, Germany*), **Mrs. M. Meuris** (*Center for Electron Microscopy at TU Dortmund*), **Dr. R. Class** and **Dr. C. B. Hartmann** (*Pharmacelsus GmbH, Saarbrücken, Germany*), and **Mrs. A. Dolderer** and **Dr. B. Nüßlein** (*Nadicom GmbH, Karlsruhe, Germany*) for technical assistance. I am grateful to **Mrs. V. Wähnert**, **Dr. B. Schäfer**, **Mrs. M. Lauerer**, **Mr. B. Meyer**, **Dr. Y. D. Shankar-Thomas**, and **Mr. A. Fläschendräger** for their kind gifts of *Camptotheca acuminata* plants from the respective botanical gardens and tissue culture laboratories in Germany. I whole-heartedly thank **Mr. H. Tian** (*Kunming Kelao Keji GmbH, China*) for helping in the collection of the plant material from China, **Prof. R. U. Shaanker** (*University of Agricultural Sciences, Bangalore, India*) for providing methanol extracts of *Nothapodytes nimmoniana* plants (collected from the Western Ghats, India), **Mr. H. Reif** (*Rombergpark botanical garden, Dortmund, Germany*) for helping with identification, taxonomy and sampling of plant material from Germany, **Dr. G. N. Qazi** (former Director, *Indian Institute of Integrative Medicine, IIIM, Jammu, India*) for allowing the deposition and accessioning of the plant materials collected in India at the herbarium of *IIIM*, **Dr. S. C. Puri** (formerly at *IIIM, Jammu, India*) for assistance in the sampling of plants from India and for his kind gift of standard demethylpodophyllotoxin.

I sincerely thank all my colleagues and friends at the *INFU* for their camaraderie and constant support. My special thanks to the technical assistants **Ms. J. Hardes**, **Mrs. G. Hardes**, **Ms. J. Gaskow** and **Mr. J. Storp** for always wearing a smile and helping me whenever necessary; that which sustained me and my search. I wish to express my heartfelt gratitude to **Mrs. B. Apitius** (*INFU*) for her constant moral support that rejuvenated my mind to sail on and on. I am thankful to **Mr. U. Schoppe** (*INFU*) for

ordering all the required stationeries, chemicals, media, instruments, and everything else necessary for my work.

I am very thankful to the **International Bureau (*IB*) of the German Federal Ministry of Education and Research (*BMBF/DLR*), Germany**, for financial support. I acknowledge the **Ministry of Innovation, Science, Research and Technology of the State of North Rhine-Westphalia, Germany**, for funding the purchase of high-resolution mass spectrometer.

Whatever good I have in my life is a result of immense sacrifices made by my **parents**. I have no words to express my heartfelt gratitude and respect towards my parents for their blessings, endless love and constant inspiration throughout my studies, and for teaching me the essence of education and integrity. I offer hearty thanks to my beloved **sister** whose unconditional love and affection has always been my strength. Praise to the Almighty who bestows success and guides our destiny. I fail to find words to express my thankfulness and gratitude for the blessings and for bestowing the ever-pervading illumination and perseverance in accomplishing this uphill task.

Table of contents

Abstract

Endophytic microorganisms are a diverse group of microbes that colonize living, internal tissues of plants without causing any immediate, overt negative effects within the hosts. A number of novel endophytic microorganisms are capable of producing host plant-specific secondary metabolites with therapeutic potential. The main objective of this study was isolation, identification, biological and biochemical characterization of endophytic fungi capable of indigenously producing camptothecin (CPT), hypericin and deoxypodophyllotoxin, harbored in *Camptotheca acuminata*, *Hypericum perforatum* and *Juniperus communis* plants, respectively. Secondary metabolites were identified and quantified by highly selective and sensitive LC-ESI-MS/MS and LC-ESI-HRMS^n.

C. acuminata plants were sampled from different botanical gardens and tissue culture laboratories across Germany as well as from China. The aerial parts were extracted and analyzed for CPT, 9-methoxycamptothecin and 10-hydroxycamptothecin. Chemometric evaluation revealed CPT to be positively correlated with both the metabolites. Endophytic fungi were isolated and characterized from all plants, only one of which was capable of producing CPT, 9-methoxycamptothecin and 10-hydroxycamptothecin in rich mycological media under axenic submerged shake-flask fermentation. The fungus was identified as *Fusarium solani* by its morphology and authenticated by ITS-5.8S rDNA analysis. CPT along with both the metabolites were additionally identified by ^{1}H NMR spectroscopy, and confirmed by comparison with authentic standards. A substantial decrease in the production of CPT by the *in vitro* cultured endophyte over repeated subculturing was observed. The survival strategy of the endophyte against CPT toxicity was evaluated by identifying the typical amino acid residues Asn352, Glu356, Arg488, Gly503, and Gly717 (numbered according to human topoisomerase I) which prevent CPT binding to topoisomerase I, and the point mutation Met370Thr on the CPT-binding and catalytic domain of its topoisomerase I enzyme (encoded by *Top1*). A cross-species biosynthetic pathway was then deciphered where the fungal endophyte utilizes indigenous *G10H* (geraniol 10-hydroxylase), *SLS* (secologanin synthase), and *TDC* (tryptophan decarboxylase) to biosynthesize CPT precursors. However, to complete CPT biosynthesis, the endophyte requires the host *STR* (strictosidine synthase). The fungal CPT biosynthetic genes destabilize *ex planta* over successive subculture generations. The seventh subculture predicted proteins exhibited reduced homologies to the original enzymes proving that such genomic instability leads to dysfunction at the amino acid level. The endophyte with an impaired CPT biosynthetic capability was artificially inoculated into the living host plants and then recovered after colonization. CPT biosynthesis could still not be restored. This demonstrated that the observed phenomenon of genomic instability is irreversible.

Several *Hypericum* species were sampled from the natural populations of Slovakia and India, extracted, and analyzed for eight pharmacologically important secondary compounds (hypericin, pseudohypericin, emodin, hyperforin, hyperoside, rutin, quercetin, and quercitrin). Chemometric evaluation not only revealed various strong positive and negative correlations among the different phytochemicals but also depicted *H. montanum* as an alternative source to *H. perforatum*. Although endophytic fungi were isolated and characterized from all plants, only one endophytic fungus was capable of indigenously producing hypericin and emodin under axenic submerged shake-flask fermentation. The fungus was identified as *Thielavia subthermophila* by its morphology and authenticated by 28S rDNA and ITS-5.8S rDNA analyses. The growth of the endophyte and production of hypericin remained independent of the illumination conditions and media spiking with emodin. Protohypericin could not be detected, irrespective of either spiking or illumination conditions. The *hyp-1* gene, suggested to encode for the Hyp-1 phenolic coupling protein in plant cell cultures, was absent in the genome of the endophyte. Thus, it is proposed that emodin anthrone is the common precursor of both hypericin and emodin in the fungal endophyte, which is governed by a different molecular mechanism than the host plant or host cell suspension cultures. Like the CPT producing endophyte, this endophyte also showed a substantial decrease in the production of hypericin and emodin *in vitro* over repeated subculturing and on storage.

Juniperus and *Podophyllum* species were collected from natural populations of India and Germany. Extraction and analyses were performed for four potential pro-drugs (podophyllotoxin, deoxypodophyllotoxin, demethylpodophyllotoxin, and podophyllotoxone). Chemometric evaluation revealed both infraspecific and infrageneric correlations among the different phytochemicals. Endophytic fungi were isolated and characterized from all plants. Only one endophytic fungus was capable of producing deoxypodophyllotoxin under axenic submerged shake-flask fermentation. The fungus was identified as *Aspergillus fumigatus* Fresenius by its morphology and 28S rDNA analysis. The growth and production kinetics showed the potential of the endophyte in the indigenous production of deoxypodophyllotoxin, but *in vitro* subculturing showed no production from the third subculture generation.

The results reported in this thesis reveal the immense potential of novel endophytic fungi as a source of important bioactive pro-drugs. Emphasis is also laid on the difficulties ahead if endophytic fungi are to be exploited for industrial production of bioactive secondary metabolites.

Zusammenfassung

Endophyten sind Mikroorganismen, die im Inneren des Vegetationskörpers einer Pflanze leben, ohne unmittelbare negative Auswirkungen für die Wirtspflanze. Eine Vielzahl dieser Endophyten ist in der Lage, pflanzenspezifische Sekundärmetaboliten mit pharma-kologischem Potential zu produzieren. Ziel dieser Arbeit war die Isolierung, Identifizierung sowie die biologische und biochemische Charakterisierung endophytischer Pilze, die Camptothecin (CPT) aus *Camptotheca acuminata*, Hypericin aus *Hypericum perforatum* und Deoxypodophyllotoxin aus *Juniperus communis* produzieren. Die sekundären Metaboliten wurden mit hochselektiver und sensitiver LC-ESI-MS/MS und LC-ESI-$HRMS^n$ identifiziert und quantifiziert.

Es wurden Pflanzen der Spezies C. *acuminata* aus verschiedenen botanischen Gärten und aus Zellkulturlaboratorien in Deutschland und China verwendet. Die oberirdischen Teile der Pflanzen wurden extrahiert und auf CPT, 9-Methoxycamptothecin und 10-Hydroxycamptothecin untersucht. Chemometrische Untersuchungen zeigten, dass die CPT-Gehalte mit denen der Metabolite positiv korrelierten. Aus den Pflanzen wurden zahlreiche endophytische Pilze isoliert und charakterisiert, aber nur einer war in der Lage, 9-Methoxycamptothecin und 10-Hydroxycamptothecin in axenischen Flüssigmedien zu produzieren. Dieser Pilz wurde morphologisch und über ITS-5.8S rDNA-Analyse als *Fusarium solani* identifiziert. CPT und dessen Metabolite wurden zusätzlich durch ^{1}H NMR und Vergleich mit authentischen Standards eindeutig identifiziert. Ein wiederholtes Überimpfen von *in vitro* Kulturen führt zu einer signifikanten Abnahme der CPT-Produktion. Die Überlebensstrategie des Endophyten gegen das toxische CPT wurde untersucht, indem die Aminosäuren Asn352, Glu356, Arg488, Gly503 und Gly717 (numeriert analog der humanen Topoisomerase I) und die Punktmutation Met370Thr des Topoisomerase I Enzyms (*Top1*) identifiziert wurden, die eine Bindung von CPT an die Topoisomerase I verhindern. Die artenübergreifende Biosynthese der CPT-Vorläufer unter Verwendung von indigenen *G10H* (Geraniol 10-Hydroxylase), *SLS* (Secologaninsynthase) und *TDC* (Tryptophandecarboxylase) des Pilzes wurde aufgezeigt. Zur vollständigen CPT-Synthese benötigte der Endophyt jedoch die von der Wirtspflanze bereitgestellte *STR* (Strictosidinsynthase). Die für die CPT-Biosynthese notwendigen Gene destabilisierten sich *ex planta* nach wiederholtem Überimpfen. In der siebten Generation wurden veränderte Proteine gefunden und damit führte die genetische Instabilität zu einer Fehlfunktion auf der Aminosäureebene. Der Endophyt mit der eingeschränkten Biosynthesefunktion wurde in die lebende Wirtspflanze inokuliert und nach Kolonisierung erneut isoliert. Es zeigte sich, dass die genetische Instabilität irreversibel ist, da die CPT-Biosynthese nicht wieder aktiviert werden konnte.

Zahlreiche Pflanzen der Spezies *Hypericum* wurden an natürlichen Standorten in der Slowakei und in Indien gesammelt, extrahiert und auf acht pharmakologisch wichtige Sekundärmetaboliten untersucht (Hypericin, Pseudohypericin, Emodin, Hyperforin, Hyperoside, Rutin, Quercetin und Quercitrin). Die chemometrische Analyse ergab zahlreiche positive und negative Korrelationen zwischen den Inhaltsstoffen und offenbarte *H. montanum* als Alternative zu *H. perforatum*. Von allen isolierten und charakterisierten Endophyten war nur einer in der Lage, Hypericin und seinen Vorläufer Emodin in axenischen Flüssigmedien zu produzieren. Der Pilz wurde mittels 28S rDNA und der ITS-5.8S rDNA-Analyse als *Thielavia subthermophila* identifiziert. Das Wachstum der Endophyten und die Bildung von Hypericin waren unabhängig von den Bestrahlungsbedingungen und der Zugabe von Emodin. Protohypericin konnte weder nach Zugabe von Emodin noch unter Bestrahlungsbedingungen nachgewiesen werden. Es wird angenommen, dass das *hyp-1*-Gen für die phenolische Kopplung des Hyp-1 Proteins in Pflanzenzellkulturen verantwortlich ist. *Hyp-1* konnte im Genom von *T. subthermophila* jedoch nicht aufgefunden werden. Vermutlich ist Emodinanthron der gemeinsame Vorläufer für Emodin und Hypericin im endophytischen Pilz und es liegt ein anderer molekularer Mechanismus als in der Pflanze oder in Pflanzenzellkulturen vor. Wie bei den CPT produzierenden Endophyten wird auch für *T. subthermophila* die deutliche Abnahme der Hypericinproduktion in späteren Generationen und bei langen Lagerzeiten festgestellt.

Juniperus und *Podophyllum* Spezies wurden von natürlichen Standorten in Indien und Deutschland gesammelt und die Extrakte auf vier potentielle Prodrugs (Podophyllotoxin, Deoxypodophyllotoxin, Demethylpodophyllotoxin und Podophyllotoxon) untersucht. Mittels chemometrischer Analysen wurden zwischen den Sekundärmetaboliten Korrelationen innerhalb der Spezies und innerhalb der Gattung festgestellt. Von den Pflanzen wurden zahlreiche endophytische Pilze isoliert und charakterisiert, einer davon konnte Deoxypodophyllotoxin in axenischen Flüssigmedien anreichern. Dieser Pilz wurde morphologisch und über seine 28S rDNA als *Aspergillus fumigatus* Fresenius identifiziert. Der Endophyt zeigte ein Potential zur indigenen Produktion des Sekundärmetaboliten, die *in vitro* Kulturen produzierten jedoch schon ab der dritten Generation kein Deoxypodophyllotoxin mehr.

Die Ergebnisse dieser Arbeit zeigen das enorme Potential von endophytischen Pilzen als Quelle von wichtigen bioaktiven Verbindungen. Bis zur großtechnischen Biosynthese von Sekundärmetaboliten aus Endophyten sind jedoch noch einige Schwierigkeiten zu überwinden.

CHAPTER 1:
INTRODUCTION

1. Introduction

Every process in the biosphere is touched by the seemingly endless capacity of microorganisms to transform the world around them (Zhao and Chen, 2008). However, it was not until Pasteur's discovery of fermentation caused by living cells that people seriously began to investigate microbes as a source for bioactive natural products (Aneja *et al.*, 2008). Then, scientific serendipity and the power of observation provided the impetus to Fleming to usher in the antibiotic era via the discovery of penicillin from the fungus *Penicillium notatum* (Strobel and Daisy, 2003; Aneja *et al.*, 2008). Since then, people have been engaged in the discovery and application of microbial metabolites with activity against both plant and human pathogens. Furthermore, the discovery of a plethora of microbes for applications that span a broad spectrum of utility in medicine (e.g., anticancer and immunosuppressant functions), agriculture and industry is now practical because of the development of novel and sophisticated screening processes in both medicine and agriculture. These processes use individual organisms, cells, enzymes, site-directed techniques, genome mining, and metabolic engineering, frequently in automated arrays, resulting in the rapid detection of promising leads for drug development (Sánchez, 2005; Zhang *et al*., 2006; Lanen and Shen, 2006; Julsing *et al*., 2007; Chemler and Koffas, 2008; Kayser, 2010). More recently, many discoveries have been made in isolating a special class of microorganisms, commonly called endophytes, which have been shown to have the natural potential for accumulation of various bioactive metabolites that may directly or indirectly be used as therapeutic agents against numerous maladies (Pirozynski and Hawksworth, 1988; Dreyfuss and Chapela, 1994; Hawksworth *et al*., 1996; Strobel and Long, 1998; Strobel and Daisy, 2003; Strobel *et al*., 2004; Zhang *et al*., 2006; Gunatilaka, 2006; Staniek *et al*., 2008; Suryanarayanana *et al*., 2009). Exciting possibilities exist in the wild and unexplored territories of the world for engaging in the discovery of novel endophytes, their biology, and their potential usefulness.

1.1. What are endophytic microorganisms?

Bacon and White (2000) gave an inclusive and widely accepted definition of endophytic microorganisms (also known as 'endophytes'): "microbes that colonize living, internal tissues of plants without causing any immediate, overt negative effects." Another classical definition is microorganisms "that colonize plant tissues without producing any apparent symptoms or obvious negative effects" (Hirsch and Braun, 1992). These organisms are known to occupy the intercellular spaces of stems, petioles, roots and leaves of plants (Strobel and Long, 1998). Endophytic microorganisms fall into several identifiable classes often in relation to their plant organ source, with the major groups as follows (Stone *et al.*, 2000; Bills *et al.*, 2004): (1) endophytic Clavicipitaceae; (2) fungal endophytes of dicots; (3) endophytic Ascomycota; (4) other systemic fungal endophytes; (5) fungal endophytes of lichens; (6)

endophytic fungi of bryophytes and ferns; (7) endophytic fungi of tree bark; (8) fungal endophytes of xylem; (9) fungal endophytes of root; (10) fungal endophytes of galls and cysts; and (11) prokaryotic endophytes of plants (including endophytic bacteria and actinomycetes). It would seem that other microbial forms, such as *Mycoplasma*, *Rickettsia*, and Archaebacteria, most certainly exist in plants as endophytes; however, no evidence for them has been presented so far. It could be noted that fungi are the most frequently encountered endophytes (Staniek *et al.*, 2008). In recent years, endophytes have been shown to be a potential source of bioactive and structurally diverse natural products and secondary metabolites.

1.2. Discovery of endophytes

Evidence of plant-associated microorganisms found in the fossilized tissues of stems and leaves has revealed that endophyte-host associations may have evolved from the time higher plants first appeared on the earth (Zhang *et al.*, 2006). The existence of fungi inside the organs of asymptomatic plants has been known since the end of the XIXth century (for example, Guerin, 1898). The term 'endophyte' (Gr. *endon*, within; *phyton*, plant) was first coined by de Bary (1866). However, except for a few sporadic works, it was not until the end of the XXth century when fungal endophytes began to receive more attention from scientists. Since the description of endophytes in the Darnel (Freeman, 1904), various investigators have isolated endophytes from different plant species, and subsequently examined them from their own perspectives. An important year in the history of endophyte research is 1977, when Charles Bacon and colleagues discovered the endophytic fungus *Neotyphodium coenophialum* as the cause of 'fescue toxicosis', a syndrome suffered by cattle fed in pastures of the grass *Festuca arundinacea* (Bacon *et al.*, 1977). Later, it was found that these infected plants contained several toxic alkaloids, and that *Neotyphodium* species could be beneficial to their plant hosts, increasing their tolerance of biotic and abiotic stress factors (Schardl *et al.*, 2004). These discoveries have led to the worldwide search for new and novel endophytic species for the better understanding and applicability of such groups of fascinating microorganisms.

1.3. Endophytes producing associated host plant-specific phytochemicals

Several researchers have reviewed the multitude of different therapeutic compounds produced by various endophytes associated with a diverse group of plants (Pirozynski and Hawksworth, 1988; Dreyfuss and Chapela, 1994; Hawksworth *et al*., 1996; Strobel and Long, 1998; Strobel and Daisy, 2003; Strobel *et al*., 2004; Zhang *et al*., 2006; Gunatilaka, 2006; Staniek *et al*., 2008; Suryanarayanana *et al*., 2009). A recent comprehensive study indicated that about 51% of biologically active substances isolated from endophytic fungi were previously unknown (Strobel and Daisy, 2003). Occasionally, novel

endophytes capable of producing high-value pro-drugs specific to their associated host plants have been discovered. This possibility was first realized and mooted by Stierle and his co-workers (1993), following their highly heralded discovery of the endophytic fungus *Taxomyces andreanae* that could produce the multi-billion dollar anticancer compound Taxol® (generic name: paclitaxel), isolated from the yew plant *Taxus brevifolia*. Spurred by this discovery, numerous efforts have been made to identify endophytic fungi as sources of plant-specific metabolites.

1.4. Rationale for bioprospecting of endophytes for host plant-specific phytochemicals

Several advantages could be envisaged of screening for endophytic microorganisms producing natural products, particularly specific to their associated host plants, for drug discovery. The important advantages of endophytes as sources of natural products are discussed here.

(a) Diversity. Natural products offer an unmatched chemical diversity with structural complexity and biological potency (Clardy and Walsh, 2004). This could be matched with the vast diversity of microorganisms, which unlike other organisms, occupy all living and nonliving niches on earth (Sánchez, 2005). It has been estimated that less than 1% of bacterial species and less than 5% of fungal species are currently known, suggesting that millions of microbial species remain to be discovered (Gunatilaka, 2006). Natural product resources, especially from the plant-associated microbes, are largely unexplored (Staniek *et al.*, 2008). Therefore, bioprospecting of endophytes holds tremendous promise in the discovery of novel lead compounds as well as plant-specific compounds with therapeutic value.

(b) Complex structure. Natural products occupy a complementary region of chemical space compared with synthetic compounds (Lam, 2007). Many natural products contain multiple ring systems with stereoselective centers, which are often complicated to obtain by synthesis. Furthermore, many of the natural products contain a vast number of functional groups, which make syntheses cumbersome, because of the complications of protecting all the functional groups and achieve a high yield simultaneously. On the other hand, microorganisms (including endophytes) produce these structurally diverse and complex molecules ('biosynthesis') using groups of enzymes that catalyze chemical reactions that are often hard to mimic. These enzymes (proteins) are in turn produced with amazing efficiency as products of a 'DNA blueprint' that is present in the microorganism's genome (Balaram, 2010).

(c) Combinatorial biosynthesis. The natural products produced by endophytes could further be used as templates for combinatorial chemistry enabling the generation of libraries of natural product analogs, which might have enhanced drug-like properties (e.g. pharmacokinetics, solubility). This application is an important turnaround because combinatorial chemistry was once expected to replace the need to

search for novel natural products. It is now accepted that both disciplines are complementary to each other (Lam, 2007). The structural diversity of the natural product libraries can be further enhanced by combining the techniques of biotransformation and combinatorial biosynthesis, in addition to a combinatorial chemistry approach.

(d) Fermentation. The natural products produced by endophytes could be optimized using controlled fermentation conditions. This could lead to an economical, environment-friendly, constant, and reproducible yield amenable to industrial scale-up. For those endophytes producing the associated host-specific compounds, production by fermentation would be independent of the varied quantities of production by the plant influenced by the vagaries of nature. This would then comply with the U.S. Federal Food and Drug Administration (FDA) that requires 'batch-to-batch' standardization procedures for drug development (Raskin *et al.*, 2002).

(e) Genome mining and metagenomics. The regulation of natural product biosynthesis in the producing endophytes could be optimized as a result of the increased understanding of genetics and biosynthesis of natural products at the present time. The biosynthesis of natural products themselves could also be manipulated to yield new derivatives with possible superior qualities and quantities. In addition to identifying new natural products, genome mining and metagenomics (Kayser and Müller, 2004; Lanen and Shen, 2006) would certainly have an impact on the understanding and manipulation of natural product production by endophytic microorganisms.

(f) Metabolic engineering. Endophytes residing within plants that produce toxic defense compounds such as anticancer compounds commonly able to interfere with the functions of basic biological units like topoisomerase I and II, tubulin, and calcium pump, have the evolutionary advantage of developed mechanisms to tolerate or resist the actions of the host compounds. Thus, metabolic engineering for important host-plant natural product biosynthesis in these endophytes could be developed for sustained and dependable high yield, without killing the engineered endophyte (Chemler and Koffas, 2008; Muntendam *et al.*, 2009; Kayser, 2010).

1.5. Rationale for plant selection

It is important to understand the methods and rationale used to provide the best opportunities to isolate novel endophytic microorganisms at the genus, species, or biotype level. Since the number of plant species in the world is so great, creative and imaginative strategies must be used to quickly narrow the search for endophytes displaying bioactivity (Mittermeier *et al.*, 1999). A specific rationale for the collection of each plant for endophyte isolation could be proposed to maximize possibility of discovering novel endophytes equipped with the capacity of producing host-specific metabolite. Several hypotheses governing this plant selection strategy are utilized:

(a) Plants from unique environmental settings, especially those with an unusual biology and possessing novel strategies for survival. Just as plants from a distinct environmental setting are considered to be a promising source of novel endophytes and their compounds, so too are plants with an unconventional biology (plants with modified structures, differently developed anatomy, etc.). A fine example of such a plant is *Hypericum perforatum* (Fig. 1a), which is commonly called St. John's wort, after the name of the famous Baptist Saint John (Hickey and King, 1981; Wichtl, 1986). This plant contains the widely used anti-depressive compound hypericin (Fig. 1b) (Brockmann *et al*., 1939, 1942, 1950). Hypericin is a photodynamic compound (Hadjur *et al*., 1996; Delaey *et al*., 2001; Kamuhabwa *et al*., 2001; Kubin *et al*., 2005) which is localized (Briskin *et al.*, 2000) and probably also synthesized in the dark glands (Fig. 1c) (Cellarova *et al.*, 1994; Onelli *et al.*, 2002), which are small specialized glandular structures dispersed over all above-ground parts of the plant (flowers, capsules, leaves, stems) but not in the roots (Hölzl and Petersen, 2003). Therefore, a plant with such an unusual biology (dark glands) for protecting itself from the photodynamic effects of its own metabolites might also contain endophytic fungi that have been evolutionarily co-adapted to accumulate the same or similar molecules.

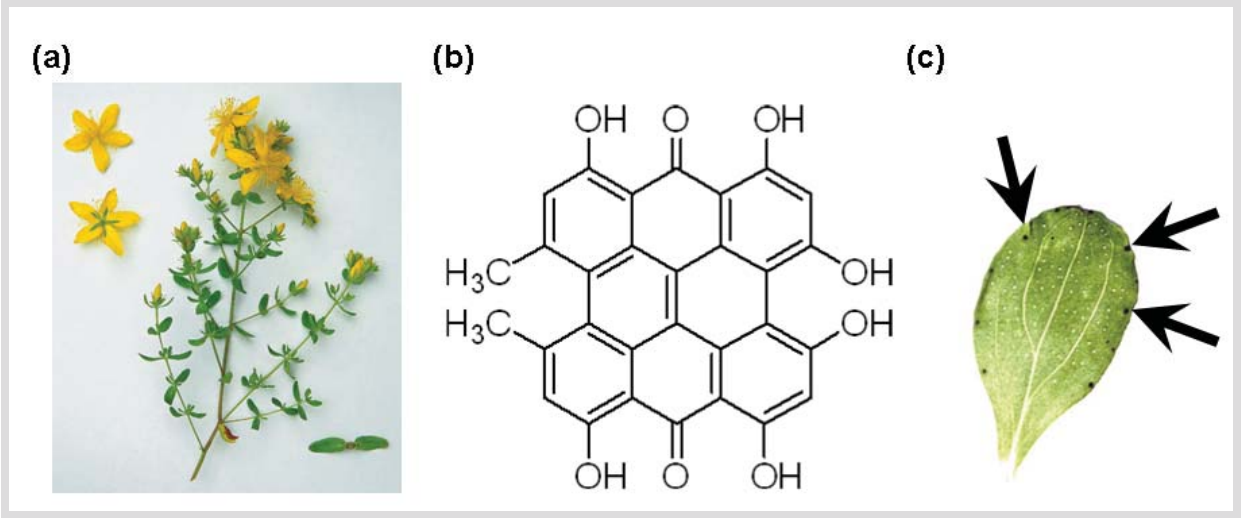

Fig. 1. (a) *Hypericum perforatum* L. (from India). (b) Hypericin. (c) Representative leaf of *H. perforatum* showing the presence of dark glands on the surface (black arrows).

(b) Plants that have an ethnobotanical history (use by indigenous people) that is related to the specific uses or applications of interest. These plants are chosen either by direct contact with local people or via local literature. *H. perforatum* serves an excellent example to describe this rationale. This plant is a pseudogamous, facultatively apomictic, perennial medicinal plant that is native to Europe, West and South Asia, North Africa, North America, and Australia (Hickey and

King, 1981; Wichtl, 1986). In general, *Hypericum* has always been a very important medicinal plant occupying a significant place in ancient history. Pedanius Dioscorides, the foremost ancient Greek herbalist, mentioned four species of *Hypericum* - *uperikon*, *askuron*, *androsaimon*, and *koris*, which he recommended for sciatica, “when drunk with 2 heim of hydromel (honey water)” (Gunther, 1959). *H. perforatum* has also been in use, at least from the time of ancient Greece (Tammaro and Xepapadakis, 1986), as an antidepressant, in healing of wounds and menstrual disorders, on account of the presence of *the-then* unknown bioactive compounds in the plant. Another example to describe this rationale is *Camptotheca acuminata*, a plant that grows in Mainland China, and is commonly called the ‘Happy Tree’ which is a direct translation of the Chinese word ‘Xi Shu’ (Fig. 2a,b). *Camptotheca* was first recorded in 1848 and scientifically described and named by Decaisne (Decaisne, 1873), Director of the Jardin des Plantes, Paris. The genus name *Camptotheca* is from the Greek *Campto* (= bent or curved) and *theca* (= a case) referring to the anthers, which are bent inward. The species name *acuminata* is derived from acuminate, which refers to the tips of leaves. This plant has been in use as traditional medicine in China for treatment of psoriasis, liver and stomach ailments and common cold (Sung *et al.*, 1998). The present application of this plant is on account of the fact that it contains substantial quantities of an important antineoplastic drug, namely camptothecin (CPT) (Fig. 2c).

Fig. 2. (a) *Camptotheca acuminata* (from China). (b) Enlarged view of plant label confirming its identity. (c) Camptothecin (CPT).

Another fine example for using this rationale is the plants of *Juniperus* (Fig. 3a-d) which contain the therapeutically important lignans podophyllotoxin and deoxypodophyllotoxin (Fig. 3e,f) (Hartwell *et al.*, 1953). This species found its use as early as in the first century A.D., when Pliny the Elder mentioned that the smaller species of *Juniperus* could be used, among other things, to stop tumors (*tumores* in Latin) or swelling (Imbert, 1998; Koulman, 2003). The use of the oil of *Juniperus* species (*J. sabina*, *J. phoenicea* and *J. communis*) for the treatment of ulcers, carbuncles and leprosy

(Gunther, 1959) has also been mentioned by Dioscorides. Generally, dried needles, called *savin*, or the derived oil was used. In 47 A.D., Scribonius Largus wrote that *savin* oil was used to soften “hard female genital parts” (Sconocchia, 1983). Later references indicated the use of *savin* to treat uterine carcinoma, venereal warts and polyps (Hartwell and Schrecker, 1958).

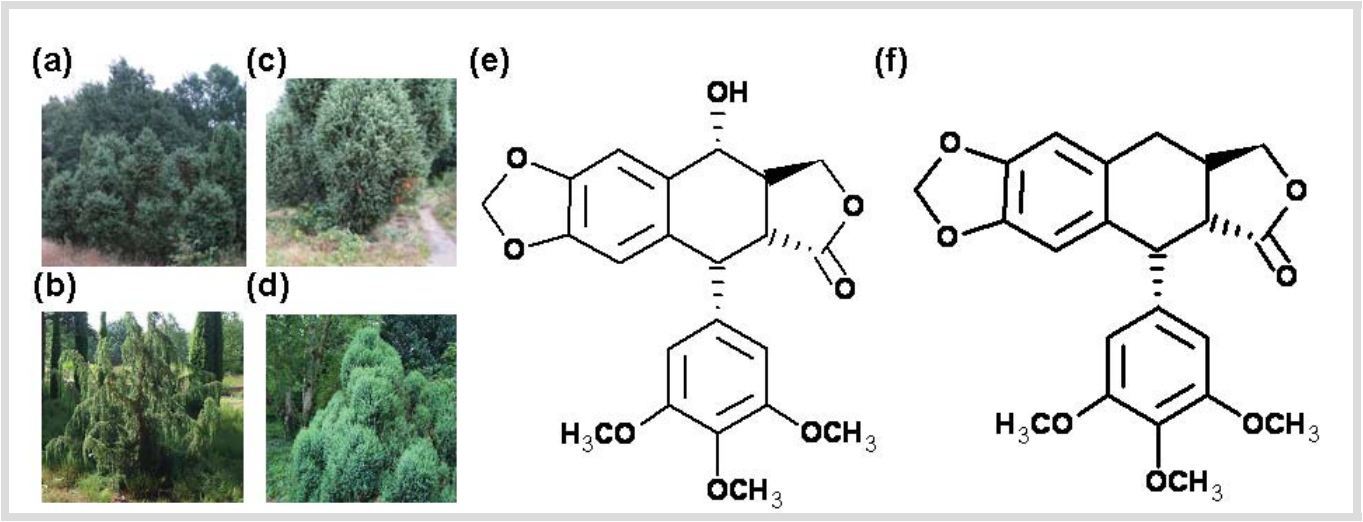

Fig. 3. (a-d) Some pictures of different *Juniperus* species growing in Rombergpark (Dortmund, Germany). (e) Podophyllotoxin. (f) Deoxypodophyllotoxin.

(c) Plants that are endemic, are endangered, have an unusual longevity, or that have occupied a certain ancient land mass, are also more likely to harbor endophytes with active natural products than other plants. *C. acuminata* plant could be mentioned here as a suitable example. This plant has been harvested ruthlessly by various sectors, including medical groups, pharmaceutical companies and scientists from around the world, to isolate CPT for various purposes (Lorence and Nessler, 2004; Sankar-Thomas, 2010). As such, in 2000 and again in 2006, *C. acuminata* was proposed for protection in the CITES (Convention for International Trade in Endangered Species), World Conservation Monitoring Centre, appendix II (Anonymous, 2006a). This appendix lists species that are not necessarily now threatened with extinction but that may become so unless trade is closely controlled. Therefore, a need for the preservation of this endangered germplasm as well as to ensure a continuous supply of CPT has been felt worldwide.

(d) Plants growing in areas of great biodiversity also have the prospect of housing endophytes with great biodiversity. It is worthy of mention that some plants growing in various parts of the world, especially in areas where a diversity of biotic and abiotic factors play essential roles, and generating bioactive natural products might have associated endophytes that produce the same or similar natural products. A general consensus has been reached on the population pressure and diversity of

endophytes in host plants growing in different ecosystems. Of particular interest has been the tropical environment; it has been postulated in general and shown in specific cases that tropical environments are the best suited setting for plant-microbe interactions (Arnold *et al*., 2000, 2003; Arnold, 2005, 2008; Rodriguez *et al*., 2009). It has been hypothesized that the optimum setting for these interactions leads to discovery of novel endophytes accumulating certain metabolites specific to the host plants themselves. Such might be the case with *Camptotheca*, *Hypericum*, *Podophyllum*, and *Juniperus*.

CHAPTER 2:
LITERATURE OVERVIEW

1. Camptothecin (CPT)

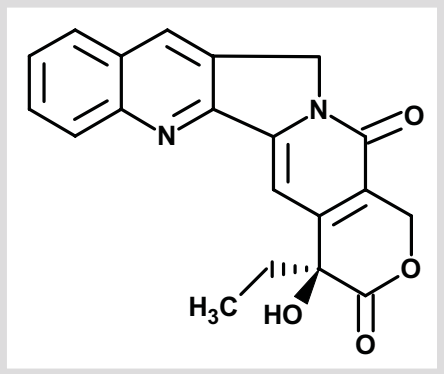

Fig. 4. Camptothecin (CPT).

1.1. Discovery

One of the most significant discoveries in the area of cancer chemotherapy originated from the laboratory of Drs. Monroe Wall and Mansukh Wani at Research Triangle Institute, North Carolina. As described by Wall (1993), the discovery of the potent antitumor activity of an extract of the leaves of *Camptotheca acuminata* Decaisne (Nyssaceae) in 1958 was somewhat serendipitous. While screening thousands of plant extracts as a possible source of steroidal precursors for cortisone (Cragg and Newman, 2004), the extracts of *C. acuminata* were identified as the only ones showing significant activity in the CA755 (adenocarcinoma) assay (Oberlies and Kroll, 2004). The isolation and structural elucidation of camptothecin (CPT) as the active agent of *C. acuminata* were made in 1966 (Wall *et al.*, 1966).

1.2. Occurrence of CPT in the plant kingdom

Discussions on occurrence of specific chemical characters within the plant kingdom, chemosystematics, have always been dependent on botanical classification (Larsson, 2007). Chemotaxonomists have compared the known distribution patterns of CPT with the phylogenetic system of classification of angiosperms, finding surprising results (Wink, 2003). Quite often, even allelochemicals of high structural specificity and complexity occur simultaneously in unrelated families of the plant kingdom (Lorence and Nessler, 2004). CPT is an illustrative example of this kind of metabolites. As depicted in Fig. 5, CPT has been isolated from samples of the following unrelated orders and families of angiosperms: Order Celastrales, Family Icacinaceae - *Nothapodytes foetida* (*N. nimmoniana*) (Aiyama *et al.*, 1988), *Pyrenacantha klaineana* (Zhou *et al.*, 2000), and *Merrilliodendron megacarpum* (Arisawa *et al.*, 1981); Order Cornales, Family Nyssaceae - *C. acuminata* (Wall *et al.*, 1966), *C. lowreyana*, and *C. yunnanensis* (Li *et al.*, 2002); Order Gentianales, Family Rubiaceae: *Ophiorrhiza mungos* (Tafur *et al.*, 1976), *O. pumila*, and *O. filistipula* (Saito *et al.*, 2001); Order

Gentianales, Family Apocynaceae - *Ervatamia heyneana* (Gunasekera *et al.*, 1979); Order Gentianales, Family Gelsemiaceae - *Mostuea brunonis* (Dai *et al.*, 1999).

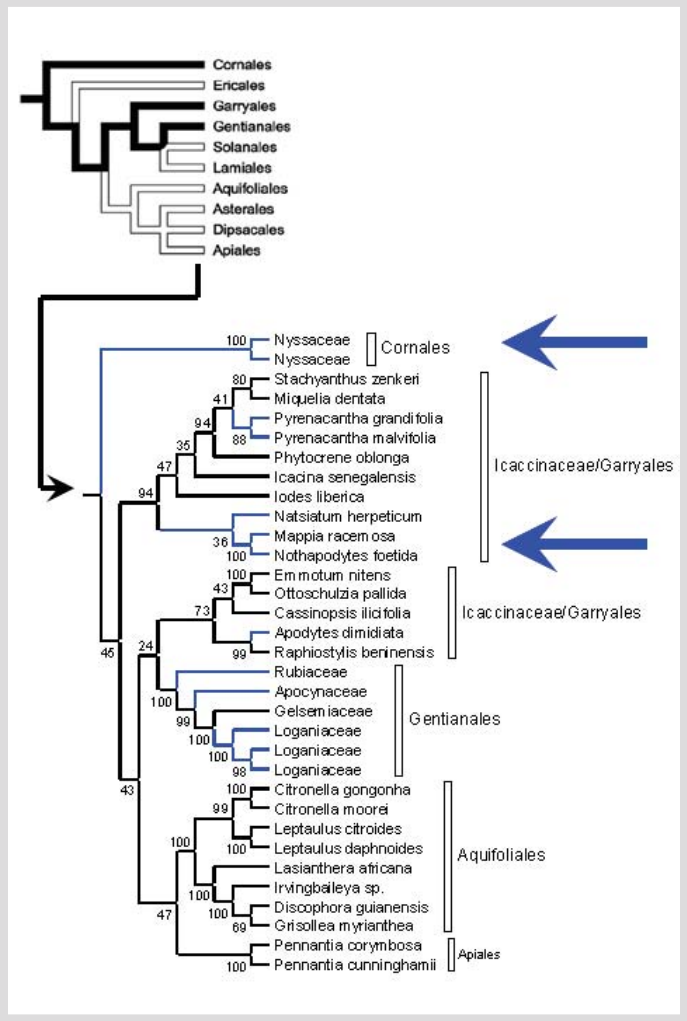

Fig. 5. Phylogeny of different orders of Asterids, modified from Larsson (2007). Clades marked with blue color contain CPT. The two blue arrows indicate the most important species containing CPT, *viz*., *C. acuminata* (Nyssaceae) and *N. foetida* (Icacinaceae).

1.3. Distribution of CPT in the plant organs

Although CPT has been reported in over nine species, the basic patterns of accumulation of CPT have been well documented only in *C. acuminata* (Chinese origin) and, to a lesser extent, in *N. nimmoniana* (Indian origin). All parts of *C. acuminata* contain some CPT. The highest levels of CPT have been reported in the leaves of *C. acuminata* (Lopez-Meyer *et al.*, 1994; Yan *et al.*, 2003). The CPT content found in young leaves (approx. 4-5 mg g^{-1} dry weight) was at least ten-fold higher than in older leaves (Yan *et al.*, 2003), 50% higher than in seeds and 250% higher than in bark (Lopez-Meyer *et al.*, 1994). In fact, the high concentration of CPT in leaves has reportedly led to the poisoning of goats that browse on the leaves and even the honey bees foraging on the floral rewards (Yan *et al.*, 2003). The higher level of CPT in leaves compared to other organs has been confirmed by studying other members of the

genus *Camptotheca* (Li *et al.*, 2002), and *O. pumila* (Yamazaki *et al.*, 2003). It has also been reported that CPT content increases with heavy shade (Liu *et al.*, 1997), while declines with leaf, branch and tree age, and with time during the growing season (Liu *et al.*, 1998). In *N. nimmoniana*, the inner root bark has been reported to yield the highest CPT content, followed by the inner stem bark. The average CPT content in the inner root bark was found to be 0.33 ± 0.21%, compared to 0.23 ± 0.15% in inner stem bark (Uma Shaanker *et al.*, 2008). Unfortunately, there is no information on the holistic analyses of the distribution of major phytochemicals like CPT and related metabolites between the organic and aqueous phases of the same plant, among different plants of the same species, among different species of the same genus, and among different related genera. There is no report on the concentration correlations of CPT and analogues relating to certain genotypes within species, infraspecific, infrageneric, or the manipulation of their existence and *in planta* expression based on their similar biosynthetic principles and/or ecological factors.

1.4. CPT as an anticancer agent

The discovery of CPT in *C. acuminata* also revealed its typical function as a “novel alkaloidal leukemia and tumor inhibitor” (Wall *et al.*, 1966). Through the initial investigations, a strong correlation between *in vitro* cytotoxicity against the 9KB (human oral epidermoid carcinoma) (Eagle, 1955) cell line and *in vivo* anticancer activity could be noted. The promising results of CPT as an antitumor agent in animal models led to its evaluation in the clinic (Moertel *et al.*, 1972). This potency of CPT is by virtue of a unique mechanism of action involving interference with eukaryotic DNA (Hsiang *et al.*, 1985; Kauh and Bjornsti, 1995; Potmesil and Pinedo, 1995; Sawada *et al.*, 1995; Torck and Pinkas, 1996); this naturally occurring enantiomer primarily targets the intranuclear enzyme DNA topoisomerase I (Topo 1), which is required for the swiveling and relaxation of DNA during molecular events, namely, DNA replication and transcription (Hsiang *et al.*, 1985) (*vide infra*). CPT also hinders the synthesis of RNA (Bendixen *et al.*, 1990). A number of reports have been published indicating the therapeutic potential of CPT (Li *et al.*, 2006), against colon cancer (Giovanella *et al.*, 1989), AIDS (Priel *et al.*, 1991), uterine, cervical, and ovarian cancer (Takeuchi *et al.*, 1991), and malaria (Bodley *et al.*, 1998).

The promising potency and efficacy of unmodified CPT are, however, compromised in therapeutic applications due to its very low solubility in aqueous media and high toxicity (Kehrer *et al.*, 2001; Li *et al.*, 2006). CPT undergoes rapid inactivation through lactone ring cleavage at physiological pH to form the water-soluble carboxylate, which is inactive and readily binds to human serum albumin (HSA), making it inaccessible for cellular uptake (Fassberg and Stella, 1992; Burke and Mi, 1993). Moreover, the sodium salt of CPT (more water soluble) is filtered by the kidneys and causes hemorrhagic cystitis and myelotoxicity, rendering it unsuitable for clinical trials (Moertel *et al.*, 1972). Additionally, the half-life

of unmodified CPT-induced Topo 1-mediated DNA breakage is far less than those of modified CPT derivatives (Holden *et al.*, 1999). Although CPT suffers from these drawbacks, its typical action-mechanism and specific target have stimulated intensive efforts to identify and develop various structural analogues (mainly by synthetic and semi-synthetic routes) to overcome the drawbacks of unmodified CPT, yet retain its potency. Extensive studies on the structure-activity relationships (SAR) of CPT (Fig. 7) have led to the formulation of various important pro-drugs having different potential benefits over CPT (Kehrer *et al.*, 2001; Li *et al.*, 2006).

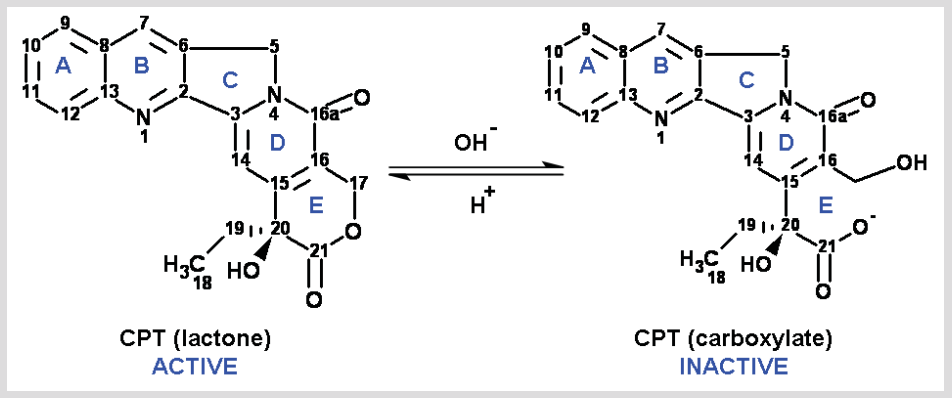

Fig. 6. Inactivation of CPT by cleavage of lactone ring under physiological pH.

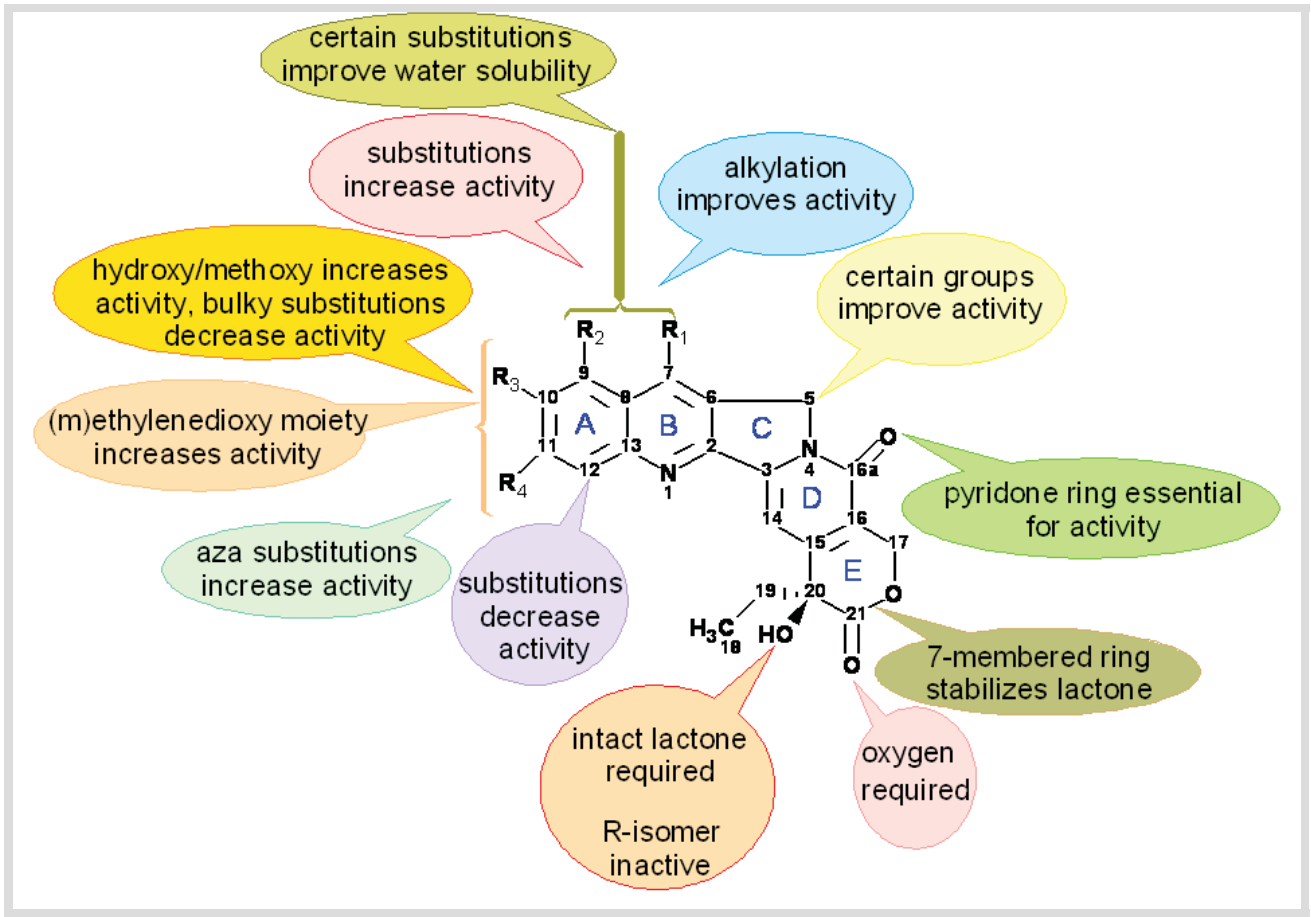

Fig. 7. Structure-activity relationships (SAR) of CPT.

In 1996, topotecan and irinotecan, two semi-synthetic derivatives of CPT (Fig. 8), received approval for human testing and application from the U.S. Food and Drug Administration (FDA) (Slichenmyer *et al.*, 1993; O'Leary and Muggia, 1998; Pommier, 2009). Topotecan, which is manufactured by SmithKline Beecham Pharmaceuticals (also known as GlaxoSmithKline) is sold under the trade name Hycamtin® (TPT) and is used to treat advanced ovarian cancers that have resisted other chemotherapy drugs (Slichenmyer *et al.*, 1993; O'Leary and Muggia, 1998).

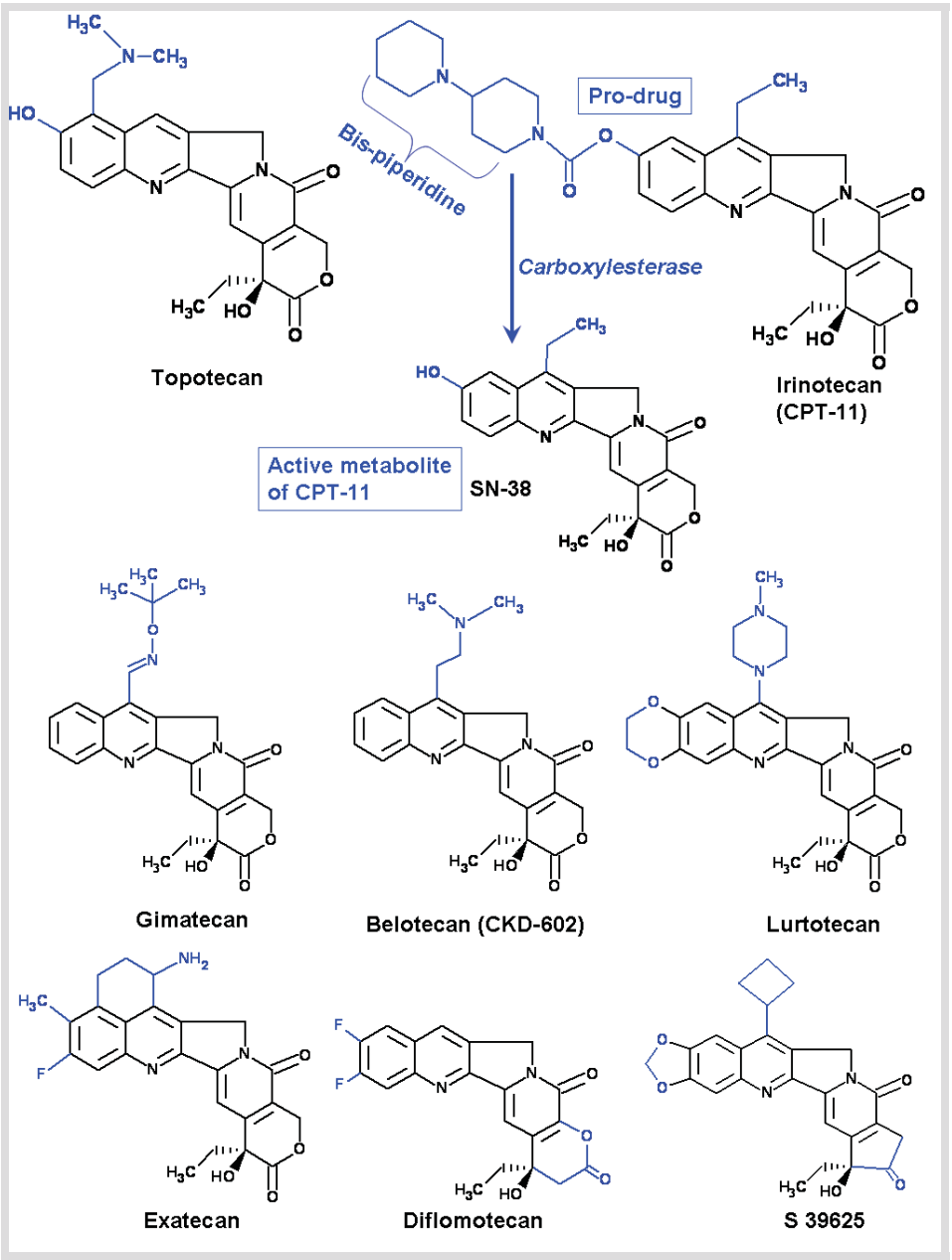

Fig. 8. Important analogues of CPT that have entered clinical trials as anticancer drug candidates.

Irrinotecan became commercially available initially in Japan in 1994, where its approved indications were cancers of the lung (small-cell and non-small-cell), cervix and ovaries (Lorence and Nessler, 2004). In 1995, the injectable irinotecan HCl was approved as a second-line agent for the

treatment of metastatic cancer of the colon or rectum (Lorence and Nessler, 2004). Irinotecan is marketed by Pharmacia and Upjohn under the trade name Camptosar® (CPT-11) (Heron, 1998). Besides the continued studies on TPT and CPT-11, much effort is being spent on the development of new structural analogues of CPT based on the SAR studies. Fig. 8 shows some important compounds that have entered clinical trials as anticancer drug candidates (Slichenmyer *et al.*, 1993; O'Leary and Muggia, 1998; Cragg and Newman, 2004; Oberlies and Kroll, 2004; Pommier, 2009).

9-Methoxycamptothecin (9-MeO-CPT) and 10-hydroxycamptothecin (10-OH-CPT) (Fig. 9) are two important 'natural' structural analogues of CPT that hold potential for their anticancer efficacy (Wu *et al.*, 1995; Sawada *et al.*, 1996) and have been reported to inhibit Topo 1 (Zhou *et al.*, 2000). These two compounds belong to the class of C-9/C-10 (R_2/R_3)-substituted CPT analogues, some of which have already entered clinical trials against various malignant diseases (Tanizawa *et al.*, 1994; Stehlin *et al.*, 1999; Kehrer *et al.*, 2001), as detailed above. Substitution at the C-9 or C-10 position with suitable groups induces superior antitumor activity (Huang *et al.*, 2007). The SAR studies show a close correlation between an ability to inhibit Topo 1 and overall cytotoxic potency based on the substitution at a particular position (Fig. 7). In general, substitutions at C-7, C-9, and C-10 (on the quinoline ring, i.e., ring A or B) tend to increase Topo 1 inhibition in addition to conferring increased water solubility. 9-MeO-CPT and 10-OH-CPT have a methoxy and a hydroxy group at the C-9 and C-10 (R_2 and R_3) position, respectively; these account for their potential therapeutic advantage over CPT.

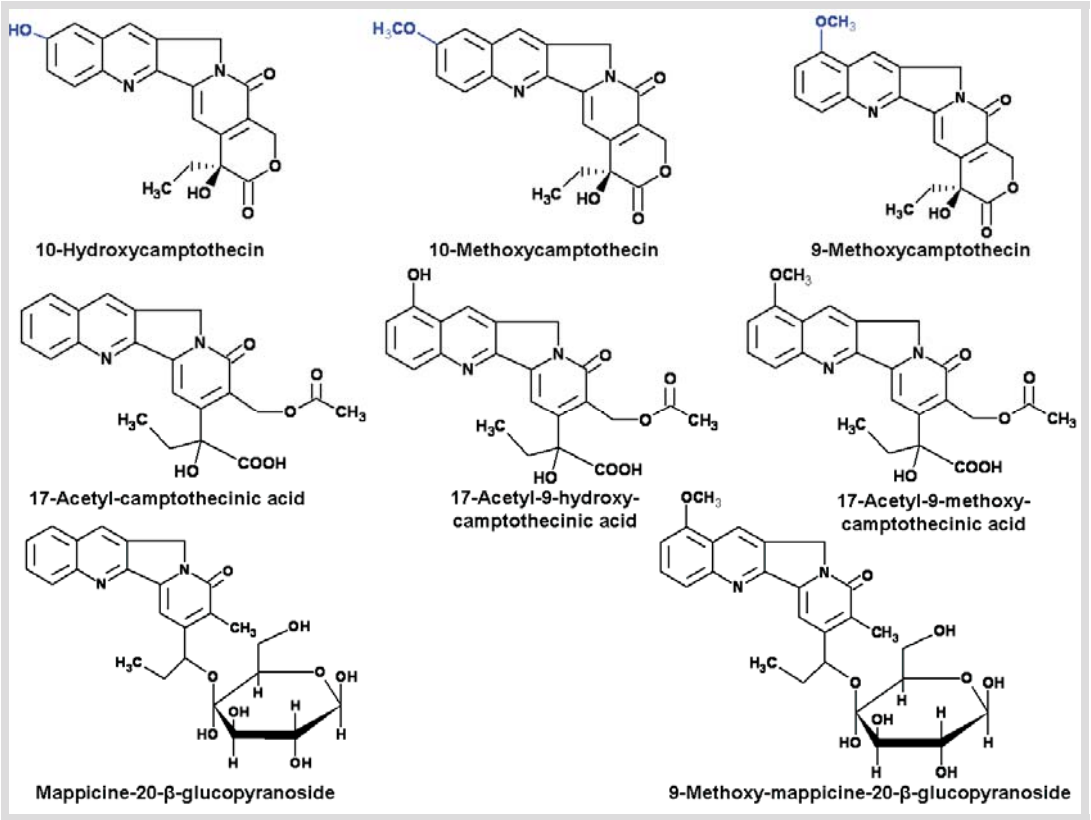

Fig. 9. Important natural analogues of CPT found in plants.

1.5. Mechanism of action of CPT: poisoning of topoisomerase I

Topoisomerases are ubiquitous enzymes that solve topological problems generated by key nuclear processes such as DNA replication, transcription, recombination, repair, chromatin assembly, and chromosome segregation (Lorence and Nessler, 2004). These enzymes are present in all organisms including Archaebacteria, viruses, yeast, flies, plants and humans (Wang, 1996). Topoisomerases modulate DNA superhelicity and perform DNA decatenation using an intricate interplay of DNA scission, manipulation, and rejoining reactions (Keck and Berger, 1999). There are two general types of topoisomerases: topoisomerase I (Topo 1) and topoisomerase II (Topo 2). Each topoisomerase type can be additionally divided into two sub-types, A and B, which are unrelated in sequence and in structure (Keck and Berger, 1999). Topo 1 catalyzes changes in the linking number of DNA (i.e., the number of times one strand of DNA crosses the other) by one per cycle of activity, by breaking and resealing phosphodiester bonds (Rasheed and Rubin, 2003; Lorence and Nessler, 2004). On the other hand, Topo 2 cleaves both strands of DNA and change the linking number of DNA by two (Wang, 1996). In all topoisomerase types, a tyrosine is used to cleave DNA forming a transient, covalent phosphotyrosyl intermediate (Keck and Berger, 1999). The Topo 1 mediated reaction can be divided into four steps (Rothenberg, 1997; Rasheed and Rubin, 2003; Lorence and Nessler, 2004; Pommier, 2009) as depicted in Fig. 10.

CPT causes DNA damage by stabilizing a normally transient covalent complex between Topo 1 and DNA (Hsiang *et al.*, 1985). CPT binds only very weakly to normal B-DNA under physiological conditions, and it does not bind to Topo 1 alone (Lorence and Nessler, 2004). Cross-linking studies have suggested that CPT interacts with the Topo 1-DNA complex, thereby forming a ternary complex that stabilizes the trans-esterification intermediate (Hertzberg *et al.*, 1990; Pommier *et al.*, 1995). Thus, by stabilizing the cleavable complex, CPT transforms the normally useful enzyme Topo 1 into an intracellular, cytotoxic poison, and hence, CPT and structural analogues are topoisomerase poisons or topoisomerase inhibitors (Lorence and Nessler, 2004). Three binding models of CPT to the cleavable complex have been proposed, all of which follow a particular pattern and none of which provides the complete explanation of all the mutations that have been found in CPT-resistant Topo 1 (Chrencik *et al.*, 2004): (1) the Pommier intercalation ‘drug-stacking’ model (Fan *et al.*, 1998); (2) the Hol base-flipping model (Redinbo *et al.*, 1998); and (3) the Pilch intercalation model (Kerrigan and Pilch, 2001). All these models follow the principle of the ‘fork collision’ model (Rothenberg, 1997) in general which can be used to explain the cytotoxic effect of CPT (Fig. 10f-i).

1.6. Resistance mechanism against CPT

The mechanism of action of CPT involving the Topo 1-DNA complex has been used to identify the

mechanism of resistance against CPT. This mechanism imposes on the survival of CPT-producing or -treated cells if means for CPT resistance is not evolved. The mode of action of CPT has been used to identify the mechanism of resistance against CPT which is caused by nucleotide polymorphisms of the gene coding for Topo 1 (*Top1* gene) resulting in non-synonymous mutations. *Top1* mutations conferring resistance to CPT have been identified in CPT-resistant human leukemia cell line CEM/C2 (Fujimori *et al*., 1995), irinotecan-treated tumor tissues (Tsurutani *et al*., 2002), and various mammalian and yeast cells (Rasheed & Rubin, 2003). The elucidation of the crystal structure of the Topo 1-DNA covalent complex (Redinbo *et al.*, 1998) as well as models of the Topo 1-DNA-CPT ternary complex and/or Topo 1-DNA-CPT analogue ternary complex (Fan *et al.*, 1998; Redinbo *et al.*, 1998; Kerrigan and Pilch, 2001) has enabled the structural mapping of these mutations. Some cell lines have shown typical Topo 1 mutations like Tyr723Phe (Y723F) and Tyr727Phe (Y727F) which confer resistance not only to CPT but also to the indolocarbazole, rebeccamycin (Woo *et al.*, 2002). Other CPT-resistant cell lines that express mutant Topo 1, including Arg364His (R364H), Gly503Ser (G503S), and Asn722Ser (N722S), are also cross-resistant to rebeccamycin (Urasaki *et al.*, 2001). Recently, a study on CPT-producing plants revealed that the Topo 1s possessing residues Lys421 (K421), Ile530 (I530), and Ser722 (S722) (Sirikantaramas *et al*., 2008) are CPT-resistant. *Top1*s of each investigated CPT-resistant genus possessed different nucleotide polymorphisms (Sirikantaramas *et al*. 2009).

The mutation-based mechanism is not the only mechanism employed for resisting CPT binding to the Topo 1-DNA complex. Recent studies have revealed that certain typical amino acid residues in Topo 1 modulate CPT-binding and three-dimensional spatial positioning of the drug at the site(s) of drug attack under physiological conditions, thereby dictating the drug-Topo 1 and/or drug-DNA interactions. For example, the amino acid residue Asn352 (N352) exhibits a dynamic mobile behavior as evidenced by the molecular dynamics of Topo 1-DNA complex (Chillemi *et al.*, 2003; Staker *et al.*, 2005). It is located in a cavity in the immediate vicinity of the A-ring of CPT, thereby dictating the chemotype-specific contact of CPT with the Topo 1-DNA complex. The importance of N352 in conferring CPT resistance has been re-confirmed by demonstrating that the point mutation Asn352Ala (N352A) produces a CPT-sensitive Topo 1 enzyme (Laco *et al.*, 2002). The amino acid residue Glu356 (E356) demonstrates conformational flexibility, being present in multiple conformations in various ternary complexes which might be a factor that is mediated through CPT-DNA interactions as well as through direct CPT-protein interactions (Staker *et al.*, 2005). The residue Arg488 (R488) contributes in CPT resistance by disrupting the CPT binding site by destroying the water-mediated contact of the E-ring of CPT to itself (Staker *et al.*, 2005). The residue Gly503 (G503) sits just behind the side chain of the active site residue R488, relative to the intercalation binding site, whose modulation disrupts the conformation of R488 (Staker *et al.*, 2005). Furthermore, the presence of a conserved residue, Gly717 (G717), within

the active site of the Topo 1 functions as a flexible hinge to facilitate the alterations in active site geometry and linker domain flexibility that affects the CPT intoxication of Topo 1 (van der Merwe and Bjornsti, 2008).

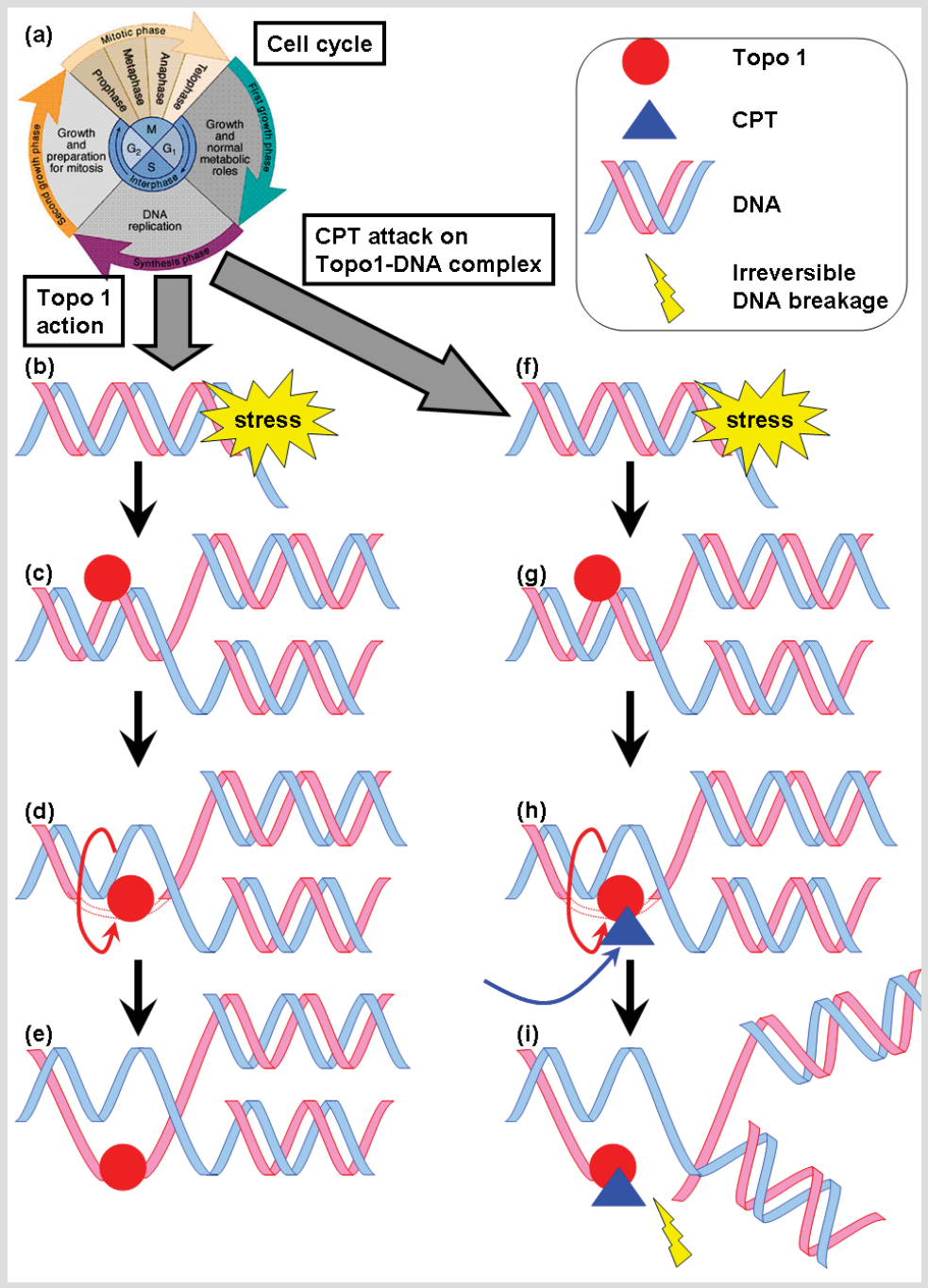

Fig. 10. The mechanism of action of Topo 1 and the mechanism of CPT attack on Topo 1-DNA complex. (a) The cell cycle; all events depicted in sections (b-i) happen in the S-phase. (b,f) Increase in tension and supercoiling of DNA. (c,g) Topo 1 binds to one DNA strand and cuts it (cleavage reaction). (d) The intact DNA passes through the nick resulting in the relaxation of the torsional strain. (e) Topo 1 reseals the cleaved DNA strand (re-ligation step). (h) Interaction of CPT with the Topo 1-DNA complex thereby forming a ternary complex that stabilizes the trans-esterification intermediate. (i) Irreversible breakage of DNA.

1.7. Other potential pharmacological effects of CPT

The typical action mechanism of CPT has led to further studies as potent inhibitors of replication, transcription, and packing of double stranded DNA-containing adenoviruses, papovaviruses, and herpes viruses, and the single-stranded DNA-containing autonomous parvoviruses (Pantazis *et al.*, 1999). CPT inhibits viral functions by attacking the host cell Topo 1 required for initiation and completion of viral functions. If properly developed, CPT could prove to be a powerful antiviral drug for several DNA viruses that are causative agents for a large number of diseases.

1.8. Biosynthetic pathway of CPT

The biosynthesis (Fig. 11) and regulation mechanism of CPT production at the molecular level are still not fully explored. Most alkaloids are derived from the amino acids, phenylalanine (Phe), tryptophan (Trp), lysine (Lys) and ornithine (Orn) (De Luca and St-Pierre, 2000), and all terpenoid indole alkaloids (TIAs) including CPT are derived from the universal precursor strictosidine (Kutchan, 1995). The biosynthesis of strictosidine involves the strictosidine synthase (*STR*; EC 4.3.3.2) mediated condensation of tryptamine with the iridoid glucoside secologanin (Stöckigt and Zenk, 1977; Stöckigt and Ruppert, 1999). The intramolecular cyclization of strictosidine yields strictosamide, a penultimate precursor of CPT in *C. acuminata* (Hutchinson *et al.*, 1979). The cDNA encoding *STR* was firstly isolated from *Rauvolfia serpentina* (Kutchan *et al.*, 1988) and then from *Catharanthus roseus* (McKnight *et al.*, 1990). *Escherichia coli*, yeast, insect cells, and tobacco, respectively, were used to heterologously express those *STR* genes (Kutchan, 1989; McKnight *et al*., 1991; Roessner *et al*., 1992; Kutchan *et al*., 1994). More recently, the Pictet-Spengler mechanism of catalysis of strictosidine synthase was evaluated (Maresh *et al.*, 2008). Tryptamine, providing the indole moiety of TIAs, is formed by decarboxylation of L-tryptophan by the enzyme tryptophan decarboxylase (*TDC*; EC 4.1.1.28) (Noé *et al.*, 1984). This reaction represents a branching point from primary metabolism into a secondary pathway. Early feeding experiments have confirmed that the tryptamine moiety is completely incorporated into the CPT molecule (Sheriha and Rapoport, 1976). Tryptophan is synthesized through the shikimate pathway (Yamazaki *et al.*, 2004), where the initial reaction between erythrose 4-phosphate and phosphoenolpyruvate leads to the formation of shikimate, which in turn is transformed to anthranilate and eventually to indole; further, the condensation of indole with a serine moiety leads to the formation of tryptophan. The cDNA clone encoding *TDC* was initially isolated from *C. roseus* (De Luca *et al.*, 1989) and later two autonomously regulated *TDC* genes (*TDC1* and *TDC2*) were isolated from *C. acuminata* and characterized (Lopez-Meyer and Nessler, 1997). The secologanin moiety is derived from a monoterpenoid, geraniol, which in turn is obtained from isopentenyl diphosphate (IPP) and dimethylallyl diphosphate (DMAPP) via formation of geranyl diphosphate (GPP).

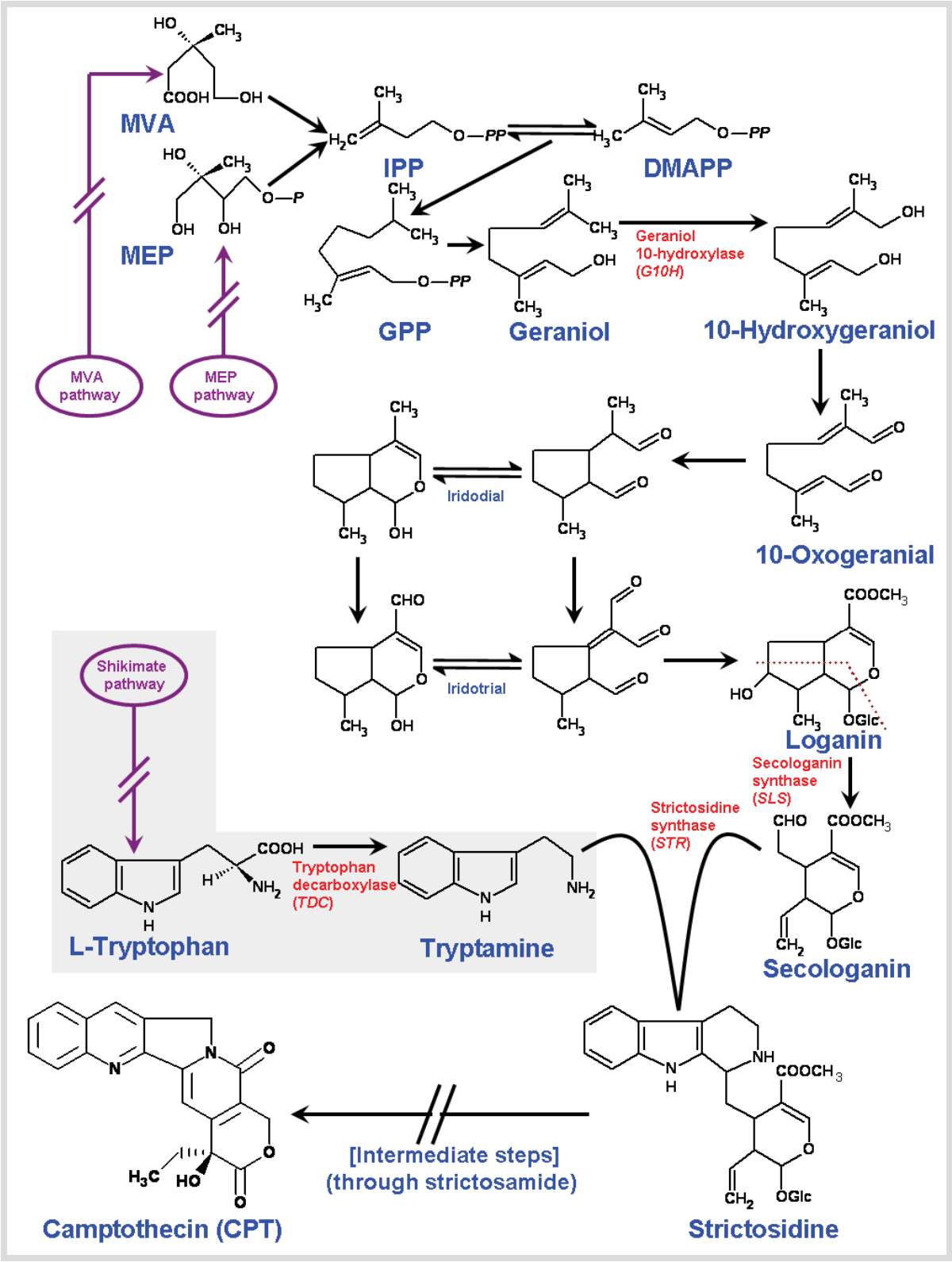

Fig. 11. The biosynthetic pathway of CPT, complied from different steps of the pathway discovered and/or verified in various CPT producing plants. Enzymes are marked in red. MVA, mevalonate; MEP, 2-C-methyl-D-erythritol-4-phosphate; IPP, isopentenyl diphosphate; DMAPP, dimethylallyl diphosphate; GPP, geranyl diphosphate.

For the formation of IPP, the precursor of terpenoid biosynthesis, the mevalonate (MVA) pathway has long been known. For many years, the MVA route was thought to be the only source of building blocks for all plant isoprenoids. Recently, 2-C-methyl-D-erythritol 4-phosphate (MEP) pathway, in which IPP is formed from 1-deoxy-D-xylulose-5-phosphate by condensation of glyceraldehyde-3-phosphate and pyruvate, was found to be present in many eubacteria, green algae, and plastids of plants (Rohmer, 1999; Rodriguez-Concepcion and Boronat, 2002; Kuzuyama and Seto, 2003). Both the isoprenoid pathways are operative simultaneously in higher plants (Lorence and Nessler, 2004). The enzyme geraniol 10-hydroxylase (*G10H*; EC 1.14.14.1) is a cytochrome P450 monooxygenase, which hydroxylates the monoterpenoid geraniol at the C-10 position leading to the formation of 10-hydroxygeraniol. This reaction forms the first committed step in the formation of secologanin (Collu *et al.*, 2001). The final step for biosynthesis of secologanin from loganin is also catalyzed by a P450 protein, secologanin synthase (*SLS*; EC 1.3.3.9) (Irmler *et al.*, 2000; Yamamoto *et al.*, 2000). Loganin is synthesized from 10-hydroxygeraniol via 10-oxogeranial and further irridotrial intermediates, by cyclization and randomization of methyl groups (Uesato *et al.*, 1986). The remaining details and precise intermediates between strictosamide and CPT are not completely defined. Therefore, it is postulated that CPT could be formed from strictosamide by three transformations (Hutchinson *et al.*, 1979). The steps following strictosamide formation remain somewhat speculative (O'Connor and Maresh, 2005). A series of chemically reasonable transformations have been proposed though there is little experimental evidence for these steps (Hutchinson *et al.*, 1979).

1.9. Requirement for alternate sustainable sources of CPT

Cancer remains a major cause of mortality worldwide. In 2006 in Europe, there were an estimated 3.2 million cancer cases diagnosed (excluding non-melanoma skin cancers) and 1.7 million deaths from cancer (Ferlay *et al.*, 2007). According to the World Health Organization (www.who.int), from a total of 58 million deaths worldwide in 2005, cancer accounts for 7.6 million (or 13%) of all deaths (Lamari and Cordopatis, 2008). The current scenario on the occurrence and mortality rates due to various forms of cancer worldwide is extremely alarming (Jemal *et al.*, 2008). Cancer rates are predicted to further increase in the future, mainly due to the steadily ageing populations in both developed and developing countries, the current trends in smoking prevalence and growing adoption of unhealthy lifestyles, and the lack of enough anticancer drugs to satisfy the current and the projected demands. CPT and its structural analogues have emerged as one of the most promising agents for cancer treatment owing to the typical action mechanism involving DNA-Topo 1. As detailed above, a large number of CPT derivatives have already entered clinical trials for various forms of cancer, in addition to TPT and CPT-11 already in the market as successful anticancer drugs. The worldwide market value for CPT

derivatives TPT and CPT-11 was estimated at about US$ 750 million in 2002 which rose to US$ 1 billion by 2003 and has reached US$ 2.2 billion in 2008 (Lorence and Nessler, 2004; Sankar-Thomas, 2010). This represents approximately 1 tonne of CPT in terms of natural material (Raskin *et al.*, 2002; Watase *et al.*, 2004). However, *C. acuminata* (from China) remains the major source of CPT and in spite of the rapid market growth, CPT is still harvested by extraction from barks and seeds of naturally grown *C. acuminata* trees (Lorence and Nessler, 2004; Sankar-Thomas, 2010), followed by *N. nimmoniana* (from India) (Uma Shaanker *et al.*, 2008). In addition to the difficulties of the practical total synthesis of these natural compounds, the unpredictable problems of nature such as erratic weather and pests have rendered these plant species vulnerable to extinction. In fact, in 2000 and again in 2006, *C. acuminata* was proposed for protection in the CITES, World Conservation Monitoring Centre, appendix II (Annonymous, 2006a). This appendix lists species that are not necessarily now threatened with extinction but that may become so unless trade is closely controlled. Similarly, it is estimated that in the last decade alone, there has been at least a 20% decline in the population of *N. nimmoniana*, leading to the red-listing of the species (Kumar and Ved, 2000; Hombe Gowda *et al.*, 2002). The few commercial nurseries for *C. acuminata* cannot meet the demand for CPT production (Sankar-Thomas, 2010). Furthermore, the yields of CPT from field trees vary widely and depend on factors that are difficult to control. For instance, plant diseases such as leaf spot and root rot are some of the major fungal diseases that can limit the cultivation of *Camptotheca* plants (Li *et al.*, 2005) and diminish the production of CPT. Cultivation of *Camptotheca* plants is limited to subtropical climates and it takes about ten years for plants to produce a stable fruit yield (Li *et al.*, 2005; Sankar-Thomas, 2010). Thus, CPT is becoming an increasingly scarce starting material for the production of TPT, CPT-11, and several other structural analogues.

1.10. Alternate sources of CPT

Currently, the combination of a high demand for CPT and its scarcity from natural plant sources has led to a different strategy: bioprospecting the endophytic fungi associated with the CPT producing plants as novel sources of CPT and related metabolites. The advantage of using fungi to produce CPT and related metabolites under controlled fermentation conditions are multifold; an economical, environment-friendly, and reproducible manner amenable to industrial scale-up for sustained production irrespective of the vagaries of nature. Recently, endophytic *Entrophospora infrequens* (Puri *et al.*, 2005; Amna *et al.*, 2006) and *Neurospora crassa* (Rehman *et al.*, 2008) isolated from *N. nimmoniana* have been reported to produce CPT. However, in both cases, there have been no further studies on how the fungi are able to produce CPT and prevent self-toxicity from the intracellular accumulated CPT. Further, no follow-up work on up-scaling the production of CPT has been performed, and there is no published

breakthrough in the commercial exploitation of these endophytic fungi as a source of CPT. There is no published report that CPT or structural analogues might be produced by any microorganism associated with *C. acuminata*. Only very recently, following our discovery of the endophytic fungus *Fusarium solani*, capable of producing CPT, 9-MeO-CPT and 10-OH-CPT, another endophytic fungus has been isolated from *Apodytes dimidiata* capable of producing the same compounds (Shweta *et al.*, 2010). Furthermore, an endophytic *Xylaria sp*. has recently been isolated from *C. acuminata* capable of producing only 10-OH-CPT, and strangely, not the parent compound CPT (Liu *et al.*, 2010). In both cases, no further follow-up studies have been reported so far.

2. Hypericin

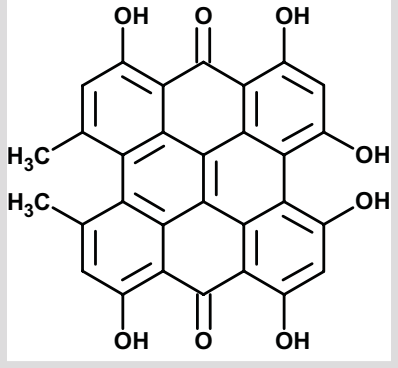

Fig. 12. Hypericin.

2.1. Discovery

Hypericin (2,2'-dimethyl-4,4',5,5',7,7'-hexahydroxy-mesonaphtodianthrone), a naphthodianthrone derivative, is a plant derived compound of high medicinal value. It is one of the main constituents of *Hypericum* species. The first detailed report of the isolation of hypericin was from the medicinal herb *Hypericum perforatum* L., published by Brockmann *et al*. (1939). The molecular formula of hypericin was first reported in 1942 by the same author as $C_{30}H_{16}O_8$ (Brockmann *et al.*, 1942) and eight years later the correct structure was published (Brockmann *et al.*, 1950).

2.2. Compounds related to hypericin

Various species of the genus *Hypericum* have long been used as medicinal plants in various parts of the world due to their therapeutic efficacy (Yazaki and Okada, 1994). Their main constituents (Fig. 13) are napthodianthrones, primarily represented by hypericin, pseudohypericin, protohypericin, protopseudophypericin (Brockmann *et al.*, 1939, 1942, 1957), the anthraquinone emodin, and derivatives occurring in very low concentrations such as isohypericin, demethyl-pseudohypericin, hyperico-dehydro-dianthrone, pseudo-hyperico-dehydro-dianthrone (Brockmann *et al.*, 1957), and

cyclopseudohypericin (Häberlein *et al.*, 1992). However, these minor constituents have not been proven to occur genuinely in plants and might be artifacts of the isolation (Hölzl and Petersen, 2003). Protohypericin and protopseudohypericin convert readily in light to hypericin and pseudohypericin, respectively. Additionally, prenylated phloroglucinol derivatives such as hyperforin and adhyperforin (Nahrstedt and Butterweck, 1997) are found. Furthermore, flavonoids such as hyperoside, rutin, quercetin and quercitrin, and biflavonoids such as I3,II8-biapigenin and I3',II8-biapigenin have been reported (Nahrstedt and Butterweck, 1997).

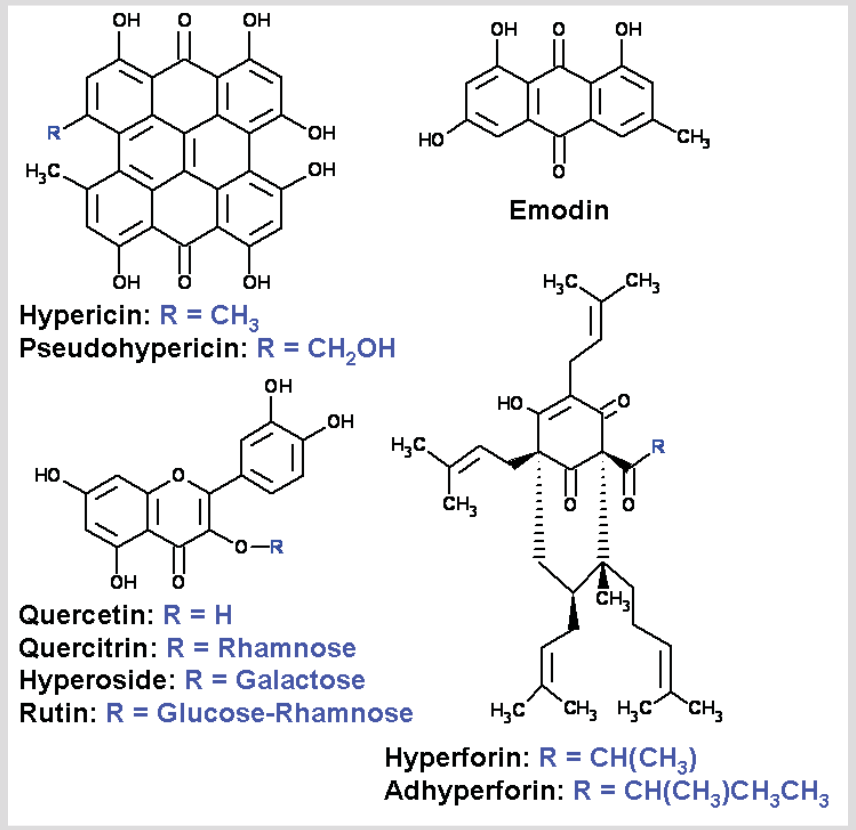

Fig. 13. The main constituents of *Hypericum* species.

2.3. Occurrence of hypericin in the plant kingdom

Hypericin mainly occurs in the plants of the genus *Hypericum* belonging to the family Clusiaceae. Formerly, *Hypericum* was placed into the families Guttiferae and then Hypericaceae (Hölzl and Petersen, 2003). Although anthrone derivatives are reported from related subfamilies, *Hypericum* is currently the only plant taxon containing condensed anthrones such as hypericin (Kitanov, 2001). *Harungana madagascariensis* belonging to the same family as *Hypericum* was reported to contain hypericin and pseudohypericin in leaves (Fisel *et al.*, 1966) and *Porospermum guineense* contains a red photosensitizing pigment in the root bark which is similar to hypericin (Hegnauer, 1966).

Hypericum is a genus comprising approximately 400 species, which are widespread in warm temperate areas throughout the world and are well represented in the Mediterranean area (Robson and

Strid, 1986), 60% of which are known to contain hypericin as a constituent (Robson, 1977, 1981). According to the Flora Europaea, 59 species are native to Europe (Hölzl and Petersen, 2003). Plants of the genus *Hypericum* have been used as traditional medicinal plants in various parts of the world (Yazaki and Okada, 1994). One of the most exploited and studied species of the *Hypericum* genus is the medicinal herb called *H. perforatum* L., commonly known as St. John's wort. It is a pseudogamous, facultatively apomictic, perennial medicinal plant that is native to Europe, West and South Asia, North Africa, North America, and Australia (Hickey and King, 1981; Wichtl, 1986). Several subspecies exist of this species, two of which are pharmaceutically important: *H. perforatum* ssp. *angustifolium* (DC) GAUDIN is mainly native to Southern Europe, whereas the subspecies *perforatum* predominantly occurs in Northern Europe (Hölzl and Petersen, 2003). These two subspecies are morphologically as well as phytochemically distinct. The narrow-leaved subspecies *angustifolium* has much higher hypericin content than the broad-leaved subspecies *perforatum*.

2.4. Distribution of hypericin in the plant organs

Hypericin is localized (Briskin *et al.*, 2000) and probably also synthesized in the dark glands (Cellarova *et al.*, 1994; Onelli *et al.*, 2002), which are small glandular structures dispersed over all above-ground parts of the plant (flowers, capsules, leaves, stems) but not in the roots (Hölzl and Petersen, 2003). The content of hypericin in the dry herb is 0.1-0.15% and in flowers and flower buds is 0.2-0.3% (Kaul, 2000). Seeds and the cotyledons of seedlings do not contain hypericins, but they can already be found in the first true leaves after germination. Although a study describing the typical distribution pattern of hypericin in plant organs of *H. perforatum* was published (Berghöfer, 1987), recent investigations reveal that the amount of hypericin in the *Hypericum* species varies considerably with the differences in climatic and soil conditions, and it is almost impossible to standardize the extraction process thereby reducing the cost-effectiveness (Smelcerovic *et al*., 2006a,b; Smelcerovic and Spiteller, 2006; Smelcerovic *et al*., 2008; Verma *et al*., 2008). Furthermore, with regard to concentrations of the active components, significant differences are evident among the different species of *Hypericum* (Umek *et al.*, 1999; Kitanov, 2001), among different populations of the same species from different localities (Kartnig *et al.*, 1989; Buter *et al.*, 1998), among different ontogenetic phases of the same individual (Tekelova *et al.*, 2000), in cell cultures (Kartnig *et al.*, 1996), and even among different plants regenerated from the same *in vitro* cultivated clone and grown under the same conditions (Cellarova *et al.*, 1994).

More recently, a series of detailed studies on the secondary metabolite contents of different *Hypericum* species were performed that included a number of species from Serbia (Smelcerovic *et al*., 2004, 2006a,b, 2007; Gudzic *et al*., 2007; Glisic *et al*., 2008), Macedonia (Smelcerovic and Spiteller, 2006),

Tenerife (Bonkanka *et al.*, 2008), and Turkey (Spiteller *et al.*, 2008; Smelcerovic *et al.*, 2008). Furthermore, studies have been made on the very important and commercially recognized *H. perforatum* from India (Buter *et al.*, 1998; Verma *et al.*, 2008). Nevertheless, it is not clear in how far the spectrum and the concentration of hypericin and related secondary compounds relate to certain genotypes within species, whether there are pronounced differences of this spectrum among different species, and whether there are clear differences in secondary compound accumulation in different aerial (leaves and stems) and non-aerial (roots) organs. It is also not understood in how far environmental factors influence the spectrum of secondary compounds and their expression. A major challenge for such comparative studies is to ensure that identical and reliable methods of secondary compound analyses are employed that ensure comparability of chemical data. Robust comparative data are needed to understand the production of secondary compounds by the plant in both a phylogenetic (evolution of biosynthetic pathways) and an environmental (factors influencing expression of metabolites) context.

2.5. Pharmacological effects of hypericin

Hypericin has long been in use, at least from the time of ancient Greece (Tammaro and Xepapadakis, 1986), as an antidepressant due to its monoamine oxidase (MAO) inhibiting capacity, having effects similar to bupropion (Nahrstedt and Butterweck, 1997) and imipramine (Raffa, 1998). Potential uses of hypericin extend to improved wound healing, anti-inflammatory effects (Zaichikova *et al.*, 1985), antimicrobial and antioxidant activity (Radulovic *et al.*, 2007), sinusitis relief (Razinkov *et al.*, 1989), and seasonal affective disorder (SAD) relief (Martinez *et al.*, 1993). Hypericin also has remarkable antiviral activity against a number of viruses including HIV-1 (human immunodeficiency virus type 1) (Lavie *et al*., 1989; Lopez-Bazzocchi *et al*., 1991; Hudson *et al*., 1991; Degar *et al*., 1992; Hudson *et al*., 1993; Lenard *et al*., 1993; Lavie *et al*., 1995; Prince *et al*., 2000; Xu and Lu, 2005), HSV-1 (*Herpes simplex* virus type 1) (Tang *et al.*, 1990; Andersen *et al.*, 1991; Cohen *et al.*, 1996; Hudson *et al.*, 1999), HSV-2 (*Herpes simplex* virus type 2) (Andersen *et al.*, 1991), BVDV (bovine viral diarrhea virus) (Prince *et al.*, 2000), influenza A (influenza virus type A) (Tang *et al.*, 1990; Lenard *et al.*, 1993; Hudson *et al.*, 1999), Para-3 (para-influenza virus type 3) (Andersen *et al.*, 1991), RadLV (radiation leukemia virus) (Lavie *et al.*, 1989; Degar *et al.*, 1993; Lavie *et al.*, 1995), Mo-MuLV (Moloney murine leukemia virus) (Tang *et al.*, 1990), VV (Vaccinia virus) (Andersen *et al.*, 1991), FLV (Friend leukemia virus) (Stevenson and Lenard, 1993; Utsumi *et al.*, 1995), VSV (vesicular stomatitis virus) (Andersen *et al.*, 1991; Lenard *et al.*, 1993), MCMV (murine cytomegalovirus) (Lopez-Bazzocchi *et al.*, 1991; Hudson *et al.*, 1991), *Sendai virus* (Lenard *et al.*, 1993), SV (Sindbis virus) (Lopez-Bazzocchi *et al.*, 1991; Hudson *et al.*, 1991, 1994), EIAV (equine infectious anemia virus) (Carpenter

and Kraus, 1991; Carpenter *et al.*, 1994; Fehr *et al.*, 1995; Park *et al.*, 1998; Kraus *et al.*, 2000), DHBV (duck hepatitis B virus) (Moraleda *et al.*, 1993), BIV (bovine immunodeficiency virus) (Tobin *et al.*, 1996), and HCMV (human cytomegalovirus) (Barnard *et al.*, 1992), either by inhibiting viral infectivity in a hypericin pre-incubation and light-dependent inactivation reaction or by inhibiting viral replication in cell cultures (Kubin *et al.*, 2005). Several recent *in vitro* studies have revealed the multifaceted cytotoxic activity of hypericin as a result of its photodynamic activity (Hadjur *et al.*, 1996; Delaey *et al.*, 2001; Kamuhabwa *et al.*, 2001; Kubin *et al.*, 2005). The peculiar attributes of hypericin are high efficiency in production of singlet oxygen and superoxide anions after irradiation with light wavelength around 600 nm, and little or no toxicity in the dark. Light-activated hypericin generates singlet oxygen (type II mechanism) and reactive oxygen species (ROS) such as superoxide radical anions, hydroxyl radicals and peroxides (type I mechanism) (Fig. 14). The radicals are cytotoxic and react with cell constituents and are the initial point of apoptosis or necrosis depending on the dosage (Kubin *et al.*, 2005).

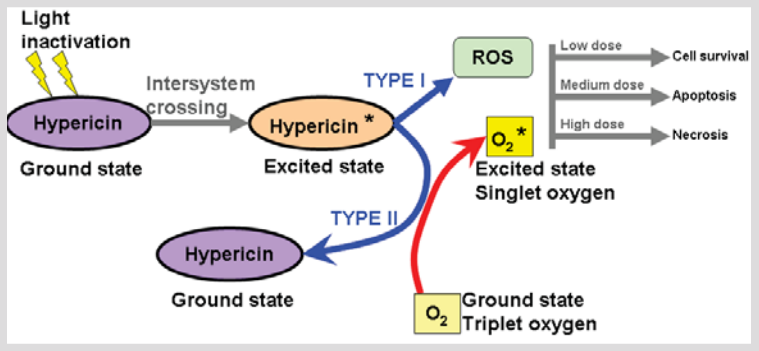

Fig. 14. The schematic representation of mechanism of hypericin photoactivation and induced damages. ROS, reactive oxygen species.

2.6. Biosynthetic pathway of hypericin

A hypothetical biosynthetic pathway was proposed shortly after the isolation and characterization of hypericin extracted from *H. perforatum* (Brockmann *et al*., 1939, 1942, 1950; Thomson, 1957). By isolating some intermediate compounds, these workers formulated a theoretical polyketide pathway based largely on the paradigm that chemical principles should apply to biosynthetic processes. The metabolism of hypericin precursors, like the polyketide metabolites in general, is presumed to follow a pathway analogous to fatty acid synthesis. A schematic representation of the proposed polyketide pathway is depicted in Fig. 15. A series of Claisen condensations between 2 carbon units (malonate) yields polyketomethylene chains, which by reduction to fatty acids and further cyclization, lead to many classes of aromatic compounds (Hertweck, 2009). Acetyl CoA serves as a starter unit for polyketide chain elongation just as in fatty acid synthesis. Malonyl CoA serves as the extender unit of the chain. A concomitant decarboxylation occurs during the attack on the carbonyl group of acetyl-S-CoA. This reaction leaves the malonyl moiety as a stronger nucleophile, so it becomes the chain extender unit.

Once the acetyl CoA starter unit is in place, the chain is elongated by subsequent additions of malonyl ACP (2C) extender units. The analogous enzymes that are proposed to catalyze the biosynthesis of poyketides are now collectively referred to as the polyketide synthases (PKSs). The PKSs appear to have a genetic organization similar to that of the enzymes of the fatty acid synthase complex (Katz and Donadio, 1993; Staunton and Weissman, 2001; Hertweck, 2009). Since this enzymatically catalyzed pathway to polyketide chains and ultimately to aromatic rings is not well characterized, it is not known what sort of reducing agent or other cofactors are required for each reaction. Exactly how the correct starter unit (acetyl CoA in the case of hypericin) is selected, how the ACP is charged with malonate, and which mechanisms determine folding and chain release are not precisely known either. Additionally, the mechanism that is accomplished with the programming that governs the number of condensations, the proper folding of the completed acyl chain, the cyclization into the correct number of rings, and the release of the resulting structure is not well understood.

In the case of hypericin biosynthesis, the homodimeric type III PKS had earlier been suggested to be responsible for the condensation of one molecule of acetyl CoA with seven molecules of malonyl CoA to form an octaketide chain that subsequently undergoes cyclizations and decarboxylation, leading to the formation of emodin anthrone (Falk, 1999; Zobayed *et al*., 2006), the first cyclization product of the polyketide pathway. The type III PKS with octaketide synthase (OKS) activity responsible for the formation of emodin anthrone has not been characterized as yet, although a PKS named HpPKS2 has recently been reported to catalyze the condensation of one acetyl CoA with two to seven malonyl CoA to yield tri- to octaketide products, but not emodin anthrone (Karppinen *et al.*, 2008). It is postulated that a dianthrone would arise from emodin anthrone, probably by oxidative coupling of the anthranol, and would lead by further oxidation of its enol form to a dehydrodianthrone and then, from a helianthrone derivative (protohypericin), to yield hypericin (Thomson, 1957). Protohypericin is readily converted to hypericin upon irradiation with visible light. The knowledge that anthrone-dianthrone inter-conversion takes place readily, coupled with a basic understanding of how anthracene nuclei are cross-linked by oxidation, contributed to the proposal of the original scheme for the biosynthesis of hypericin from emodin anthrone (Brockmann *et al*., 1942, 1950; Thomson, 1957).

On the other hand, Chen *et al*. (1995) characterized the enzyme emodinanthrone-oxygenase that catalyzes the fixation of molecular oxygen into emodin anthrone to yield the anthraquinone emodin. Furthermore, Bais *et al*. (2003) reported the biochemical and molecular characterization of an enzyme, Hyp-1, from dark grown *H. perforatum* cell cultures, that specifically catalyzes the direct conversion of emodin to hypericin *in vitro* (Fig. 15c). More recently, a study on the expression of the *hyp-1* gene in different organs of *H. perforatum* seedlings in early stages of development, purporting to locate the sites of biosynthesis of hypericin, was published (Kosuth *et al.*, 2007).

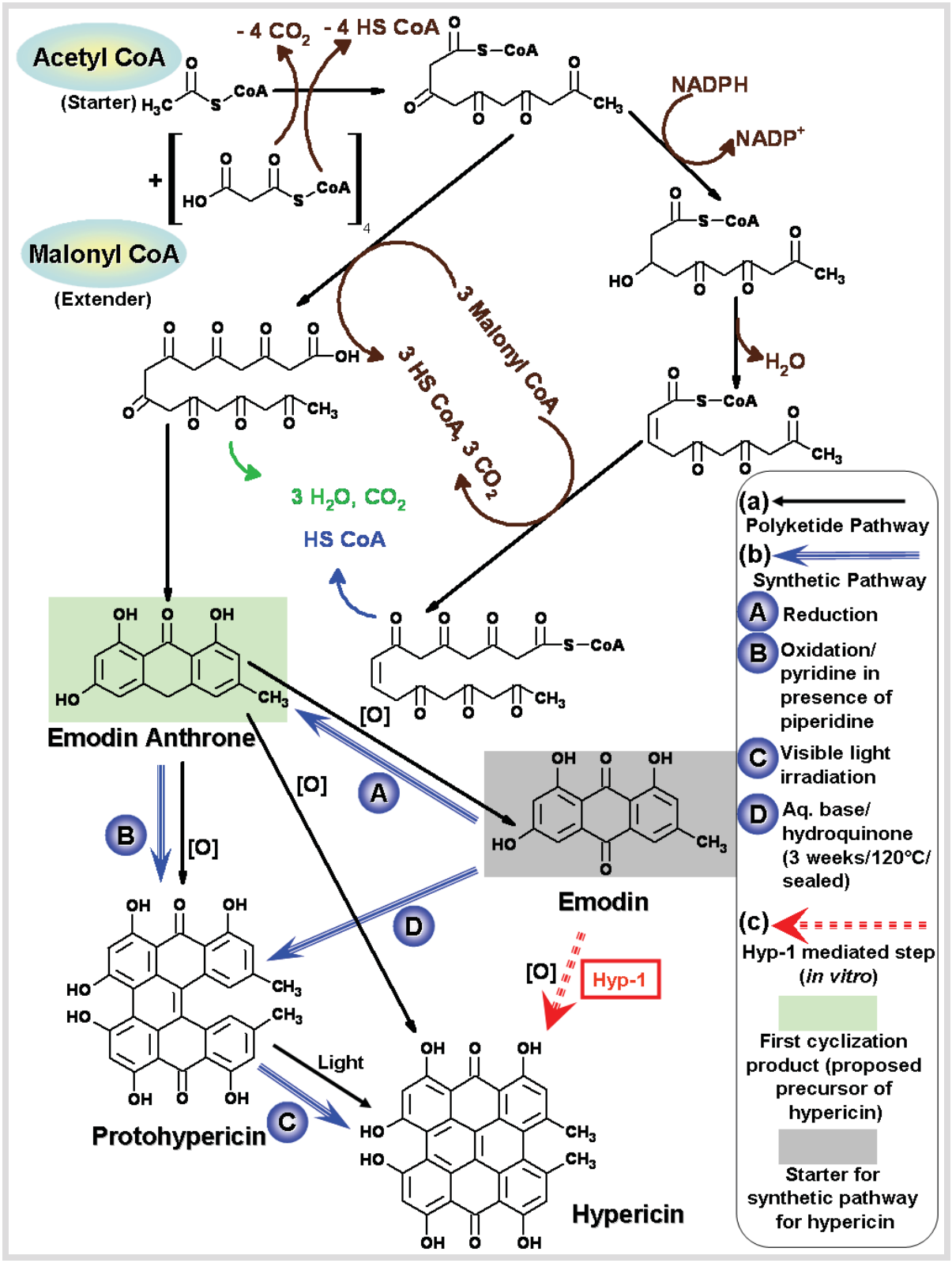

Fig. 15. The schematic representation of different manners of hypericin production. (a) Hypothetical polyketide pathway adapted from the originally proposed pathway (Brockmann *et al.*, 1950; Thomson, 1957). (b) The synthetic routes of preparing hypericin. (c) Hyp-1 mediated pathway from emodin to hypericin proposed by Bais *et al.* (2003).

This study, however, showed that the sites of biogenesis and accumulation of hypericin in the *Hypericum* plants are independent of the expression of the *hyp-1* gene. Moreover, Michalska *et al*. (2010) also failed to reproduce the experiments of Hyp-1 catalyzed conversion of emodin to hypericin as claimed by Bais *et al*. (2003), thus questioning the function of Hyp-1 in plants.

Concomitantly, the chemical synthesis of hypericin follows the pattern of the proposed biogenesis. Emodin anthrone is the precursor of hypericin synthesis and is obtained either by the reduction of emodin isolated from the bark of the breaking buckthorn (Falk *et al.*, 1993) or by synthesizing emodin as first described by Brockmann *et al*. (1957). The synthetic routes to hypericin (Mazur *et al.*, 1992; Falk *et al.*, 1993; Falk, 1999) are shown in Fig. 15b. Additionally, a new high-yield synthetic route to emodin anthrone with commercially available *o*-cresotinic acid as precursor has been developed by Falk and Schoppel (1991).

2.7. Requirement for alternate sustainable sources of hypericin

Due to the efficacy of hypericin, St. John's wort is one of the best-selling herbal medicines worldwide (Annonymous, 2006b; Julsing *et al.*, 2007). In the U.S., a monograph for St. John's wort and its powder is part of the twentieth edition of the national formulary included into the USP 25 published in 2002 (Meier, 2003). In the U.S. alone, the annual sales figure is around US$ 200 million (Ernst, 2003). In 2009, St. John's wort has been one of the top-twenty herbal dietary supplements in the Food, Drug, and Mass Market (FDM) Channel as determined by the Information Resources Inc. (IRI) in the U.S. with total sales worth US$ 8,758,233 (Cavaliere *et al.*, 2010). On the other hand, the European Pharmacopoeia included a monograph for St. John's wort in the 2000 Addendum to Ph Eur 3 (Meier, 2003). The monograph is fully integrated in the actual issue of Ph Eur 4. The eighth edition of the Swiss Pharmacopoeia has recently included the monograph for the freshly harvested plant (*Herba hyperici recens*) as the herbal drug for the production of the oily macerate (Meier, 2003). In Europe, St. John's wort has always been one of the top-selling drugs. In Germany, St. John's wort is listed in the German Drug Codex, approved as a medicine in the Commission E monographs, and licensed as a standard medicinal tea infusion (Annonymous, 1998). It is used in psychiatric drugs in forms including ampoule (Hyperforat®), coated tablet (LI 160, Jarsin®, Lichtwer Pharma, Berlin), juice (Kneipp® Johanniskraut Pflanzensaft N), tea (Kneipp® Johanniskraut-Tee), and tincture (Psychotonin® M). It is used in some urological preparations affecting micturition (e.g., Inconturina®) (Schilcher, 1997). In German pediatric medicine, St. John's wort aqueous infusions, alcoholic fluid extracts, and some proprietary products [such as Sedariston®, a combination of St. John's wort and valerian (*Valeriana officinalis*) extracts] are used to treat depressive states in young people. For example, St. John's wort is a component of a sedative tea for children, composed of 30% lemon balm leaf (*Mellissa officinalis*),

30% lavender flower (*Lavandula officinalis*), 30% passion flower herb (*Passiflora spp.*), and 10% St. John's wort herb (Schilcher, 1997). Unfortunately, hypericin is not abundant and is only available in the plants of *Hypericum* species. The concentration of hypericin varies significantly with the differences in climatic and soil conditions, among different species of *Hypericum*, among different populations of the same species from different localities, among different ontogenetic phases of the same individual, in cell cultures, and even among different plants regenerated from the same *in vitro* cultivated clone and grown under the same conditions. As a result, there is a problem in sourcing hypericin and standardizing extracts to meet the current and projected demands available from the natural sources. Therefore, it is desirable to find alternative sources of hypericin to meet the pharmaceutical demand by establishing an inexhaustible, cost-effective, and renewable resource of this compound using fermentation technology (involving a microbe) that promises reproducible and dependable productivity.

3. Deoxypodophyllotoxin

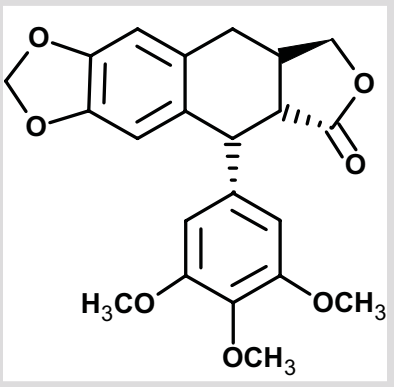

Fig. 16. Deoxypodophyllotoxin.

3.1. Discovery

The first literature report on the extraction of 'Podophyllum' was that of King, who called the resin he obtained from alcohol extraction as 'podophyllin' (King, 1857). 'Podophyllum' is the dried roots and rhizomes of species of *Podophyllum*, which was described and its first modern botanical name given by Linnaeus (1753) (Fig. 17a). The first successful chemical investigation was later carried out by Podwyssotzki (1881, 1882, 1884). The correct empirical formula for podophyllotoxin first advanced by Borsche and Niemann (1932) and later confirmed (Gensler *et al*., 1954; Gensler and Wang, 1954; Petcher *et al*., 1973).

Strikingly, the first documented proof of the discovery of deoxypodophyllotoxin was not from *Podophyllum*. The Leech book of Bald (Fig. 17b), 900-950 A.D., an early English medicinal book, has reported on the use of root of *Anthriscus sylvestris* (Imbert, 1998). These roots were reported contain lignans such as deoxypodophyllotoxin and were used in ointments prepared from a large number of

plants and plant extracts like *savin* to cure cancer (Cockayne, 1961). In China and Japan, the roots of this plant were also used as a kind of crude drug called '*qianhu*' in China (Kozawa *et al.*, 1978) and '*zengo*' in Japan (Kozawa *et al.*, 1982). On the other hand, as early as in the first century A.D., Pliny the Elder mentions that the smaller species of *Juniperus* could be used, among other things, to stop tumors ('*tumores*' in Latin) or swelling (Imbert, 1998; Koulman, 2003). Pedanius Dioscorides mentions the use of the oil of *Juniperus* species (*J. sabina*, *J. phoenicea* and *J. communis*) for the treatment of ulcers, carbuncles and leprosy (Gunther, 1959). Generally, dried needles, called *savin*, or the derived oil was used. In 47 A.D., Scribonius Largus wrote that *savin* oil was used to soften "hard female genital parts" (Sconocchia, 1983). Later references indicated the use of *savin* to treat uterine carcinoma, venereal warts and polyps (Hartwell and Schrecker, 1958). At present, we know that the pharmacological activity of *J. sabina* needles is to be ascribed to the lignans deoxypodophyllotoxin and podophyllotoxin (Hartwell *et al.*, 1953).

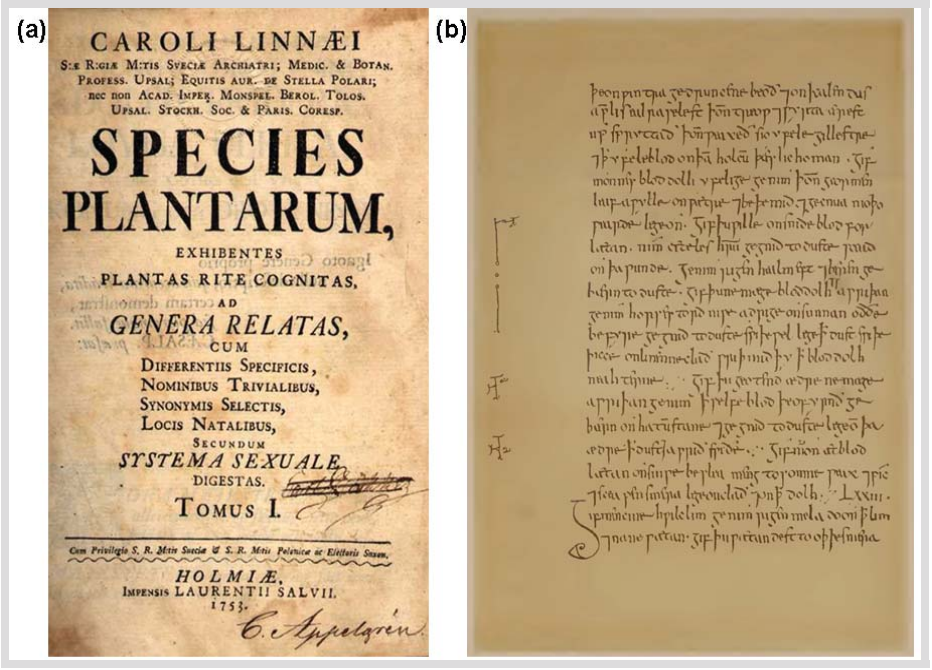

Fig. 17. (a) Cover page of the first edition of 'Species Plantarum' by Linnaeus (1753), where *Podophyllum* was named and described for the first time. (b) A facsimile of a page from the 'Bald's Leechbook' where lignan deoxypodophyllotoxin was described for the first time. These images have been released into the 'public domain' applicable to the United States, Australia, and European Union.

3.2. Lignans related to deoxypodophyllotoxin

Parallel to the discovery of podophyllin (King, 1857) and deoxypodophyllotoxin (Imbert, 1998), the natives of the Himalayas as well as the American Indians independently discovered that extracts of *Podophyllum* rhizomes possessed a cathartic action and could be used as traditional medicine (Koulman, 2003). The Indians introduced podophyllin, a resin obtained by ethanolic extraction of the *Podophyllum* roots and rhizomes. The main constituents in podophyllin are the lignans podophyllotoxin, 4'-demethylpodophyllotoxin, and α- and β-peltatin (Koulman, 2003) (Fig. 18). Podophyllin was included

in the first U.S. Pharmacopoeia, dating from 1820, as a cathartic and cholagogue (Koulman, 2003). However, initial expectations regarding the clinical utility of podophyllotoxin were tempered largely due to its unacceptable gastrointestinal toxicity (Ayres and Loike, 1990).

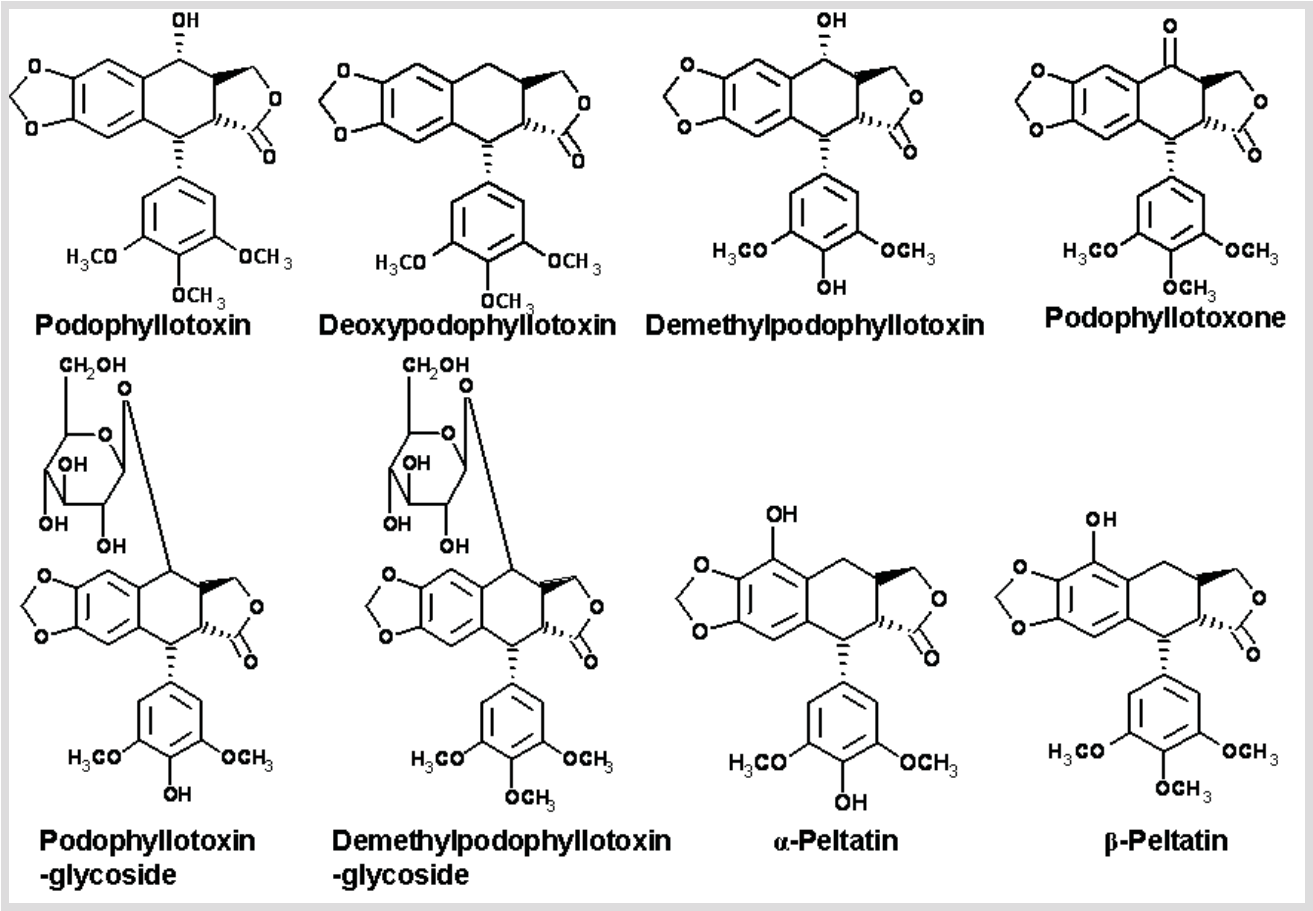

Fig. 18. Important lignans present in plants of the genera *Podophyllum* and *Juniperus*.

This led researchers to investigate the possibility that the *Podophyllum* lignans might occur naturally as glycosides (Stähelin and von Wartburg, 1991). Using special procedures to inhibit enzymatic degradation, these researchers indeed obtained the podophyllotoxin-β-*D*-glucopyranoside as the main component and its 4'-demethyl derivative from the Indian *Podophyllum* species, among other related lignans like podophyllotoxone (Imbert, 1998; Canel *et al.*, 2000; Wong *et al.*, 2000). The research efforts were then focused on a program to chemically modify both the glycosides and aglycones of a wide range of podophyllotoxin derivatives. Extensive structure activity relationship (SAR) studies were carried out using several podophyllotoxin analogues (Fig. 18). It was revealed that the core structure of deoxypodophyllotoxin is responsible for the cytotoxicity (Koulman, 2003; Liu *et al.*, 2007). The extra methoxy group (6-methoxypodophyllotoxin) on the position-6 does not significantly change the *in vitro*

cytotoxicity compared to podophyllotoxin. Also the methyl group on the 4'-position of the pendent ring has little effect on the cytotoxicity (Middel *et al.*, 1995; Hadimani *et al.*, 1996). Nearly 600 derivatives were prepared and tested over a period of about 20 years (Stähelin and von Wartburg, 1991). This resulted in the development of the clinically important anticancer drugs, etoposide (Eposin®, VePesid®, VP-16) and teniposide (Vumon®, VM-26) (Imbert, 1998; Koulman, 2003; Liu *et al*., 2007) (Fig. 19).

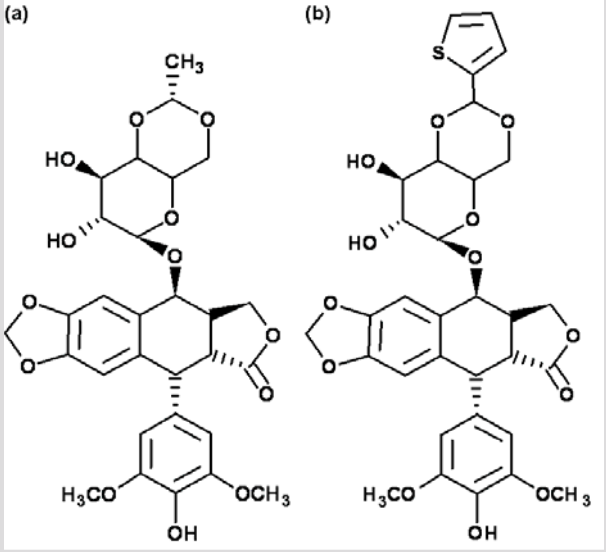

Fig. 19. (a) Etoposide. (b) Teniposide.

By 1983, Bristol-Myers Squibb Co. took over license for both etoposide and teniposide. In 1996, the phosphate analogue called etopophos was also approved (Koulman, 2003). Etoposide is still used, often in combination with cisplatin and for instance bleomycin, for the treatment of metastatic testicular germ-cell tumors (Flechon *et al.*, 2001). Etoposide alone is also used for the treatment of small-cell lung cancer (Mascaux *et al.*, 2000). With these success stories, further investigations have generated exciting chemotherapeutic candidates and successful applications of drug development from podophyllotoxin-related leads, such as NK611, GL-331, Azatoxin, TOP53, and Tafluposide (Liu *et al.*, 2007).

3.3. Occurrence of deoxypodophyllotoxin in the plant kingdom

Based on the classification of Cronquist (1988), podophyllotoxins (including deoxypodophyllotoxin) can be found in the order Pinales of the Gymnospermae and in the four orders of the Magnoliopsida. In total, there are 13 families distributed over the whole plant kingdom producing podophyllotoxin and related lignans (Koulman, 2003). Presently, at least 35 different plant species are cited in the literature to produce podophyllotoxin (Koulman, 2003). Podophyllotoxin, deoxypodophyllotoxin, and related structural analogues are not only present in Podophyllaceae (Berberidaceae), but also in other families like Juniperaceae (Cupressaceae), Polygalaceae, and Linaceae (Kupchan *et al*., 1965; San Feliciano *et*

al., 1989a,b; Broomhead and Dewick, 1989, 1990a,b; Yu *et al*., 1991; Kuhnt *et al*., 1994; Konuklugil, 1996a,b; Muranaka *et al*., 1998; Petersen and Alfermann, 2001). Another 20 different species have been reported that do not produce podophyllotoxin but only related lignans like certain species of the *Bursera* genus, which produce deoxypodophyllotoxin and α-peltatin-*A*-methylether (Jolad *et al*., 1977; Wickramaratne *et al*., 1995). Also within the plant kingdom, the biosynthesis of podophyllotoxin seems restricted to the vascular plants. There are more lignans with the 2,7'-ring closed like the justicidines, originally isolated from *Justicia procumbens* (Fukamiya and Lee, 1986). These type of arylnaphthalene lignans are also isolated from different *Linum* species (Mohagheghzadeh *et al.*, 2002; Koulman and Konuklugil, 2004), *Haplophyllum patavinum* (Innocenti *et al.*, 2002), *Cleistanthus collinus* (Fukamiya and Lee, 1986) and other *Justicia* species (Rajasekhar *et al.*, 1998; Day *et al.*, 1999; Navarro *et al.*, 2001).

3.4. Distribution of deoxypodophyllotoxin in the plant organs

Although the discovery of podophyllotoxin and deoxypodophyllotoxin dates back to more than a century, not much progress has been made with regard to their chemosystematics and ecology. Currently, the commercial source of podophyllotoxin is the rhizomes and roots of *Podophyllum emodi* Wall., Berberidaceae (syn. *P. hexandrum* Royle), an endangered species from the Himalayas (Bedir *et al.*, 2002). The yield of podophyllotoxin from *P. peltatum* is low (approx. 0.25% based on the dry weight) and the supply of *P. hexandrum* rhizomes, which contain about 4% of podophyllotoxin by dry weight, is becoming increasingly limited due to both intensive collection and lack of cultivation (Choudhary *et al.*, 1998; Rai *et al.*, 2000). Nevertheless, except for the very few sporadic works on the essential oils, podophyllotoxin and occasionally a few of its structural analogues, in small groups of plants or even single plants, there has not been much progress.

There is absolute dearth of information on the distribution of deoxypodophyllotoxin in the plant organs. There is no information on the holistic analyses of the distribution of major phytochemicals like podophyllotoxin and structural analogues between the organic and aqueous phases of the same plant, among different plants of the same species, among different species of the same genus, and among different related genera. It is not clear in how far the continuum and the concentration of podophyllotoxin and related secondary compounds relate to certain genotypes within species, if there are prominent differences of this continuum among different species, and how far the ecological factors manipulate the spectrum of secondary compounds and their *in planta* expression. A major challenge for such comparative studies is to guarantee that identical and reliable methods of secondary compound analyses are employed that ensure comparability of chemical data.

3.5. Pharmacological effects of deoxypodophyllotoxin

In addition to being a potential precursor of the antineoplastic moiety podophyllotoxin, deoxypodophyllotoxin itself is an important lignan that possesses therapeutic efficacy against a plethora of malignancies. Deoxypodophyllotoxin has been shown to demonstrate remarkable anticancer activities against a number of tumor cell lines including A549, SK-OV-3, SK-MEL-2, HCT15, B16F10 and K562 (Kim *et al.*, 2002; Masuda *et al.*, 2002). It is also active against *Herpes simplex* virus (Sudo *et al.*, 1998) and has considerable antiproliferative effects (Ikeda *et al.*, 1998). Furthermore, it has been documented that deoxypodophyllotoxin exhibits antiplatelet aggregation activity (Chen *et al.*, 2000), *in vivo* antiasthmatic activity (Lin *et al.*, 2006), and has a broad spectrum of insecticidal activity (Inamori *et al.*, 1985; Gao *et al.*, 2004). Recently, deoxypodophyllotoxin was reported to be antiallergic because it not only inhibits the passive cutaneous anaphylaxis (PCA) reaction but also has a dual cyclooxygenase (COX)-2 selective/5-lipoxygenase (LOX) inhibitory activity (Lee *et al*., 2004; Lin *et al*., 2004). In addition to this, potential uses of deoxypodophyllotoxin in the treatment of hyperpigmentation caused by UV radiation or by pigmented skin disorders have been reported (Choi *et al.*, 2004).

3.6. Mechanism of action of deoxypodophyllotoxin

Podophyllotoxin and deoxypodophyllotoxin share the same action mechanism based on the core structure of deoxypodophyllotoxin as evidenced by the SAR studies. Deoxypodophyllotoxin, like podophyllotoxin, inhibits the formation of the microtubules, i.e., inhibits the formation of the mitotic spindle, resulting in an arrest of the cell division process in metaphase and clumping of the chromosomes (Imbert, 1998; Canel *et al.*, 2000; Liu *et al.*, 2007). Under *in vitro* conditions, it binds to tubulin dimers giving lignan-tubulin complexes. This stops further formation of the microtubules at one end but does not stop the disassembly at the other end leading to the degradation of the microtubules. This mode of action is comparable to the alkaloid colchicin, and for their mode of action these compounds are called ‘spindle poisons’ (Liu *et al.*, 2007). Other spindle poisons in clinical use are paclitaxel and vincristine-like alkaloids (Koulman, 2003). These cause the cells to enter the mitosis, but the duplicated chromosomes are not separated. In this way, the cells cannot duplicate and growth is stopped. The specific interaction of these compounds with the microtubules’ growth is, however, different as they stop degradation and not assembly (Ayres and Loike, 1990; Stähelin and von Wartburg, 1991). Strikingly, the clinically applied podophyllotoxin-derivatives etoposide, teniposide and etopophos have a completely different mode of action. These compounds are topoisomerase II (Topo 2) inhibitors (Stähblin, 1973; Ayres and Loike, 1990; Hande, 1998; Imbert, 1998; Canel *et al.*, 2000; Liu *et al.*, 2007). A major advantage of the newly introduced etopophos (etoposide phosphate) is the improved solubility in water (Witterland *et al.*, 1996). Etopophos is a pro-drug of etoposide. After

administration, the phosphate group is hydrolyzed in the human body to yield etoposide, which is bioactive (Witterland *et al.*, 1996).

3.7. Biosynthetic pathway of deoxypodophyllotoxin

The biosynthetic pathways of podophyllotoxin, deoxypodophyllotoxin and related lignans are still a matter of debate, although much work has been done on the pharmacological aspects of these lignans. Due to the large number of lignan producing plant species, this research field is scattered rather than concentrated on one model species. Different research groups focus on different species; therefore, it is not clear to which extent there are similarities in the biosynthesis of podophyllotoxin in the different species. Generalized conclusions cannot be drawn yet and it is only possible to speculate about major parts of the podophyllotoxin biosynthesis (Fig. 20). All lignans are ββ-dimers of phenylpropanoid derivatives and are biosynthetically derived from the phenylpropanoid pathway (Canel *et al*., 2000; Koulman, 2003). The sequence leading to formation of (-)-matairesinol, the presumed precursor of podophyllotoxin in *P. hexandrum*, was elucidated using *Forsythia intermedia* as a model system (Davin *et al.*, 1997). In the presence of a one-electron oxidant, e.g. laccase, and a 78 kDa dirigent protein, *E*-coniferyl alcohol is converted into (+)-pinoresinol via regio- and stereoselective intermolecular 8,8'-coupling of the putative enzyme-bound intermediate radical. Sequential stereoselective reduction of (+)-pinoresinol then occurs to consecutively generate (+)-lariciresinol followed by formation of (-)-secoisolariciresinol. The stereoselectivity of this process results in inversion of the configuration at C-2 and C-5 of (+)-pinoresinol, a process that is envisaged to occur either by a concerted S_N2 mechanism or via reduction of an intermediate quinomethane. Stereoselective dehydrogenation of (-)-secoisolariciresinol then occurs to give (-)-matairesinol. The efficient incorporation of (-)-[^{14}C]matairesinol into podophyllotoxin, β-peltatin, 4'-demethylpodophyllotoxin and α-peltatin in *Podophyllum* demonstrates that (-)-matairesinol is probably the common precursor to both groups of the *Podophyllum* lignans (Broomhead *et al.*, 1991). Thus, (-)-matairesinol is presumably converted to yatein or 4'-demethylyatein which are transformed into podophyllotoxin/β-peltatin or 4'-demethylpodophyllotoxin/α-peltatin, respectively, via the appropriate quinomethane intermediates. Furthermore, it was proven for *Podophyllum* that (-)-matairesinol, yatein, and deoxypodophyllotoxin can be converted into podophyllotoxin (Jackson and Dewick, 1984; Kamil and Dewick, 1986). Labeled possible precursors of podophyllotoxin were fed to roots of *P. hexandrum* and the formation of metabolites was monitored. The results demonstrated that *Podophyllum* could convert (-)-matairesinol, yatein and deoxypodophyllotoxin to podophyllotoxin. The oxidized analogue of yatein, anhydropodorhizol, was not converted to podophyllotoxin. Van Uden *et al*. (1995) delivered further evidence for this theory by feeding deoxypodophyllotoxin to *Linum* cells, which resulted in the formation

of 6-methoxypodophyllotoxin and podophyllotoxin. Cell suspension cultures of *Linum flavum* are able to convert large amounts of deoxypodophyllotoxin into the glycoside of 6-methoxypodophyllotoxin (Van Uden *et al.*, 1997). Recently, the metabolic stereoselectivity of recombinant human cytochrome P450 (CYP3A4) towards deoxypodophyllotoxin was predicted *in silco* and experimentally validated (Julsing *et al.*, 2008).

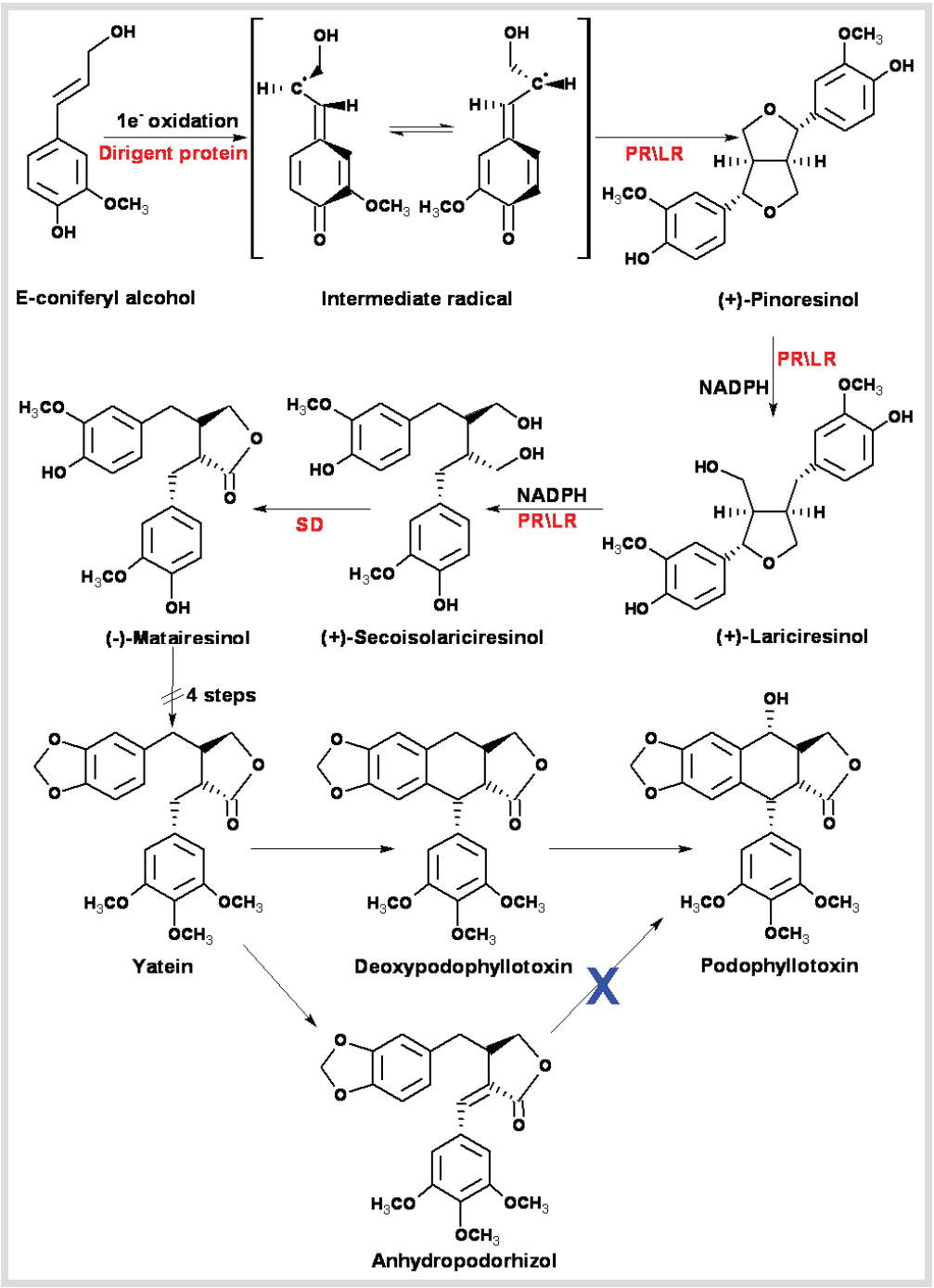

Fig. 20. The proposed biosynthetic pathway of podophyllotoxin and/or deoxypodophyllotoxin. PR\LR, pinoresinol–lariciresinol reductase; SD, secoisolariciresinol dehydrogenase.

3.8. Requirement for alternate sustainable sources of deoxypodophyllotoxin

Podophyllotoxin and deoxypodophyllotoxin are clinically relevant plant compounds serving as the unique starting compounds for the production of two widely used anticancer drugs, etoposide and teniposide, among many other derivatives currently under clinical trials, as detailed above. U.S. sales of etoposide tripled in 1995 and have since risen at an annual rate of more than 10% (Canel *et al.*, 2000). Etoposide is used in combination therapy in refractory testicular, lymphoid and myeloid leukemia, stomach, ovarian, brain, breast, pancreatic, and small and large cell lung cancers (Canel *et al.*, 2000). Even the use of pure podophyllotoxin, in creams (like Wartec®) and gels (Condylox®), is nowadays very common (Koulman, 2003). In addition, numerous new podophyllotoxin derivatives are currently under development and evaluation as topoisomerase inhibitors and potential anticancer drugs. Recently, a Swedish company (Conpharm) started clinical trials with a new podophyllotoxin derived drug CPH82 (Reumacon®) for the treatment of rheumatoid arthritis (Koulman, 2003). Reumacon® is a mixture of two podophyllotoxin glucosides (podophyllotoxin-4,6-*O*-benzylidene-α-D-glucopyranoside, AS 3738; and 4'-demethylpodophyllotoxin-4,6-*O*-benzylidene-α-D-glucopyranoside, AS 3739). However, the major problem is the steady supply of the starting compounds to satisfy the current and projected demands for anticancer drugs. The total synthesis of both podophyllotoxin and deoxypodophyllotoxin is cumbersome on account of the presence of four chiral centers, a rigid *trans*-γ-lactone and an axial 7'-aryl substituent (Gordaliza *et al.*, 2004). The rhizome of *P. peltatum* and *P. hexandrum* plants is also an inefficient source owing to the yields being very low, and further the plants becoming increasingly limited due to both intensive collection and lack of cultivation (Choudhary *et al.*, 1998; Rai *et al.*, 2000). As a result, the species *P. hexandrum* is listed in appendix II of CITES, World Conservation Monitoring Centre. This appendix lists species that are not necessarily now threatened with extinction but that may become so unless trade is closely controlled (Annonymous, 2001). Metabolic engineering approaches have not been feasible since all the enzymes or genes involved in podophyllotoxin biosynthesis are not precisely known. Therefore, an alternative to the synthesis and isolation from natural sources is production by biotechnological techniques starting from deoxypodophyllotoxin. Deoxypodophyllotoxin shares the same fate as podophyllotoxin and is not readily available from commercial sources because of its scarcity from natural sources and cumbersome extraction procedures. Hence, it is desirable to develop alternative sources for the production of the aryl tetralin lignan, deoxypodophyllotoxin, which might be used as a precursor (pro-drug) to develop anticancer drugs and as a substrate for bioconversion studies.

3.9. Alternate sources of deoxypodophyllotoxin

For establishing an alternative, inexhaustible, cost-effective and a renewable resource of the high-value

deoxypodophyllotoxin, fermentation technology (involving a microorganism) appears promising since industrial production requires reproducible and dependable productivity. There are three reported discoveries of podophyllotoxin-producing endophytic fungi: *Phialocephala fortinii* isolated from *P. peltatum* (Eyberger *et al.*, 2006), *Trametes hirsuta* isolated from *P. hexandrum* (Puri *et al.*, 2006), and *Fusarium oxysporum* isolated from *Juniperus recurva* (Kour *et al.*, 2008). However, in all the three cases, there has been no follow-up work on scale-up, and there is no published breakthrough in the commercial exploitation of these endophytic fungi as a source of podophyllotoxin.

CHAPTER 3:
AIMS AND OBJECTIVES

1. Aim

The aim of this study was to isolate, identify, and biologically and biochemically characterize endophytic fungi capable of indigenous production of camptothecin (CPT), hypericin and deoxypodophyllotoxin, harbored in *Camptotheca acuminata*, *Hypericum perforatum* and *Juniperus communis* plants, respectively.

The goals of this thesis are composed of the following steps:

- Sampling of *C. acuminata* plants from different botanical gardens and tissue culture laboratories across Germany as well as from China. For *Hypericum* species, sampling of plants from the natural populations of Slovakia and India. Sampling of *Juniperus* and *Podophyllum* species from the natural populations of India and Germany.
- Extraction of different organs to identify and quantify the important secondary metabolites comprising of CPT, 9-MeO-CPT and 10-OH-CPT (from *C. acuminata*); hypericin, pseudohypericin, emodin, hyperforin, hyperoside, rutin, quercetin, and quercitrin (from *Hypericum*); podophyllotoxin, deoxypodophyllotoxin, demethylpodophyllotoxin, and podophyllotoxone (from *Juniperus* and *Podophyllum*).
- Chemometric evaluation of the infraspecific and infrageneric variability and correlation among the secondary metabolites studied, to understand their distribution in plants based on their biosynthetic pathways and synergistic or antagonistic principles.
- Isolation of endophytic fungi harbored in different organs of all the studied plants.
- Identification and characterization of the endophytic fungi capable of indigenous production (i) of CPT, 9-MeO-CPT and 10-OH-CPT (isolated from *C. acuminata*); (ii) of hypericin and emodin (isolated from *H. perforatum*); and (iii) of deoxypodophyllotoxin (isolated from *J. communis*).
- Investigation of macroscopic and microscopic morphology, biochemical and molecular characterization of the three desired endophytes, as well as evaluating their growth and production kinetics.
- Generation studies of the three desired endophytes over seven successive subcultures for evaluating the *ex planta* secondary metabolite production under *in vitro* axenic conditions.

1.1. Further specific investigation of the CPT producing endophyte

- Investigation of the primary structure of endophyte topoisomerase I emphasizing on the CPT-binding and catalytic domains to understand how the fungus ensures self-resistance before being incapacitated by self and host CPT biosynthesis.
- Investigating the key steps of the CPT biosynthetic pathway in the endophyte and its host to elucidate the cross-species mutualistic biosynthesis shared by them.
- Deciphering the cause of *ex planta* impaired CPT biosynthesis in the endophytic fungus over successive subculture generations.
- Investigating the fate of the endophyte after artificially inoculating it in *C. acuminata* host plants followed by recovery after successful colonization to understand the consequence on its morphology and impaired CPT biosynthetic capability.

1.2. Further specific investigation of the hypericin producing endophyte

- Investigation of the growth and production kinetics of the endophyte in the presence and absence of light to evaluate the effect of illumination on fungal hypericin biosynthesis.
- Investigating the effect of spiking media with emodin (the proposed precursor of hypericin in plants) on the production of hypericin and its own accumulation in light and under light protection, and the effect of growth on production and vice versa.
- Investigating the cytotoxic and photodynamic effects of fungal hypericin and emodin on human acute monocytic leukemia cells (THP-1).
- Investigating whether the candidate *hyp-1* gene, suggested encoding for the coupling protein as the key enzyme in the biosynthesis of hypericin in *H. perforatum* cell cultures, is present and/or expressed in the endophyte as well.

1.3. Further specific investigation of the deoxypodophyllotoxin producing endophyte

- Investigation of the *in vitro* antimicrobial effects of fungal deoxypodophyllotoxin on a panel of pathogenic bacterial strains.

CHAPTER 4:
MATERIALS AND METHODS

1. Reference standards

CPT was purchased from Sigma-Aldrich Chemie GmbH (Steinheim, Germany) and 10-hydroxycamptothecin (10-OH-CPT) from LKT Laboratories Inc. (St. Paul, MN). Unfortunately, 9-methoxycamptothecin (9-MeO-CPT) is not available commercially. Hence, 9-MeO-CPT was first isolated and established as an authentic standard from *N. nimmoniana* plant using preparative HPLC, LC-HRMS^3, and ^{1}H NMR spectroscopy.

Hypericin (≥95% purity) was purchased from Sigma-Aldrich Chemie GmbH (Steinheim, Germany), pseudohypericin (≥95% purity) from Calbiochem (Darmstadt, Germany), emodin (≥99% purity) from AppliChem GmbH (Darmstadt, Germany), hyperforin (≥90% purity) from Cayman Chemical (Michigan, U.S.A.), hyperoside (≥97% purity) from Merck (Darmstadt, Germany), rutin (≥97% purity) from Acros Organics BVBA (Geel, Belgium), quercetin (≥98% purity) from ABCR GmbH & Co. KG (Karlsruhe, Germany), and quercitrin (≥85% purity) from Sigma-Aldrich Chemie GmbH (Steinheim, Germany).

Podophyllotoxin was purchased from Sigma-Aldrich Chemie GmbH (Steinheim, Germany). The reference standard demethylpodophyllotoxin was a kind gift from Dr. S. C. Puri [formerly at the Indian Institute of Integrative Medicine (IIIM), Canal Road, Jammu, India] which was authenticated by multi-component high-resolution tandem mass spectrometry (LC-ESI-HRMS^n) and comparing with the literature data (Wong *et al.*, 2000).

All the standard solutions were stored in the dark at -20°C.

2. Camptothecin (CPT)

2.1. Plant sampling and phytochemical profiling of host plants

2.1.1. Collection, identification and authentication of plant material

Living plants and fresh aerial plant parts were collected from different botanical gardens and tissue culture laboratories across Germany. Table 1 contains data concerning the identity of *Camptotheca* species under study, names/sites of sampling, and the plant codes used. All plant specimens have been identified, authenticated, and are currently maintained (live plants) at the respective collection centers. Therefore, it was not necessary to deposit the plants collected from Germany separately in any depository. Furthermore, fresh aerial parts from a fully matured *C. acuminata* tree were collected (August 2007) from the Southwest Forestry University (SWFU) campus, Kunming, Yunnan Province, People's Republic of China. This specimen is presently being maintained at the Southwest Forestry University, and therefore, additional deposition of plant material was not required.

Table 1. Plant codes and sampling points of *C. acuminata* plants.

Taxon	Plant Code	Obtained from
Camptotheca acuminata	INFU/Ca	Southwest Forestry University (SWFU) campus, Kunming, Yunnan Province, People's Republic of China
Camptotheca acuminata	Lp4	Universität Hamburg, Biozentrum Klein Flottbek und Botanischer Garten, Hamburg
Camptotheca acuminata	Mp36	Universität Hamburg, Biozentrum Klein Flottbek und Botanischer Garten, Hamburg
Camptotheca acuminata	Bp81	Universität Hamburg, Biozentrum Klein Flottbek und Botanischer Garten, Hamburg
Camptotheca acuminata	Bp81seed	Universität Hamburg, Biozentrum Klein Flottbek und Botanischer Garten, Hamburg
Camptotheca acuminata	Fre	Botanischer Garten der Albert-Ludwigs-Universität, Freiburg
Camptotheca acuminata	Stu	Botanischer Garten der Universität Hohenheim, Stuttgart
Camptotheca acuminata	Bay	Ökologisch-Botanischer Garten der Universität Bayreuth, Bayreuth
Camptotheca acuminata	Mai	Botanischer Garten der Johannes Gutenberg-Universität, Mainz
Camptotheca acuminata	Ham	Universität Hamburg, Biozentrum Klein Flottbek und Botanischer Garten, Hamburg
Camptotheca acuminata	Hal	Botanischer Garten der Martin-Luther-Universität, Halle

2.1.2. Preparation of plant extracts

C. acuminata plants were cut into aerial parts viz. stems and leaves, in two sets in parallel in each case (Fig. 21). One set was used fresh for extraction and the other set was completely air-dried in the oven at 25°C. The fresh and dried plant materials, respectively, were ground to dust under liquid nitrogen. Then, 5.0 g of the dust for each plant part was extracted independently with 50 mL MeOH:$CHCl_3$ (80:20) by ultra-sonication in chilled conditions (ice-bath aided, ≤4°C) using a Branson B-12 apparatus (Danbury, Connecticut) operating at 20 kHz and 60 W for 20 min. The final solution was filtered using Whatman filter paper under vacuum. The filtrate was used as the final organic extract. The residue was extracted with 50 mL H_2O:MeOH (90:10) by ultra-sonication for 20 min using the same procedure. The sonicated solution was filtered again using Whatman filter paper under vacuum. The filtrate was used as the final aqueous extract. The final residue (if any) was discarded. The final extracts were concentrated to dryness by rotary evaporation in vacuum at 30°C, reconstituted in 1 mL analytical grade MeOH, and then stored in the dark at -20°C till the commencement of the analyses by LC-ESI-HRMS/MS.

2.1.3. Determination of metabolite contents

CPT, 9-MeO-CPT, and 10-OH-CPT were identified by LC-HRMS and LC-$HRMS^3$ fragment spectra

(LTQ-Orbitrap spectrometer, Thermo Scientific), which were consistent with the reference standards, and quantified using TSQ Quantum Ultra AM mass spectrometer (Thermo Finnigan, U.S.A.) equipped with an ESI ion source (Ion Max). The mass spectrometer was equipped with a Dionex HPLC system Ultimate 3000 consisting of pump, flow manager, and autosampler (injection volume 0.6 µL). Nitrogen was used as sheath gas (6 arbitrary units), and helium served as the collision gas. The separations were performed by using a Phenomenex Gemini C_{18} column (3 µm, 0.3 × 150 mm) (Torrance, CA) with a H_2O (+ 0.1% HCOOH) (A)/acetonitrile (+ 0.1% HCOOH) (B) gradient (flow rate 4 µL min^{-1}). Samples were analyzed by using a gradient program as follows: 95% A isocratic for 5 min, linear gradient to 60% A within 12 min, and to 100% B in 29 min. After 100% B isocratic for 5 min, the system returned to its initial condition (95% A) within 1 min and was equilibrated for 7 min. The spectrometer was operated in positive mode (1 spectrum s^{-1}; mass range: 200-800) with nominal mass resolving power of 60000 at *m/z* 400 with a scan rate of 1 Hz, with automatic gain control to provide high-accuracy mass measurements within 2 ppm deviation using one internal lock mass; *m/z* 391.284286; bis-(2-ethylhexyl)-phthalate. MS^2 led to the corresponding CO_2 loss of the precursor (CID of 45). The final MS^3 measurement was performed under CID of 45 and resulted in characteristic fragments of the compounds.

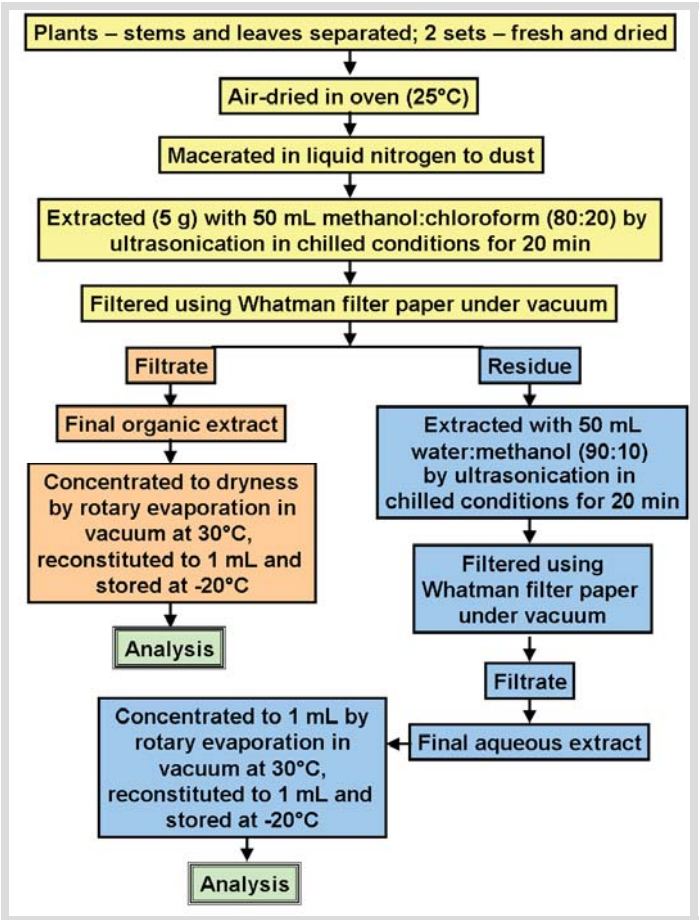

Fig. 21. The scheme for the extraction of the plant materials.

2.1.4. Data analysis

The LC-MS/MS data were subjected to a number of different chemometric evaluations for metabolite profiling and correlating the phytochemical loads among the various *Camptotheca* plants (infraspecific), among the organic and aqueous phases, and among the different aerial tissues (dry and fresh in parallel) to reflect the metabolomic profiles of the studied plants. The analyses included multivariate analysis (MVA), Kruskal's multidimensional scaling (MDS), principal component analysis (PCA), linear discriminant analysis (LDA), and hierarchical agglomerative cluster analysis (HACA). All analyses were performed using the statistical software XLSTAT-Pro version 2009.1.02 (Addinsoft, NY, U.S.A.), except for MVA which was performed using the statistical software QI Macros version 2008.11 (KnowWare International Inc., CO, U.S.A.). Both the statistical software packages were used in combination with Microsoft Excel 2003 version SP3-11.8237.8221 (part of Microsoft Office Professional 2003, Microsoft Corporation, U.S.A.). For the purpose of statistical precision and ease of evaluation, all values lesser than the limit of quantitation (<LOQ) were considered as null.

2.1.4.1. Multivariate analysis (MVA)

MVA (QI Macros) was performed allowing the evaluation of the phytochemical variability due to differences between categories (ordination), namely the different plant species, genera, as well as the organic and aqueous extracts. Furthermore, the total phytochemical load (total metabolite continuum) for each category was evaluated by calculating the individual average. The MVA chart depicted the high and low values as well as each data point in each category. The spread provided the idea of the variation for each category relative to the other categories. Additionally, it depicted the data load (holistic phytochemical load) for each category relative to the others by calculating the individual average for each category.

2.1.4.2. Multidimensional scaling (MDS)

In order to scrutinize the relationships between the metabolite contents among the investigated *C. acuminata* plants, MDS analysis using Kruskal's algorithm based on Pearson correlation coefficiency (Kruskal-type MDS, or Kruskal's MDS), was performed (Kruskal, 1964). The method was performed in a 3-dimensional (3D) mode to develop a 3D map of the series of phytochemicals under study from a proximities matrix (by dissimilarities) between the categories. Furthermore, a 3D surface analysis was executed using the 3D distance in space between the phytochemicals to construct the exact map of the phytochemical relativity within about the given symmetry of the 3 axes in 3 different dimensions. To achieve an optimal representation of the data points in 3D, a criterion called the 'Kruskal's stress' was evaluated (closer the stress to 0, the better and accurate the representation). The Shepard diagram

gave an idea about the quality of the representation. It corresponded to a scatter plot, where the abscissa was the observed dissimilarities, and the ordinates, the distance on the configuration generated by the MDS. The further the points were spread, the lesser the MDS map was reliable. The reliability of the chart was evaluated on whether the ranking of the abscissa was respected on the ordinates (i.e., reliable), or the points were on the same line (i.e., ideal quality).

2.1.4.3. Principal component analysis (PCA)

A 2-dimensional (2D) visualization of the arrangement of the metabolites relative to each other was generated by depicting the values of the principal components (metabolites under study) relative to the species. This was accomplished by running the PCA using the numerical data structured in *M* observations versus *N* variables (quantity of each phytochemical under study for each sample). Thereafter, the analyzed *M* observations (initially described by the *N* variables) were visualized on a scaled-down dimensional map (i.e., in 2D) to obtain the optimal view for each variability criterion. However, in order to assess the quality of the projection from the multi-dimensional primary table to a lower-dimension (2D), the 2D chart was related to a mathematical object called the 'eigenvalue'. Each eigenvalue corresponded to a factor (linear combination of the initial variables, each un-correlated with the other, i.e., the Pearson correlation coefficient, r = 0), and each factor to a dimension. The eigenvalues and the corresponding factors were sorted out by descending order of how much of the initial variability they represented (converted to %). This was achieved by plotting the 'Scree Plot' using the variability in the useful dimensions versus the cumulative variability, relative to the eigenvalues. Since the final PCA was depicted in a 2D spacing, the cumulative variability for the first two factors of the Scree Plot was the reliability factor for the analysis. The PCA was represented in the form of a Correlation Circle (on two factors) depicting the projection of the variables in the 2D space. When two variables were far from the center but close to each other, they were significantly positively correlated (i.e., r tends to 1). If two variables were orthogonal, they were not correlated (i.e., r tends to 0). However, if two variables were on the opposite side of the center, then they were significantly negatively correlated (i.e., r tends to -1). In all tests, the significance level at which the critical values were assessed, differences were 5% (i.e., $\alpha \leq 0.05$).

2.1.4.4. Linear discriminant analysis (LDA)

In order to establish the statistical correlations among different plant samples under study (different species as well as the same species from different locations), LDA based on the classification method originally developed by Fisher (1936), was computed. Individually, *Camptotheca* was used as the training and test set, respectively; which depended on a variable *X*. The variable *X* was the

phytochemical load on the individual species as evaluated by LC-MS/MS. The objective was to test if (and how) the four phytochemicals under study allowed to discriminate the species, and to visualize the observations on a 2D map that depicted how separated the groups were in a precise manner.

2.1.4.5. Hierarchical agglomerative cluster analysis (HACA)

The LC-MS/MS data were statistically processed using HACA by average linkage. Dissimilarity was measured by Euclidean distance using data of all four standard constituents under study, as well as for the different plant samples. This permitted the assignment of the compounds measured into groups of high correlation, and for assembling the plant species into similar groups based on their metabolic profiles. The results were visualized by dendrograms.

2.2. Biological characterization of CPT producing endophytic fungus

2.2.1. Isolation and establishment of *in vitro* culture of CPT producing endophytic fungus

Explants was carefully excised from the host (Fig. 22), collected in clean, dry, plastic bags, and processed within 48 h of collection. The explants were washed thoroughly in running tap water followed by deionized (DI) water to remove any dirt sticking to them and stored at 4°C until the isolation procedure. Surface-sterilization of the explants was done following the previously established methods (Lodge *et al*., 1996; Strobel *et al*., 2004; Puri *et al*., 2005), suitably modified. The explants were thoroughly washed in running tap water, and small fragments of approximately 10 mm (length) by 5 mm (breadth) were cut with the aid of a flame-sterilized razor blade. Then, the small fragments were surface-sterilized by sequential immersion in 70% ethanol for 1 min, 1.3 M sodium hypochlorite (3-5% available chlorine) for 3 min, and 70% ethanol for 30 s. Finally, these surface-sterilized explant pieces were rinsed three times in sterile, double-distilled water for 1 min each, to remove excess surface sterilants. The excess moisture was blotted on a sterile filter paper. Surface-sterilized explant fragments, thus obtained, were evenly spaced in Petri dishes (TPP, Trasadingen, Switzerland) containing water agar (WA) medium (DIFCO, cat. no. 214530) amended with streptomycin (100 mg L^{-1}) to eliminate any bacterial growth. Petri dishes were sealed using Parafilm (Pechiney, Chicago, IL) and incubated at 28 ± 2°C in an incubator until fungal growth started. To ensure proper surface-sterilization, unsterilized explants were prepared simultaneously and incubated under the same conditions in parallel, to isolate the surface-contaminating fungi. The cultures were monitored every day to check the growth of endophytic fungal colonies from the sample segments. The hyphal tips, which grew out from

sample segments over 4-6 weeks, were isolated and subcultured onto a rich mycological medium, Sabouraud dextrose agar (SA) medium (DIFCO, cat. no. 210950), and brought into pure culture.

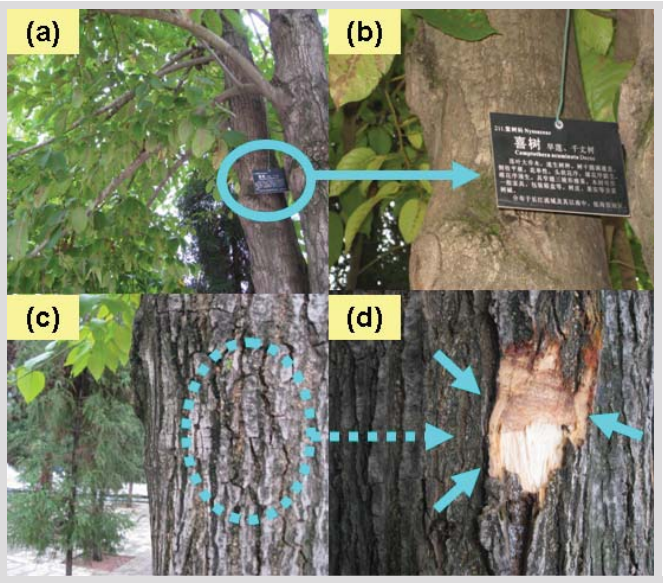

Fig. 22. *C. acuminata* plant from which the CPT producing endophytic fungus, INFU/Ca/KF/3, was isolated. (a,b) The plant is maintained at the Southwest Forestry University (SWFU) campus, Kunming, Yunnan Province, People's Republic of China. (c,d) The position on the trunk from where the inner bark was explanted for the isolation of the endophytes.

2.2.2. Maintenance and storage of the endophytic isolate

The CPT-lacking (reference) and CPT-producing axenic endophytic fungal isolates, obtained above, were coded as INFU/Ca/KF/2 and INFU/Ca/KF/3, respectively, and preserved by lyophilization, as well as by cryopreservation at -70°C in the microbial library of our institute. The endophytic fungus capable of producing CPT and two structural analogues (INFU/Ca/KF/3) has been deposited at the German Collection of Microorganisms and Cell Cultures (*Deutsche Sammlung von Mikroorganismen und Zellkulturen GmbH*, DSMZ), Braunschweig, Germany (accession number DSM 21921).

2.2.3. Identification of the endophytic isolate

The endophytic fungi were grown on SA for 5 days at 28 ± 2°C. In each case, the mycelium was scraped directly from the surface of the agar culture (5 days old) and weighed. Nucleic acid was extracted and purified using the AppliChem DNA isolation kit for genomic DNA (AppliChem GmbH, Darmstadt, Germany) using the Chomczynski method (Chomczynski and Sacchi, 1987), suitably modified. For identification and differentiation, the Internal Transcript Spacer regions (ITS1 and ITS2) and the intervening 5.8S rRNA region were amplified and sequenced (White *et al.*, 1990) using electrophoretic sequencing on an ABI 3730xl DNA analyzer (Applied Biosystems, Foster City, CA) using BigDye Terminator v 3.1 cycle sequencing kit. The ITS regions of each fungus were amplified using PCR (PeqStar thermocycler, PeqLab GmbH, Erlangen, Germany) and the universal ITS primers, ITS1 (5´-TCC GTA GGT GAA CCT GCG G-3´) and ITS4 (5´-TCC TCC GCT TAT TGA TAT GC-3´).

The PCR products were purified and desalted using the Chargeswitch purification kit (Invitrogen, Carlsbad, CA) and then sequenced. The sequences were aligned and prepared with the software DNAstar Lasergene SeqMan (Madison, WI) and matched against the nucleotide-nucleotide database (BLASTn) of the U.S. National Center for Biotechnology Information (NCBI) for final identification of the endophytic isolates. The ITS-5.8S rDNA sequences obtained have been deposited at the EMBL-Bank (European Molecular Biology Laboratory) under the accession numbers FN667579 (for INFU/Ca/KF/2) and FM179605 (for INFU/Ca/KF/3).

2.2.4. Morphological studies of the endophytic fungus

The endophytic fungus, INFU/Ca/KF/3, growing on potato dextrose agar (PDA; DIFCO cat. no. 213400), SA and Czapek-Dox agar (CDA; Merck, cat. no. 1.05460) was examined after 2, 3, 4, 5, and 10 days to study the macroscopic morphology. Shake-flask fermentations were performed in Sabouraud dextrose broth (SB; DIFCO, cat. no. 238230) at 28 ± 2°C with shaking (200 rev min^{-1}) to study the macroscopic morphology under submerged broth culture conditions. Hyphae on the agar plate were aseptically transferred to slides for microscopy. A Leica DM-R light microscope (Leica Microsystems GmbH, Wetzlar, Germany) was used to examine the microscopic features of the fungus.

2.2.5. Establishment of CPT production as a function of time

The endophyte was cultured in SB consisting of dextrose (2%) as the sole carbon source and enzymatic digest of casein (1%) as the sole nitrogen source. A set of 10 conical flasks of 500 mL capacity was used, each with four indentations and containing 100 mL SB, adjusted to pH 5.6 before autoclaving. The fungus was inoculated into each flask from the parent axenic culture. These flasks were incubated at 28 ± 2°C with shaking (200 rev min^{-1}) on a rotary shaker (Heidolph UNIMAX 2010, Germany). Each flask represented one time point of fermentation termination followed by extraction and analysis for the determination of production of CPT, 9-MeO-CPT and 10-OH-CPT. The first sample was taken after 2 h of inoculation (0 h) and subsequently the other samples were taken after every 24 h, up to 216 h. Three replicates of each experiment set were considered to get reproducible data.

2.2.6. Preparation of cell-free extract

Shake-flask fermentations were performed with the fungus under specific conditions as detailed above, and the special morphological features under the submerged culture conditions were noted. The cell-free extract was prepared by filtering the incubated culture through muslin cloth under vacuum. The mycelia and spent broth were treated separately. The mycelial pellet was dried in an oven (25°C) to obtain the dry weight and was resuspended in deionized water (DI). This suspension was then

sonicated in an ultrasonicator operating at 20 kHz and 60 W under chilled conditions (ice-bath aided, ≤4°C) for 20 min. The milky fluid, thus obtained, was extracted three times with 50 mL of $CHCl_3$:MeOH (4:1, *v/v*). The organic solvent was removed after each extraction by rotary evaporation under vacuum at 30°C, yielding the organic extract. The spent broth (100 mL) was extracted directly in the same way. To ensure the production of 9-MeO-CPT by the cultured endophyte, extractions were performed with $CHCl_3$:CD_3OD (4:1, *v/v*) in a similar fashion in parallel and analyzed.

2.3. Biochemical characterization of CPT producing endophytic fungus

2.3.1. Structural elucidation and quantification of CPT, 9-MeO-CPT, and 10-OH-CPT

CPT, 9-MeO-CPT, and 10-OH-CPT were identified by LC-HRMS and LC-$HRMS^3$ fragment spectra (LTQ-Orbitrap spectrometer), and quantified using TSQ Quantum Ultra AM mass spectrometer (Thermo Finnigan, U.S.A.) equipped with an ESI ion source (Ion Max), similar to what was performed for the plant extracts (*vide supra*). The ^1H NMR measurements for 9-MeO-CPT and 10-methoxycamptothecin (10-MeO-CPT) were made at 298 K with a Bruker DRX-400 spectrometer using 5 mm tubes with $CDCl_3$ (Merck, Darmstadt, Germany) as solvent.

2.3.2. Generation studies on the endophytic isolate

The established axenic isolate INFU/Ca/KF/3 was subcultured from the first generation using the 'hyphal-tip method' to obtain the second-generation isolate. Subsequent subcultures were made in a similar way to obtain up to the seventh generation of the endophytic isolate. Shake-flask fermentations were performed with the isolates for each generation, and the extraction and metabolite analysis were performed using the methods detailed above. Three replicates of each experiment set were taken to get reproducible data. The results were statistically analyzed using the Box and Whisker's plot method. Attempts were made to optimize the fermentation conditions by using various compositions of different basic liquid media, liquid media supplemented with different carbon and nitrogen sources, and with trace minerals, monotonic carbon-only media, monotonic nitrogen-only media, basic liquid media supplemented with some putative precursors without and with additional supplements, and basic liquid media spiked with various forms of surface-sterilized host intact tissues and tissue aqueous extracts (Table T1, in Appendix A).

2.3.3. Screening, characterization and modeling of topoisomerase I (*Top1*)

Top1 cDNA fragments from *C. acuminata* and CPT producing and lacking endophytes were amplified

by RT-PCR (reverse transcriptase-polymerase chain reaction) with degenerate primers. The template for RT-PCR (cDNA) was prepared by reverse transcription of total RNA with 200 U M-MLV reverse transcriptase (Promega, Madison, WI) and 10 mM anchored oligoT primer at 42°C. The RNA from the plant and the endophytes were isolated by RNeasy-Plant Mini Kit (Qiagen, Valencia, CA). The PCR primers (Table 2) were designed using the GenTool Lite 1.0 software based on the nucleotide sequence alignment (ClustalX 2.0) of *Top1* coding sequences from *C. acuminata* (AB372511), *F. culmorum* (FJ938238), and hypothetical protein from *G. zeae* (XM_387050).

Table 2. The various degenerate and/or gene-specific primers employed for the present study.

Primer name	Primer sequence	Target gene	Target protein
TOP1-F4	5'-GGGTAGAAAGGAGAAGGTCGGCAAC-3'	*Top1*	Topoisomerase I
TOP1-R4	5'-CGTTGTCTTGGGTGCCTTTTTGA-3'	*Top1*	Topoisomerase I
TOP1-F5	5'-TGTCGACGYYCAGGTKTTCAAGA-3'	*Top1*	Topoisomerase I
TOP1-R5	5'-GCCTTGCGCTTTTCGTTGTCCKY-3'	*Top1*	Topoisomerase I
TOP1-R6	5'-ATCGCCCATCGGAACTTGTYWM-3'	*Top1*	Topoisomerase I
SLS-F1	5'-TGGGCATGGTTTACTCCTAA-3'	*SLS*	Secologanin synthase
SLS-R1	5'-AGGAATTCCTACCGTAAGTATTGAT-3'	*SLS*	Secologanin synthase
G10H-F1	5'-TGGGCAATGTCAGAAATGCTTAAA-3'	*G10H*	Geraniol 10-hydroxylase
G10H-R1	5'-ACCGAACGGAATCAGCTCGAAAT-3'	*G10H*	Geraniol 10-hydroxylase
TDC-F1	5'-TACGGCTCTGATCARACTCAT-3'	*TDC*	Tryptophan decarboxylase
TDC-R1	5'-TGGACTMAGACTCARTGAGTCA-3'	*TDC*	Tryptophan decarboxylase
STR-F1	5'-CCATTGTGTGGGAGGACATATGA-3'	*STR*	Strictosidine synthase
STR-R1	5'-TGGCCCTTCTAGCCAATACTT-3'	*STR*	Strictosidine synthase
STR-F2	5'-GTCCCGAAGGTGTGGAAGAAA-3'	*STR*	Strictosidine synthase
STR-R2	5'-TGGCCATCAGAATTCCTCTTT-3'	*STR*	Strictosidine synthase

Several sets of PCR primers were constructed to cover the whole functional and direct/indirect CPT-binding domains of *Top1*. The desired products were amplified by touchdown style RT-PCRs. PCRs were performed in 30 µL reaction volume [0.5 µM forward and reverse primer; 1x iQ Supermix (Biorad, Hercules, CA) containing 0.2 mM dNTPs; 3 mM $MgCl_2$, and 0.7 U hot start iTaq DNA polymerase; and 30-50 ng reverse transcribed RNA/cDNA]. The reaction conditions were: 4 min at 95°C, 30 cycles (30 s at 94°C, 30 s at 69°C decreased by 0.4°C per cycle, 45 s at 72°C), 20 cycles (30 s at 94°C, 30 s at 54°C, 50 s at 72°C), and 4 min at 74°C. The sizes of the amplified products were checked by electrophoresis in 2% agarose TAE gel stained with GoldView (0.005% *v/v*, SBS, Beijing, China). The amplified products were purified by Wizard, SV Gel and PCR Clean-Up System (Promega, Madison, WI) and directly sequenced with the forward and reverse primer. Overlapping fragments of *Top1* were assembled and aligned with available *Top1*s. Based on the ORF (open reading frame) alignments, the

acquired sequences were interpreted and putative amino acid sequences were deduced (numbered according to human Topo 1) and compared with the coding amino acid sequences from different plants and fungi. The sequences obtained have been deposited at the EMBL-Bank under the accession numbers FN669774 (for INFU/Ca/KF/3) and FN669775 (for INFU/Ca/KF/2). The three-dimensional model structure of Topo 1 of endophytic *F. solani* was constructed with MODELLER (Sali and Blundell, 1993), using the published human Topo 1-DNA-topotecan complex (Protein Data Bank entry 1RRJ) as the template (Chrencik *et al.*, 2004). Structure alignment figure was prepared with RasMol 2.7.5 (www.rasmol.org).

2.3.4. Detection, screening, amplification and characterization of CPT biosynthetic genes

The endophytic fungus (first and the seventh generation in parallel, viz. INFU/Ca/KF/3/I and INFU/Ca/KF/3/VII) was grown on SA for 5 days at 28 ± 2°C; then the mycelia were scraped directly from the agar-surface, weighed, and the total genomic DNA (gDNA) was then isolated and purified using the Macherey Nagel NucleoSpin Plant II Maxi Genomic DNA extraction kit strictly following the manufacturer's guidelines (Anonymous, 2008). Fresh *C. acuminata* bark tissue (5 g) that did not contain INFU/Ca/KF/3, INFU/Ca/KF/2, or other CPT producing endophytes was used for isolating plant gDNA. Here, an additional purification step was performed for plant gDNA in order to completely eliminate any contaminants and interfering agents, by precipitation of 2 × 500 µL DNA solution with 2% (*v/v*) isopropanol, then pooling, followed by Q-sepharose cation purification, and final clean-up and concentration with a QIAGEN MinElute purification kit (QIAGEN, Hilden, Germany) to a final volume of 12 µL. The purified DNA template qualities were evaluated by NanoDrop Micro-Volume UV-Vis spectrophotometer. Amplification of *G10H*, *SLS*, *TDC* and *STR* genes from the endophytic fungal gDNAs (two clones in parallel each from the different generations) as well as from the plant gDNAs (duplicates) was attempted using the gene-specific and/or degenerate primers designed for each gene by aligning the nucleotide sequences (Clustal 2.0) of the respective genes reported so far and choosing the maximum conserved regions of these sequences (Table 2). The PCRs were performed in triplicates by optimizing the conditions in each case based on the template used and the target product as detailed in Table T2, in Appendix A. The PCR products were purified and desalted using the Chargeswitch purification kit and sequenced (bi-directional, at least 2x coverage) on an ABI 3730xl DNA analyzer. The final base sequences were established by base calling (noting the data quality and confidence for each base) and trimming with the Phred 0.020425c software. The final sequences were subjected to six-frame translation and interpreted on the basis of the ORFs to obtain the putative amino acid sequences of the expected products. The final product alignments were performed by the

EMBOSS-WATER bioinformatics tool based on the Smith-Waterman local alignment algorithm (Smith and Waterman, 1981) and the EMBOSS-NEEDLE bioinformatics tool based on the Needleman-Wunsch global alignment algorithm (Needleman and Wunsch, 1970), respectively, using the Blosum62 matrix (EMBL). The sequences of all the products have been deposited at the EMBL-Bank under the accession numbers FN582355-FN582360 (*G10H*, *SLS*, *TDC*), and FN667580-FN667581 (*STR*).

2.3.5. High-precision isotope-ratio mass spectrometry (HP-IRMS)

CPT biosynthesized by the cultured endophyte (first generation, INFU/Ca/KF/3/I) outside the host plant and that from the tissues of original host plant (*C. acuminata*, from SWFU), respectively, were the samples that were analyzed by HP-IRMS. The fungal CPT was obtained by shake-flask fermentation in nitrogen-free potato dextrose broth (PDB; DIFCO cat. no. 254920), followed by extraction and analysis as detailed above. The host plant CPT was extracted from the tissue that did not contain INFU/Ca/KF/3, INFU/Ca/KF/2, or other CPT-producing endophytes, and pure CPT was isolated by preparative HPLC and identified by LC-ESI-HRMS^n. The samples were readied for HP-IRMS in each case by placing 0.5 mg CPT in 3.5 × 5 mm tin capsules (HEKAtech GmbH, Germany), lyophilizing completely and finally rolling the capsules into small spheres. The HP-IRMS measurements were performed by suitable modifications of established methods (Kennedy and Krouse, 1990; Preston, 1992; Handley and Raven, 2000; Apostol *et al*., 2001; Blessing *et al*., 2009). The HP-IRMS measurements were performed in compound-specific carbon isotope (CSCI) and compound-specific nitrogen isotope (CSNI) modules, using a FlashEA 1112 elemental analyzer (Thermo Fisher, Italy) coupled to a DELTA V Plus isotope-ratio mass spectrometer (Thermo Fisher, Bremen, Germany) interfaced through a ConFlo IV universal continuous flow interface (Thermo Fisher, Bremen, Germany). The combustion furnace (oxidation reactor) was maintained at 1020°C, and flash combustion was initiated by injecting a pulse of O_2 at the time of sample drop. Helium was used as the carrier with a flow rate of 120 mL min^{-1}. NO_x species were reduced to N_2 in a reduction furnace at 680°C. Water was removed by phosphorus pentoxide in a water trap and CO_2 was separated from N_2 using a Porapak-packed N_2/CO_2-separation column (3 m × 6.5 mm, Thermo Electron S. p. A.) operated isothermally at 85°C. Each sample was analyzed in quadruplet. Acetanilide (Fisons Instruments) was used as the reference standard.

2.3.6. Preparative HPLC and LC-ESI-HRMS^n for isolation of pure CPT from *C. acuminata*

For isolation of pure CPT, gradient separation was performed using a Gilson preparative HPLC system (Middleton, U.S.A.) with a model 322 pump, a model 152 UV/VIS detector (288 nm), a model 204 fraction collector (collection of CPT peak at t_R 18.5 min) and the Gilson-Unipoint software. Compounds

were separated at a flow rate of 4 mL min^{-1} on a C_{18} column (Alltima, 5µ, 10 × 250 mm) using Millipore water (solvent A) - distilled methanol (solvent B) gradient: 70% A isocratic for 2 min, linear gradient to 100% B within 25 min. After 100% B for 9 min, the system was returned to its initial conditions within 1 min and held for 6 min. Purity of the fraction collected was checked by multi-component high-resolution tandem mass spectrometry (LC-ESI-$HRMS^n$) as detailed above.

2.3.7. *In vitro* inoculation of *F. solani* in living *C. acuminata* and its recovery after colonization

Endophytic fungi were isolated from the aerial parts (leaves and stems) of the above plants with special emphasis on whether they contained the same endophyte under study (*F. solani* INFU/Ca/KF/3) and whether any of the endophytes isolated was capable of biosynthesizing CPT or structural analogues. Only those plants were selected as suitable target hosts where INFU/Ca/KF/3 was not one of the endophytes and which did not produce CPT or structural analogues. Finally, using the rationale that the associated co-existing endophytes might pose additional antagonistic selection pressure to dictate the existence and *in planta* metabolomics of INFU/Ca/KF/3 after its artificial colonization post-inoculation in the target hosts, the *in vitro* antagonism of each isolated endophyte was evaluated with INFU/Ca/KF/3 and with each other, and also between that of INFU/Ca/KF/3 and INFU/Ca/KF/2 (Fig. 23). Only those plants were considered as potential target hosts for the artificial fungal inoculation, which did not possess any *in vitro* antagonistic association with each other and with endophytic *F. solani* INFU/Ca/KF/3.

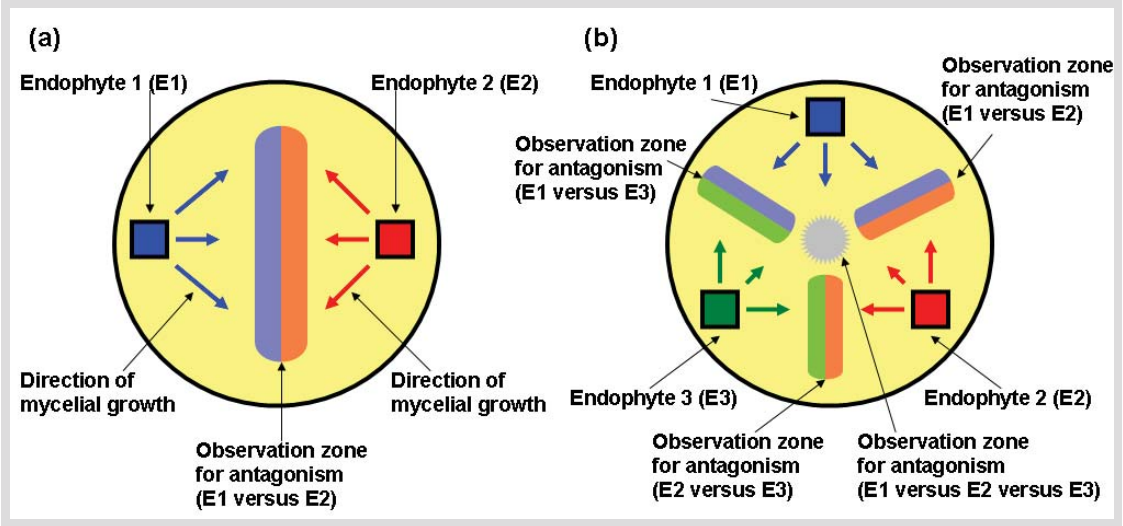

Fig. 23. The *in vitro* agar-plate based antagonism study between the various endophytic fungi. (a) The schematic representation of the inoculation zones, directions of growth and zone(s) for observation of the *in vitro* antagonism between two endophytes. (b) The schematic representation of the inoculation zones, directions of growth and zone(s) for observation of the *in vitro* antagonism between three endophytes simultaneously.

The seventh generation of endophytic *F. solani* (INFU/Ca/KF/3/VII), with its CPT biosynthetic potential impaired, was used to inoculate the selected target *C. acuminata* host plants using previously reported methodology (Strobel *et al.*, 2007), suitably modified. The plants were first acclimatized in the controlled laboratory conditions at the site of the infection studies for a few weeks, by planting them in medium-sized pots containing high-value fertile potting soil (Floragard Vertriebs GmbH, Germany) with very specific physicochemical properties (Table 3) and maintaining them in a moderate-humidity chamber with natural light.

Table 3. The physicochemical properties of the soil employed in the present study.
Basic properties: Mixture of slightly- and well-decomposed raised bog peat (white and black), green compost, flax fibers, organic compound fertilizer, lime, and with balanced NPK. Complies with the directives issued by the international authorities for organic-biological and biodynamic agriculture. Deviation according to the quality parameters established by the *Gütegemeinschaft Substrate für Pflanzen e.V.* (Quality Assurance Association Growing Media for Plants).

Feature/Characteristic	Details
Total soil volume (packed)	40 l (DIN EN 12580)
pH	5.6 ($CaCl_2$)
Salinity	1.6 g/l (KCl)
Nitrogen (N)	180 mg/l
Phosphate (P_2O_5)	220 mg/l (calculated)
Potassium (K_2O)	340 mg/l (calculated)
Magnesium (Mg)	270 mg/l (total)
Magnesium (MgO)	210 mg/l ($CaCl_2$)
Sulfur (S)	350 mg/l (total)

The temperature was maintained at 25-28°C and the plants were watered moderately on alternate days. Using the rationale that the plants in their natural environment constantly interact with their dynamic surroundings, only a precisely controlled and not a totally sterile environment was maintained during the experiments. Each plant was inoculated at the leaves and stems in triplicates in three zones, viz. upper (towards the apex), central, and lower (towards the base/roots) in order to get an overall idea whether the age or physiology of host tissue dictates the endophyte affinity, infectivity and metabolomics. The target sites of infection were briefly decontaminated from the unwanted surface microorganisms by swabbing the surfaces with sterile paper tissues dampened with 70% ethanol. Each plant site was inoculated by placing a 10 day old mycelial mat of endophytic *F. solani* carefully teased from the SA surface, over the tissue surface (leaf and stem), then puncturing both mat and plant surface with sterilized needles (Fig. 24a-e, g-j). The puncture wounds allowed the breakage of both the mycelia and the plant tissue at the same point. This provided the perfect opportunity for the new hyphae growing at the fungal wound site where the mycelial mat was damaged to enter the plant tissue

through the plant wound site. The mycelial mats adhering to the plant surfaces were wrapped with Parafilm to prevent dislocation of wound sites and monitored regularly without disturbance (Fig. 24f,k,l). A control set of leaves and stems was also set up but without the fungal inoculum having been placed on the surface. A week after inoculation, the incubation was terminated by removing the fungal mycelial mats from the plant surfaces. The surfaces were again swabbed with sterile paper tissues dampened with 70% ethanol. The infected leaves and stems (including the wound sites) were then excised from the plants followed by surface-sterilization and then recovery of the colonized endophyte using the established procedures (detailed above). The recovered endophytes were pure-cultured in SA as and when they emerged from the plant tissue explants into the water agar (supplemented with antibiotic) media.

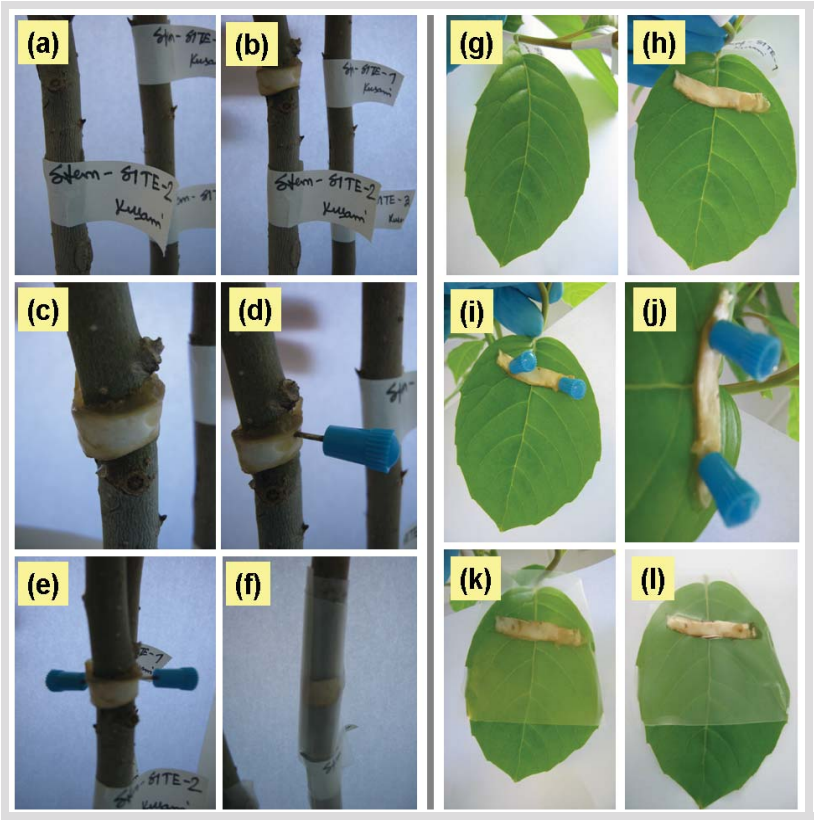

Fig. 24. Representative pictures of artificial *in vitro* establishment of the seventh generation of endophytic *F. solani* in the stems and leaves of the target *C. acuminata* host plants.
(a,g) Representative target stem and leaf for artificial inoculation of endophyte.
(b,c,h) 10 day old mycelial mat placed over the surface-sterilized stem and leaf surface.
(d,e,i,j) Pin-point puncture wounds created through the mycelial mat into the stem and leaf surface below with sterilized needles mediating breakage of mycelia and plant tissue at the same point.
(f,k,l) Undisturbed experimental set-up for endophyte infection and colonization within the living host tissues.

2.3.8. Microscopic examination of endophytic fungus before infection and after recovery

The endophytic hyphae emerging from the plant tissues were directly observed and characterized under a bright field stereo microscope to evaluate the emergence-pattern of the colonized endophyte from the plant tissues. A Leica S8 APO Greenough stereo microscope (Leica Microsystems GmbH, Wetzlar, Germany) equipped with a Schott KL 1500 compact halogen cold light source (Schott AG, Mainz, Germany) was used to examine the microscopic features of the plant-associated and axenic

endophytic fungi. The images were captured using Leica EC3 digital camera (Leica Microsystems), which were then processed using the Leica Application Suite LAS EZ ver. 1.6.0 (Leica Microsystems). The *F. solani* inoculum and the recovered endophytes were further processed for SEM (scanning electron microscopy). The fungi growing on SA were processed as described earlier (Ezra *et al.*, 2004; Strobel *et al.*, 2007), with suitable modifications, by placing the fungal preparations (mycelia-agar plugs) into 2% glutaraldehyde in 0.1 M sodium cacodylate buffer (pH 7.2–7.4) with Triton X, a wetting agent, aspirated for 5 min and left overnight. The next day, these were washed five times in water for 20 min each, followed by a 20 min dip in 10% ethanol, a 20 min dip in 30% ethanol, a 20 min dip in 50% ethanol and five 20 min dips in 70% ethanol, and were left overnight or longer in 70% ethanol. They were then rinsed for 20 min in 95% ethanol and then for three 20 min dips in absolute ethanol, followed by three 20 min dips in acetone. This was finally desiccated in a vacuum-operated desiccator for 30 min. The dehydration process was done slowly, to minimize hyphal shriveling. The obtained fungal material was critical-point dried, carbon coated and micrographs were recorded with a Hitachi S4500 SEM in an accelerating voltage of 1.0 kV using a secondary electron detector.

3. Hypericin

3.1. Plant sampling and phytochemical profiling of host plants

3.1.1. Collection, identification and authentication of plant material

Living plants were collected in Slovakia from wild populations of *Hypericum hirsutum* L., *Hypericum montanum* L., *Hypericum tetrapterum* Fr., and *Hypericum maculatum* Crantz, the latter from four different natural populations, and of *Hypericum perforatum* L., representing a natural population in Jammu and Kashmir, India. Table 4 contains data concerning the identity of the *Hypericum* species under study, voucher numbers of the deposited herbarium specimens including the name of the depositories, and sites of collections. All the plant species were collected at bloom stage from their natural populations at each location. Plants were collected in June (in India) and July (in Slovakia) 2007.

3.1.2. Preparation of plant extracts

The extraction process used has been optimized and validated in previous work (Smelcerovic *et al.*, 2006a). The plants were cut into roots, stems and leaves, and were air-dried at room temperature (25°C). The plant materials were then ground to dust under liquid nitrogen. Then, extraction was

performed similar to *C. acuminata* (Chapter 4: section 2.1.2) and stored in the dark at -20°C till commencement of analyses by LC-MS/MS.

Table 4. Locality and voucher information of the *Hypericum* species studied. Specimens of the Slovakian plants are deposited in the herbarium of the Botanical Garden Berlin-Dahlem and of the Indian material in the herbarium of the Indian Institute of Integrative Medicine (IIIM), Canal Road, Jammu 180 001, India.

Plant Taxon	Voucher Number	Collection Site
Hypericum perforatum L.	112/IIIM-S	**India**, Harwan, Jammu & Kashmir, (34°07′ N, 74°52′ E, 1587 m altitude), 10 km from Srinagar, rocky vegetation
Hypericum maculatum Crantz s. l.	T. Borsch & J. Kosuth 3900	**Slovakia**, Spisska Tomašovca N of Kosice, (48°56′ N, 20°27′ E, 620 m NN), meadow vegetation
Hypericum hirsutum L.	T. Borsch & J. Kosuth 3901	**Slovakia**, Spisska Tomašovca, N of Kosice, (48°54′ N, 20°27′ E, 620 m NN), *Abies-Fagus* forest
Hypericum maculatum Crantz s. l.	T. Borsch & J. Kosuth 3902	**Slovakia**, Tatra Mountains, Térry Cottage (49°11′ N, 20°12′ E, 1680 m NN), tall herb vegetation close to stream
Hypericum montanum L.	T. Borsch & J. Kosuth 3903	**Slovakia**, hillside N of Kosice (48°44′ N, 21°13′ E, 327 m NN), *Querco-Carpinetum* forest
Hypericum tetrapterum Fr.	T. Borsch & J. Kosuth 3913	**Slovakia**, valley close to Nová Sedlica (49°01′ N, 22°20′ E, 306 m NN), *Scirpus*-dominated swampy tall herb vegetation
Hypericum maculatum Crantz s. l.	T. Borsch & J. Kosuth 3908	**Slovakia**, Hačava, (48°40′ N, 20°49′ E, 440 m NN), meadow vegetation
Hypericum maculatum Crantz s. l.	T. Borsch & J. Kosuth 3907	**Slovakia**, Hačava, (48°40′ N, 20°52′ E, 460 m NN), meadow vegetation

3.1.3. Determination of metabolite contents

Metabolite content was determined by small modifications of a previously described method (Bonkanka *et al.*, 2008). The compounds were separated on a Luna C_{18} 100 Å column (3 µm, 250 mm; Phenomenex, Torrance, CA) at 30°C. Chromatographic conditions were optimized for the separation of hypericin, pseudohypericin, hyperforin and emodin (gradient 1), and for the separation of flavonoids (gradient 2) at the Surveyor HPLC system (Thermo Finnigan, U.S.A.). The mobile phase consisted of 10 mM ammonium acetate buffer adjusted to pH 5.0 with glacial acetic acid (A) and a 9:1 mixture of acetonitrile and methanol (B). Gradient 1: gradient elution was performed using the following solvent gradient: from 55A/45B held for 2 min to 0A/100B in 8 min, thereafter holding for 13 min; each run was followed by an equilibration period of 6 min. The flow rate was 0.3 mL min^{-1} and injection volume was 3 µL. Gradient 2: gradient elution was performed using the following solvent gradient: start for 2 min at 95A/5B, in 6 min to 75A/25B, then in 2 min to 50A/50B and in another 2 min to 100B. After holding for 13 min returned to initial conditions (95A/5B) within 1 min and held for 8 min. The eluent flow rate was 0.25 mL min^{-1} and the injection volume was 5 µL.

Highly selective and sensitive selected reaction monitoring (SRM) was performed using a TSQ Quantum Ultra AM mass spectrometer (Thermo Finnigan, U.S.A.) equipped with an ESI ion source (Ion Max) operating in negative mode. Nitrogen was employed as both the drying and nebulizer gas. The capillary voltage was 5 kV and capillary temperature was set at 200°C. Sheath gas (nitrogen) was set at 45 arbitrary units and collision gas pressure was 1.5 mTorr. Each mass transition was monitored at a peak width of 0.5 and dwell time of 0.3 s. Retention times, precursor and product ions, together with collision energies for the compounds under study are shown in Table 5. All the secondary metabolites were re-verified using the highly selective and sensitive LC-ESI-HRMS^n (LTQ-Orbitrap spectrometer). External calibration was performed in the range 0.01-10 μg mL^{-1} for emodin, 0.05-50 μg mL^{-1} for hyperforin, pseudohypericin, and hypericin, as well as 0.5-100 μg mL^{-1} for hyperoside, rutin, quercetin, and quercitrin. Correlation coefficient for the calibration curves were >0.99 for all analytes. The relative standard deviation (RSD) of the analytical method was determined by eight injections of an extract and was below 6% for all compounds. The LOD (limit of detection) and LOQ were determined by minimum signal to noise ratio of 3 and 9, respectively. Instrumental LOQ of the compounds varied between 0.003 μg mL^{-1} (emodin) and 2 μg mL^{-1} (quercitrin).

Table 5. Retention times, precursor ions, product ions, and collision energies of the compounds analyzed. [a]compounds analyzed with gradient 1; [b]compounds analyzed with gradient 2.

Compound	Retention time (min)	Precursor ion $[M-H]^-$ (*m/z*)	Product ion (*m/z*)	Collision energy (V)
Emodin[a]	6.5	269.0	225.0	38
Pseudohypericin[a]	7.3	519.3	487.0	52
Hypericin[a]	9.3	503.2	405.0	57
Hyperforin[a]	9.4	535.5	313.1	40
Rutin[b]	9.5	609.2	300.0	40
Hyperoside[b]	9.8	463.0	300.0	34
Quercitrin[b]	10.4	447.1	300.0	32
Quercetin[b]	10.9	300.9	151.0	30

3.1.4. Data analysis

The LC–MS/MS data were subjected to a number of different statistical evaluations for metabolite profiling and correlating the phytochemical loads among the various parts of the plants of the studied *Hypericum* samples (same and different species), between the organic and aqueous extracts, among the different species, among populations of the same species from different locations, among populations of different species from the same locations, as well as among populations of different species from different locations. The analyses included MVA, Kruskal's MDS, PCA, LDA, and HACA. All the analyses were performed using the statistical software XLSTAT-Pro version 2008.7.02, except

for MVA which was performed using the statistical software QI Macros version 2008.11. Both the statistical softwares were used in combination with Microsoft Excel 2003 version SP3-11.8237.8221. The chemometric algorithms and methodologies were used similar to those used for the *C. acuminata* plants (Chapter 4: section 2.1.4).

3.2. Biological characterization of hypericin producing endophytic fungus

3.2.1. Isolation and establishment of *in vitro* culture of hypericin producing endophyte

The wild specimens of *Hypericum* plants collected from Slovakia and India were removed from the soil and transported to our institute for processing within 24 h of collection. The plants were washed thoroughly in running tap water followed by DI water to remove any soil and dirt adhering to the plant parts. The leaves, stems and roots were cut for the isolation of endophytic fungi. Surface-sterilization of the cut explants and isolation of endophytes were carried out following the established methods (Lodge *et al.*, 1996; Strobel *et al.*, 2004; Puri *et al.*, 2005), suitably modified, similar to that used for *C. acuminata* (Chapter 4: section 2.2.1). Only one endophytic fungus was able to produce hypericin and its proposed precursor (in plants) emodin, and was taken up for further studies.

3.2.2. Maintenance and storage of the endophytic isolate

The axenic culture, obtained above, was coded as INFU/Hp/KF/34B and was routinely maintained on PDA, SA, and CDA in active form. For long-term storage, the colonies were preserved in the vegetative form in 15% (*v/v*) glycerol at -70°C. Agar blocks impregnated with mycelia were used directly for storage of the vegetative forms. Furthermore, the endophytic fungus has been deposited at DSMZ (accession number DSM 21024).

3.2.3. Identification of hypericin producing endophytic fungus

Total genomic DNA was isolated from the mycelial mass using the Macherey Nagel (MN) Food DNA extraction kit strictly following manufacturer's guidelines (Anonymous, 2007). About 100 mg of fungal tissue was scraped from the PDA surface and transferred to a tube for homogenizing using a homogenizer. The homogenized samples were transferred into MN Tube Strips (lysis) and added 1 mL buffer (CF, supplied with MN kit) preheated to 65°C, 10 µL of proteinase K solution, 10 µL of RNase A and mixed vigorously. The setup was incubated at 65°C for 30 min. The samples were centrifuged for 20 min at 5600 x g. 300 µL clear supernatant was transferred to a round well block, added 300 µL buffer (C4, supplied with MN kit) and 200 µL ethanol. The contents were mixed by vigorous vortexing

for 15-30 s followed by a brief spin for 30 s at 1500 x g to collect any sample from cap strips. The samples were then transferred into the wells of the NucleoSpin® Food Binding Strips. 100 µL pre-warmed TE buffer (10 mM Tris-HCl, pH 8.0, 1 mM EDTA, 70°C) was dispensed to each well of the NucleoSpin® Food Binding Strips directly onto the membranes followed by incubation at room temperature for 2-3 min. Finally, centrifugation was performed at 5600 × g for 2 min to obtain the genomic DNA.

The genomic DNA obtained was subjected to PCR analysis (ABI GeneAmp PCR System 9700, Applied Biosystems, Foster City, CA) using primers directed to the D2 region (variable) of the large subunit (LSU, 28S) rDNA. The PCR performed in 25 µL reaction volume contained 2.5 µL of 10x Taq polymerase reaction buffer (Fermentas GmbH, St. Leon-Rot, Germany), 2.5 µL of 25 mM $MgCl_2$, 0.2 µL of Taq polymerase enzyme (Fermentas GmbH), 1 µL of 100x BSA (Fermentas GmbH), 2 µL of 10 µM dNTPs (Fermentas GmbH), 1.25 µL of 100 pM forward primer LR0R (ACCCGCTGAACTTAAGC), 1.25 µL of 100 pM reverse primer LR7 (TACTACCACCAAGATCT), 1.30 µL of 100 pM control primer/template LR5 (TCCTGAGGGAAACTTCG), 0.5 µL extracted genomic DNA (suspension), and 12.5 µL of water. The control was added as per manufacturer's guidelines. The results from the control helped in determining whether failed reactions (if any) were the result of poor primer quality or reaction failure. The reaction conditions were as follows: 95°C for 15 min, 34 cycles (95°C – 45 s, 45°C – 45 s, 72°C – 90 s) and 72°C for 7 min followed by cooling to 4°C. PCR product was sequenced on an ABI 3730xl DNA Analyzer using BigDye® Terminator v 3.1 Cycle sequencing kit. Briefly, the amplified DNA was resuspended in BigDye® Terminator sequencing buffer and Hi-Di™ formamide (Applied Biosystems), and loaded into the instrument capillary array (50 cm) by electro-kinetic injection with the help of an autosampler. The array was pre-filled with a special polymer called POP-7™ (Applied Biosystems), a medium that prevents the DNA fragments to stick together. The DNA sequence fragments were separated by size as they travelled through the polymer-filled capillary array (electrophoresis). As they reached the detection window, a laser beam was used to excite the molecules and emissions from samples were collected simultaneously and spectrally separated by a spectrograph. The emissions were focused as columns of light onto the attached CCD camera, which were read and interpreted by the 3730xl Data Collection software (Applied Biosystems) and displayed as an electropherogram. The sequences were aligned and prepared with the software DNAstar Lasergene SeqMan and matched against the nucleotide-nucleotide database (BLASTn) of the NCBI for final identification of the endophytic isolate. For ITS-5.8S rDNA analysis, the endophytic fungus was prepared and processed similar to *F. solani* isolated from C. *acuminata* (Chapter 4: section 2.2.3).

The partial 28S rRNA gene, ITS1, 5.8S rRNA gene and ITS2 sequence obtained has been deposited at the EMBL-Bank under accession number AM909688.

3.2.4. Morphological studies of the endophytic fungus

The endophytic fungus, INFU/Hp/KF/34B, growing on PDA, SA, and CDA was examined after 2, 3, 4, 5, and 10 days to study the macroscopic morphology. Hyphae from the agar plate were aseptically transferred to slides for microscopy. A Leica DM-R light microscope and a Leica S8 APO Greenough stereo microscope equipped with a Schott KL 1500 compact halogen cold light source were used to examine the microscopic features of the axenic endophytic fungus. The images were captured using Leica EC3 digital camera and processed using the Leica Application Suite LAS EZ ver. 1.6.0.

3.2.5. Establishment of hypericin and emodin production as a function of time

The endophyte was cultured in PDB. A set of 10 conical flasks (500 mL) was used, each with four indentations and containing 100 mL of PDB, adjusted to pH 5.6 before autoclaving. The fungus was inoculated into each flask from the parent axenic culture. These flasks were incubated at 28 ± 2°C with shaking (200 rpm) on a rotary shaker. Each flask represented one time point for termination of fermentation followed by extraction and analysis for determination of the production of hypericin and emodin. The first sample was taken after 2 h of inoculation (0 h), and subsequently the other samples were taken after every 24 h, up to 216 h. For each sample, the dry weight of biomass was determined after termination of fermentation to the desired time point. Three replicates of each experiment set were undertaken.

3.2.6. Preparation of cell-free extract

The cell-free extract was prepared by filtering the incubated culture through muslin cloth under vacuum. The mycelia and broth were treated separately. The mycelial pellet was dried in an oven (≤30°C) to obtain the dry weight and was first extracted three times with ethyl acetate (50 mL), followed by extraction (both mycelia and spent broth) similar to that used for the endophytes isolated from *C. acuminata* plants (Chapter 4: section 2.2.6).

3.3. Biochemical characterization of hypericin producing endophytic fungus

3.3.1. Structural elucidation and quantitation of hypericin

Quantitation of the hypericin and emodin was performed by using a Thermo Finnigan Surveyor HPLC system consisting of Surveyor MS-pump and Surveyor Autosampler-Plus (injection volume 5 µL). The compounds were separated on a Luna C_{18} (50 × 3 mm, 3 µm particle size) column from Phenomenex

(Torrance, CA). The mobile phase consisted of water containing 10 mM ammonium acetate (pH 5.0) (A) and acetonitrile-methanol, 9:1 (B). Samples were separated using a gradient program as follows: (flow rate of 250 µL min^{-1}) 55% A isocratic for 2 min, linear gradient to 100% B over 6 min (flow rate 300 µL min^{-1}). After 100% B isocratic for 7 min, the system was returned to its initial conditions (55% A) within 1 min and was equilibrated for 4 min before the next run was started. MS detection (multiple reaction monitoring mode) was performed by using a TSQ Quantum Ultra AM spectrometer equipped with an ESI ion source (Ion Max) operating in negative mode. Nitrogen was employed as both the sheath (50 arbitrary units) and auxiliary (8 arbitrary units) gas, and argon served as the collision gas with a pressure of 1.5 mTorr. The capillary temperature was set at 250°C. External calibration was performed in the range 0.01-10.0 µg mL^{-1} for hypericin and 0.005-10.0 µg mL^{-1} for emodin. Correlation coefficients for the linear calibration curves were >0.995 for both compounds.

Hypericin and emodin were identified by HRMS fragment spectra (LTQ-Orbitrap spectrometer), which were consistent with authentic standards. The spectrometer was equipped with a Dionex HPLC system Ultimate 3000 consisting of pump, flow manager, and autosampler (injection volume 1 µL). Nitrogen was used as sheath gas (6 arbitrary units), and helium served as the collision gas. The separations were performed by using a Phenomenex Gemini C_{18} column (3 µm, 0.3 × 150 mm) (Torrance, CA) with a H_2O (+0.1% HCOOH, +1 mM ammonium acetate) (A)/acetonitrile (+0.1% HCOOH) (B) gradient (flow rate 4 µL min^{-1}). Samples were analyzed by using a gradient program as follows: 30% A isocratic for 1 min, linear gradient to 100% B over 10 min; after 100% B isocratic for 60 min, the system was returned to its initial condition (30% A) within 1 min and was equilibrated for 9 min. The spectrometer was operated in negative mode (1 spectrum s^{-1}; mass range 50–1000) with nominal mass resolving power of 60000 at *m/z* 400 with a scan rate of 1 Hz with automatic gain control to provide high-accuracy mass measurements within 2 ppm deviation using one internal lock mass (*m/z* 386.7149314; CsI_2^-).

3.3.2. HRMS screening for emodin anthrone and protohypericin

Additional screening for emodin anthrone and protohypericin was performed in full scan negative mode. The spectrometer was equipped with a Thermo Surveyor system consisting of a LC-pump and autosampler (injection volume 5 µL). N_2 was used as sheath gas (5 arbitrary units), and He served as the collision gas. The separations were performed by using a Phenomenex Synergi Fusion RP column (4 µm, 2 × 150 mm) with a H_2O (+0.1% HCOOH, +10 mM NH_4OAc) (A)/MeCN (+0.1% HCOOH) (B) gradient (flow rate 0.25 mL min^{-1}). Samples were analyzed by using a gradient program as follows: 50% A isocratic for 2 min, linear gradient to 100% B over 8 min; after 100% B isocratic for 48 min, the system was returned to its initial condition (50% A) within 1 min and was equilibrated for 6 min. The spectrometer was operated in negative mode (1 spectrum s^{-1}; mass range 200-1000) with mass

resolving power of 60000 at *m/z* 400 with a scan rate of 1 Hz with automatic gain control to provide high-accuracy mass measurements within 2 ppm deviation.

3.3.3. Establishment of hypericin and emodin production as a function of time in light and under light protection

A set of 10 conical flasks (500 mL) was used, each with four indentations and containing 100 mL of PDB, adjusted to pH 5.6 before autoclaving. The fungus was inoculated into each flask from the parent axenic culture. These flasks were incubated at 28 ± 2°C with shaking (200 rpm) on a rotary shaker. Each flask represented one time point for termination of fermentation followed by extraction and analysis for determination of the production of hypericin and emodin. The first sample was taken after 2 h of inoculation (0 h), and subsequently the other samples were taken after every 24 h, up to 216 h. For each sample, the dry weight of biomass was determined after termination of fermentation to the desired time point. A similar set of 10 flasks was prepared simultaneously and processed in parallel in the same way. The only difference was that the entire procedure was performed under complete light protection, from inoculation through fermentation to extraction and analysis of hypericin and emodin. Three replicates of each experimental set were undertaken.

3.3.4. Emodin spiking under submerged fermentation conditions

The spiking experiments were performed in a similar fashion to the fermentation for kinetic studies. Groups of three conical flasks of 500 mL capacity were used, each with four indentations and containing 100 mL of PDB adjusted to pH 5.6 before autoclaving. The fungus was inoculated into each flask from the parent axenic culture. These flasks were incubated at 28 ± 2°C with shaking (200 rpm) on a rotary shaker for 216 h. The first set was the control and was not fed with emodin. In the second and third sets, 3 and 5 mM concentrations of emodin, respectively, were fed before commencing with the shake-flask fermentation. A similar setup of three sets was prepared simultaneously and processed in parallel under complete light protection from inoculation through fermentation to extraction and analysis of hypericin and emodin. The dry weight of biomass in each case was determined after termination of fermentation. Three replicates of each experimental set were undertaken.

3.3.5. Detection of the *hyp-1* gene in the fungal endophyte

Nucleic acids for detection of the presence and expression of the *hyp-1* gene in the endophyte by PCR and RT-PCR, respectively, were isolated using DNeasy- and RNeasy-Plant Mini Kits (Qiagen, Valencia, CA). The *hyp-1* gene-specific primers were designed on the basis of the published full-length cDNA of

hyp-1 from *H. perforatum* (accession number AY148090). Two sets of primers amplifying 368 bp (hyp-for1 5´-AGGCTGTTTAAGGCATTGGTCC-3´, hyp-rev1 5´-GCTTTCTTTTCCCCGATCTTGAC-3´) and 570 bp long gene fragments (hyp-for2 5´-TTTCTGAATATGGCGGCGTACAC-3´, hyp-rev2 5´-CAAGCATCGCAAAACACAAGACC-3´) were used. The expected lengths of the PCR products were based on the published *hyp-1* cDNA from *H. perforatum*. The binding sites of the PCR primers were localized inside the translated region of the gene (hyp-for1/rev1) or covered the whole translated region of *hyp-1* gene (hyp-for2/rev2). Approximately 500 ng of total RNA was reverse transcribed by 10 mM anchored oligo-T primer and 200 U M-MLV reverse transcriptase (Invitrogen) according to the manufacturer's instructions. DNA and cDNA from *H. perforatum* were used as positive controls of the PCRs. The amplification reactions were performed in 30 µL reaction volume containing 1x diluted Taq polymerase reaction buffer with 1.5 mM $MgCl_2$ (Finnzymes, Espoo, Finland), 1.0 U DyNAzyme II DNA polymerase (Finnzymes), 0.2 mM dNTP (Finnzymes), 0.5 µM forward and reverse primer, and 50 ng of DNA or reverse transcribed RNA (cDNA). The reaction conditions were as follows: 95°C for 3 min, 30 cycles (94°C for 30 s, 58°C for 30 s, and 72°C for 30 s), and 74°C for 4 min, in MJ-Mini thermocycler (BioRad, Hercules, CA). Initially, gradient PCR (annealing from 52 to 60°C) was applied to obtain distinct and specific PCR products. The length of the desired amplification product was verified by electrophoresis in 2% agarose gel dyed with GoldView (0.005% *v/v*). The distinct PCR products from the endophyte were purified by Wizard SV gel and PCR Clean-Up System and directly sequenced with the forward and reverse primer. The assembled nucleotide sequences were aligned and compared with the publicly available database of DNA sequences by BLASTn to verify the nucleotide similarity with the *hyp-1* gene.

3.3.6. Generation studies on the endophytic isolate

In order to establish the production pattern of hypericin and emodin over successive generations, a study was devised to understand the variance of metabolite production from one generation to another and to correlate that with the fungal growth pattern. This was done similar to that of endophytic *F. solani* isolated from *C. acuminata* (Chapter 4: section 2.3.2). Furthermore, the axenic cultures were stored at 4°C till different time points to study the production of hypericin and emodin by the endophyte on storage. The initial production (August 2007) were compared with those of February 2009 and October 2009. Three replicates of each experiment set were performed to get reproducible data.

3.3.7. Culturing of the THP-1 cell line

The human acute monocytic leukemia cell line (THP-1), bearing DSMZ number ACC 16, was used. The THP-1 cells were grown in tissue culture flasks in complete growth medium in an atmosphere of 5%

CO_2 and 90% relative humidity in a carbon dioxide incubator. The complete growth medium was prepared by using RPMI-1640 supplemented with 2 mM L-glutamine, 10% FBS, and penicillin (100 IU mL^{-1}, just before use) in double-distilled water. The pH of the medium was adjusted to 7.2, and the medium was sterilized by filtering through 0.2 µm filters in a laminar air flow hood under aseptic conditions.

3.3.8. Subculturing of the THP-1 cell line

For subculturing, the medium of the flask having subconfluent growth was changed 1 day in advance. The entire medium from the flask was taken out and discarded. Cells were washed with PBS. Then 0.5 mL of Trypsin-EDTA in PBS (pre-warmed at 37°C) was added to make a thin layer on the monolayer of the THP-1 cells. The flask was incubated for approximately 5 min at 37°C and observed under a microscope. If the cells were found to be detached, complete growth medium (1 mL, pre-warmed at 37°C) was added to make the cell suspension. An aliquot was taken out and cells were counted and checked for viability with Trypan blue. Cell stock of more than 98% cell viability was accepted for determination of the *in vitro* cytotoxicity. The cell density was adjusted to 5.0×10^4 cells mL^{-1} by addition of more complete growth medium.

3.3.9. Preparation of test materials for cytotoxic assay

The stock solution for the cytotoxicity assays was prepared by pooling together all the fungal extracts obtained from multiple fermentations and dissolving in DMSO. A final concentration of 7.2 mg mL^{-1} (filter-sterilized through 0.2 µm filter under vacuum after dissolving) could be achieved with the pooled extracts. From the stock solution, working concentrations were prepared such that the maximum concentration was 288.0 µL mL^{-1} and minimum concentration was 0.044 µL mL^{-1}, with a dilution factor (DF) of 3. Since the relative concentrations of hypericin and emodin in the pooled fungal extract were unknown, the working solutions were prepared in µL mL^{-1} rather than in µM.

3.3.10. Cytotoxic assay

The *in vitro* cytotoxicity against the human cancer cell line THP-1 was determined using 96-well flat bottom tissue culture plates (Corning B. V. Life Sciences, The Netherlands), with the parameters as shown in Fig. 25. The aliquots of 100 µL of cell suspension (5.0×10^4 cells mL^{-1}) were added to each well and incubated for 24 h at 37°C. The samples (100 µL in each well) of the desired concentrations were added under strictly subdued light conditions to the wells, giving a final well-volume of 200 µL and final cell concentration of 2.5×10^4 cells mL^{-1}. The cells were allowed to grow in the presence of different sample concentrations for another 48 h at 37°C in the complete absence of light. In order to

estimate the photodynamic cytotoxicity of the samples, a similar set was prepared in parallel and run simultaneously as follows: the plates containing the cells and the samples were exposed to light for 20 min before incubation, by placing them on 3 mm transparent plastic slides 7 cm above a set of three 20 W halogen lamps. The plates were constantly moved to avoid shadows.

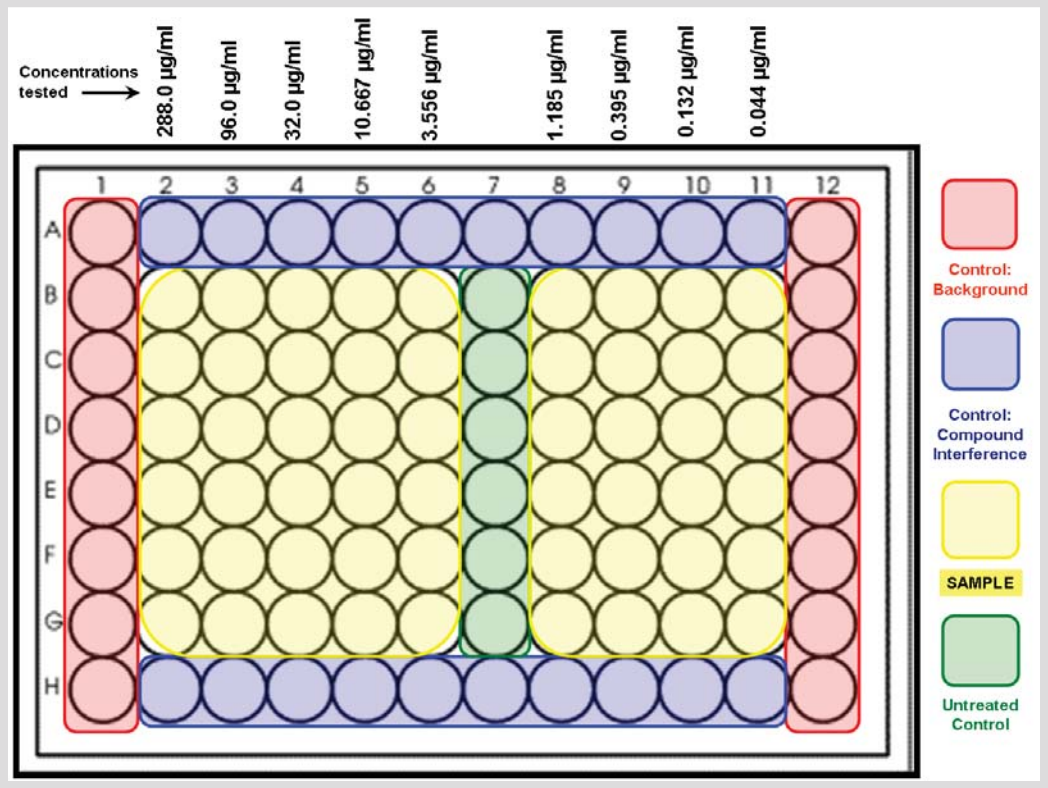

Fig. 25. The diagrammatic layout of the 96-well plates representing the parameters of the cytotoxic assays using both the resazurin and ATPlite methods.

During irradiations, the temperatures never exceeded 32°C. All experimental sets were repeated six times. Three sets of controls were used, in parallel, in light and dark conditions, to validate the experimental data. The first control was the negative control, which consisted of media only, in six replicates. The second control was the background control in eight replicates. A third additional control was designed to test the sample-indicator interaction and interference, at all concentrations, and in duplicates. Two different methods were used in all cases in parallel to quantify the viable cells using a VICTOR X3 multi-label plate reader (PerkinElmer Life And Analytical Sciences, Inc., Boston, MA). The first method consisted of quantification using resazurin (Sigma-Aldrich Chemie GmbH), to measure the mitochondrial activity. The second method consisted of quantifying using ATPlite (PerkinElmer Life and Analytical Sciences, Inc.), to measure the available ATP concentration. The final relative viabilities were calculated and represented in percent fractional survival (FS).

3.3.11. Morphological changes of human cancer cell line THP-1 on treatment with fungal metabolites

The THP-1 cells (both untreated and treated) were centrifuged at 2000 rpm for 10 min, spread over sterile glass slides, and allowed to air-dry under strict aseptic conditions. The air-dried smears were fixed in absolute MeOH for 2 min and stained with Giemsa (Sigma-Aldrich Chemie GmbH). These were subjected to microscopic studies using a Leica DM-R light microscope (Leica Microsystems GmbH) and photographed using the built-in digital camera.

4. Deoxypodophyllotoxin

4.1. Plant sampling and phytochemical profiling of host plants

4.1.1. Collection, identification and authentication of plant material

Living plants were collected (a) from the natural populations in Dortmund (Germany) of *Juniperus communis* L. Horstmann, *Juniperus communis* L. Meyer, *Juniperus communis* L. Wilseder Berg, *Juniperus communis* Hibernica, *Juniperus blaaws*, *Juniperus procumbens* Tremonia, *Juniperus x-media* Pfitzeriana, and *Juniperus squamata* Wilsonii; (b) from the natural populations in Haltern (Germany) of *Juniperus communis* var. *communis*, *Juniperus communis* (male cones), and *Juniperus communis* (female cones); (c) from the natural populations of *Juniperus recurva* at three sites in Yarikha, Bonera, and Sonamarg (Jammu and Kashmir, India), respectively; and (d) from the natural populations of *Podophyllum hexandrum* at five sites in Yarikha, Gulmarg, Pahalgam, Aru, and Sonamarg (Jammu and Kashmir, India), respectively. Table 6 contains data concerning the identity of the *Juniperus* and *Podophyllum* species collected from various populations in India, including voucher numbers of the deposited herbarium specimens, the name of the depository, and the sites of collections. The *Juniperus* species collected from Germany were sampled from the natural populations at the Rombergpark botanical garden, Dortmund, North-Rhine Westphalia, Germany and around the Haltern lake, North-Rhine Westphalia, Germany. These plant species are currently maintained (live plants) at the Rombergpark botanical garden, Dortmund, Germany. Therefore, it was not necessary to deposit the plants collected from Germany separately in any depository. All plants were collected in June 2007 in both India and Germany.

4.1.2. Preparation of plant extracts

The extraction of the plant materials was performed using suitable modification of our previously

established and validated method (for *Hypericum* species). The plants were cleaned and cut into small pieces, and were air-dried at room temperature (25°C). The plant materials were then ground to dust under liquid nitrogen. Then, 5.0 g of the dried dust for each plant (aerial parts; 1:1 *w/w* stem:needle for *Juniperus*, 1:1 *w/w* stem:leaf for *Podophyllum*; in triplicates) was extracted similar to that of *Hypericum* plants (Chapter 4: section 3.1.2) and stored in the dark at -20°C till commencement of analyses by LC-MS/MS.

Table 6. Locality and voucher information of the *Juniperus* and *Podophyllum* species collected in India. The specimens have been deposited in the herbarium of the Indian Institute of Integrative Medicine (IIIM), Jammu, India. The *Juniperus* species collected in Germany are maintained (live plants) at the Rombergpark botanical garden (refer to the text for details).

Plant Taxon	Voucher Number	Collection Site
Juniperus recurva	101/IIIM-S	**India**, Yarikha, Dist. Baramula, Jammu & Kashmir, 2200 m altitude, 50 km from Srinagar
Juniperus recurva	106/IIIM-S	**India**, Bonera, Jammu & Kashmir, plain land, 33 km from Srinagar
Juniperus recurva	110/IIIM-S	**India**, Sonamarg, Hapatgand, Jammu & Kashmir, 3000 m altitude, 90 km from Srinagar
Podophyllum hexandrum	103/IIIM-S	**India**, Yarikha, Dist. Baramula, Jammu & Kashmir, 2200 m altitude, 50 km from Srinagar
Podophyllum hexandrum	105/IIIM-S	**India**, Gulmarg, Jammu & Kashmir, 2750 m altitude, 60 km from Srinagar
Podophyllum hexandrum	108/IIIM-S	**India**, Pahalgam, Betab valley, Jammu & Kashmir, 2300 m altitude, 98 km from Srinagar
Podophyllum hexandrum	109/IIIM-S	**India**, Aru, Jammu & Kashmir, 2200 m altitude, 50 km from Srinagar
Podophyllum hexandrum	111/IIIM-S	**India**, Sonamarg, Hapatgand, Jammu & Kashmir, 2900 m altitude, 87 km from Srinagar

4.1.3. Determination of metabolite contents

HPLC analysis of the extracts was performed using a Surveyor HPLC system. Compounds were separated on a Hydro-RP column (150 × 2 mm, 4 µm particle size) from Phenomenex (Torrance, CA). The mobile phase consisted of 10 mM ammonium acetate in distilled water (A) and acetonitrile with 0.1% formic acid (B). Gradient elution was performed using the following solvent gradient: from 85A/15B (held for 3 min) in 16 min to 17A/83B, then in 1 min to 0A/100B and after 7 min, back to the initial conditions (85A/15B); each run was followed by an equilibration period of 8 min. The flow rate was 0.22 mL min^{-1} and the injection volume was 5 µL. All separations were performed at 30°C.

Mass spectra were obtained using a TSQ Quantum Ultra AM mass spectrometer equipped with an ESI ion source (Ion Max) operating in positive mode. Nitrogen was employed as both the drying and

nebulizer gas (40 AU). The MS/MS parameters are shown in Table 7. Capillary temperature was 200°C and capillary voltage was 3.5 kV. The calibration curves of the reference compounds podophyllotoxin and demethylpodophyllotoxin were constructed by dilution of external standards with methanol to give the desired concentrations. The concentrations of standard solutions were 0.1, 0.5, 1, 5, 10, 50, 80, 120, and 160 µg mL^{-1}. Correlation coefficient for the linear calibration curve was >0.99 for both podophyllotoxin and demethylpodophyllotoxin. All procedures were carried out under light protection. Concentrations of the commercially unavailable compounds deoxypodophyllotoxin and podophyllotoxone were calculated with the assumption of similar precursor ion response like that of podophyllotoxin. The LOQs were 0.05 µg mL^{-1} (demethylpodophyllotoxin) and 0.2 µg mL^{-1} (podophyllotoxin, deoxypodophyllotoxin, and podophyllotoxone), respectively. The LOD (3 times noise intensities) and LOQ (10 times noise intensities) were calculated/estimated from signal to noise ratio using signal intensities of the analytes and the noise near the retention time of the analytes. Estimation was necessary for the derivatives (deoxypodophyllotoxin and podophyllotoxone) due to absence of reference standards.

Table 7. Retention times, precursor and product ions, and collision energies for the compounds under study. SRM, selected reaction monitoring.

Compound	Retention time (min)		Precursor ion (*m/z*) $[M+NH_4]^+$	Product ion (*m/z*)	Collision energy (V)
Podophyllotoxin	13.31	SRM I	432.1	247.0	23
		SRM II	432.1	229.0	27
		SRM III	432.1	185.0	42
Demethylpodophyllotoxin	10.93	SRM I	418.1	247.0	20
		SRM II	418.1	229.0	23
Podophyllotoxone	15.41	SRM I	430.1	245.0	23
		SRM II	430.1	201.0	35
Deoxypodophyllotoxin	16.27	SRM I	416.1	231.0	25

All the secondary metabolites were re-verified using the highly selective and sensitive LC-ESI-$HRMS^n$. HPLC analysis of the extracts was performed using an Agilent (Santa Clara, U.S.A.) 1200 HPLC system consisting of LC-pump, PDA detector (λ = 254 nm), autosampler (injection volume 10 µL) and column oven (30°C). Compounds were separated using a Synergi Fusion RP80 column (150 x 3 mm, 4 µm particle size) from Phenomenex (Torrance, CA) with a H_2O (+ 0.1% HCOOH, + 10 mM ammonium acetate) (A)/acetonitrile (+ 0.1% HCOOH) (B) gradient (flow rate 400 µL min^{-1}). Samples were analyzed by using gradient program: 95% A isocratic for 3 min, linear gradient to 100% B over 20 min, after 100% B isocratic for 10 min, the system returned to its initial condition (95% A) within 1 min, and was

equilibrated for 5 min. The FT-full scan and MS/MS spectra were obtained with an LTQ-Orbitrap XL spectrometer (Thermo Fisher, U.S.A.) equipped with H-ESI-II source. The spectrometer was operated in positive mode (1 spectrum s^{-1}; mass range: 250-1000) with nominal mass resolving power of 60000 at *m/z* 400 with a scan rate of 1 Hz with automatic gain control to provide high-accuracy mass measurements within 2 ppm deviation using an internal standard; bis(2-ethylhexyl)phthalate: *m/z* 391.284286. MS/MS experiments were performed in HCD (higher-energy C-trap dissociation, 35 eV) mode. The following parameters were used for experiments: spray voltage 5 kV, capillary temperature 260°C, and tube lens 70 V. Nitrogen was used both as sheath gas (45 AU) and auxiliary gas (10 AU). Helium served as the collision gas.

4.1.4. Data analysis

The LC-MS/MS data were subjected to a number of different chemometric evaluations for metabolite profiling and correlating the phytochemical loads among the various plants of the studied *Juniperus* and *Podophyllum* species (infraspecific), between the organic and aqueous extracts, among populations of the same species from different locations, among populations of different species from the same location, among populations of different species from different locations, as well as among populations of different genera (infrageneric) from the same and different locations. The analyses included MVA, Kruskal's MDS, PCA, LDA, and HACA. All the analyses were performed using the statistical software XLSTAT-Pro version 2009.1.02, except for MVA which was performed using the statistical software QI Macros version 2008.11. Both statistical software packages were used in combination with Microsoft Excel 2003 version SP3-11.8237.8221. The chemometric algorithms and methodologies were used similar to those used for the *C. acuminata* plants (Chapter 4: section 2.1.4).

4.2. Biological characterization of deoxypodophyllotoxin producing endophytic fungus

4.2.1. Isolation and establishment of *in vitro* culture of deoxypodophyllotoxin producing endophyte

The plant twigs (*Juniperus*) or stems and leaves (*Podophyllum*) were thoroughly washed in running tap water followed by DI water. Small fragments of *Juniperus* twigs (containing about 5–10 needles) and *Podophyllum* stems/leaves (10 mm × 5 mm) were cut with the aid of a flame-sterilized razor blade. Surface-sterilization of the explants was done following the previously established method (Lodge *et al.*, 1996; Strobel *et al.*, 2004; Puri *et al.*, 2005) suitably modified, similar to that used for the

endophytes isolated from *Hypericum* plants (Chapter 4: section 3.2.1).

4.2.2. Maintenance and storage of the endophytic isolate

One endophytic fungus capable of producing deoxypodophyllotoxin was obtained above, which was coded as INFU/Jc/KF/6 and was routinely maintained on PDA, SA, and CDA in active form. For long-term storage, the colonies were preserved in the form of spores as well as vegetative form in 15% (*v/v*) glycerol at -70°C. Agar blocks impregnated with mycelia were used directly for storage of the vegetative forms. Furthermore, the endophytic fungus has been deposited at DSMZ (accession number DSM 21023).

4.2.3. Isolation of total genomic DNA, PCR amplification of LSU (28S) rDNA and sequencing

Total genomic DNA was isolated from the mycelial mass using the Macherey Nagel (MN) Food DNA extraction kit strictly following manufacturer's guidelines (Anonymous, 2007), similar to that of *T. subthermophila* isolated from *H. perforatum* (Chapter 4: section 3.2.3). The DNA sequence obtained has been deposited at the EMBL-Bank under accession number FM179606.

4.2.4. Morphological studies of the endophytic fungus

The endophytic fungus, INFU/Jc/KF/6, growing on PDA, SA and CDA was examined after 2, 3, 4 and 5 days to study the macroscopic morphology. Hyphae on the agar plate were aseptically transferred to slides for microscopy. A Leica DM-R light microscope was used to examine the microscopic features of the fungus.

4.2.5. Establishment of deoxypodophyllotoxin production as a function of time

A set of 10 conical flasks of 500 mL capacity was used, each with four indentations and containing 100 mL SB, adjusted to pH 5.6 before autoclaving, and fermentations were performed in triplicates similar to that of endophytic *F. solani* isolated from *C. acuminata* (Chapter 4: section 2.2.5).

4.2.6. Preparation of cell-free extract

The cell-free extract was prepared by filtering the incubated culture through muslin cloth under vacuum. The mycelia and broth were treated separately. The mycelial pellet was dried in an oven (≤30°C) to obtain the dry weight. Mycelial and broth extractions were performed similar to that used for the endophyte isolated from *C. acuminata* (Chapter 4: section 2.2.6).

4.3. Biochemical characterization of deoxypodophyllotoxin producing endophytic fungus

4.3.1. Structural elucidation and quantitation of deoxypodophyllotoxin

All spectra were recorded with an LTQ-Orbitrap spectrometer. The spectrometer was operated in positive mode (1 spectrum s^{-1}; mass range: 50–1000) with nominal mass resolving power of 60000 at *m/z* 400 with a scan rate of 1 Hz with automatic gain control to provide high accuracy mass within 1 ppm deviation using one internal lock mass, polydimethylcyclosiloxane – $[(CH_3)_2SiO]_6$: *m/z* 445.120025. The spectrometer was equipped with a Dionex HPLC system Ultimate 3000 consisting of pump, flow manager and autosampler (injection volume 0.5 µL). Nitrogen was used as sheath gas (5 AU) and helium served as the collision gas. The separations were performed by using a Phenomenex Gemini C_{18} column (3 µm, 0.3 × 150 mm) (Torrance, CA, U.S.A.) with a H_2O (+0.1% HCOOH) (A) / acetonitrile (+0.1% HCOOH) (B) gradient (flow rate 4 µL min^{-1}). Samples were analyzed by using a gradient program as follows: 90% A isocratic for 2 min, linear gradient to 100% B over 8 min, after 100% B isocratic for 10 min, the system was returned to its initial condition (90% A) within 1 min, and was equilibrated for 9 min. The quantitation of the compound was achieved by accurate mass (maximum deviation 1 ppm) single ion monitoring (SIM) of the $[M+H]^+$ ion of deoxypodophyllotoxin. Since deoxypodophyllotoxin is unavailable from commercial sources, the calibration was performed using podophyllotoxin as standard and detector response was assumed to be in the same range. The calibration graph was linear from 50 ng mL^{-1} up to 10000 ng mL^{-1}. Furthermore, a high-resolution full scan run was performed in order to check for the accumulation of structural analogues of podophyllotoxin and deoxypodophyllotoxin by the cultured endophyte.

4.3.2. Generation studies on the endophytic isolate

In order to establish the production pattern of deoxypodophyllotoxin over successive subculture generations, a study was devised to understand the variance of metabolite production from one generation to another and to correlate that with the fungal growth pattern. This was done similar to that of endophytic *F. solani* isolated from *C. acuminata* (Chapter 4: section 2.3.2).

4.3.3. Antimicrobial assay

The *in vitro* antimicrobial activities of the crude fungal extracts (mycelial and spent broth extracts pooled together, and thereafter filter-sterilized using a 0.45 µm membrane filter) were tested against a panel of laboratory standard pathogenic control strains belonging to DSMZ. Both for mycelia and spent broth,

the samples for antimicrobial studies were taken from multiple days and pooled together. Before commencing with the antimicrobial studies, the final pooled sample was measured by high-resolution LC-MS. The final concentration of fungal deoxypodophyllotoxin that could be achieved was 2 µg mL^{-1} (justified to whole number). Gram-positive bacterium *Staphylococcus aureus* subsp. *aureus* (DSM 799), and Gram-negative bacteria *Klebsiella pneumoniae* subsp. *ozaenae* (DSM 681), *Pseudomonas aeruginosa* (DSM 1128) and *Escherichia coli* (DSM 682) were used. The medium used for the activation of the microorganisms was Nutrient broth (NB; Merck, Darmstadt, Germany) and activation was performed strictly according to DSMZ guidelines following our previously established protocols (Kusari *et al.*, 2009; Sukul *et al.*, 2009). The activated test microbial strains were inoculated and cultured on Nutrient agar (NA) medium (DIFCO, cat. no. 213000) at 37°C for 24 h (stationary culture), and maintained at 4°C until use. Logarithmic phase fresh cultures were prepared from the above by inoculating five colonies into 5 mL of the NB and further incubation for 48 h at 37°C. The turbidity was corrected by comparison with a McFarland turbidity standard, by adding isotonic NaCl solution until 1 × 10^{-8} colony-forming units (CFU mL^{-1}) were attained (Brantner *et al.*, 1996). All procedures were followed under strict aseptic conditions.

A disk diffusion method, according to Clinical and Laboratory Standards Institute (CLSI) (Wikler, 2006), was employed for the determination of the antimicrobial activity of the samples. All agar plates were prepared in 90 mm sterile Petri dishes with 22 mL of agar, giving a final depth of 4 mm. 100 µL of inoculum suspension of the tested microorganisms were spread on the solid media plates using the standard spread-plate technique (Kusari *et al.*, 2009; Sukul *et al.*, 2009). Sterile assay paper disks (Schleicher & Schuell GmbH, Dassel, Germany; 6.0 mm in diameter) were impregnated with 40 µL of the samples, air-dried under the laminar air flow hood and placed on inoculated plates. These plates, after standing at 4°C for 2 h, were incubated at 37°C for 24 h. Three sets of control were used. One control was the organism control and consisted of a seeded Petri dish with no sample. In the second control, samples were introduced to the unseeded Petri dishes to check for sterility. To ensure the nullification of the solvent effect (if any), disks imbued with 40 µL of HPLC grade methanol was run simultaneously as a third control. Standard podophyllotoxin was also used as a reference agent in parallel (same concentration as that of fungal deoxypodophyllotoxin used, i.e. 2 µg mL^{-1}) to understand the comparative antimicrobial efficacy of the fungal deoxypodophyllotoxin against the tested organisms. The diameters of the inhibition zones were measured in millimeters (to the nearest mm). Each test was repeated six times and the mean values (±SD) were calculated.

CHAPTER 5:
RESULTS

1. Camptothecin (CPT)

1.1. Phytochemical profiling of host plants

1.1.1. Phytochemical profiling by multivariate analysis (MVA)

All together, eleven different *C. acuminata* plants from independent locations were analyzed for three different secondary metabolites (CPT, 9-MeO-CPT, and 10-OH-CPT). Fig. 26 shows the high-resolution MS^3 spectra of plant CPT, 9-MeO-CPT, and 10-OH-CPT compared to the reference standards showing the characteristic fragments. The concentrations of CPT, 9-MeO-CPT, and 10-OH-CPT in the organic, aqueous and total (organic and aqueous) phases, as well as that for the fresh and dried aerial tissues (stems and leaves) are shown in Table T3 (Appendix A). Based on LC-MS/MS analyses, it was revealed that the fresh stems of *C. acuminata* from China had the highest holistic metabolite load followed by the fresh stems of the plant from Halle, Germany. On evaluating independently, the highest content of CPT, 9-MeO-CPT, and 10-OH-CPT, respectively, was found in the fresh stems of *C. acuminata* from China. The fresh leaves of the plant from Mainz, Germany had the second highest content of CPT, followed by that in the fresh stems of the plant from Halle. Following the plant from China, the highest contents of 9-MeO-CPT and 10-OH-CPT were found in the fresh leaves of *C. acuminata* from Halle followed by the fresh stems of the same plant, and the fresh leaves of *C. acuminata* from Bayreuth followed by the fresh leaves of the plant from Halle, respectively.

MVA of the LC-MS/MS data was carried out to evaluate the individual and holistic phytochemical variability due to differences between categories, namely, different plants from the different locations, organic and aqueous extracts, as well as dried and fresh extracts (Fig. 27). From the MVA, it was evident that the tested compounds were mostly favored in the organic phases, although considerable ratios of CPT, 9-MeO-CPT, and 10-OH-CPT were also found in the aqueous phases in the *Camptotheca* genus. For all organs (i.e., leaves and stems), the content of the tested secondary metabolites decreased on drying. This was irrespective of the location from where the plants were sampled. Computation of the individual averages for each category also revealed the highest holistic phytochemical load in the fresh leaves of *C. acuminata* from China, followed by the fresh stems of the plant from Halle.

1.1.2. Multidimensional scaling (MDS)

Kruskal's MDS algorithm based on the Pearson correlation matrix was used to investigate, for the first time, the relationships between the metabolite contents (total) among the *Camptotheca* plants (Fig. 28).

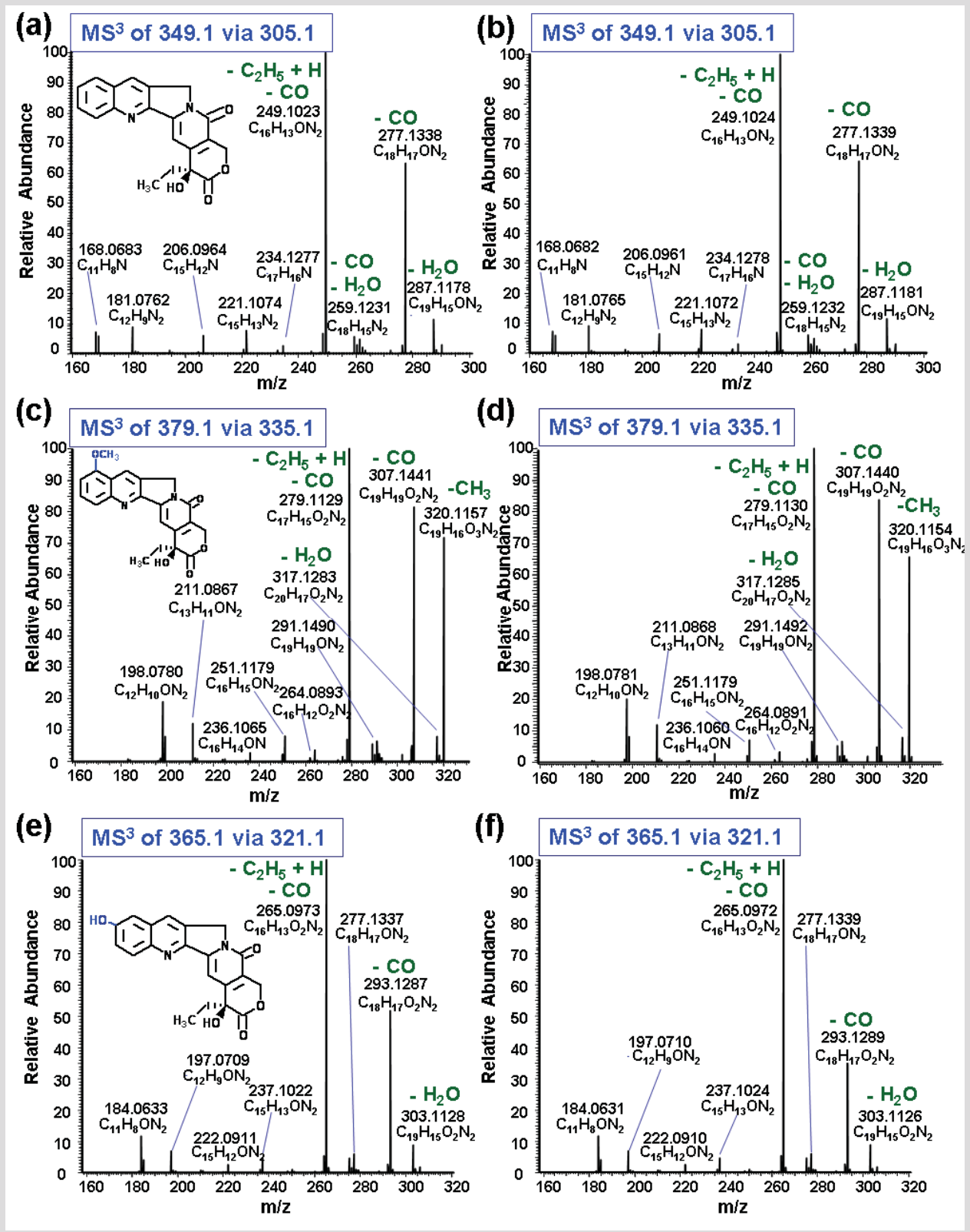

Fig. 26. High-resolution MS^3 product ion spectra of standard references and respective compounds in *C. acuminata* plants. (a) Standard CPT. (b) Plant CPT. (c) Standard 9-MeO-CPT. (d) Plant 9-MeO-CPT. (e) Standard 10-OH-CPT. (f) Plant 10-OH-CPT.

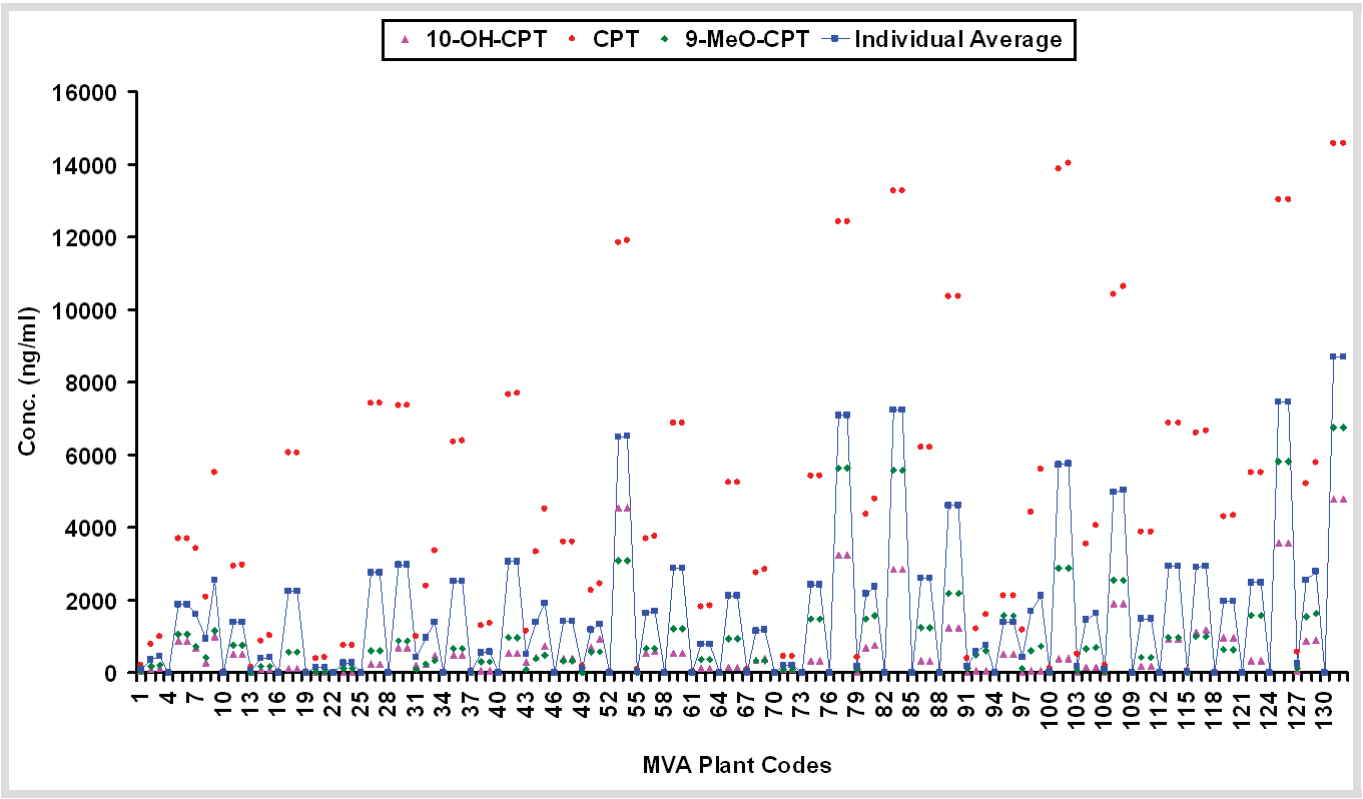

Fig. 27. MVA plot of the LC-MS/MS data for *C. acuminata*. The MVA codes '1-132' are represented in Table T3 (Appendix A) with detailed explanation.

This was done for the fresh and the dried aerial tissues in parallel. The method was executed in a 3-dimensional (3D) module to build a 3D map of the series of phytochemicals under study from the proximities matrix (by dissimilarities) between the categories (Fig. 28a,b). Furthermore, a 3D surface analysis was performed using the 3D distance in space between the phytochemicals to build the exact map of the phytochemical relativity within about the given symmetry of the 3 axes in 3 different dimensions (Fig. 28c,d). In order to achieve an optimal representation of the data points in 3D, Kruskal's stress was computed and found to be negligible in all evaluations (6.004×10^{-5} for fresh tissue extracts, and 4.872×10^{-5} for dried tissue extracts).

Moreover, to have an overall idea of the quality of the representation, the Shepard diagram based on Kruskal's stress in 3D was evaluated in each case. The Shepard diagram revealed that the observed dissimilarities and disparities (distances) were on the same linear curve for each evaluation (Fig. 29), confirming the reliability of the MDS representation in 3D.

The Pearson correlation matrix for the fresh tissue extracts (Table 8) revealed a significant positive correlation between all the three phytochemicals; CPT was positively correlated to 9-MeO-CPT (Pearson correlation coefficient, $r = 0.862$, $\alpha \leq 0.05$) as well as to 10-OH-CPT ($r = 0.801$, $\alpha \leq 0.05$). Furthermore, 9-MeO-CPT and 10-OH-CPT were found to be positively correlated ($r = 0.868$, $\alpha \leq 0.05$).

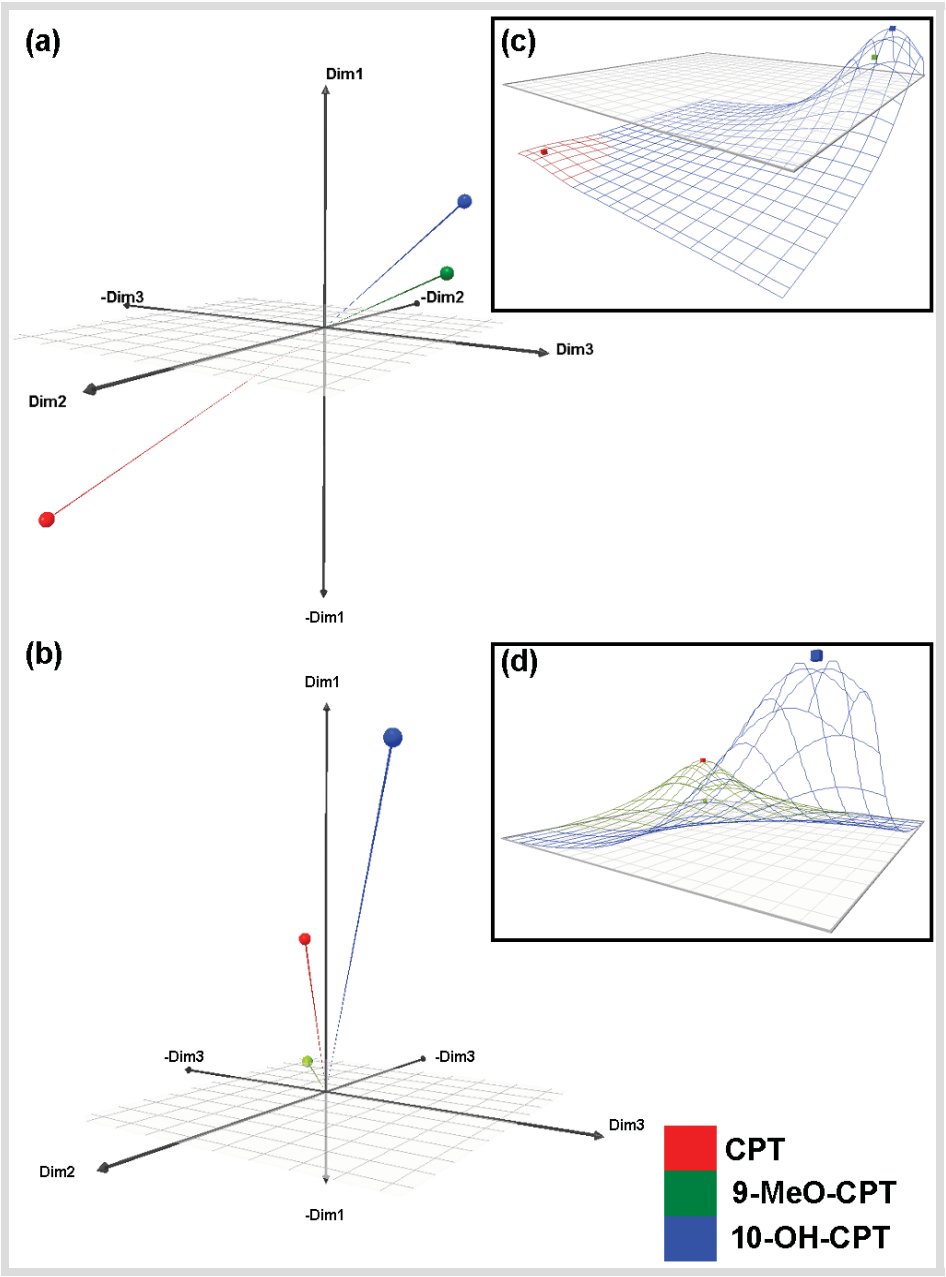

Fig. 28. Kruskal's MDS based on Pearson correlation used to investigate the relationships between the metabolite contents among investigated *Camptotheca* species. (a) 3D MDS map of the three metabolites under study from the proximities matrix (by dissimilarities) between the categories considering the dry tissue extracts' metabolite spectra. (b) 3D MDS map of the three metabolites under study from the proximities matrix (by dissimilarities) between the categories considering the fresh tissue extracts' metabolite spectra. (c,d) The respective 3D surface analysis map showing the spatial 3D distance about the given symmetry of the 3 axes in 3 different dimensions.

However, for the dried tissues, a positive correlation was found only between CPT and 9-MeO-CPT ($r = 0.640$, $\alpha \leq 0.05$); such a correlation was absent between CPT and 10-OH-CPT, as well as between 9-MeO-CPT and 10-OH-CPT. Interestingly, when comparing the degree of relativity between CPT and 9-MeO-CPT in the fresh and the dried tissues, a decrease could be observed on drying. This corroborated the observations by MVA that drying of the plant aerial tissues led to reduction in the secondary metabolites that could be extracted and thus, the difference in the phytochemical correlations in fresh and dried tissues could be understood at the infraspecific level.

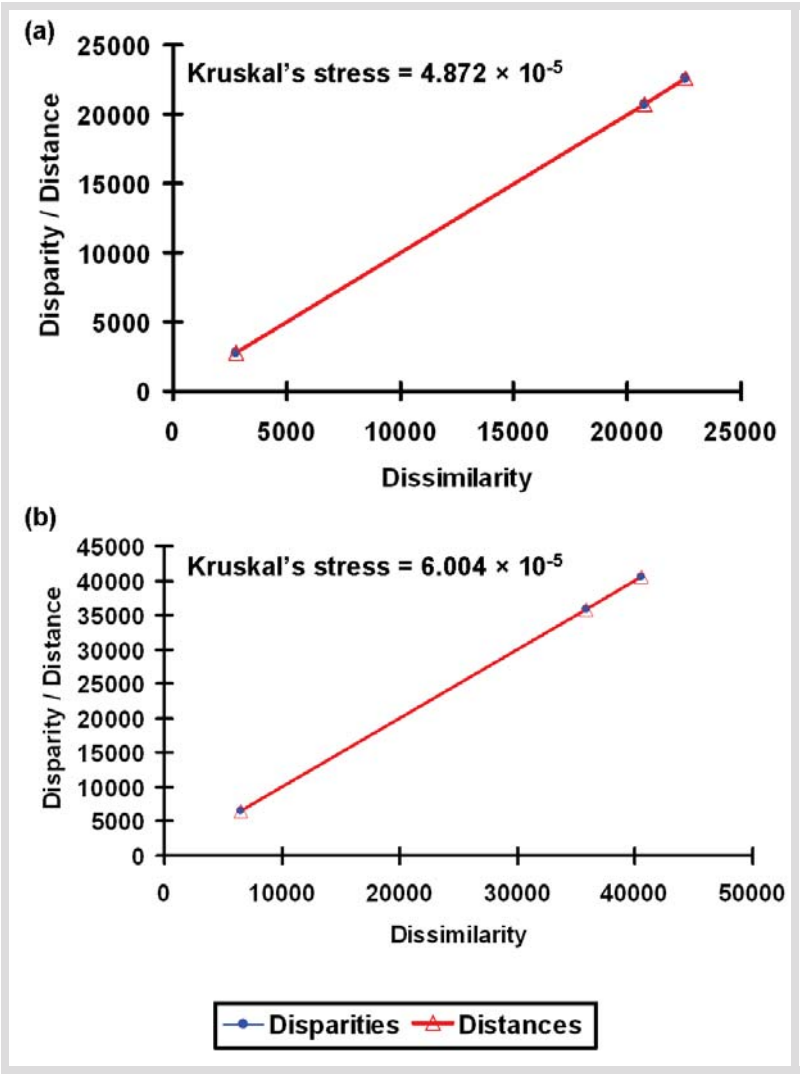

Fig. 29. The Shepard diagram for the MDS analysis in 3D. (a) For dry tissue extracts. (b) For fresh tissue extracts. In order to achieve an optimal representation of the data points in 3D, Kruskal's stress was computed and found to be negligible in all evaluations.

Table 8. Correlations between all the three tested phytochemicals by Pearson correlation matrix. Positive correlations are marked in bold.

Tissue type	Variables	10-OH-CPT	CPT	9-MeO-CPT
Fresh tissues	**10-OH-CPT**	-		
	CPT	**0.801**	-	
	9-MeO-CPT	**0.868**	**0.862**	-
Dried tissues	**10-OH-CPT**	-		
	CPT	0.350	-	
	9-MeO-CPT	0.365	**0.640**	-

1.1.3. Principal component analysis (PCA)

A 2-dimensional (2D) visualization of the respective position of the secondary metabolites relative to

each other was created by depicting the values of the principal components (metabolites) corresponding to the species. This was achieved by running the PCA. In order to evaluate the reliability of the PCA in 2D, a Scree Plot was computed in each case using the data variability in the useful dimensions (in this case, up to F3, i.e., 3rd dimension) versus the cumulative variability, relative to the eigenvalues (Fig. 30a,b). From the Scree Plots, it was revealed that the PCA analyses were reliable in 2D spacing (F1/F2 *Camptotheca* fresh tissue extracts = 96.23%, and F1/F2 *Camptotheca* dried tissue extracts = 88.0%). The PCA in each case was represented in the form of a Correlation Circle depicting the projection of the variables in the 2D space.

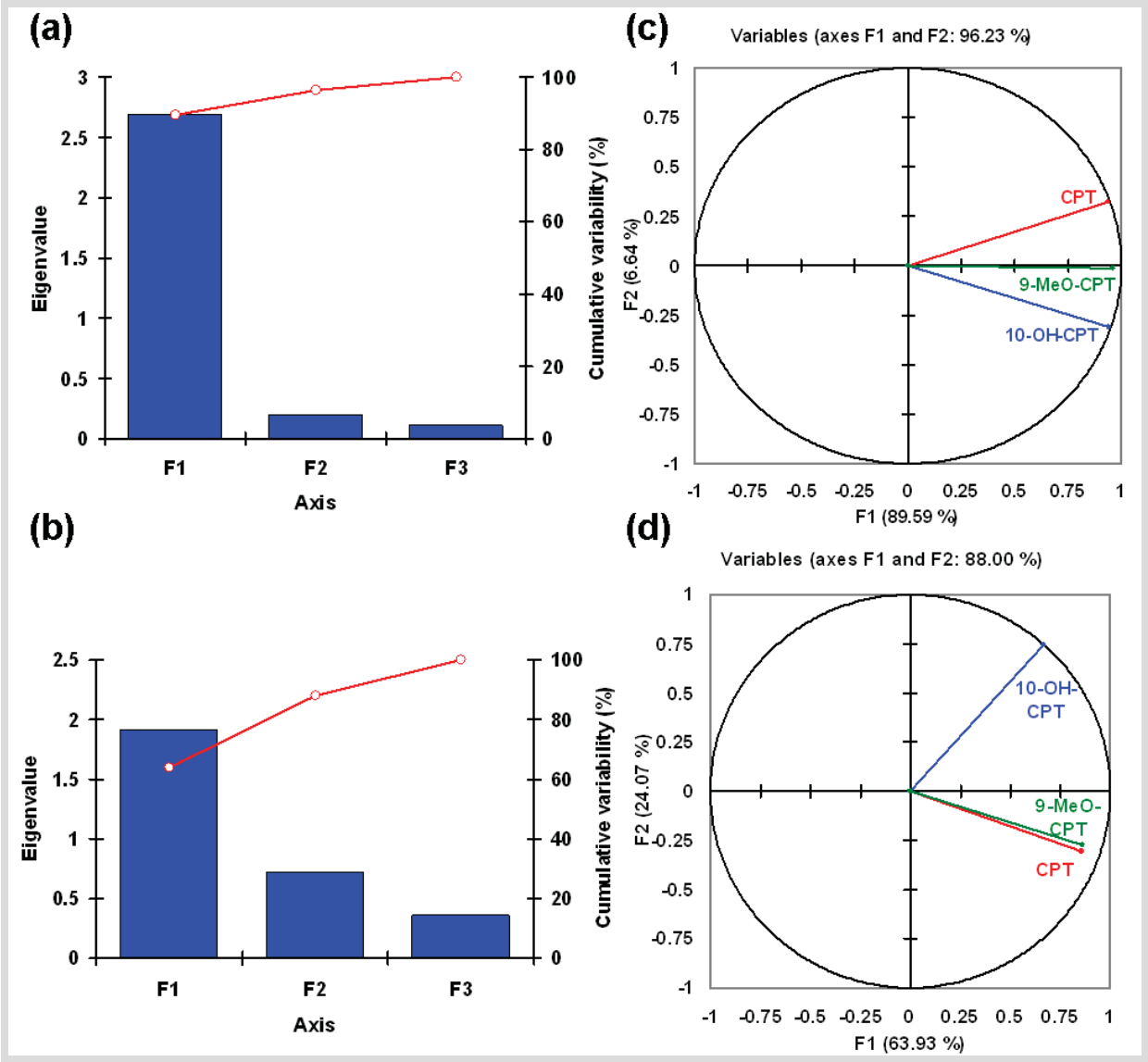

Fig. 30. PCA. (a) Scree Plot depicting the data variability in the three dimensions versus the cumulative variability, relative to the eigenvalues in the fresh tissue extracts of *Camptotheca*. (b) Scree Plot of the dried tissue extracts of *Camptotheca*. (c) The PCA Correlation Circle depicting the projection of the variables (phytochemicals) in the 2D space in *Camptotheca* for the fresh tissue extracts. (d) The PCA Correlation Circle for the dried tissue extracts.

The PCA for fresh tissues revealed CPT content to be positively correlated to both 9-MeO-CPT and 10-OH-CPT contents among the studied plants (Fig. 30c), corroborating the MDS. Like the MDS, the phytochemical correlations were observed to be reduced on drying. The PCA for the dried tissue extracts showed CPT to be positively correlated to 9-MeO-CPT and not to 10-OH-CPT; the Correlation Circle which depicted a near-orthonormal projection between CPT and 10-OH-CPT. Hence, an infrageneric correlation could not be drawn between these two metabolites. The F1/F2 comparison in the Scree plots further depicted the loss of phytochemical stability on drying.

1.1.4. Linear discriminant analysis (LDA)

In order to evaluate the chemotaxonomic significance (specificity of secondary metabolite profiles for individual plants) of the different plant samples under study and to visualize how the three metabolic constituents allowed discriminating the species (infraspecific), a LDA was computed, each based on the metabolite profiles of fresh and dried tissues, respectively. The results were visualized on a 2D map that depicted the degree of separation between the groups (Fig. 31).

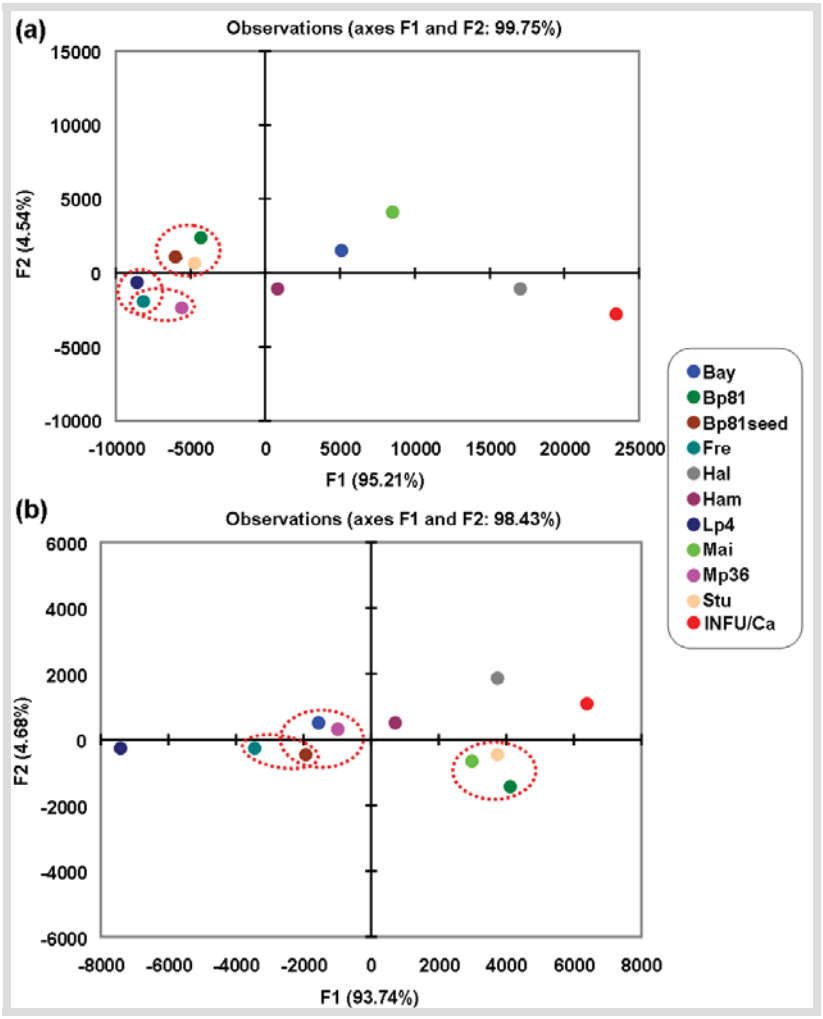

Fig. 31. 2D map of LDA. (a) Based on metabolite profiles of the fresh tissue extracts. (b) Based on metabolite profiles of the dried tissue extracts.

The LDA projection for *Camptotheca* taking into account the fresh tissue metabolite profiles (Fig. 31a) revealed that *C. acuminata* from China (INFU/Ca) was well separated from the rest of the plants. From the MVA, it was observed that this plant had the highest holistic phytochemical load among the all the tested plants, and therefore, the LDA projection classified this plant as distinct in metabolite spectrum and demarcated from other plant samples. Furthermore, the two plants from Hamburg (Bp81 and Bp81seed) along with the plant from Stuttgart, and the plants from Hamburg (Lp4) and Freiburg, and Hamburg (Mp36) and Freiburg were grouped in close confidence. On the other hand, the LDA projection taking into account the dried tissue metabolite profiles closely grouped *C. acuminata* from Hamburg (Bp81), Mainz, and Stuttgart, as well as the plants from Hamburg (Mp36) and Bayreuth, and Hamburg (Bp81seed) and Freiburg, respectively.

1.1.5. Hierarchical agglomerative cluster analysis (HACA)

For a clearer arrangement, the compounds measured were grouped in a manner that assigned similar behavior using HACA method by average linkage (Fig. 32).

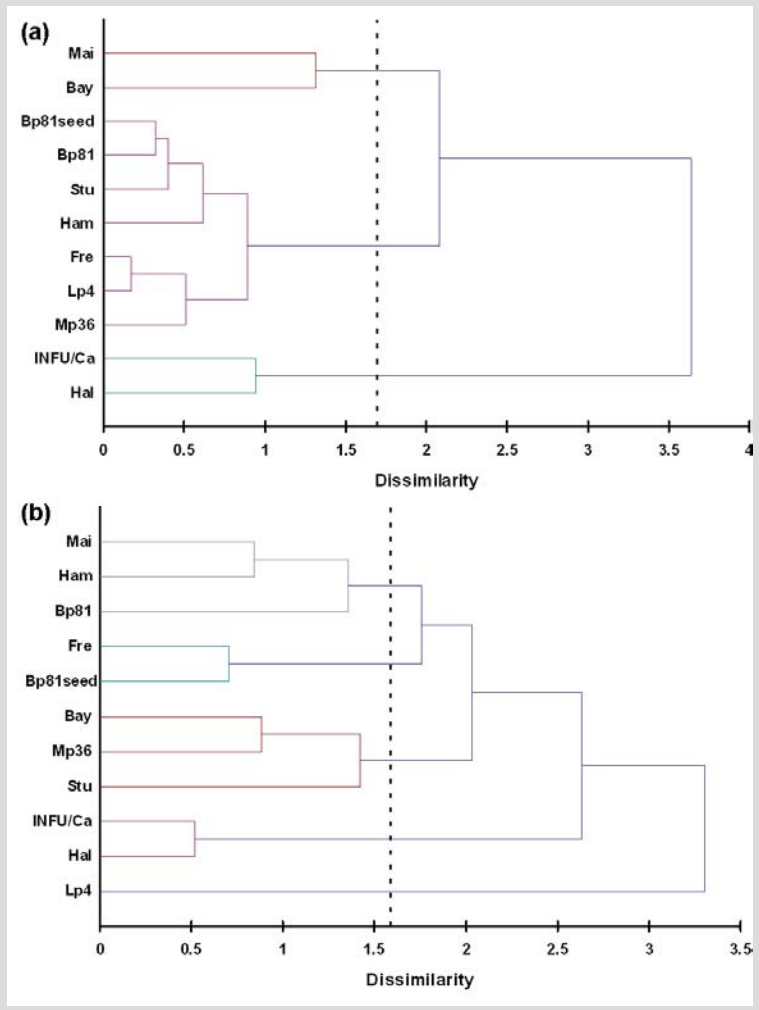

Fig. 32. Dendrograms by HACA plotting the various *Camptotheca* plant species under study versus CPT, 9-MeO-CPT, and 10-OH-CPT. (a) Fresh tissue extracts. (b) Dried tissue extracts.

Dissimilarity was measured by Euclidean distance using data of all three standard constituents under study, as well as for the different plant samples. The results were visualized by dendrograms. The dendrogram obtained by HACA plotting various *Camptotheca* plants versus each of the three phytochemical under study showed that *C. acuminata* from China (INFU/Ca) was well separated from all the other plants from all other locations except that from Halle (Hal) because the latter also contained high quantities of CPT and the two related metabolites. The fresh extracts led to *C. acuminata* from Hamburg (Bp81 and Bp81seed) and Stuttgart, as well as from Hamburg (Lp4 and Mp36) and Freiburg being in close confidence with each other. These relationships corroborate those represented by the LDA evaluations.

The dendrogram obtained by HACA plotting the various *Camptotheca* plant species (in dry extracts) under study versus each of the three secondary metabolites under study depicted the plants from Hamburg (Bp81 and Ham) and Mainz, as well as from Hamburg (Bp81seed) and Freiburg (Fre), and Bayreuth (Bay) and Hamburg (Mp36) into close confidence. Again, some of the original correlations were lost on drying the tissues.

1.2. Biological characterization of CPT producing endophytic fungus

1.2.1. Isolation and *in vitro* culture of the endophytic fungus

C. acuminata was chosen as the source for isolating the endophytes, since this plant contains CPT and related metabolites distributed in various organs (Wall *et al*., 1966; Lopez-Meyer *et al*., 1994; Yan *et al*., 2003). The analyses of *C. acuminata* from various parts of Germany and from China showed considerable amounts of CPT, 9-MeO-CPT and 10-OH-CPT in the host plants themselves. Therefore, a selective search for fungal endophytes was pursued using the rationale that the plants containing these antineoplastic molecules may also contain endophytic fungi that are able to accumulate the same or similar molecules.

Table 9 shows the number of endophytic fungi isolated from various organs of the *C. acuminata* plants, which were different morphologically from the strains isolated from unsterilized explants (surface-contaminating fungi). The selective media supporting the pure culture of fungi was noted, and the isolation of the endophytes was verified by performing the isolation of surface-contaminating fungi in parallel. Out of all endophytes, only one was able to produce CPT, 9-MeO-CPT and 10-OH-CPT (strain INFU/Ca/KF/3), and was taken up for further studies. Another endophytic fungus incapable of producing CPT (strain INFU/Ca/KF/2) was also obtained from the same bark explant as *F. solani* (INFU/Ca/KF/3), which was isolated for using as a reference organism in the Topo 1 (*Top1*) studies.

Table 9. The number of endophytic fungi isolated from different organs of the *C. acuminata* plants from various locations.

Plant	Plant Code	Organ	Number of isolated endophytic fungi
C. acuminata	INFU/Ca	Inner bark	11
		Leaves	4
C. acuminata	Lp4	Stems	6
		Leaves	3
C. acuminata	Mp36	Stems	7
		Leaves	3
C. acuminata	Bp81	Stems	4
		Leaves	5
C. acuminata	Bp81seed	Stems	5
		Leaves	5
C. acuminata	Fre	Stems	9
		Leaves	7
C. acuminata	Stu	Stems	4
		Leaves	2
C. acuminata	Bay	Stems	6
		Leaves	5
C. acuminata	Mai	Stems	6
		Leaves	1
C. acuminata	Ham	Stems	7
		Leaves	3
C. acuminata	Hal	Stems	9
		Leaves	6

1.2.2. Macroscopic morphological characteristics of the endophytic fungus on agar medium

The fungus (INFU/Ca/KF/3) was grown on various types of rich mycological media. The growth was rapid on SA, PDA, and CZA, though profuse growth could be observed on SA and PDA. On SA, copious amounts of aerial, surficial and submerged hyphae were observed that reached about 6-7 cm diameter in 5 days at 28 ± 2°C. The mycelia, initially white in color, sometimes became off-white to creamy at later stages of growth. Sporodochia could be seen as raised points by the naked eye, mostly creamy to pink in color (bluish-green to bluish-brown color not observed in this case). From the reverse side of the Petri dish, the color was creamy to creamy-orange. The morphology, however, became substantially altered on continuous subculturing. From the 3rd subculture generation onwards, the mycelia gradually became typically white to off-white in color even at the later stages of growth. The sporodochia could not be distinguished easily by the naked eye and the amount of aerial hyphae became multifold. The differences in the morphology on subculturing are shown in Fig. 33, wherein the

representative morphologies in the 1st and the 7th generations are depicted.

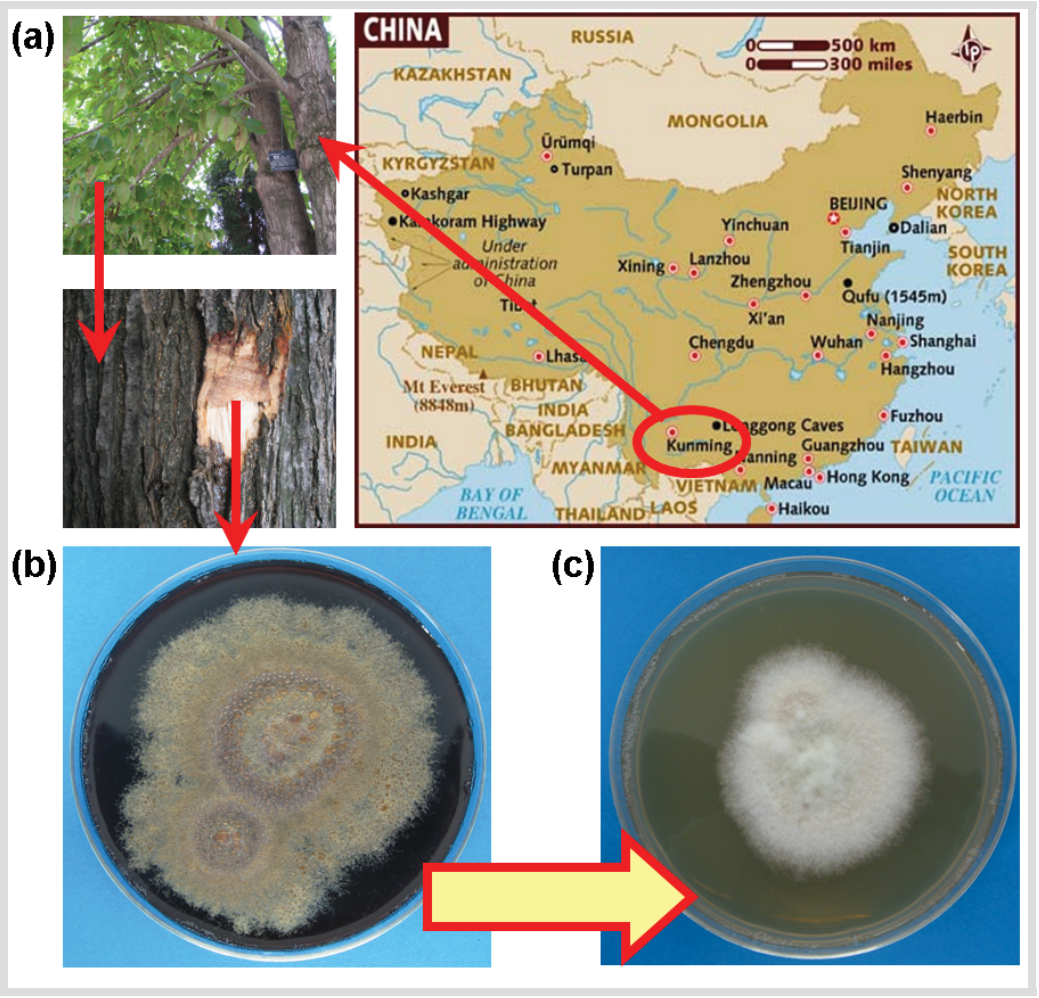

Fig. 33. Endophytic fungus, INFU/Ca/KF/3, isolated from *C. acuminata* (SWFU, China) growing on rich medium (SA) plate. (a) Kunming, China from where the *C. acuminata* inner bark was explanted for isolation of the CPT-producing endophyte. (b) The representative 1st generation morphology. (c) The representative 7th generation subculture morphology.

1.2.3. Macroscopic morphological characteristics of the endophytic fungus in broth medium

Under shake-flask conditions in SB, the fungus grew as white, non-sticky, and small to medium, round balls (Fig. 34). Pellicle formation at the edge of the flask was light and slightly sticky. Interestingly, the fungal mycelia did not show any coloration in submerged culture conditions, though the spent medium at the end of 5 days turned a little viscous and developed a dark brown to chocolate color. There was no change in the submerged morphology even on repetitive subculturing, though the viscosity and color change of the spent media were eventually reduced at the later generations (especially from the 4th generation onwards).

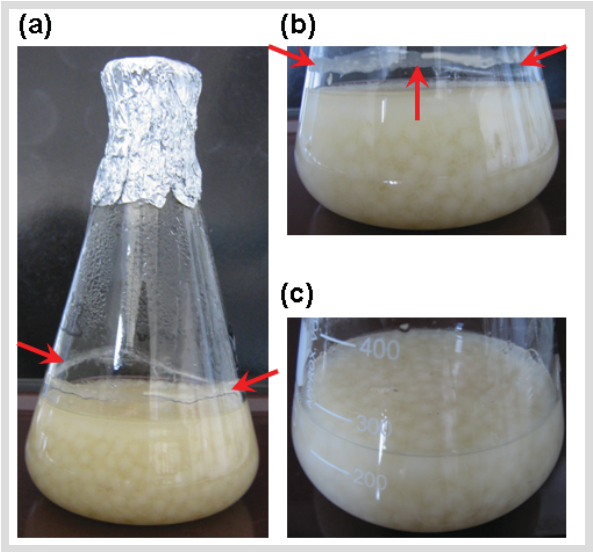

Fig. 34. The macroscopic morphological characteristics of the endophytic fungus in SB medium. (a) Fungal growth as white, non-sticky, small to medium, round balls. (b,c) Enlarged view at two different angles for closer visibility. The pellicle formation is shown by red arrows.

1.2.4. Microscopic morphological characteristics of the endophytic fungus

Microscopic studies of the fungus revealed the hyphae as septate and hyaline (Fig. 35). Conidiophores were simple (non-branched) and macroconidia were moderately curved, stout, thick-walled, 2-5 septate, measured up to about 70 µm long, and were borne on short conidiophores; these conidiophores could soon form sporodochia. Microconidia were borne from long monophialides, were one to three-four celled, about 2-5 x 8-16 µm long, and occurred in false heads only (in clusters of conidia at the tip of the phialide).

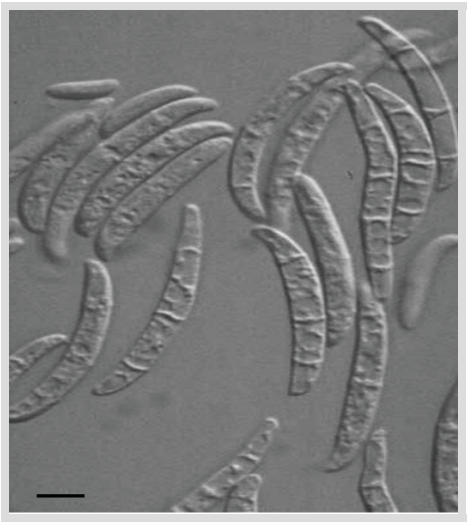

Fig. 35. The microscopic morphological characteristics of the endophytic fungus on SA medium. The characteristic curved, stout, macroconidia are clearly visible.

1.2.5. Identification and authentication of the endophytic fungus

The fungus has been identified as *Fusarium solani* based on its macroscopic and microscopic morphology, and authenticated by the molecular analysis (Fig. 36) of the ITS region of rDNA containing

ITS1, and ITS2, and the intervening 5.8S rRNA gene. The ITS-5.8S rDNA sequence obtained has been deposited into EMBL-Bank under accession number FM179605. The endophytic fungus has been deposited at DSMZ (accession number DSM 21921). The reference endophytic fungus (INFU/Ca/KF/2) was also treated in a similar manner and identified as *Albonectria rigidiuscula*. In turn, the ITS-5.8S rDNA sequence obtained for *A. rigidiuscula* has been deposited into EMBL-Bank under accession number FN667579.

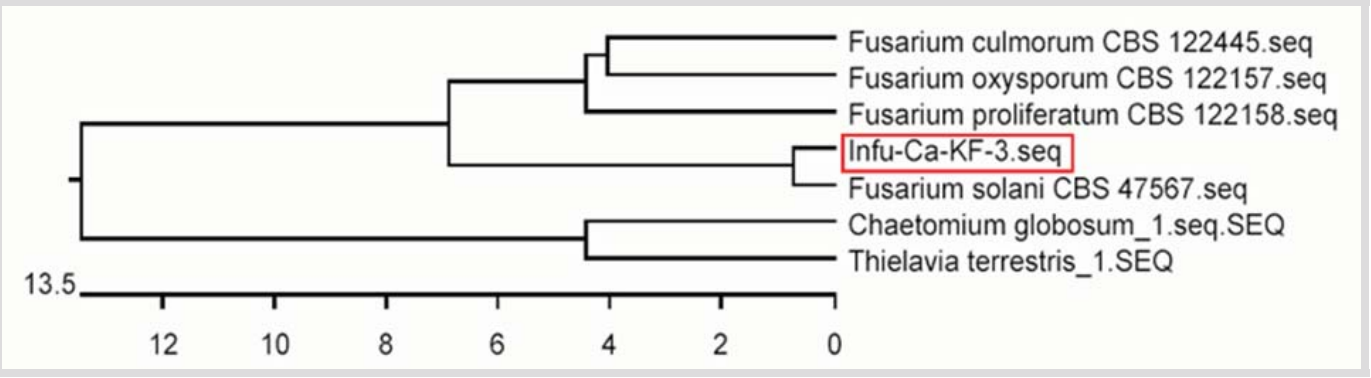

Fig. 36. Dendrogram showing the phylogenetic position of the CPT producing fungal isolate.

1.3. Biochemical characterization of CPT producing endophytic fungus

1.3.1. Structural elucidation of CPT, 9-MeO-CPT, and 10-OH-CPT

Both the fungal biomass and the culture media from grown cultures were assessed for the presence of CPT, 9-MeO-CPT, and 10-OH-CPT. The culture media did not yield any trace of these compounds. The identification of the compounds in the fungal biomass was achieved using LC-HRMS, LC-HRMS^2 and LC-HRMS^3 and by comparison with the authentic reference standards. Unfortunately, the 9-MeO-CPT produced by the cultured endophyte was not successfully elucidated by LC-NMR due to interference from other metabolites in the fungal extract, which were inseparable. Hence, 9-MeO-CPT was first isolated and established as an authentic standard from *N. nimmoniana* using LC-HRMS^3 and ^{1}H NMR spectroscopy in order to elucidate the exact position of the methoxy group, and thereafter fungal 9-MeO-CPT was confirmed. The ^{1}H NMR for 9-MeO-CPT (Fig. 37) is as follows:

9-MeO-CPT: ^{1}H NMR ($CDCl_3$, 400 MHz) δ 0.96 (3H, t, J = 7.5 Hz, H-18), 1.85 (2H, m, H-19), 3.99 (3H, s, OCH_3), 5.22/5.62 (4H, m, H-5/H-17), 6.91 (1H, d, J = 7.5 Hz, H-10), 7.64 (1H, s, H-7) 7.67 (1H, t, J = 7.5 Hz, H-11), 7.71 (1H, d, J = 7.5 Hz, H-12), 8.79 (1H, s, H-14).

Furthermore, we synthesized 10-methoxycamptothecin (10-MeO-CPT) from standard 10-OH-CPT by its reaction with an ether solution of diazomethane (30 min), which was identical to the 10-MeO-CPT from the host *C. acuminata* plant. The ^{1}H NMR for 10-MeO-CPT (Fig. 37) is as follows:

10-MeO-CPT: ^{1}H NMR ($CDCl_3$, 400 MHz) δ 1.03 (3H, t, J = 9 Hz, H-18), 1.88 (2H, m, H-19), 3.97 (3H, s, OCH_3), 5.29/5.72 (4H, m, H-5/H-17), 7.14 (1H, s, H-9), 7.47 (1H, d, J = 9 Hz, H-11) 7.61 (1H, s, H-7), 8.10 (1H, d, J = 9 Hz, H-12), 8.25 (1H, s, H-14).

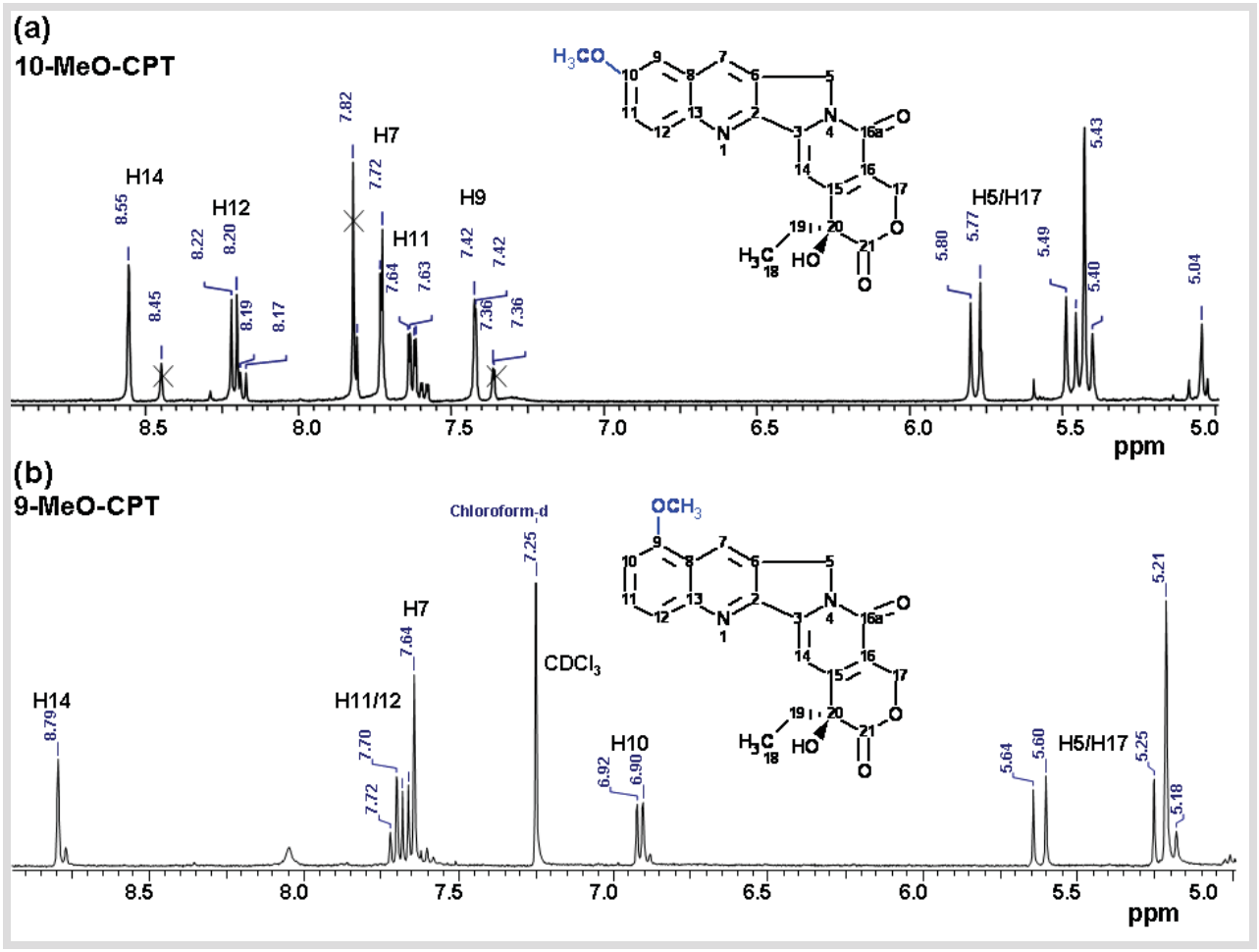

Fig. 37. The ^{1}H NMR spectra of MeO-CPT with methoxy group at positions 10 and 9.

The characteristic fragments of MS^3, together with a brief interpretation of the fragments and the comparison of the retention times, are presented in Figs. 38 and 39. It can be seen from Fig. 39e,f that there is a difference not only in the retention times between 9-MeO-CPT and 10-MeO-CPT but also in the intensities of the MS^3 fragments (*m/z* 320). Furthermore, there was no incorporation of the CD_3OD into the CPT moiety proving that 9-MeO-CPT was indeed the secondary metabolite produced by the cultured endophyte and not adduct. Interestingly, an additional isomeric-OH-CPT was accumulated by the cultured endophyte in addition to 10-OH-CPT in some generations only, having a different retention time (t_R) than 10-OH-CPT ($t_{R\ 10\text{-OH-CPT}}$ 22.29 min, $t_{R\ \text{isomeric-OH-CPT}}$ 22.95 min) but identical mass spectra, as shown in Fig. 38h. It is most probably the 9-OH-CPT isomer, which was lost completely in the later subculture generations.

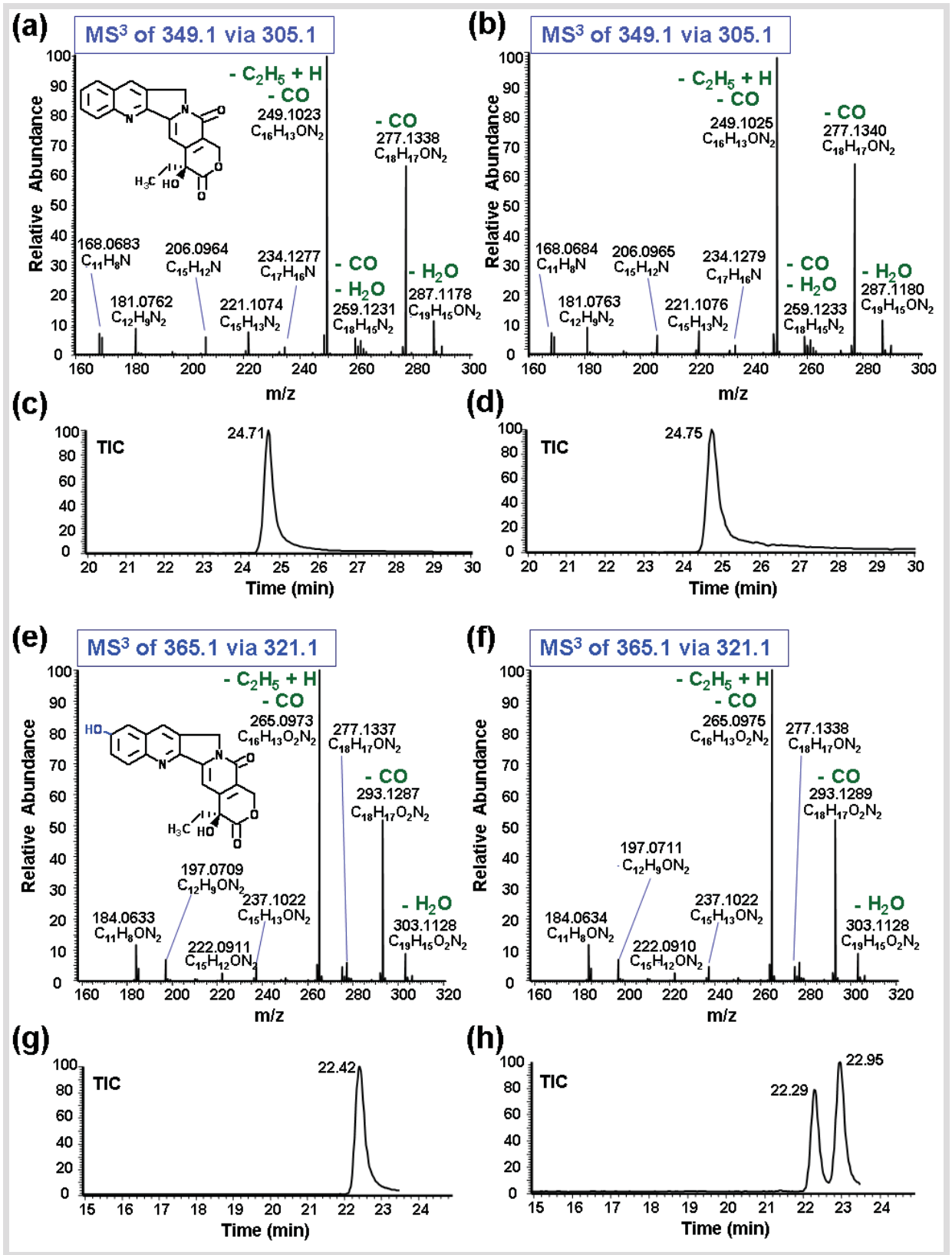

Fig. 38. High-resolution MS^3 product ion spectra and TICs of the tested compounds. (a,c) Standard CPT. (b,d) Fungal CPT. (e,g) Standard 10-OH-CPT. (f,h) Fungal 10-OH-CPT.

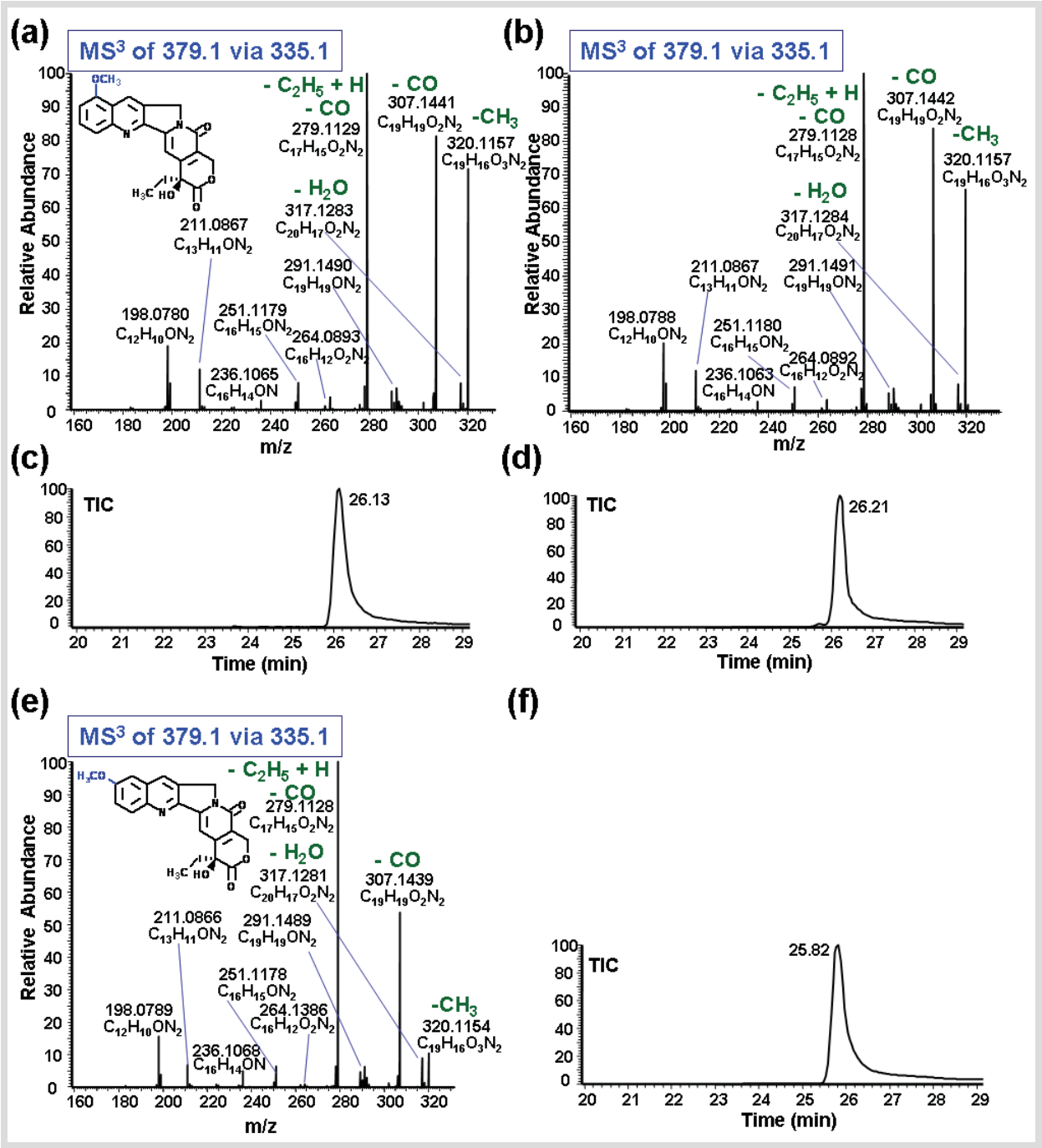

Fig. 39. High-resolution MS^3 product ion spectra and TICs of the tested compounds. (a,c) Standard 9-MeO-CPT. (b,d) Fungal 9-MeO-CPT. (e,f) 10-MeO-CPT (from *C. acuminata* host plant).

1.3.2. Growth kinetics of the endophytic fungus

The growth kinetics of the endophytic fungus was examined up to the ninth day (216 h) of incubation. The endophyte exhibited an exponential increase in the dry weight of mycelia up to the ninth day (216

h) of incubation under submerged axenic conditions (Fig. 40). Growth commenced immediately after the fermentation was started. The steep biomass accumulation revealed the immediate onset of tropophase of the endophyte (vigorous growth phase).

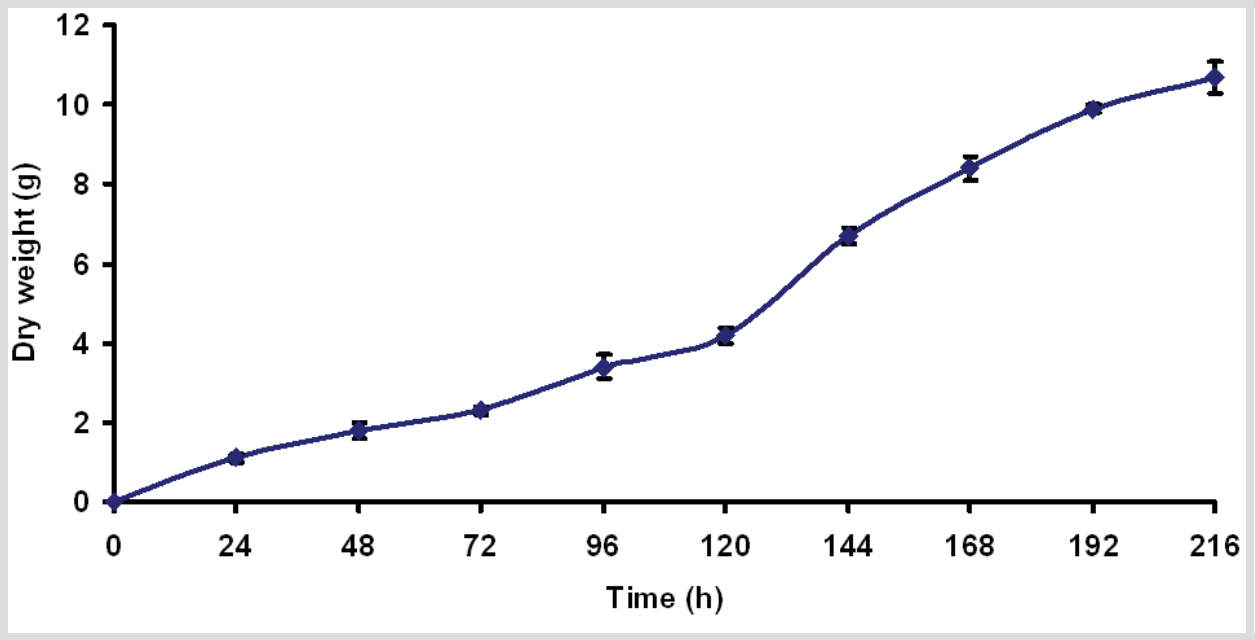

Fig. 40. Growth kinetics of the cultured endophytic fungus, *F. solani*.

1.3.3. Production kinetics of the endophytic fungus

In order to study the production kinetics of CPT, 9-MeO-CPT, and 10-OH-CPT, the mycelia were collected every 24 h and metabolites were isolated from both the mycelia and spent broth. The contents of CPT, 9-MeO-CPT, and 10-OH-CPT in the organic extracts of mycelia and broth, collected at periods of regular time intervals, were determined to provide an insight into the production kinetics as a function of time (Fig. 41). Maximum production of both CPT and 9-MeO-CPT was observed on day 3 (72 h) in terms of µg 100 g^{-1} dry weight of mycelia, although their formation started as early as 24 h. Their content gradually declined after 72 h of incubation till the termination of fermentation (216 h). On the other hand, 10-OH-CPT could be detected from 24 h till the termination of fermentation in only two replicates, but could not be quantified at any stage of fermentation (<LOQ). None of the three metabolites was detected in the spent medium (broth) revealing that these were accumulated as intracellular metabolite without being released into the medium. Furthermore, the formation of neither CPT, 9-MeO-CPT, or 10-OH-CPT could be observed in inoculated, extracted and processed culture broths at the start of the experiment (0 h). This eliminated the possibility that any of these secondary metabolites had been carried-over from the original plant material to the fungus via the mycelia

(inoculum plugs). This study thereby unequivocally established the novel production of CPT, 9-MeO-CPT, and 10-OH-CPT by the endophytic fungus.

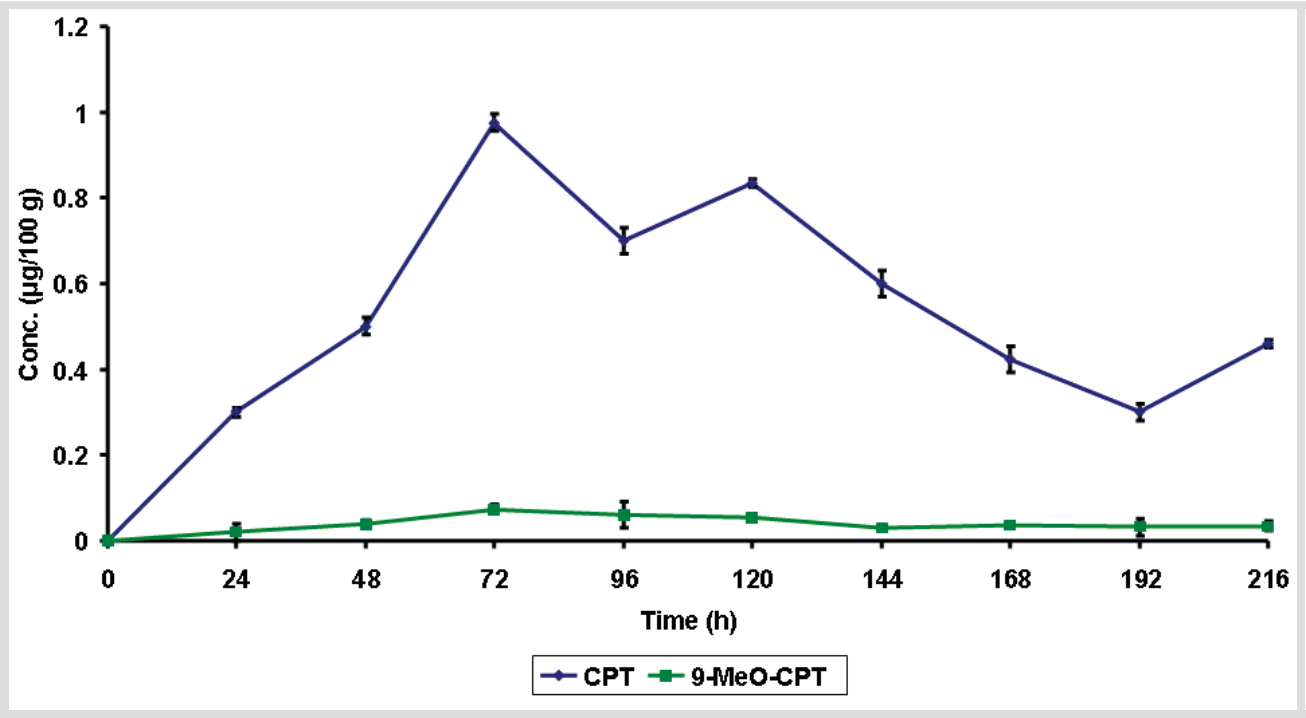

Fig. 41. Intracellular secondary metabolite concentration of the cultured endophyte at different time points of fermentation.

1.3.4. Reduction of CPT, 9-MeO-CPT and 10-OH-CPT production on subculturing

A detailed study of metabolite production was undertaken over generations (Fig. 42). In shake-flask incubations of the endophytic fungus, an inverse relation between the hyphal biomass and the respective CPT and 9-MeO-CPT production across the first to the seventh generation was found. The inverse relation was strong from the third to the seventh generation, where the levels of CPT and 9-MeO-CPT were substantially reduced. Interestingly, the endophytic production of 10-OH-CPT was detected only from the fourth generation, which remained almost constant through to the seventh generation. However, 10-OH-CPT could not be quantified because the production up to the third generation was below the limit of detection (<LOD) and from the fourth to seventh generation was below the limit of quantitation (<LOQ). Optimized fermentation conditions and addition of precursors as well as various host plant tissue extracts (Table T1, Appendix A) did not restore the production of CPT, 9-MeO-CPT or 10-OH-CPT; although the biomass accumulation varied with different nutrient source and host extract. It was observed that the addition of the various forms of host extract substantially increased the biomass accumulation without restoring the biosynthesis of the cultured endophyte.

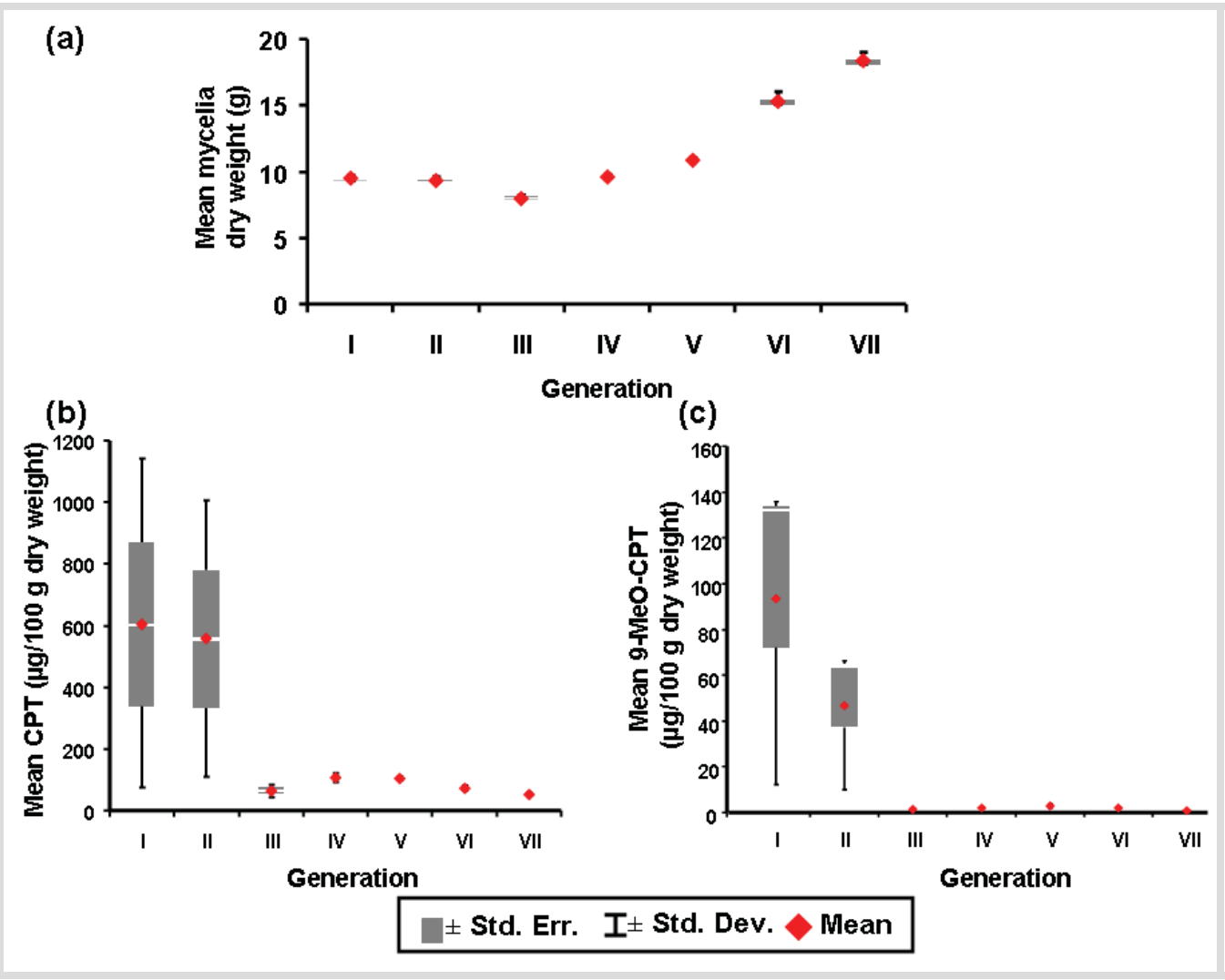

Fig. 42. Box and Whisker's plot of the metabolite production pattern by the endophytic fungal isolate from the 1st to the 7th subculture generation under shake-flask conditions and their correlation with the fungal biomass accumulation. (a) Mean fungal biomass dry weight. (b) Mean CPT. (c) Mean 9-MeO-CPT. n = 3.

1.3.5. Topo 1 (*Top1*) structure of endophytic *F. solani*

CPT induces cell death by targeting Topo 1, the enzyme that catalyzes changes in DNA topology. The primary structure of the Topo 1 (translated by *Top1* gene) in endophytic *F. solani* was studied (Fig. 43a-d). In addition, the Topo 1 structure of endophytic *A. rigidiuscula* (coded INFU/Ca/KF/2) was evaluated. This was obtained as an associated endophytic fungus incapable of biosynthesizing CPT, isolated from the same bark explant as that of *F. solani*. The reason for such a comparison was to understand the fate and relationship of other associated endophytes present in *C. acuminata* that do not produce CPT, but which might be exposed to the accumulated host-CPT. This comparison was further extended to

the Topo 1s of host *C. acuminata* (Ca), two other CPT-producing plants *Ophiorrhiza liukiuensis* (Ol) and *Ophiorrhiza pumila* (Op), CPT-lacking *Ophiorrhiza japonica* (Oj), *Saccharomyces cerevisiae* (Sc), *Homo sapiens* (Hs), and *Fusarium culmorum* (Fc); the latter belongs to the same genus as the CPT-producing endophyte with a reported *Top1* sequence.

This study revealed that neither the CPT-producing nor the CPT-lacking fungal Topo 1 possessed the three amino acid residues which are proposed to cause CPT resistance in the CPT producing plants. Instead, *F. solani* revealed amino acid residues N421 (similar to Op and Ol), L530 (similar to Ca), and N722 (dissimilar to all other CPT-producing plants compared), respectively (Fig. 43b). Both fungal Topo 1s revealed residues N352, E356, and G503 which modulate the CPT-Topo1-DNA binding. Also, the highly conserved residues at the active site (R488, K532, R590, H632 and Y723) assigning the catalytic function were not altered in the endophytes. Several other known mutations triggering previously identified or predicted CPT resistance in Topo 1 were not found in the endophytes. Tyrosine T370 in the endophytes' Topo 1s represented the same residue as found in mutated Topo 1 (M370T) of human CPT resistant cancer cells (CEM/C2) as also in CPT sensitive *S. cerevisiae*; therefore, the mutation might not contribute to CPT resistance (Fujimori *et al*., 1995). The comparison of the endophytic Topo 1 sequences with mutations associated with CPT resistance revealed only variation at the residue G653 in both endophytes and closely related *F. culmorum*. The previously reported mutation of A653P in the linker of human Topo 1 increased the rate of enzyme-catalyzed DNA religation, thereby rendering Topo 1 resistant to CPT (Fiorani *et al*., 2003). Although the residue at position 653 was not the same as that published by Fiorani *et al*. (2003) for the CPT resistant Topo 1, the changes in flexibility or orientation of the linker might alter the geometry of active site and thereby the kinetics of DNA cleavage/religation catalyzed by Topo 1 (Lasasso *et al*., 2007). Even though the evaluation of the Topo 1 structure of endophytic *F. solani* with emphasis on the CPT binding and catalytic domain bound with the published or predicted resistance-mediating amino acids revealed variation only in one residue (G653), higher difference between human or plant and fungal Topo 1s is present (Fig. 43d).

1.3.6. CPT biosynthetic steps in the endophytic fungus

The key steps of CPT biosynthesis in the endophytic fungus, *F. solani*, were elucidated in order to understand the mutualistic association of the endophyte with the host plant and the reason for the reduction of CPT production on subculturing. The presence of the *G10H* (geraniol 10-hydroxylase), *SLS* (secologanin synthase), *TDC* (tryptophan decarboxylase) and *STR* (strictosidine synthase) genes in the endophytic fungal genome (first generation, coded INFU/Ca/KF/3/I) were screened using the gene-specific and/or degenerate primers. Amplification products of the expected sizes were obtained using the primers designed for *G10H*, *SLS* and *TDC* (Fig. 44a and Table T4 in Appendix A).

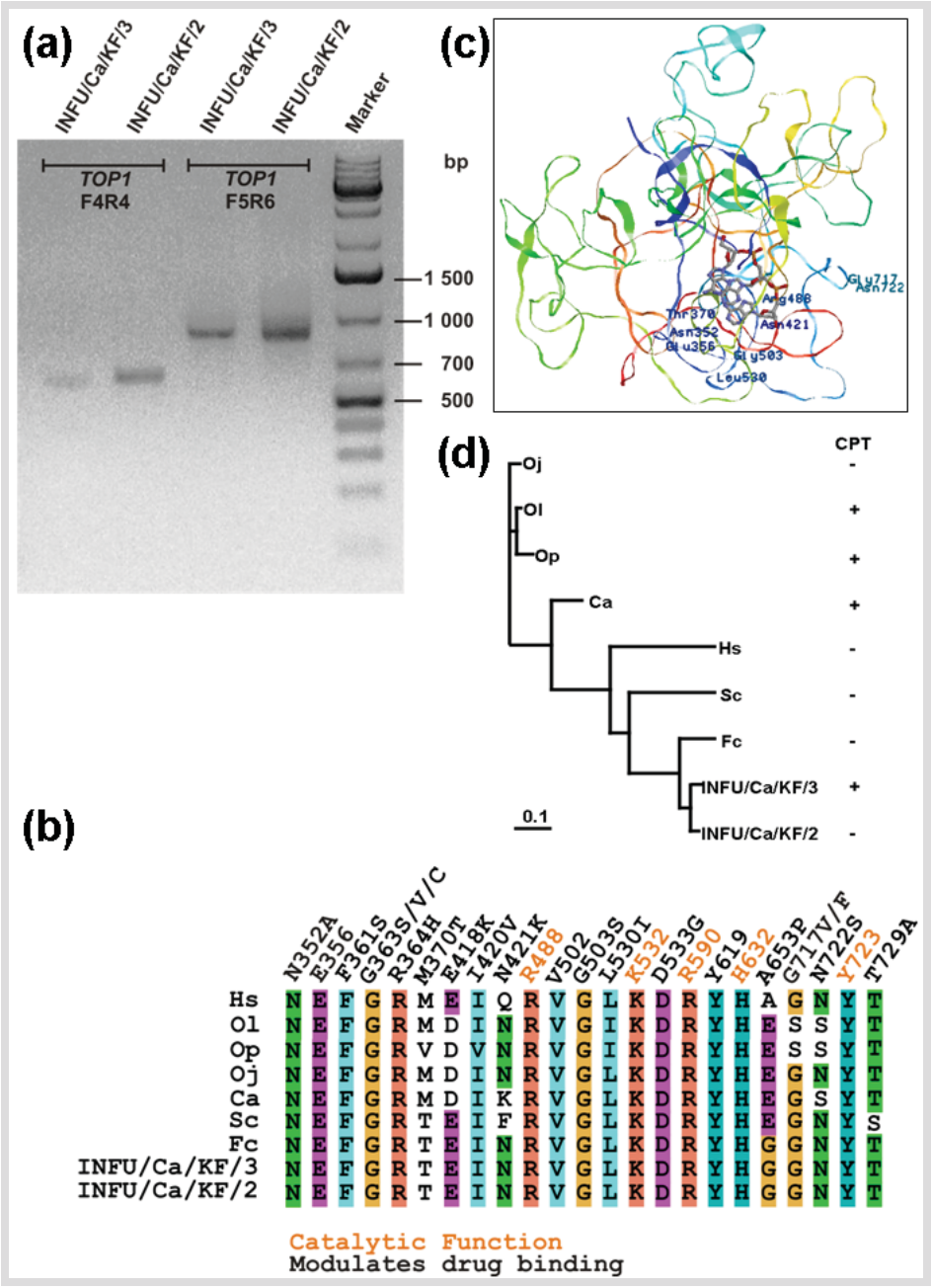

Fig. 43. The architectural study of Topo 1 encoded by *Top1* in endophytic *F. solani* INFU/Ca/KF/3 compared to other related and non-related taxa. (a) The stained agarose gel of RT-PCR-amplified partial cDNA from *F. solani* and associated *A. rigidiuscula* encoding Topo 1. Desired products were obtained using gene-specific and/or degenerate primers under optimized PCR conditions with specific templates. (b) Variability of the amino acid sequence in the Topo 1 associated with its function or modulation of CPT binding in *F. solani* (INFU/Ca/KF/3) as compared to its associated *A. rigidiuscula* (INFU/Ca/KF/2), the host *C. acuminata* (Ca), two CPT-producing plants *O. liukiuensis* (Ol) and *O. pumila* (Op), CPT-lacking *O. japonica* (Oj), *F. culmorum* (Fc), *S. cerevisiae* (Sc), and *H. sapiens* (Hs). The residues of the catalytic domain are marked in orange color. Known CPT resistance mutations are marked. The residues are numbered according to the human Topo 1. (c) The schematic representation of the three-dimensional structure of *F. solani* Topo 1 showing the amino acid residues on the CPT binding and catalytic domains as detailed in the text. (d) Dendrogram depicting the neighbor-joining phylogram analysis based on *Top1* of endophytic *F. solani* as compared to others. CPT production is indicated by '+' or '-'.

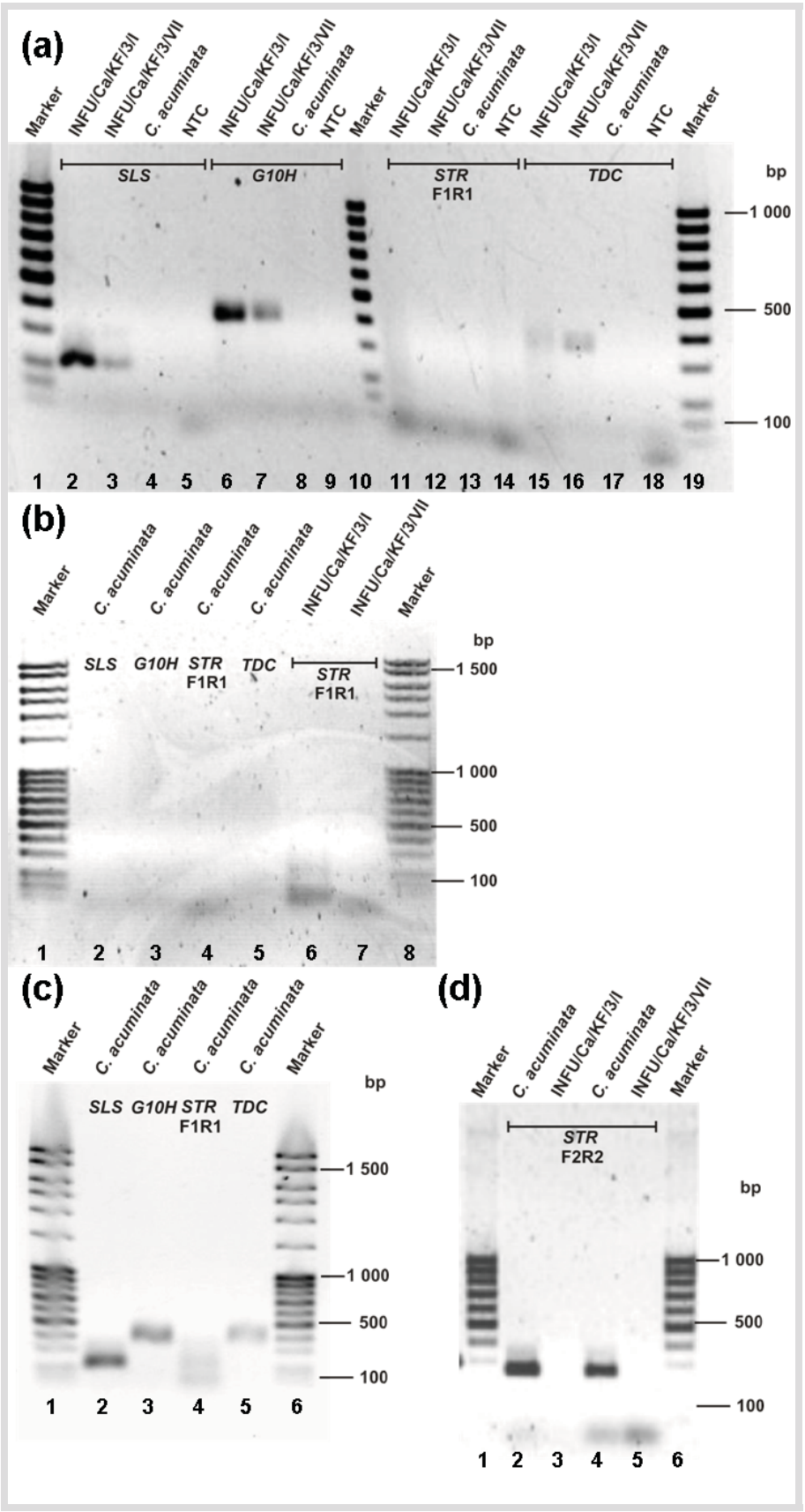

Fig. 44. The stained agarose gels of PCR-amplified DNA from endophytic *F. solani* in its first (INFU/Ca/KF/3/I) and seventh (INFU/Ca/KF/3/VII) generation subcultures, and from the *C. acuminata* host plant, encoding geraniol 10-hydroxylase (*G10H*), secologanin synthase (*SLS*), tryptophan decarboxylase (*TDC*) and strictosidine synthase (*STR*). (a-d) Desired products were obtained in each case using gene-specific and/or degenerate primers under optimized PCR conditions with specific templates, as detailed in the text. NTC, No Template Control.

The deduced amino acid sequence of the fungal *G10H* revealed 100% homology to the geraniol 10-hydroxylase enzyme (EC 1.14.14.1; UNIPROT: Q8VWZ7). The translated product of fungal *SLS* exhibited 100% homology to the cytochrome P450 (UNIPROT: Q42700) and secologanin synthase enzyme (EC 1.3.3.9; UNIPROT: Q05047). The translated *TDC* protein sequence from the endophyte *F. solani* showed homology (100%) to tryptophan decarboxylase enzyme (EC 4.1.1.28; UNIPROT: P93082). Interestingly, no product was obtained with any *STR* gene-specific primers (located in highly conserved regions) under any PCR conditions (Fig. 44b,d). Since no gene coding for strictosidine synthase that is responsible for the condensation of secologanin and tryptamine was found in the genome of the endophytic fungus, the contribution of the host plant in completing the biosynthesis of CPT could be attributed.

1.3.7. Use of the host strictosidine synthase by the endophytic fungus

In order to evaluate whether the host plant (*C. acuminata*) actually contributes to the completion of the *in planta* fungal CPT biosynthesis, the *STR* gene was isolated and characterized from the *C. acuminata* genome using *STR* gene-specific primers. An amplification product of desired size was obtained using suitable *STR* primer set, under optimized PCR conditions and multiple purification of the gDNA from interfering agents (Fig. 44c,d and Table T4 in Appendix A). The deduced amino acid sequence revealed 100% (UNIPROT: P18417) and 86% (UNIPROT: P68175) homology to the strictosidine synthase enzyme (EC 4.3.3.2). Thus, it was revealed that the endophytic fungus utilized host strictosidine synthase to condense tryptamine with secologanin to form strictosidine, which it would have carried-over into its biomass during the isolation procedure. The absence of *STR* in the endophytic fungus (Fig. 44d) and the analyses of the plant *G10H*, *SLS*, and *TDC* sequences (Fig. 44c) further confirmed that none of the genes identified in the endophyte were the remnants of host plant DNA in the fungal biomass. Thus, a cross-species CPT biosynthetic pathway was deciphered. However, this biosynthetic mechanism is not the sole cause of the observed reduction of *in vitro* fungal CPT biosynthesis (*vide infra*) for all attempts in reversing it have been unsuccessful.

1.3.8. High-precision isotope-ratio mass spectrometry confirmed contribution of the host plant

Using the high-precision isotope-ratio mass spectrometry (HP-IRMS) by compound-specific carbon isotope (CSCI) and compound-specific nitrogen isotope (CSNI) modules, it was confirmed that the endophytic fungus actually utilizes host strictosidine synthase. The CPT produced by the cultured endophyte (first generation, INFU/Ca/KF/3/I) outside the host plant in a nitrogen-free media was compared to CPT from the tissue (not containing *F. solani* INFU/Ca/KF/3) of original *C. acuminata* host

(from SWFU) to check both the $\delta^{13}C/^{12}C$ (by CSCI) and the $\delta^{15}N/^{14}N$ (by CSNI). It was possible to trace the exact pattern of the accumulation of both 'carbons' and 'nitrogens' with the source of the enzyme(s) (fungal or plant) concerned up to and including the formation of CPT in the endophytic fungus and in the host plant. The $\delta^{13}C/^{12}C$ of the endophytic and plant CPT were found to be 27.65 ± 0.1‰ and 28.46 ± 0.08‰, respectively (Fig. 45a). This significant difference between the stable carbon isotope ratios of the CPT biosynthesized by the endophyte and the plant, thus, corroborates the conclusion from the homology-based approach that the building of the carbon skeleton in the endophyte has been achieved indigenously by the fungal enzymes. The carbon signature of the culture media contributed partly towards the observed variation in $\delta^{13}C/^{12}C$ values. On the other hand, the $\delta^{15}N/^{14}N$ ratios of the endophyte and plant CPT were found to be 5.13 ± 0.1‰ and 5.10 ± 0.03‰ (Fig. 45b). That is, no significant difference between the stable nitrogen isotope ratios of the CPT produced by the endophyte and the plant was observed. This established without doubt that the endophytic fungus utilizes the plant strictosidine synthase enzyme, which has been carried-over into the biomass of the isolated endophyte.

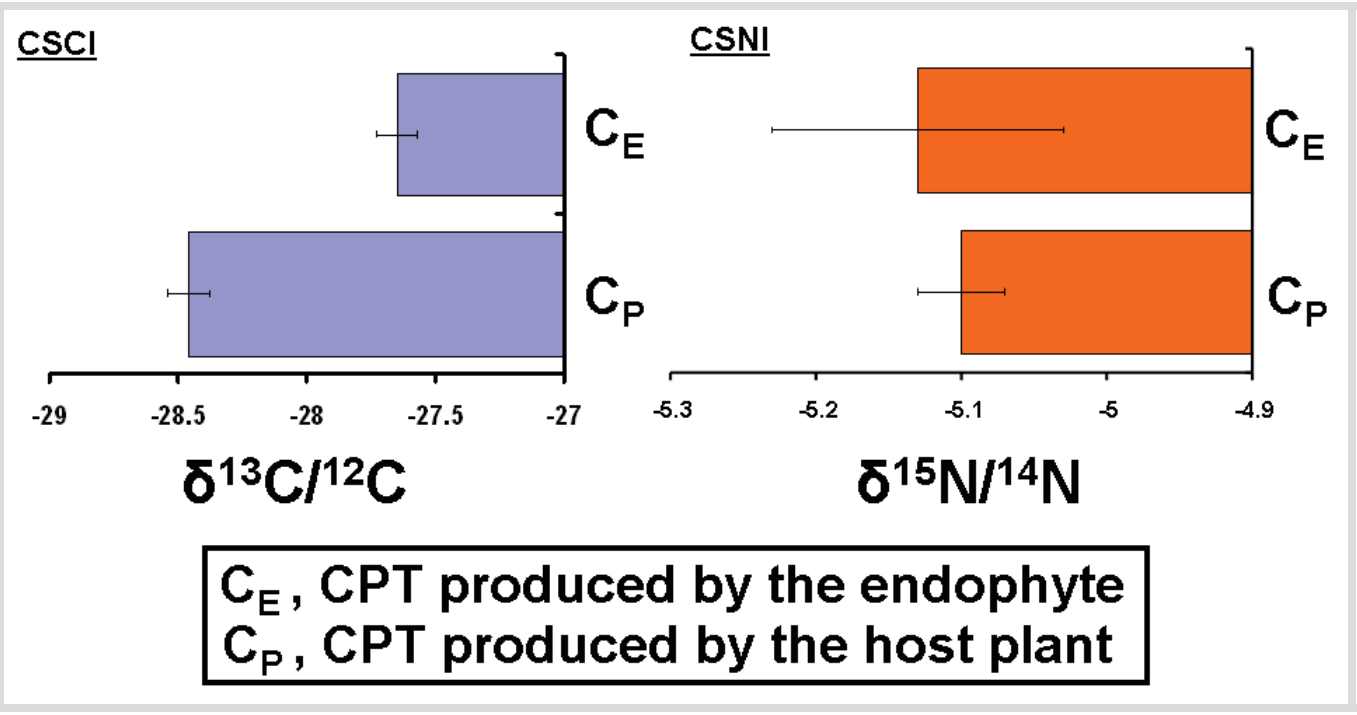

Fig. 45. HP-IRMS plots by CSCI and CSNI showing the $\delta^{13}C/^{12}C$ and the $\delta^{15}N/^{14}N$ ratios between the CPT biosynthesized by the endophytic fungus (*F. solani* INFU/Ca/KF/3) and the original host plant (*C. acuminata*), respectively.

1.3.9. *Ex planta* genomic instability from first to seventh generation subculture

The elucidation of the key CPT biosynthetic steps in the first generation of the fungus paved the way to ascertain whether the *ex planta* environment (i.e., *in vitro* axenic conditions) led to the instability of the

CPT biosynthetic genes over subculture generations, thereby impairing CPT biosynthesis. The same products were isolated from the genome of the endophytic fungus in its seventh subculture (INFU/Ca/KF/3/VII) as it was done for the first generation. Using the same primers and PCR conditions as for the first generation, specific products with the desired sizes were obtained for *G10H*, *SLS* and *TDC* in the seventh generation (Fig. 44a and Table T4 in Appendix A). Like the first generation, *STR* was not found in the seventh generation (Fig. 44b,d). The obtained PCR products were sequenced to check whether there might be some alteration or instability in the endophytic genome under *in vitro* conditions over several subcultures. This approach consisted of comparing all deduced translation products with the databases, as it was carried out with the first generation. *G10H*, *SLS*, and *TDC* revealed non-synonymous mutations which exhibited highly reduced homologies to the original products: at least 96% for *G10H*, 86% for *SLS*, and 48% for *TDC* at the amino acid level. The homologies always varied in different replicates revealing that the mutations in CPT biosynthetic genes were not always the same on repeated subculturing. Hence, instability of the fungal CPT biosynthetic genes under axenic conditions was ascertained.

1.3.10. Instability of CPT biosynthetic genes led to dysfunctional proteins

The effects of genomic alterations on the final enzyme identities were evaluated to confirm the cause of impaired CPT biosynthesis. The EMBOSS-WATER bioinformatics tool based on the Smith-Waterman local alignment algorithm (Smith and Waterman, 1981) was utilized, to align (local) and compare the predicted structure of the fungal enzymes in the seventh generation subculture to that of the original enzymes in the first generation. Genomic alterations leading to irreversible dysfunction at the amino acid level were revealed; the seventh generation predicted proteins exhibited only 98.1 to 99.4% (*G10H*), 92.0 to 98.8% (*SLS*), and 47.6 to 81.7% (*TDC*) similarities to the original enzymes. The homologies always varied within this range in different replicates revealing that the mutations in CPT biosynthetic genes were not always of the same type on repeated subculturing. Furthermore, the EMBOSS-NEEDLE bioinformatics tool based on the Needleman-Wunsch global alignment algorithm (Needleman and Wunsch, 1970) was used, to evaluate the optimal globally aligned dynamic scores of the seventh generation predicted proteins with that of the general structures of the actual enzymes. The results agreed with the local alignment scores, revealing that degradation of CPT biosynthetic genes under *ex planta* axenic conditions led to dysfunctional proteins; the seventh generation predicted proteins exhibited only 86.6 to 99.1% (*G10H*), 84.6 to 98.2% (*SLS*), and 22.4 to 70.2% (*TDC*) similarities to the general structures of the original proteins, in different replicates. The primary structure of the control gene *Top1* was, however, not degraded or destabilized over repeated *in vitro* sub-culturing, revealing that instability of the CPT biosynthetic genes was not reflected on the primary

metabolic processes in the endophytic fungus. Furthermore, the ribosomal RNA gene in the endophytic isolate at its seventh generation was checked. It was revealed that the fungal rDNA was still intact as the first parent isolate even in the seventh subculture. Thus, it was proved that the primary metabolic processes and the functions of the housekeeping genes were not destabilized on repeated subculturing.

1.3.11. *In vitro* inoculation of endophytic *F. solani* for *in planta* colonization to restore CPT biosynthesis

Endophytic *F. solani* starts to lose its genetic programming for the biosynthesis of CPT in axenic conditions. Drawing analogy to the golden standards laid down by Koch's postulates for classical microbiology (Hildebrand *et al.*, 2004; Partida-Martinez and Hertweck, 2005), attempts were made to reverse the impaired CPT biosynthesis by artificially re-infecting the *C. acuminata* host with the endophytic *F. solani* at its seventh generation subculture (INFU/Ca/KF/3/VII). The different target host plants were selected on the basis of the criteria for setting up the experimental model for the artificial inoculation of endophytic *F. solani* with the aim of recovering and characterizing it after *in planta* colonization. Firstly, none of the endophytic fungi isolated from the target host plants were capable of producing CPT or structural analogues. Secondly, none of the isolated endophytic fungi was *F. solani* (strain INFU/Ca/KF/3). Finally, *in vitro* antagonism of each of the isolated endophytes with INFU/Ca/KF/3 and with each other, and between that of INFU/Ca/KF/3 and INFU/Ca/KF/2 (Fig. 46) were evaluated.

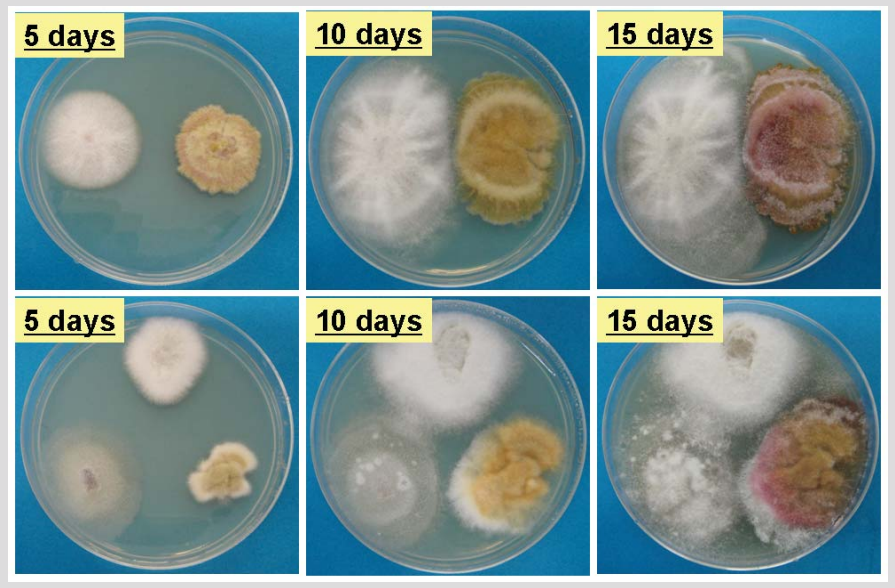

Fig. 46. The *in vitro* agar-plate based antagonism study between the various endophytic fungi. Representative plates showing how the agar-plates were observed when considering the antagonism study between two endophytes and three endophytes in parallel. The growth after 5, 10 and 15 days are shown.

The endophyte was inoculated into the leaves and stems of the target host plants. No apparent stress was observed in the plants after successfully inoculating the fungal endophyte, and there was no visible damage to the leaves and stems apart from the puncture wounds themselves (Figs. 47a-c, 48a-g), similar to the control. From the leaf inoculations, fungi with white or off-white mycelia emerged on the agar plates both from the site of wound and in many cases, from the edge of the leaf blades too (Fig. 47d-h) after 48 to 72 h. The fungi always emerged out first at the wound site followed by emergence from the blade edge. The position on the plant where the leaf was situated did not affect the success of inoculation and recovery of the endophytic fungus. In those cases where the fungus emerged from the leaf blades (a few cm from the inoculation wound), tissue colonization had occurred well away from the inoculation site demonstrating the affinity and specificity of the endophyte for the host. Additionally, there was no visible manifestation of the artificially established endophyte in the live host tissues even at the wound sites corroborating the host-affinity and the true endophytic nature of *F. solani* (INFU/Ca/KF/3). In case of stem inoculations, recovery was higher for the inoculations in the upper part of the plants. The fungi emerging from the wound-inoculated stem pieces were visible only after 120 h of incubation indicating that the colonization by the established endophyte was much slower in the stems than in the leaves. It might be due to the compactness of the stem tissues. Unlike the leaves, no fungi emerged from the wound sites; they emerged on all sides of the excised stem pieces starting close to the wound and then later further away (Fig. 48h,i). The colonized endophyte emerged from the leaf and stem tissues within 10-12 days, whereas no other resident endophyte emerged so fast, as expected, thus demonstrating a possible ‘axenic growth inertia’ resulting from repeated *in vitro* subculture.

1.3.12. CPT pathway not restored in recovered endophytic *F. solani*

The axenic morphology of the infecting *F. solani* (INFU/Ca/KF/3/VII) was compared with that of the recovered fungi (Fig. 49a,b). Strikingly, the morphology of recovered *F. solani* was similar to that of the original *F. solani* INFU/Ca/KF/3 culture in its first generation. The emergence-pattern of the established endophyte from the plant tissues was evaluated (Fig. 49c,d). The straight and pointed hyphae of the emerging fungi corroborated the plausible ‘axenic growth inertia’ gained during their existence under *in vitro* conditions. Furthermore, SEM was performed on both the endophyte used for inoculating the plants and the recovered endophytes for comparative evaluation (Fig. 49e-i). SEM revealed that the infecting *F. solani* was composed primarily of straight, overlapping, compact and pointed hyphae in a particular direction before the host-infection. However, the recovered *F. solani* contained several intertwined, criss-cross, and meshed hyphae resembling a net. This was possibly due to the conversion of the ‘axenic growth inertia’ (*ex planta*) to the ‘inertia of exploration’ (*in planta*).

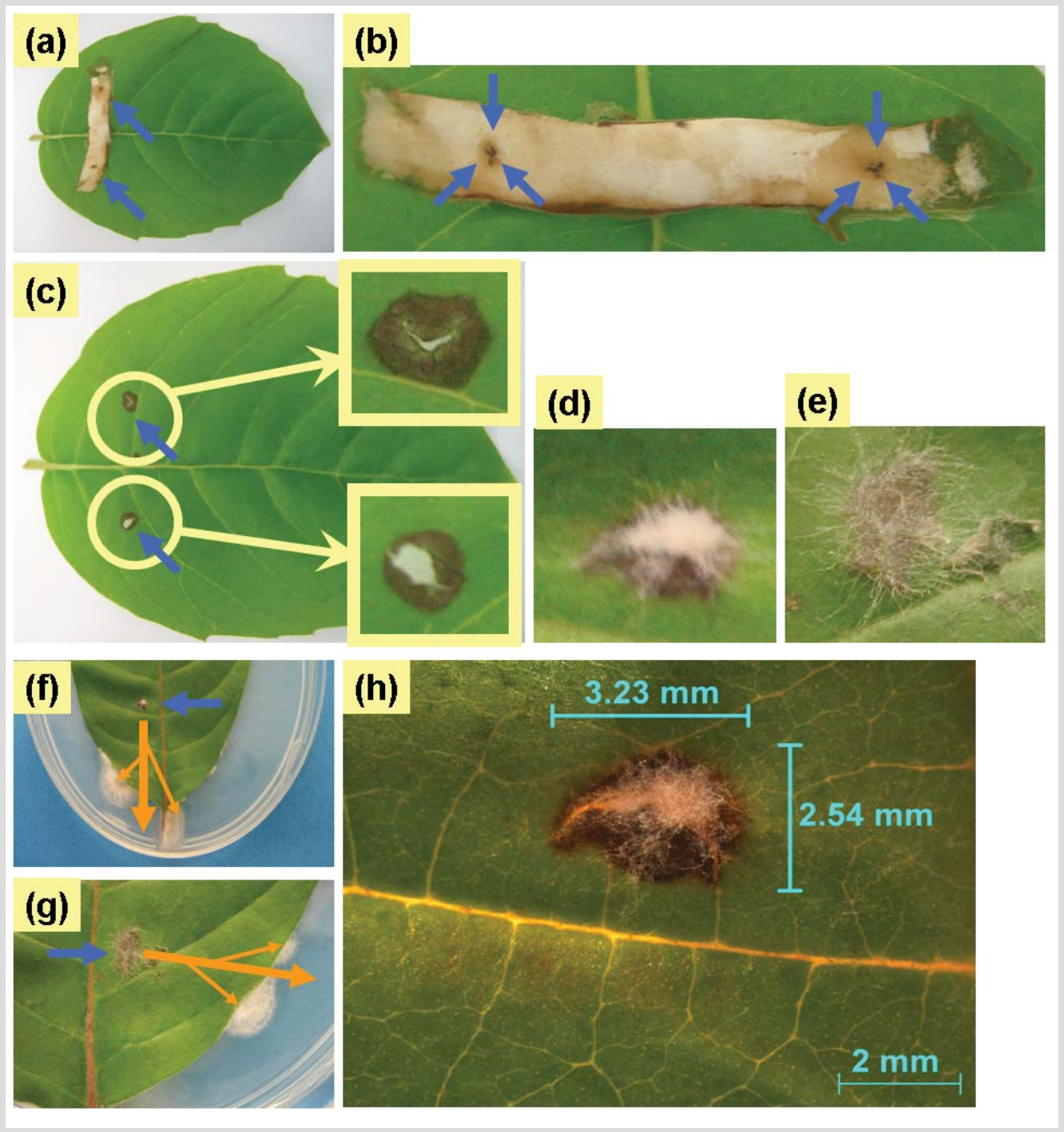

Fig. 47. Representative pictures of artificial *in vitro* inoculation and *in planta* colonization of the seventh generation of endophytic *F. solani* (INFU/Ca/KF/3/VII) in the leaves of the target *C. acuminata* host plants followed by recovery, in an attempt to reverse the observed impairment of CPT biosynthesis by the endophyte. (a,b) No apparent stress or visible manifestation could be observed except for the puncture wounds after removal of Parafilm (blue arrows), or after removal of endophytic mycelial mat (see c). (d,e) Endophytic *F. solani* could be recovered first at the site of wound. (f,g) Endophytic *F. solani* could be recovered later at the leaf-blade emerging few cm away (orange arrows) from the original wound site (blue arrow) demonstrating the tissue colonization away from site of inoculation. (h) Close-up view of recovered endophytic *F. solani* INFU/Ca/KF/3 at the wound site clearly showing no visible manifestation at other parts of the intact leaf.

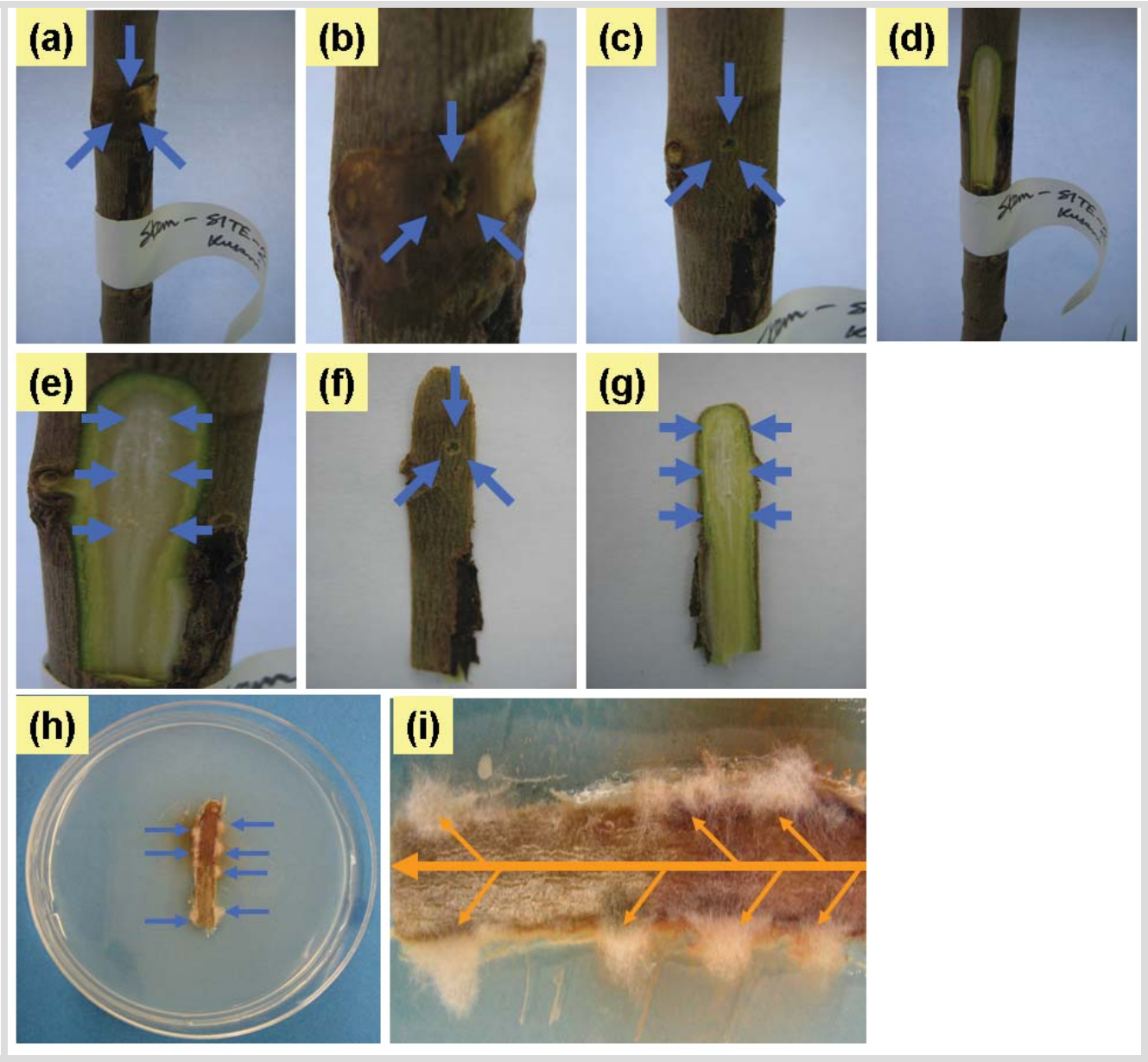

Fig. 48. Representative pictures of artificial *in vitro* inoculation and *in planta* colonization of the seventh generation of endophytic *F. solani* (INFU/Ca/KF/3/VII) in the stems of the target host plants followed by recovery, in an attempt to reverse the observed impairment of CPT biosynthesis by the endophyte. (a,b) Stem surface view with intact mycelia after one week of incubation. (c-g) Stem outer and inner surface view after removal of mycelial mat. (h,i) Endophytic *F. solani* could not be recovered at the site of wound. However, it could be recovered later at the stem-edges emerging few cm away demonstrating the tissue colonization away from site of inoculation. The orange arrows show the direction of tissue colonization based on the gradual delay in recovery (emergence).

All recovered fungi were established as axenic cultures, confirmed identical to the original *F. solani*, cultured under shake-flask conditions, extracted and analyzed using the same procedures as that for the original endophytic *F. solani*. All recovered *F. solani* had completely stopped producing CPT

demonstrating the irreversible biosynthetic dysfunction. The reactive intermediates of the elucidated CPT pathway could not also be isolated and identified with LC-ESI-HRMS^n. Thus, even though the endophyte could be successfully established in its host (*C. acuminata*), the CPT biosynthetic pathway was not restored.

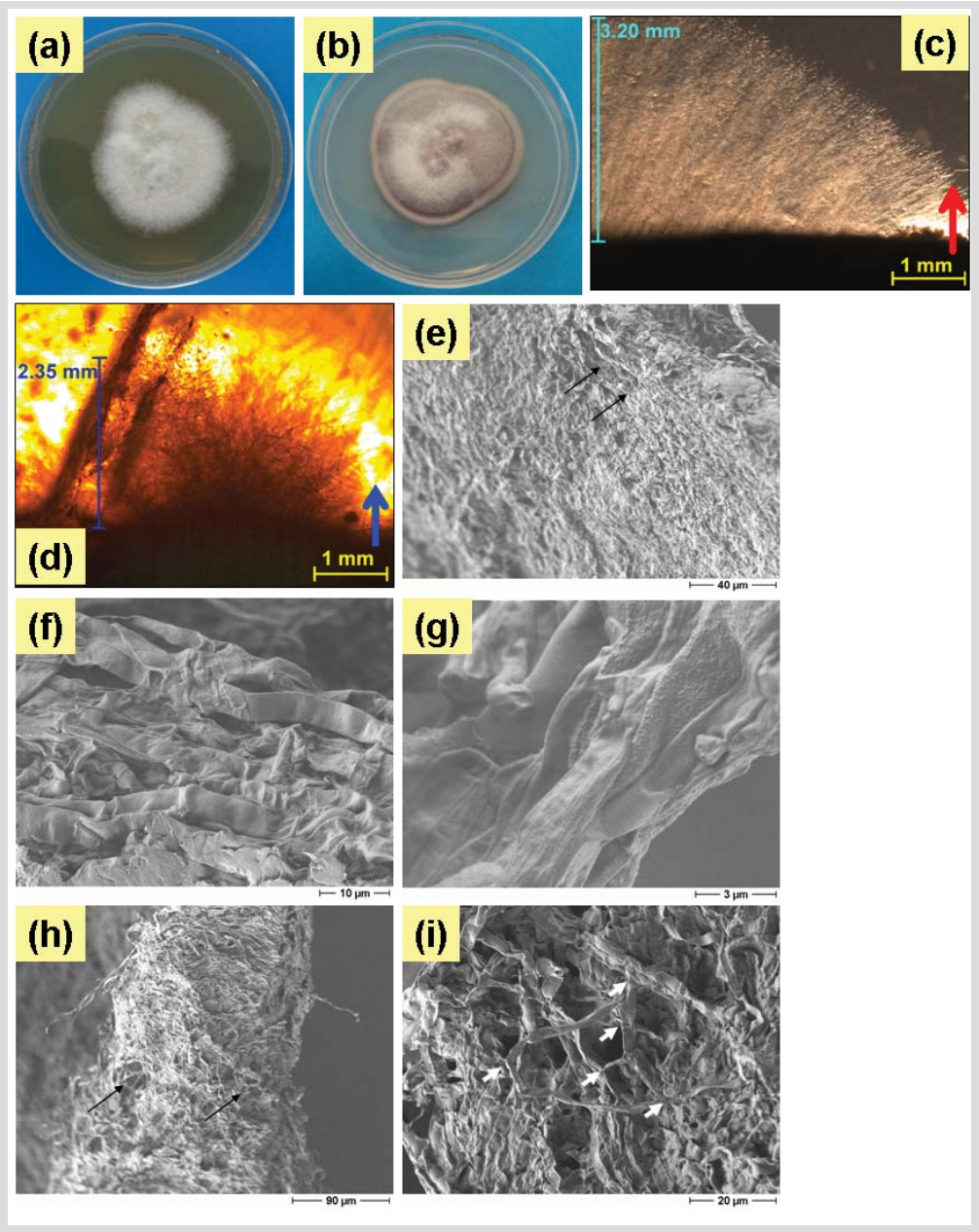

Fig. 49. Macroscopic and microscopic evaluation of endophytic *F. solani* artificially inoculated in the target host *C. acuminata* plants as compared to the recovered *F. solani* post-infection. (a) The seventh-generation of *F. solani* on SA medium before infection. (b) The representative morphology of the recovered *F. solani* after colonization in the target hosts on SA medium. (c) A representative bright field picture of endophytic hyphae emerging out of the *C. acuminata* leaf during recovery of *F. solani*. (d) A representative bright field picture of endophytic hyphae emerging out of the *C. acuminata* stem during recovery of *F. solani*. (e,f,g) The SEM micrographs of the original *F. solani* before establishment in the host plants. (h,i) The SEM micrographs of the recovered *F. solani* after colonization in the host plants.

2. Hypericin

2.1. Phytochemical profiling of host plants

2.1.1. Phytochemical profiling by multivariate analysis (MVA)

All together, eight different plants representing five species of *Hypericum* were extracted and analyzed. The concentrations of hypericin, pseudohypericin, emodin, hyperforin, hyperoside, rutin, quercetin, and quercitrin in leaves, stems and roots, found in organic, aqueous and total (organic and aqueous) phases, are shown in Table T5 (Appendix A). Based on LC–MS/MS analyses, it was revealed that *H. montanum* had the highest contents of hypericin, pseudohypericin, and their probable precursor emodin. Hypericin was found in all species from all localities, which is in agreement with the study of hypericins in *Hypericum* species from Bulgaria (Kitanov, 2001). Pseudohypericin and emodin were also observed in all the species studied. The highest content of hyperforin was found in *H. perforatum* followed by *H. maculatum* (specimen 3907). This corroborates the previously published data on the content of hyperforin in *H. maculatum* (Smelcerovic and Spiteller, 2006). All species studied contained hyperforin, which is in agreement with the data obtained before (Smelcerovic and Spiteller, 2006). However, not all *Hypericum* species contain hyperforin (Umek *et al.*, 1999; Maggi *et al.*, 2004). *H. maculatum* (specimen 3907) also contained the highest amount of rutin. The highest contents of hyperoside and quercitrin were found in individuals of *H. maculatum* from two Slovakian populations located in close proximity (specimens 3907 and 3908). The greatest amount of quercetin was found in *H. perforatum*, which is in line with a previous investigation (Smelcerovic *et al.*, 2008).

MVA of the LC–MS/MS data was carried out to evaluate the individual and holistic phytochemical variability due to the differences among categories, namely, the different plant species, the different plant parts (leaves, stem and roots), as well as the organic and aqueous phases (Fig. 50). From the MVA, it was evident that the highest contents of hypericin, pseudohypericin, emodin, hyperforin, and quercitrin in the respective species of *Hypericum* were present only in the organic extracts of the leaves. However, for the stronger polar molecules of rutin, hyperoside, and quercetin, the highest contents were found in the combined organic and aqueous extracts of the leaves. Computation of the individual averages for each category revealed the highest holistic phytochemical load in the leaves of *H. perforatum*, followed by *H. maculatum* (specimen 3907), *H. hirsutum*, *H. montanum*, and *H. maculatum* (specimen 3902). It is interesting to note that even though *H. perforatum* did not contain the highest amounts of all tested active principals individually, the total spectrum of metabolic load on it was the highest. This is interesting when considering the fact that *H. perforatum* so far is the most

widely used medicinal plant among all the 400 species (approx.) of *Hypericum* (Smelcerovic *et al.*, 2006b, 2007; Verma *et al.*, 2008).

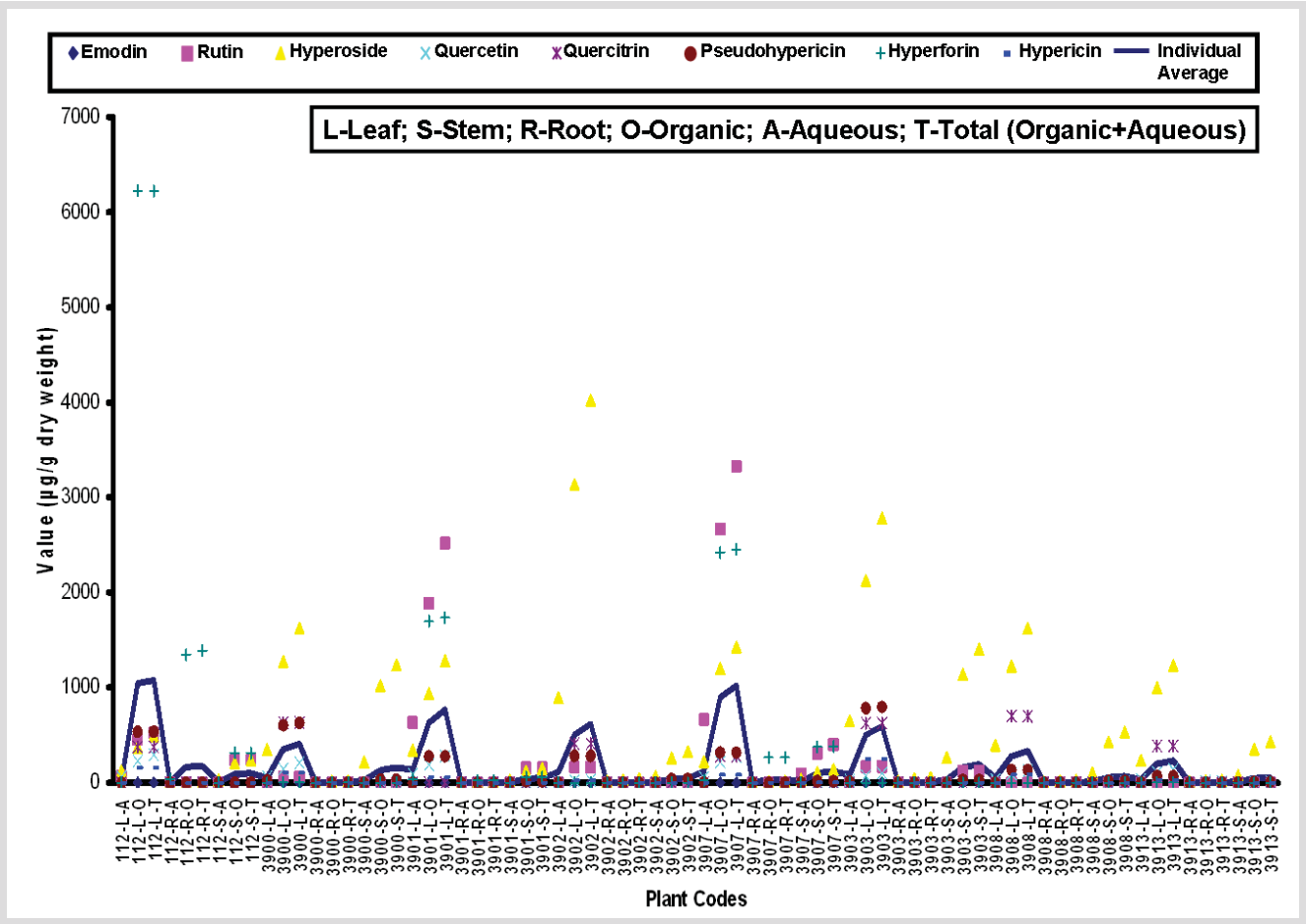

Fig. 50. MVA of the organic and aqueous phases of plant parts in the studied species of *Hypericum* genus. Plant codes depict the voucher number of the respective plant sample.

2.1.2. Multidimensional scaling (MDS)

Kruskal's MDS algorithm based on the Pearson correlation matrix was used to investigate the relationships between the metabolite contents (total) among the investigated *Hypericum* species (Fig. 51). The method was executed in a 3-dimensional (3D) module to build a 3D map of the series of phytochemicals under study from the proximities matrix (by dissimilarities) among the categories (Fig. 51a). Furthermore, a 3D surface analysis was performed using the 3D distance in space among the phytochemicals to build the exact map of the phytochemical relativity within about the given symmetry of the 3 axes in 3 different dimensions (Fig. 51b). In order to achieve an optimal representation of the data points in 3D, Kruskal's stress was computed and found to be 0.015 (negligible stress). Moreover, to have an overall idea of the quality of representation, evaluation of the Shepard diagram based on

Kruskal's stress in 3D was performed. The Shepard diagram revealed that the observed dissimilarities and the disparities (distances) were on the same linear curve (Fig. 51c), confirming the reliability of the MDS representation in 3D.

The Pearson correlation matrix (Table 10) revealed a significant positive correlation between hypericin and pseudohypericin contents of the species studied (Pearson correlation coefficient, r = 0.946, $\alpha \leq 0.05$). A similar hypericin-pseudohypericin correlation was observed previously by Sammon's MDS in 17 *Hypericum* species from Turkey (Smelcerovic *et al.*, 2008), in *H. perforatum* from different populations within India (Verma *et al.*, 2008), and also in *H. perforatum* cell cultures (Kartnig *et al.*, 1996). Furthermore, a significant positive correlation was observed between the contents of hypericin and emodin (r = 0.925, $\alpha \leq 0.05$). So far, only Zobayed *et al*. (2006) described high concentrations of both emodin and hypericin/pseudohypericin in the dark glands of *H. perforatum* suggesting their biosynthesis in these organs. A more universal positive correlation of emodin and hypericin contents in this study may be explained by parallel enhancement of a common precursor in the biosynthetic pathways. The detected positive correlation between emodin and hypericin is of considerable importance given the proposed hypericin biosynthesis via the polyketide pathway in *Hypericum*. Biosynthesis of hypericin has been suggested to start with the condensation of one molecule of acetyl-CoA with seven molecules of malonyl-CoA to form an octaketide chain that subsequently undergoes cyclizations and decarboxylation leading to the formation of emodin anthrone, which further oxidizes to emodin, which in turn undergoes oxidative dimerization to finally form hypericin (Brockmann *et al.*, 1950; Birch, 1967; Thomson, 1957).

Table 10. The Pearson correlation matrix depicting the correlations between the eight metabolites under study. The positive correlations are marked in bold.

Variables	Emodin	Rutin	Hyperoside	Quercetin	Quercitrin	Pseudo-hypericin	Hyperforin	Hypericin
Emodin	-							
Rutin	0.062	-						
Hyperoside	0.552	0.242	-					
Quercetin	0.476	0.706	0.403	-				
Quercitrin	0.862	0.115	0.708	0.589	-			
Pseudo-hypericin	0.808	0.330	0.653	0.698	0.798	-		
Hyperforin	0.236	0.473	0.035	0.688	0.221	0.452	-	
Hypericin	**0.925**	0.298	0.563	0.672	0.809	**0.946**	0.470	-

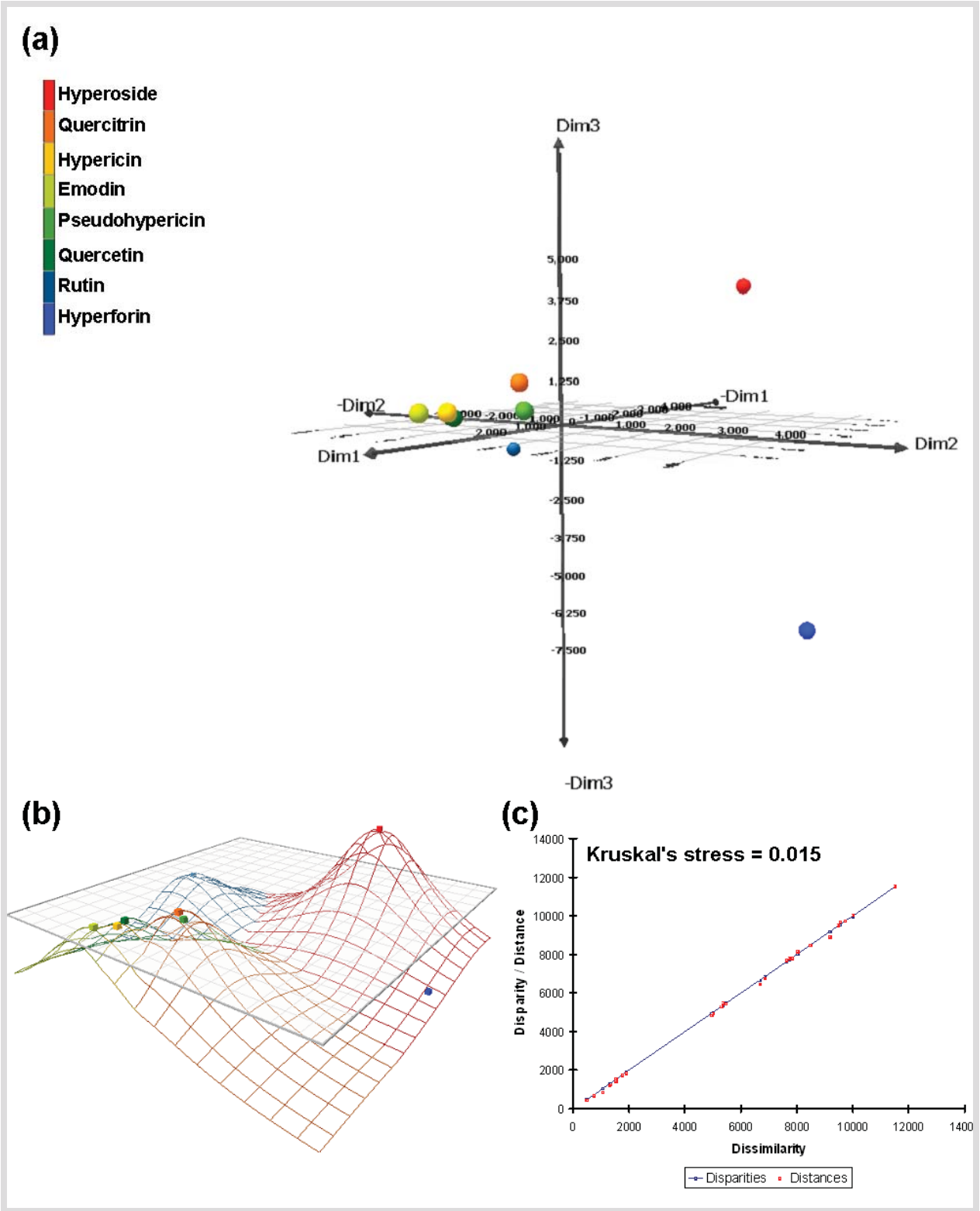

Fig. 51. Kruskal's MDS based on Pearson correlation used to investigate the relationships between the metabolite contents among the investigated *Hypericum* species. (a) 3D MDS map of the eight phytochemicals under study from the proximities matrix (by dissimilarities) between the categories. (b) 3D surface analysis map showing the spatial 3D distance about the given symmetry of the three axes in three different dimensions. (c) The Shepard diagram for the MDS analysis in 3D.

Although there is very little information on the polyketide biosynthetic pathways, Bais *et al*. (2003) characterized an enzyme putatively catalyzing the condensation of emodin to hypericin in *H. perforatum*. More recently, Karppinen and Hohtola (2008) found tissue specific expression of two new polyketide synthases in *H. perforatum*, obviously correlating with hypericin and pseudohypericin concentrations. However, there are still many open questions relating to the specificity of certain enzymes or genes for the conversation of specific compounds versus more general roles in catalyzing certain kinds of chemical reactions. Interestingly, a positive correlation was also found between pseudohypericin and emodin ($r = 0.808$, $\alpha \leq 0.05$), pseudohypericin and quercitrin ($r = 0.798$, $\alpha \leq 0.05$), hypericin and quercitrin ($r = 0.809$, $\alpha \leq 0.05$), emodin and quercitrin ($r = 0.862$, $\alpha \leq 0.05$), hyperoside and quercitrin ($r = 0.708$, $\alpha \leq 0.05$), and, rutin and quercetin ($r = 0.706$, $\alpha \leq 0.05$). The evaluation for this study corroborates the previously reported positive inter-correlations among rutin, hyperoside, quercitrin and quercetin in *H. perforatum* plants of Indian origin (Verma *et al.*, 2008). It is interesting that quercitrin which was positively correlated with hypericin, was also in positive association with pseudohypericin and emodin. This could be explained by emodin and hypericins lying on the same biosynthetic pathway, as also by their synergistic contribution to the chemical makeup of the studied plants.

2.1.3. Principal component analysis (PCA)

A 2-dimensional (2D) visualization of the relative position of the metabolites relative to each other was created by depicting the values of the principal components (metabolites under study) relative to the species. This was achieved by running the PCA. In order to evaluate the reliability of the PCA in 2D, a Scree Plot was computed using the data variability in the useful dimensions (in this case, up to F8, i.e. 8^{th} dimension) versus the cumulative variability, relative to the eigenvalues (Fig. 52a). From the Scree Plot, it was revealed that the PCA analysis was reliable in 2D spacing (F1 versus F2 = 81.348%). The PCA was represented in the form of a Correlation Circle (Fig. 52b) depicting the projection of the variables in the 2D space. The PCA revealed a significant positive correlation between the hypericin and pseudohypericin contents among the studied plant species, similar to the MDS. A positive correlation was also observed between hypericin and emodin, pseudohypericin and emodin, hypericin and quercitrin, and, rutin and quercetin. All these positive correlations corroborate to Kruskal's MDS. However, the PCA revealed some very interesting novel correlations that were not elucidated by the MDS based on Kruskal's algorithm. For the first time, hyperforin could be correlated with another metabolite in the genus *Hypericum*, as evidenced by its positive correlation with quercetin. It was also evident that rutin showed a negative correlation with emodin as well as with quercitrin. In a previous study, a similar negative correlation has been found between rutin and quercitrin among six *Hypericum* species from Slovenia (Umek *et al.*, 1999). The Correlation Circle also depicted an orthonormal

projection between hyperforin and emodin, rutin and hyperoside, and, hyperforin and hyperoside. Hence, it was concluded that these metabolites were not correlated with each other for the studied species. The independent existence of these metabolites without any correlation with each other could be interpreted as the differences in the biosynthetic pathways for their accumulation in the plants.

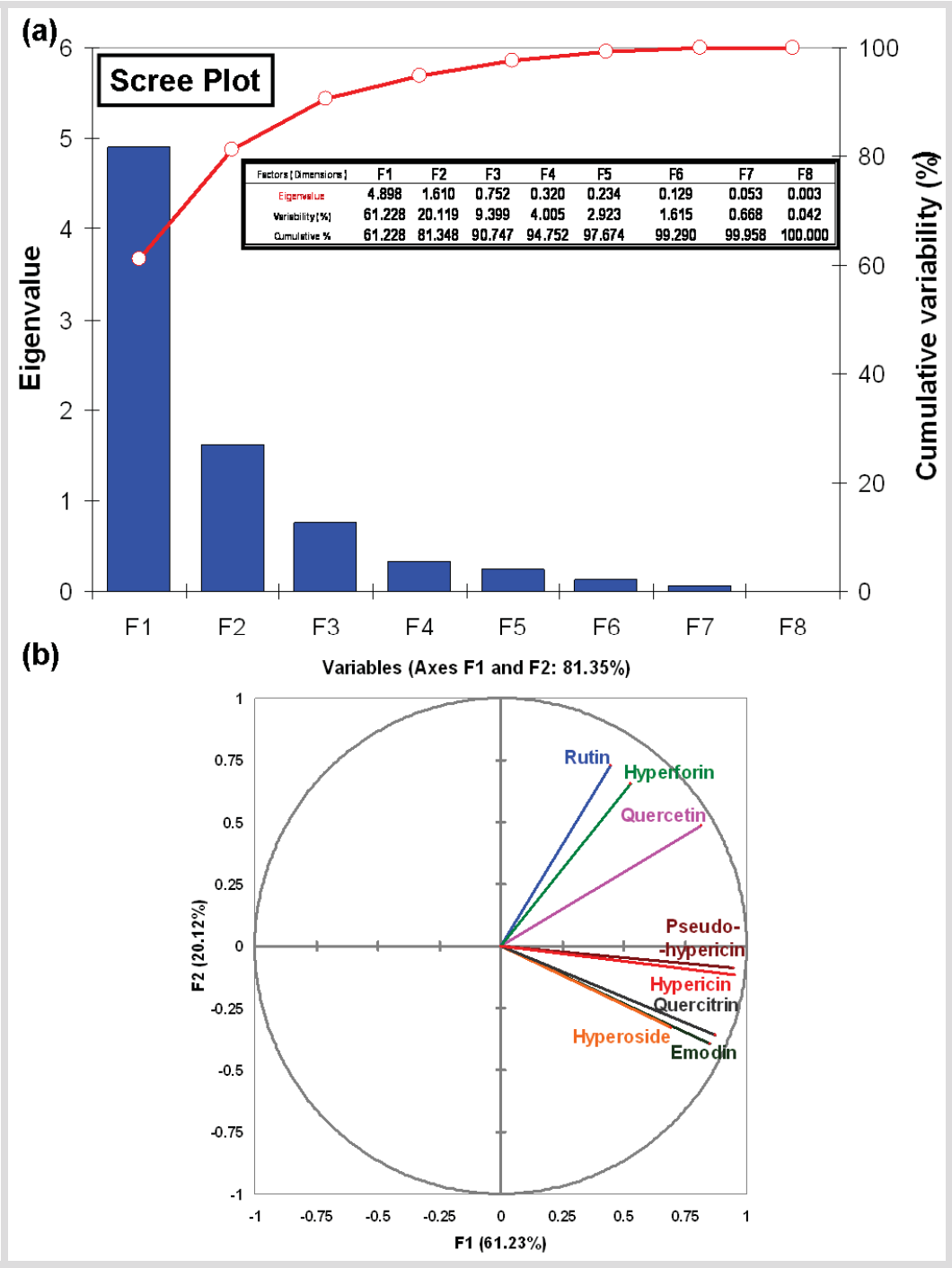

Fig. 52. PCA. (a) The Scree Plot depicting the data variability in eight dimensions versus cumulative variability, relative to the eigenvalues. (b) The projection of the variables (phytochemicals) in the 2D space shown by the PCA Correlation Circle.

2.1.4. Linear discriminant analysis (LDA)

The chemotaxonomic significance (specificity of secondary compound profiles for individual species) of the different plant samples under study was evaluated by LDA. The results were visualized on a 2D map that depicted the degree of separation between the groups (Fig. 53). The LDA projection revealed that *H. perforatum* was well separated from the rest of the species. From the MVA, it was observed that *H. perforatum* had the highest holistic phytochemical load, and therefore, the LDA projection clarified that this species is distinct in metabolite spectrum and demarcated from other species. Interestingly, the loads of the tested metabolites on different individuals of *H. maculatum* were different from each other. This could be the result of genotypic differences within the same species or due to environmental factors influencing biosynthesis and expression of the respective compounds. Further studies on the genotypic diversity of selected *Hypericum* species and experiments testing the influence of environmental variables on known genotypes are needed.

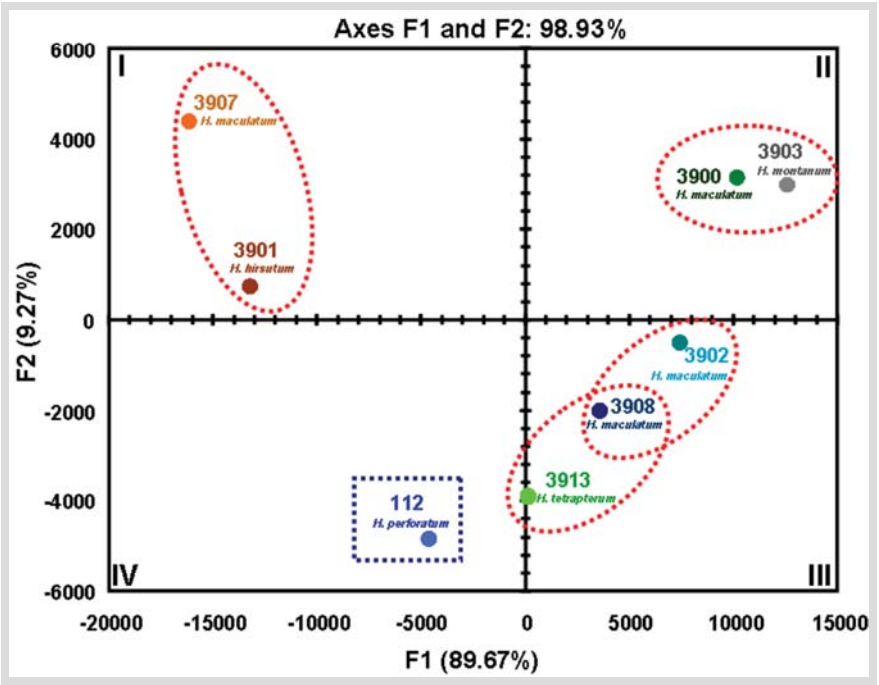

Fig. 53. 2D map of LDA.

2.1.5. Hierarchical agglomerative cluster analysis (HACA)

For a clearer arrangement, the compounds measured were grouped in a manner that assigned similar behavior using HACA method by average linkage. The dendrogram obtained by HACA plotting the data of all the eight compounds under study versus the plant species (Fig. 54a) showed that hypericin and pseudohypericin were grouped separately from the other components. Furthermore, emodin was grouped at an equal distance from both hypericin and pseudohypericin. This observation, like the Kruskal's MDS analysis by Pearson correlation matrix, yet again indicated a presumed parallel

enhancement of a common precursor (emodin) in the biosynthetic pathways (of hypericin and pseudohypericin). This relationship, therefore, is in line with the previous reports that emodin might be a common precursor of hypericin and pseudohypericin in plants via the polyketide pathway (Brockmann *et al*., 1950; Birch, 1967; Thomson, 1957; Bais *et al*., 2003).

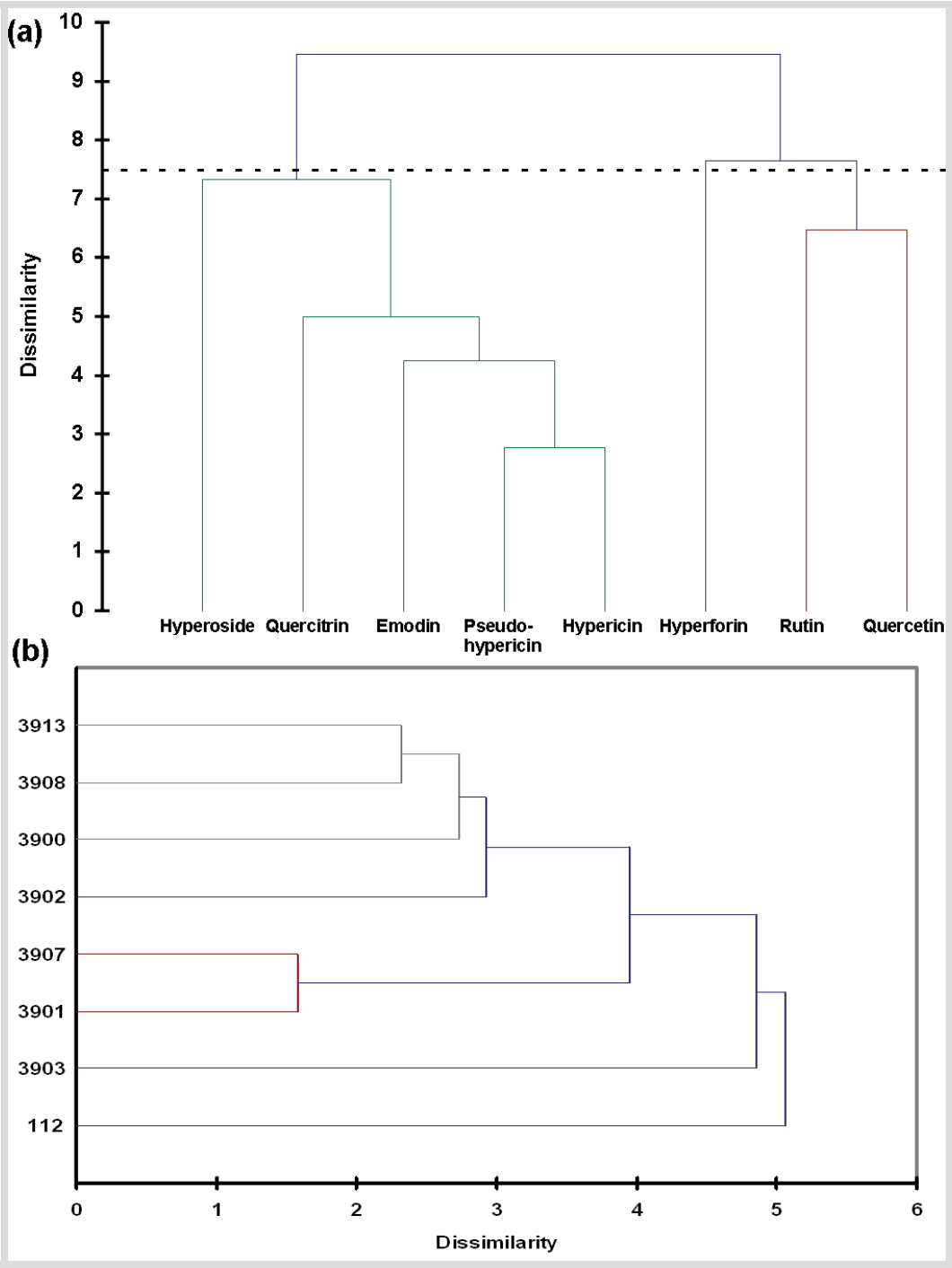

Fig. 54. HACA by average linkage. (a) Dendrogram obtained by plotting the data of all the eight compounds under study versus the plant species. (b) Dendrogram obtained by plotting the various plant species under study versus each of the eight metabolites under study.

Interestingly, rutin and quercetin were also grouped together and they possessed equal dissimilarity to the other components, which might be explained by their positive correlation and synergistic effects in *Hypericum* species (by Kruskal's MDS). The dendrogram obtained by HACA plotting the various plant species under study versus each of the eight phytochemical (Fig. 54b) showed that *H. perforatum* (specimen 112) was well separated from all other species. HACA revealed that *H. maculatum* (specimen 3907) and *H. hirsutum*, and, *H. tetrapterum* and *H. maculatum* (specimen 3908) formed single sub-cluster (similar to LDA). Therefore, a significant relationship among the eight pharmacologically important compounds could be observed.

2.2. Biological characterization of hypericin producing endophytic fungus

2.2.1. Isolation and *in vitro* culture of the endophytic fungus

Using the rationale that the plants containing hypericin may also contain endophytic fungi that are able to accumulate the same or similar molecules, a selective search for fungal endophytes was pursued. Hypericin is found only in the species of *Hypericum*, which also contains other related phytochemicals like pseudohypericin, emodin, hyperforin, hyperoside, rutin, quercetin, and quercitrin, distributed in various organs. The analyses of *Hypericum* species from various populations of Slovakia and from India showed considerable amounts of hypericin and related phytochemicals in the host plants themselves. Table 11 shows the number of endophytic fungi isolated from various organs of the *Hypericum* plants, which were morphologically different from the strains isolated from unsterilized explants (surface-contaminating fungi). The selective media supporting the pure culture of fungi were noted, and the isolation of the endophytes was verified by performing the isolation of surface-contaminating fungi in parallel. Only one endophytic fungus was able to produce hypericin and emodin (its proposed precursor in plants), coded INFU/Hp/KF/34B, and was taken up for further studies.

2.2.2. Macroscopic morphological characteristics of the endophytic fungus on agar medium

The fungus produced copious amounts of aerial, surficial and submerged hyphae on rich medium (PDA) that reached 6 cm diameter in about 5 days at 28 ± 2°C (Fig. 55). The mycelia, initially white and cottony, gradually turned dark grey to black with white to light grey, cottony centers. The aerial hyphae were almost all medium to dark grey, slender, and with pointed tips. The surface hyphae were light to dark grey or black, and slender with pointed growing tips. No sporulation was observed in rich medium (PDA). The fungus did not even sporulate in other rich mycological media as well, like SA and MEA,

though the characteristic color development of the mycelia was always prominent at later stages of growth. From the reverse side of Petri dish, the color was tan or brown to black. Interestingly, the fungus showed very good rate of growth and survival even up to 38-40°C, revealing its thermotolerant capabilities.

Table 11. The number of endophytic fungi isolated from different organs of the *Hypericum* plants sampled from various locations.

Plant	Specimen	Organ	Number of isolated endophytic fungi
H. perforatum	112	Stems	37
		Leaves	12
		Roots	18
H. maculatum	3900	Stems	7
		Leaves	11
		Roots	13
H. hirsutum	3901	Stems	28
		Leaves	17
		Roots	9
H. maculatum	3902	Stems	24
		Leaves	12
		Roots	15
H. montanum	3903	Stems	26
		Leaves	21
		Roots	13
H. maculatum	3907	Stems	31
		Leaves	16
		Roots	15
H. maculatum	3908	Stems	23
		Leaves	21
		Roots	14
H. tetrapterum	3913	Stems	26
		Leaves	20
		Roots	12

2.2.3. Macroscopic morphological characteristics of the endophytic fungus in broth medium

Under shake-flask conditions in PDB, the fungus grew as white, non-sticky, and medium to big, round balls. Pellicle formation at the edge of the flask was light and slightly sticky. Interestingly, the fungal mycelium did not show any coloration (Fig. 56) unlike on solid medium (PDA). At the end of 5 days, the spent medium looked more viscous than the fresh medium, although it retained its color.

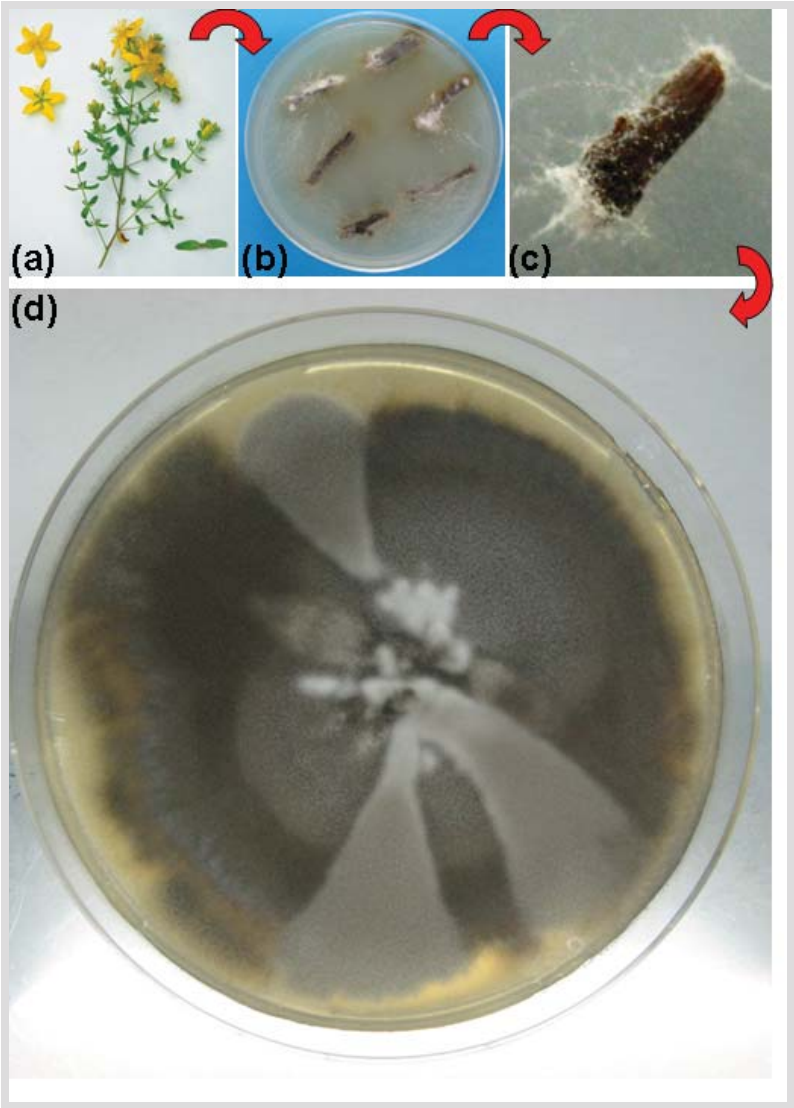

Fig. 55. The endophytic fungus, INFU/Hp/KF/34B, growing on PDA media. (a) *H. perforatum* host plant. (b) Representative surface-sterilized stem explants in a Petri dish containing WA supplemented with streptomycin. (c) The tips of hyphae of INFU/Hp/KF/34B emerging out of the surface-sterilized stem segment. (d) The macroscopic morphology of the endophyte on PDA.

Fig. 56. The macroscopic morphological characteristics of the endophytic fungus in PDB medium.

2.2.4. Microscopic morphological characteristics of the endophytic fungus

Light microscopic studies have revealed that the hyphae were intertwined into rope-like strands, sometimes coiled, and branched. The hyphae preferably grew on the surface of the media, while still developing hyphal coils, hyphal stranding and right-angled branching. Each strand contained uniform, elongated, rectangular hyphal cells; the terminal cells were almost always oval to pointed (towards the periphery) giving the overall appearance of pointed tips. Branching was by structural changes in single terminal hyphal cells that started dividing bi-directionally first, followed by uniform growth in both directions. Branching was right-angled most of the times, though branching at lesser angular distance was visible in most peripheral hyphae. The overall colony appearance was fan-like, spreading from the center towards the edges. Detailed microscopic studies of the fungus (Fig. 57) revealed that the conidia (aleuriospores, chlamydospores) forming laterally or terminally on the hyphae or on short branches were broadly clavate or pyriform, with a truncate base, single-celled, hyaline or light brown and measured 5-7 × 3-5 µm. The ascomata developing within the mycelial mat were spherical, black, and 90-200 µm in diameter. The thin and dark wall of the ascomata was composed of textura epidermoidea or of flattened, irregular outlined, 6-8 µm sized cells and was often covered with dark hyphae. The ascospores were fusiform or ellipsoidal, single-celled, brown, and 14-20 × 8-10 µm in size, with a distinct, subapical germ pore.

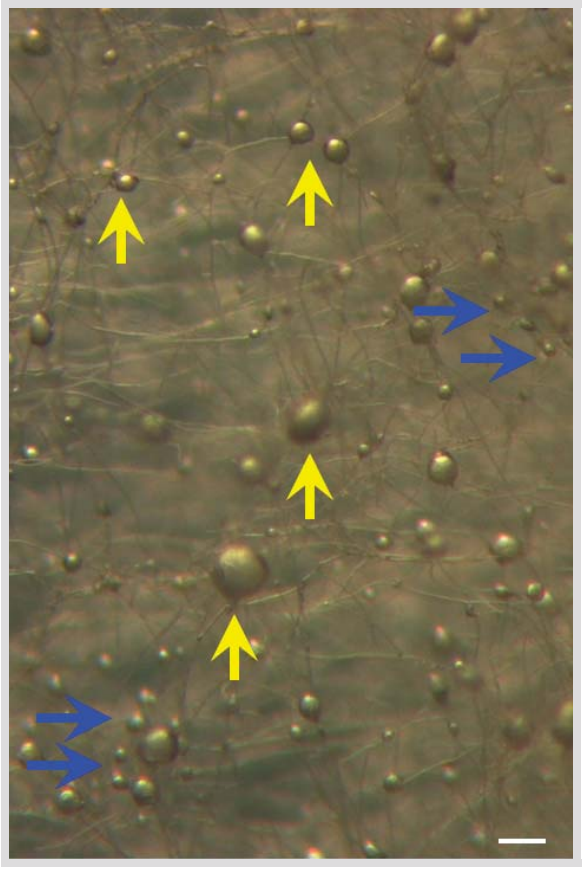

Fig. 57. The microscopic morphological characteristics of the endophytic fungus on PDA medium. The terminal (yellow arrow) and lateral (blue arrow) conidia are visible.

2.2.5. Identification and authentication of the endophytic fungus

The macroscopic and microscopic morphological characteristics of the endophytic fungus revealed that it belongs to the genus *Thielavia*. Further, the molecular analysis of the fungus based on a large subunit (LSU) 28S rRNA gene revealed 99% similarity to another fungal isolate, 9097 (accession number EF420068), similarly to other related taxa, for example, *Chaetomium globosum* (98%, accession number AY545729) and unidentified fungal isolate 9038 (98%, accession number EF420066); thus, 28S rDNA analysis was inconclusive. The final assignment of the species could, therefore, be done by resorting to the molecular analysis of the ITS region of the rDNA containing ITS1, and ITS2, and the intervening 5.8S rRNA gene (Fig. 58). The ITS-5.8S rDNA sequence obtained has been deposited into EMBL-Bank under accession number AM909688. On the basis of the ITS-5.8S rDNA analysis, in addition to its morphology, the endophytic fungus, INFU/Hp/KF/34B, has been identified as *Thielavia subthermophila*, and deposited at DSMZ under accession number DSM 21024.

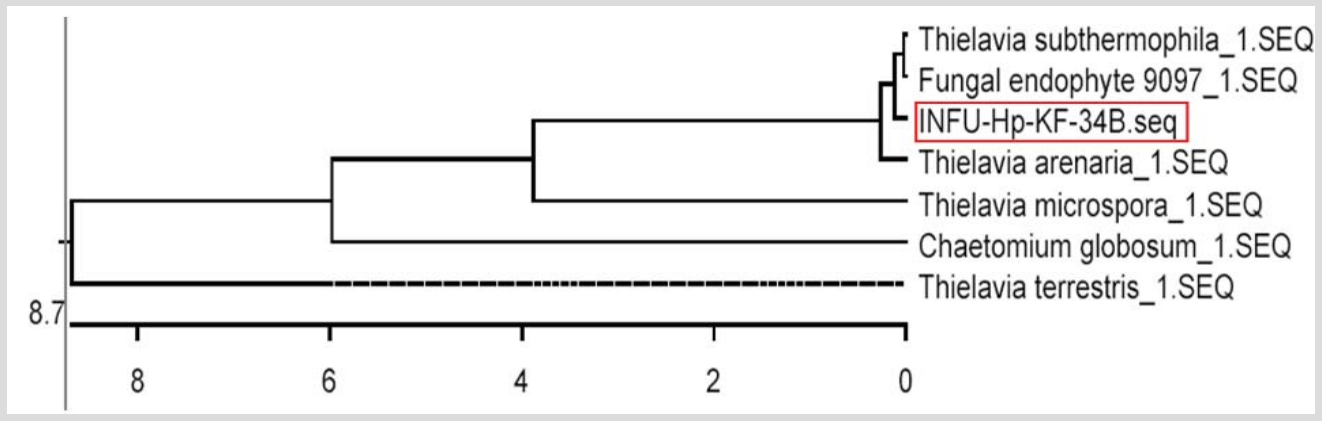

Fig. 58. The dendrogram showing the phylogenetic position of the fungal isolate.

2.3. Biochemical characterization of hypericin producing endophytic fungus

2.3.1. Structural elucidation and quantitation of hypericin and emodin

Both the fungal biomass and the culture media from grown cultures were assessed for the presence of hypericin and emodin. The culture media did not yield any trace of these compounds. The identification of hypericin and emodin in the fungal biomass was achieved by comparison with authentic reference standards using LC-HRMS, LC-MS/MS, and LC-HRMS/MS. The quantitative analysis by LC-MS/MS indicated a yield over a range of 35 ± 2 µg 100 g^{-1} (for hypericin) and 113 ± 1 µg 100 g^{-1} (for emodin) dry weight of fungal mycelia under shake-flask conditions after 7 days of incubation of the isolated

microorganism. The retention times and the ESI-MS/MS spectra (Fig. 59) of fungal hypericin and emodin were identical to the data obtained for the authentic standards. The high-resolution measurement confirmed the molecular formulas of the compounds: hypericin $[M-H]^-$ 503.07724 ($C_{30}H_{16}O_8$); emodin $[M-H]^-$ 269.04555 ($C_{15}H_{10}O_5$), and the characteristic fragments.

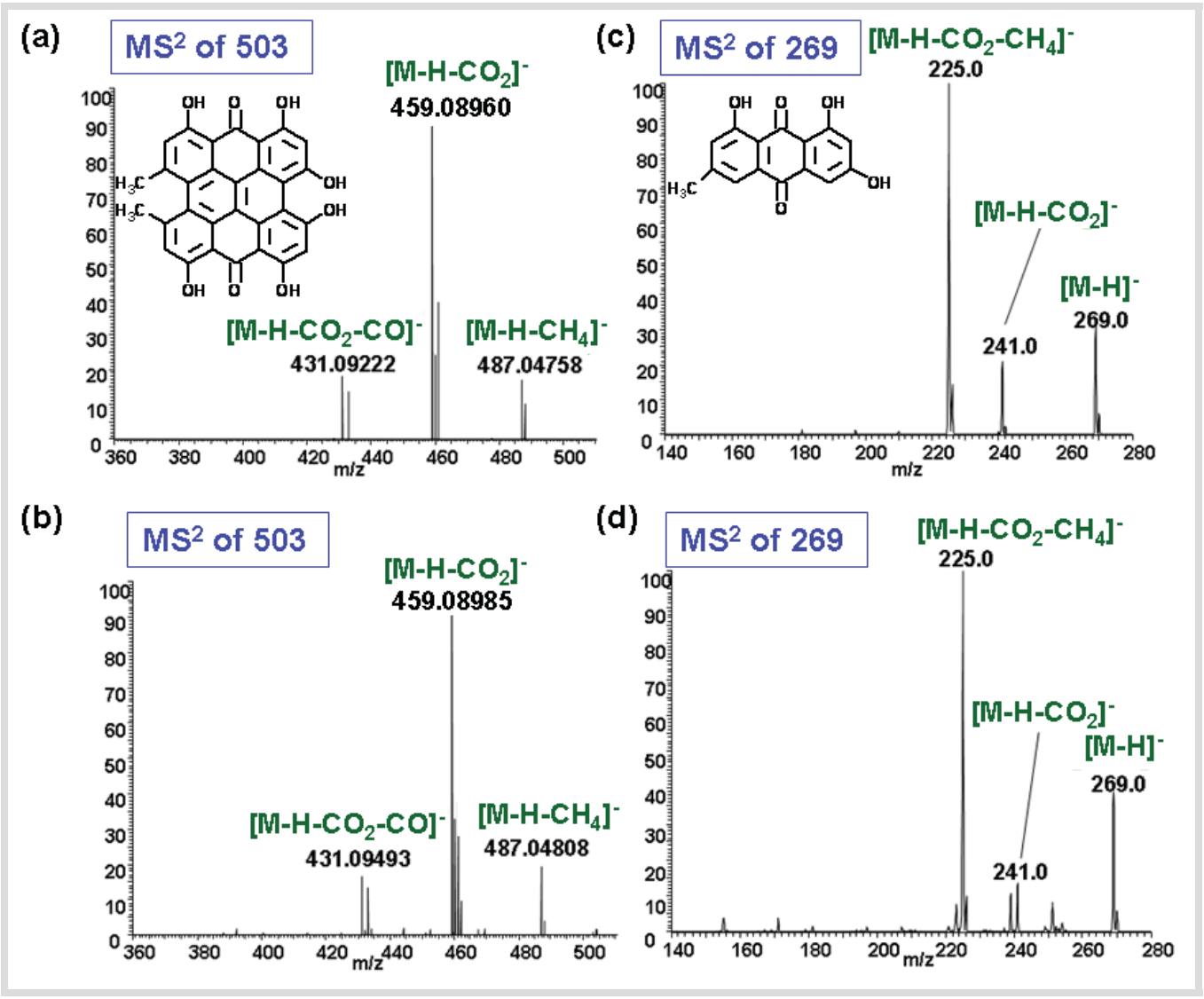

Fig. 59. High-resolution MS/MS product ions of (a) standard hypericin and (b) fungal hypericin; nominal mass MS/MS product ions of (c) standard emodin and (d) fungal emodin.

2.3.2. Growth kinetics of the endophyte in the light and in darkness

The growth kinetics of the endophytic fungus INFU/Hp/KF/34B was examined up to the ninth day (216 h) of incubation. The endophyte exhibited an exponential increase in the dry weight of mycelia up to the ninth day (216 h) of incubation both in the light and in darkness (Fig. 60). The growth kinetics was

similar in both light and dark conditions. Interestingly, the amounts of biomass produced by the fungus after submerged fermentation under light and dark conditions were comparable for each time period throughout the whole experiment. Growth commenced immediately after the fermentation was started. The biomass accumulation at the end of fermentation (216 h) was the same under both conditions.

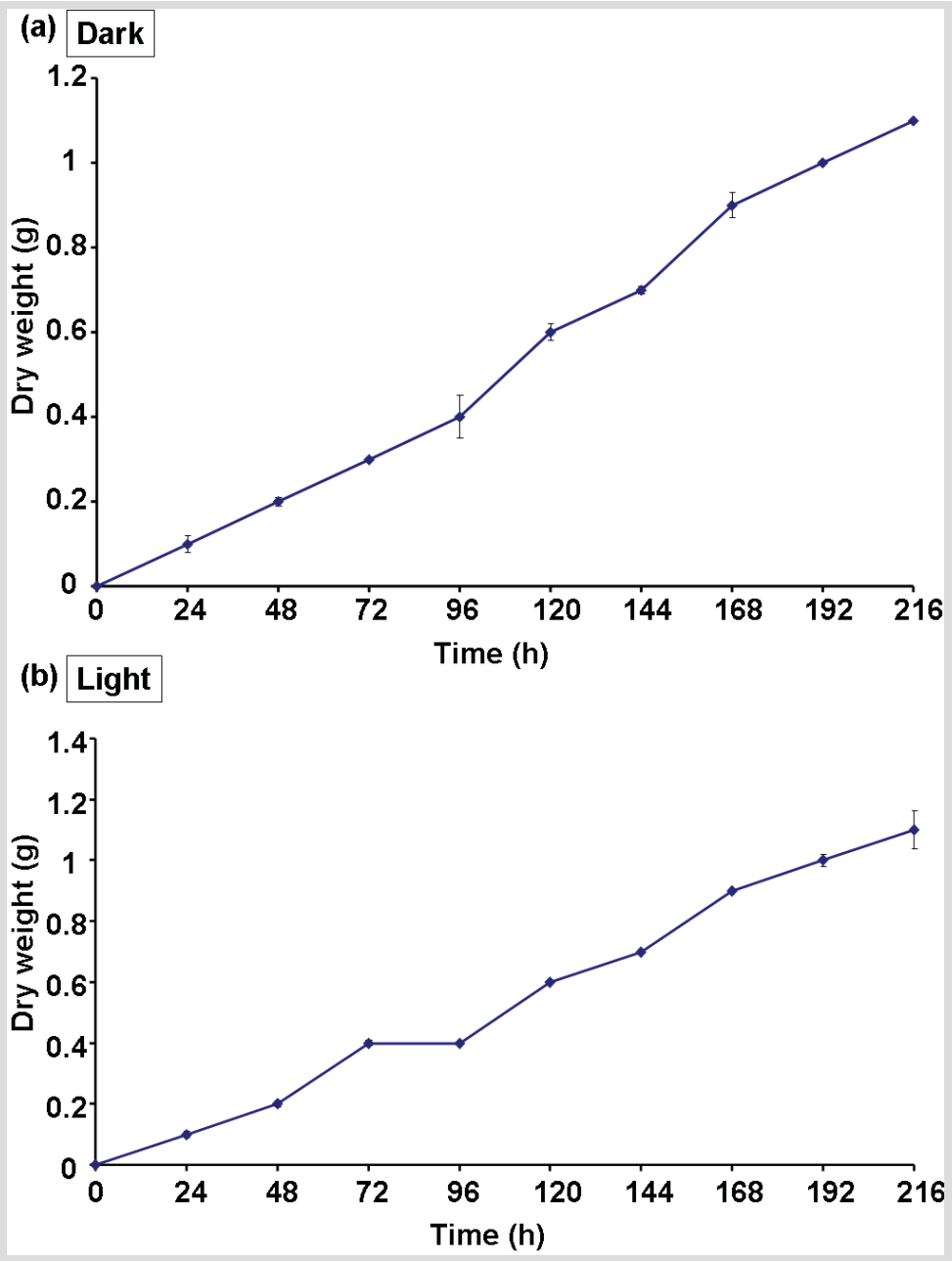

Fig. 60. Growth kinetics of the cultured endophyte INFU/Hp/KF/34B.
(a) Under light protection.
(b) Without light protection.

2.3.3. Production kinetics of the endophyte in the light and in darkness

In order to study the production kinetics of hypericin and emodin, the mycelia were collected every 24 h and metabolites were isolated from both the mycelia and spent broth. The contents of hypericin and

emodin in the organic extracts of mycelia and broth, collected at periods of regular time intervals, were determined to provide an insight into the production kinetics as a function of time (Fig. 61).

Under both light and dark conditions, the production of emodin commenced as early as 24 h (Fig. 61a). The content of emodin gradually increased until 48 h, after which it remained almost the same, with some minor changes between 168 and 216 h. In order to obtain a smooth curve depicting the overall pattern production of emodin, the 'moving averages' were evaluated, taking into account the values preceding and succeeding a particular point in time. The amount of emodin produced by the endophyte after fermentation for 9 days was comparable under both light and dark conditions. The intracellular concentration kinetics revealed that the accumulation of emodin in the cells started immediately irrespective of the conditions of illumination, and the concentration of emodin increased steeply in the first 24 h followed by a sharp decrease afterward (Fig. 62a). Emodin was not detected in the spent medium (broth) under both light and dark conditions (LOD = 3.0 pg mL^{-1}), revealing that it was accumulated as intracellular metabolite. Furthermore, emodin was not found at 0 h. Hence, emodin had not been carried over from the original plant material via the mycelia of the fungus, i.e., via the inoculum plugs.

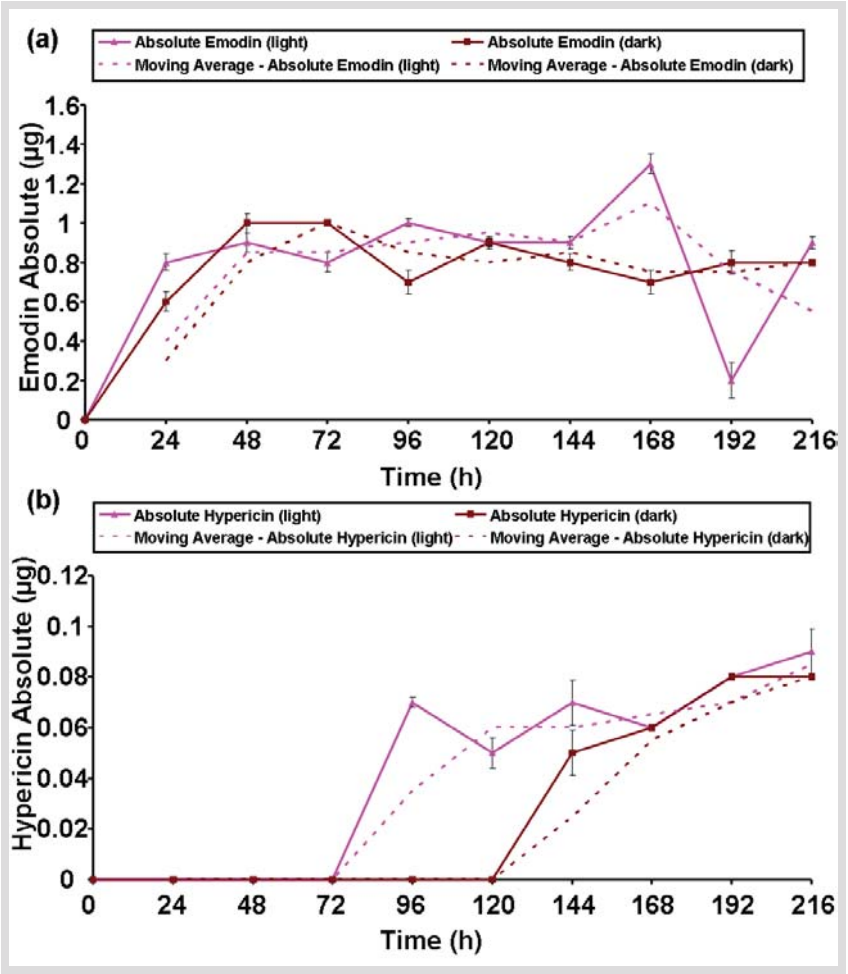

Fig. 61. Production kinetics of the cultured endophyte under light and darkness at different time points of fermentation.
(a) Emodin production kinetics.
(b) Hypericin production kinetics.

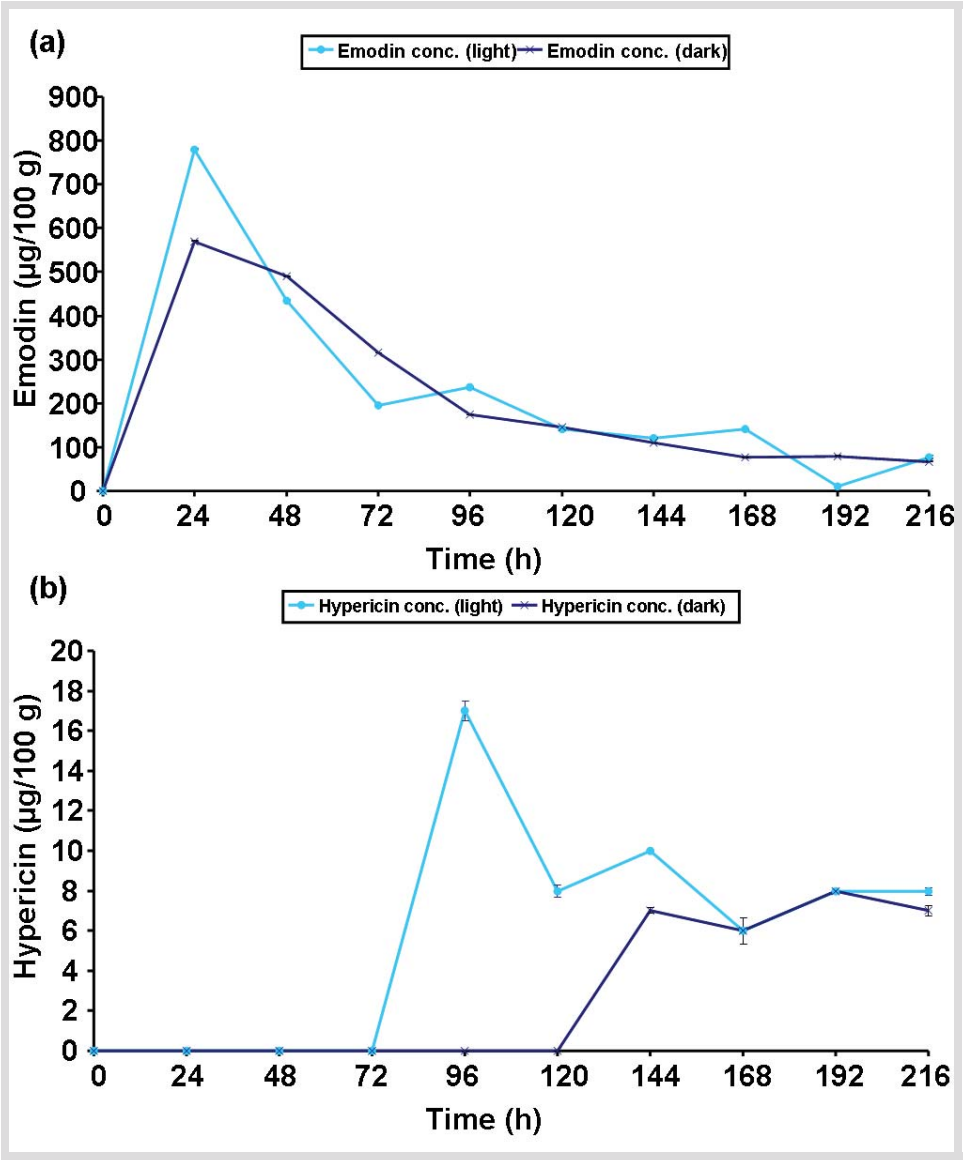

Fig. 62. Intracellular concentration kinetics of the cultured endophyte under light and darkness at different time points of fermentation.
(a) For emodin.
(b) For hypericin.

The production of hypericin did not start immediately in the light (Fig. 61b). It could be detected only from 96 h of submerged fermentation onward, after which it gradually increased up to the end of the ninth day. Interestingly, however, the production of hypericin commenced much later in darkness, only from 144 h onward (Fig. 61b). Nevertheless, final concentrations and contents at 216 h were similar on illumination and in the darkness. It could, therefore, be concluded that although illumination was not a potent external factor in determining the microbial biosynthesis of hypericin, it definitely had an effect, to some extent, on hastening the start of the biosynthesis. The evaluation of the intracellular concentrations of hypericin (Fig. 62b) revealed that in both light and dark conditions, there was a sharp increase in the post-production initial concentrations for around 24 h, after which it remained constant and did not decrease, unlike emodin. As with emodin, hypericin was not detected in the spent medium

or at the start of the experiment (0 h) under conditions of either light or darkness. It was evident that light had no effect on the production of either hypericin or emodin by the cultured endophyte, although it had some effect on the kinetics of production of hypericin. Furthermore, there was no detectable production of protohypericin in any experiment. Hence, it was proved that both hypericin and emodin were actual metabolic products that were accumulated by the endophyte. Strikingly, the production of hypericin and emodin by the first generation of the cultured endophyte observed during the study on growth and production kinetics (February 2009) was less than what was initially observed (August 2007).

2.3.4. Presence/expression of the *hyp-1* gene in the endophyte

It was proposed that in the host plant cell cultures, direct and complex enzymatic conversion of emodin to hypericin is governed by the product of the candidate *hyp-1* gene, the Hyp-1 phenolic coupling protein (Bais *et al.*, 2003). This enzyme was considered to be responsible for several subsequent reactions leading to hypericin. However, as previously reported (Kosuth *et al.*, 2007), the transcript level of the respective gene *in planta* did not correspond with tissue-specific accumulation of hypericin. Furthermore, Michalska *et al*. (2010) also failed to reproduce the experiments of Hyp-1 catalyzed conversion of emodin to hypericin as claimed by Bais *et al*. (2003), thus questioning the function of Hyp-1 in plants. In an attempt to isolate a homologous sequence from *T. subthermophila*, the presence of the gene was tested by PCR amplification with two pairs of *H. perforatum hyp-1* gene-specific primers. No specific amplification product homologous to the *hyp-1* gene was amplified on either DNA or RNA/cDNA template from *T. subthermophila*. Distinct amplification product was obtained only by RT-PCR with a second set of primers (amplifying a 570 bp long fragment on cDNA in *H. perforatum*). The amplified product was longer than in *H. perforatum* (Fig. 63).

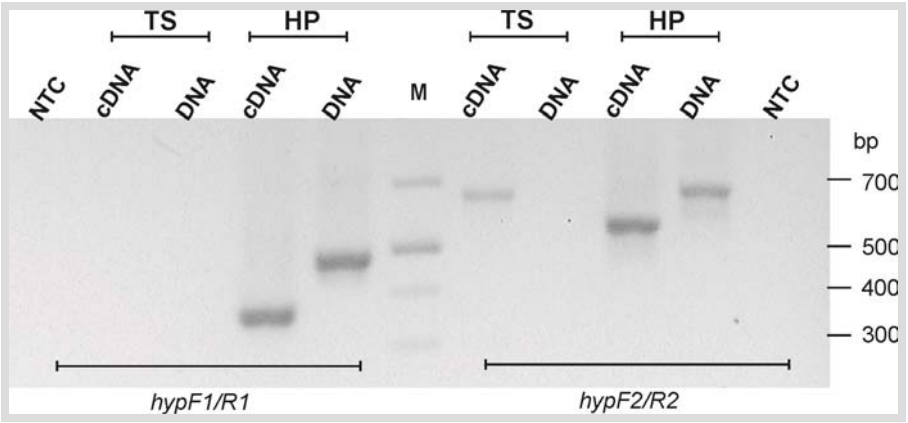

Fig. 63. PCR/RT-PCR of the *hyp-1* gene by using two sets of *H. perforatum* gene-specific primers (*hypF1/R1*, *hypF2/R2*). DNA or cDNA from *Thielavia subthermophila* (TS) and *H. perforatum* (HP) were used in the amplification reactions. NTC, no template control; M, DNA size marker.

Sequencing of this cDNA gene fragment did not reveal any nucleotide similarity with the published cDNA of the *hyp-1* gene from *H. perforatum*. The size difference between the *hyp-1* gene transcript and

the genomic fragment amplified on DNA template from *H. perforatum* was due to the presence of intron within the gene sequence. The absence of the homologous sequence of the *hyp-1* gene in *T. subthermophila* indicated that if the *hyp-1* gene is involved in the biosynthesis of hypericin in the host plant in the proposed manner (Bais *et al.*, 2003), then the biosynthetic pathway in the endophytic fungus might be different and/or governed by a different molecular mechanism than the host plant or host cell suspension cultures.

2.3.5. Effect of emodin spiking on growth and production

The endophytic fungus was spiked with different concentrations of emodin under submerged fermentation conditions, similar to those of the kinetics study, in order to study the effects of the additional spiking on the growth and production of hypericin and emodin by the axenic endophyte *in vitro* (Fig. 64) .

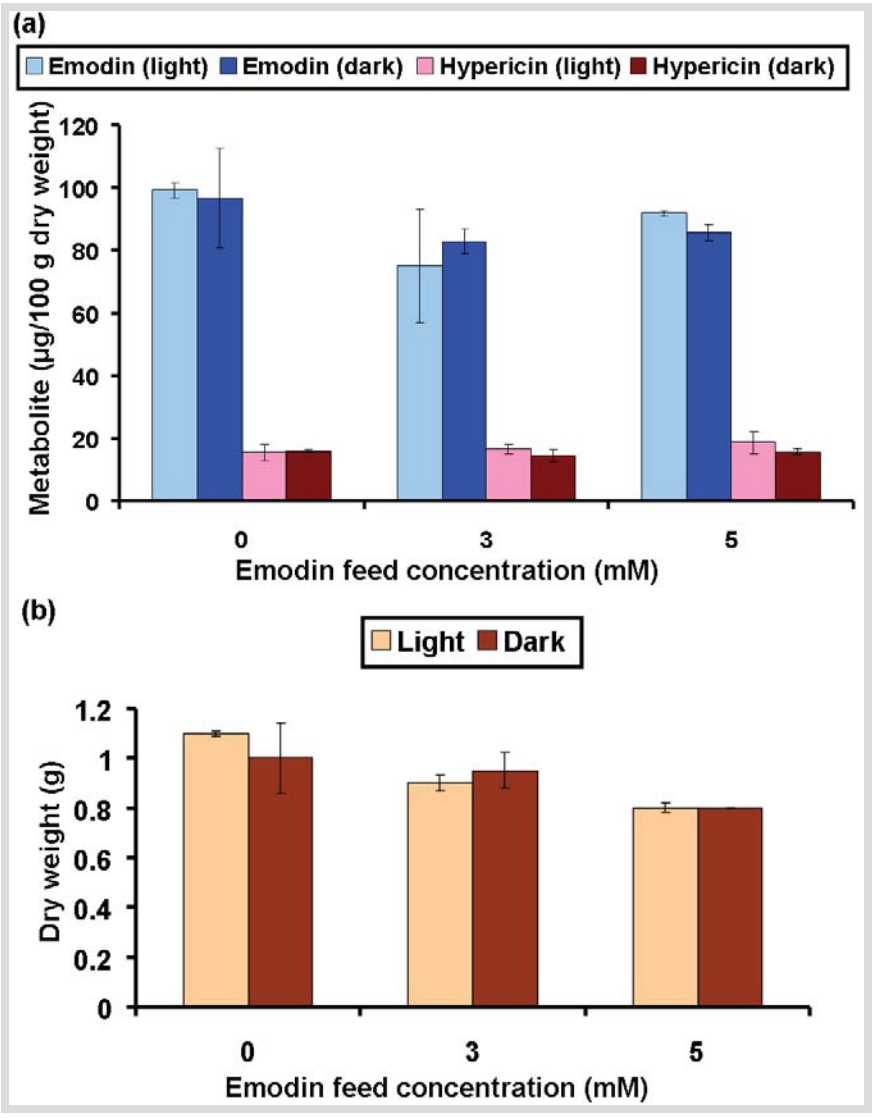

Fig. 64. (a) The accumulation of hypericin and emodin by the cultured endophytic fungus under submerged shake-flask conditions with additional feeds of different emodin concentrations. (b) Effect of additional emodin feeding on the growth of the cultured endophyte. All values represent after fermentation for 216 h.

The spiking was performed under conditions of both light and darkness. It was observed that the addition of emodin to the growth media did not stimulate or inhibit the production of either hypericin or emodin by the cultured endophyte even with or without the illumination conditions (Fig. 64a). Analyses of the spiked spent broths revealed that the endophyte did not take up emodin from the media. Interestingly, however, the addition of emodin had a negative impact on the growth of the endophyte both in the light and in darkness (Fig. 64b). The growth was inversely proportional to the amount of emodin added and independent of the presence or absence of the irradiation.

2.3.6. Reduction of hypericin and emodin biosynthesis on subculturing

A detailed study of metabolite production was undertaken over generations (Fig. 65). In shake-flask incubations of the endophytic fungus, a clear decrease in the production of both hypericin and emodin was observed from the first to the seventh generation subculture, which ceased completely from the fifth generation onwards. Interestingly, a negative correlation between the biosynthesis and growth was also observed, similar to what was observed for endophytic *F. solani* (INFU/Ca/KF/3).

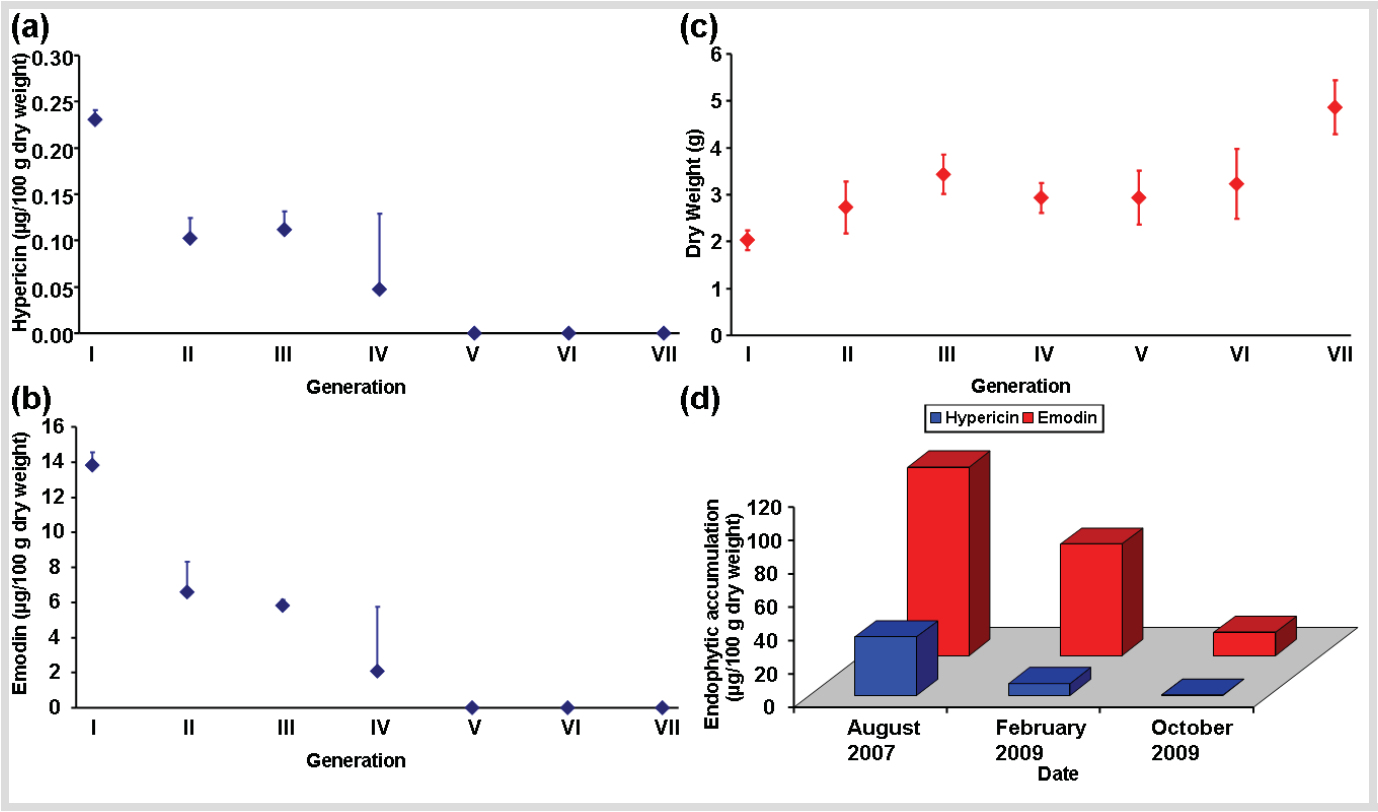

Fig. 65. Hypericin and emodin production pattern by the endophytic fungal isolate from the first to the seventh subculture generation under shake-flask conditions and on storage, and the correlation with the fungal biomass accumulation. (a) Mean hypericin production pattern. (b) Mean emodin production pattern. (c) Mean fungal biomass dry weight. (d) Effect on fungal production after storage at 4°C.

The production of hypericin and emodin by the first generation of the cultured endophyte on storage at 4°C was evaluated during February 2009 and October 2009, compared to the initial values (August 2007). The endophyte showed a substantial reduction in the production of both hypericin and emodin under storage conditions, similar to subculturing (Fig. 65d). Interestingly, the impact of storage on the decrease in hypericin production was more pronounced as compared to that on emodin.

2.3.7. Cytotoxic and photodynamic efficacies of the fungal metabolites

In order to investigate the exploratory *in vitro* cytotoxic effects of photoactivated fungal extract containing hypericin and emodin metabolized by the fungus, THP-1 cells were incubated in parallel with the various concentrations of the fungal extract in the dark and after light activation, respectively. The cytotoxicity was assessed using the resazurin-based assay to measure the THP-1 mitochondrial succinoxidase inhibition (Fig. 66), as well as by using the ATPlite assay to measure the THP-1 cytoplasmic ATP depletion (Fig. 67). The cytotoxic effect of the fungal extract was found under both dark and light-activated conditions. In both conditions, a concentration-dependent cytotoxicity was observed. However, the cytotoxicity of the fungal extract was much more pronounced after irradiation with light for 20 min in both the assay types, revealing the photodynamic properties of the fungal metabolites. The resazurin assay revealed the greatest viability gap at a concentration of 1.185 μg mL^{-1} [92.7 (dark) versus 4.9% (light)] (Fig. 66b). Similarly, the ATPlite assay also revealed the greatest viability gap at the same concentration [91.1 (dark) versus 1.0% (light)] (Fig. 67b). The interference of the sample with the dye under both illuminated and dark conditions was considered when evaluating the assays (Figs. 66c,d and 67c,d).

2.3.8. Effect of fungal metabolites on morphology of human cancer cell line THP-1

In order to ascertain the effect of the fungal metabolites on the THP-1 morphology under dark and photoactivated states, microscopic studies of untreated and treated cells were performed (Fig. 68). The untreated cells were round, single cells in suspension, and some cells were in clusters. The treated cells showed reduction in size and condensation of the nucleus, and the protoplasmic extensions were reduced. The cells treated with photoactivated metabolites showed even more visible apoptosis with drastic condensation of the cytoplasm and nucleus and marginalization of the chromatin material in the nuclei (Fig. 68b). This, yet again, revealed the high photodynamic properties of the fungal metabolites that would necessitate some form of regulation of endophytic production of these metabolites.

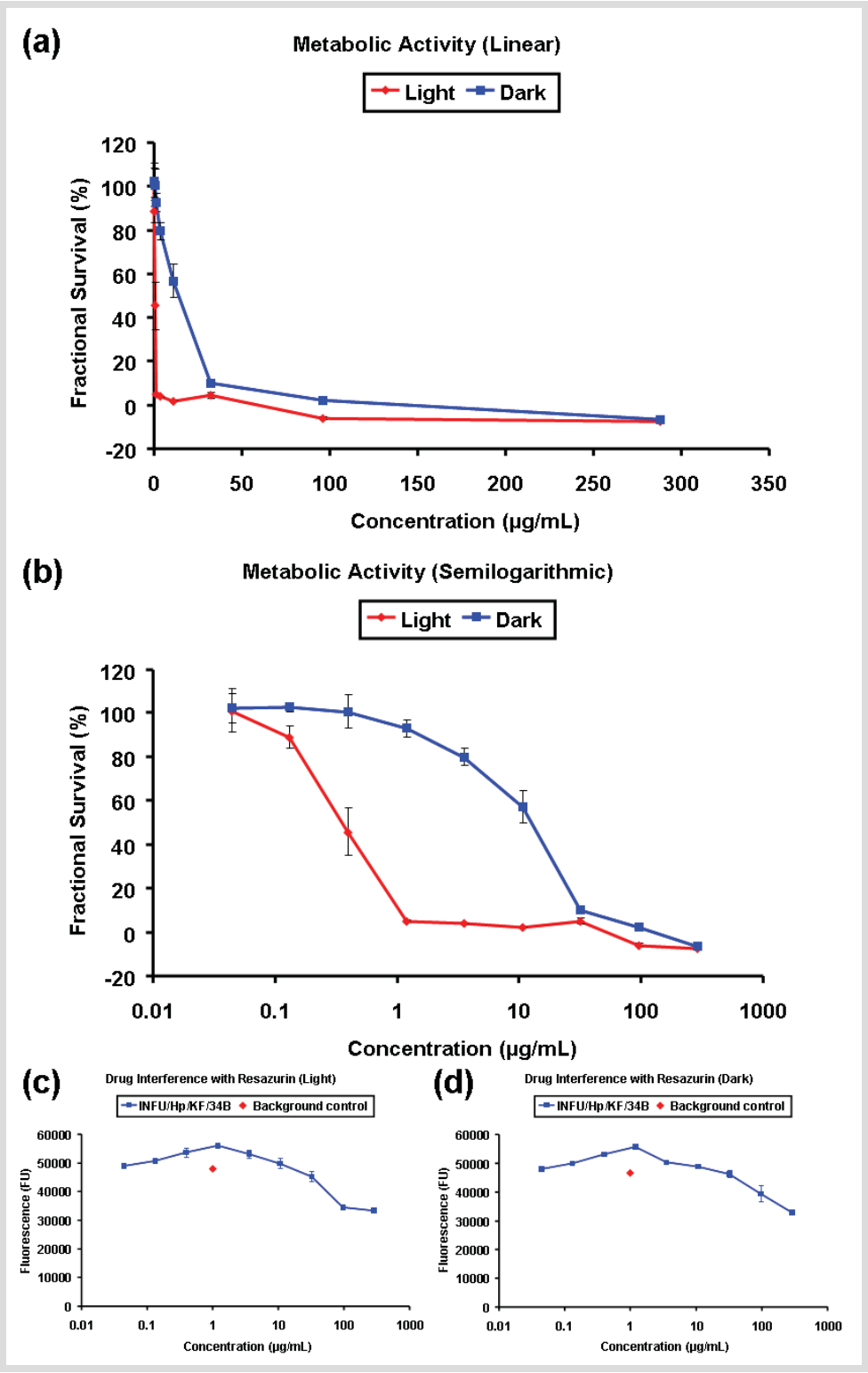

Fig. 66. Resazurin-based *in vitro* cytotoxic assay of the fungal extract against THP-1 cells under light protection and after light activation. (a) Linear representation of fractional survival (FS) of THP-1 as a function of concentration. (b) Semilogarithmic representation of the FS of THP-1 as a function of concentration. (c) Interference of the sample with the indicator (resazurin) in light conditions. (d) Interference of the sample with the indicator (resazurin) in dark conditions.

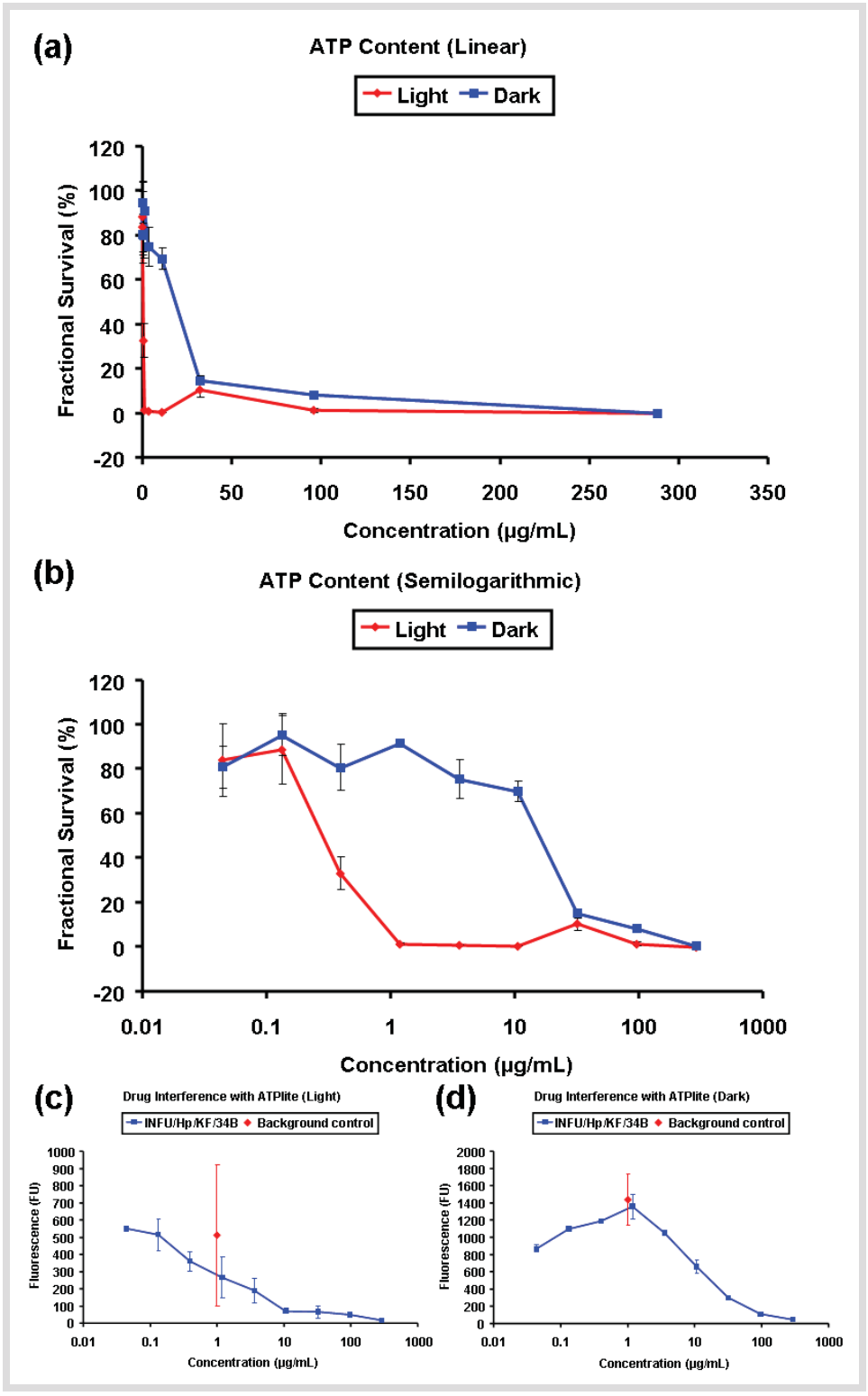

Fig. 67. *In vitro* cytotoxic assay of the fungal extract against THP-1 cells using ATPlite under light protection and after light activation. (a) Linear representation of fractional survival (FS) of THP-1 as a function of concentration. (b) Semilogarithmic representation of the FS of THP-1 as a function of concentration. (c) Interference of the sample with the indicator (ATPlite) in light conditions. (d) Interference of the sample with the indicator (ATPlite) in dark conditions.

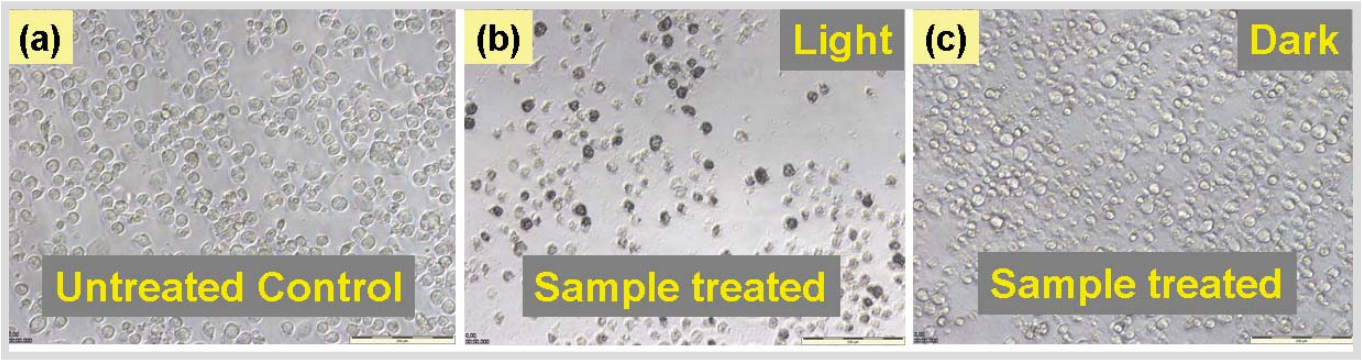

Fig. 68. Representative microscopic pictures depicting the morphology of the THP-1 cells. (a) Untreated. (b) Treated with light-activated fungal metabolites. (c) Treated with fungal metabolites not photo-activated.

3. Deoxypodophyllotoxin

3.1. Phytochemical profiling of host plants

3.1.1. Phytochemical profiling by multivariate analysis (MVA)

All together, thirteen different *Juniperus* plants and five different *Podophyllum* plants were analyzed for four different secondary metabolites. The concentrations of podophyllotoxin, deoxypodophyllotoxin, podophyllotoxone, and demethylpodophyllotoxin in the organic, aqueous and total (organic and aqueous) phases are shown in Table T6 (Appendix A) for *Juniperus* and Table T7 (Appendix A) for *Podophyllum*. Fig. 69 shows the characteristic fragmentation pathway for the four tested compounds, and their high-resolution precursor and product ions in plants. Based on LC-MS/MS analyses, it was revealed that *P. hexandrum* (from Pahalgam) had the highest contents of both podophyllotoxin and podophyllotoxone, whereas *P. hexandrum* (from Yahrika) had the highest contents of deoxypodophyllotoxin (infraspecific) and demethylpodophyllotoxin, respectively. *J. x-media* Pfitzeriana showed the highest contents of all the tested metabolites (infraspecific), except demethylpodophyllotoxin. Strikingly, it contained the highest amounts of deoxypodophyllotoxin, even higher than *P. hexandrum* which is currently exploited for harvesting podophyllotoxin and related compounds. Therefore, *J. x-media* Pfitzeriana might be an alternative to *P. hexandrum* currently being widely used worldwide for harvesting the anticancer pro-drug podophyllotoxin. Nevertheless, it is worth mentioning that any phyto-drug produced from *J. x-media* Pfitzeriana would obviously have to pass through the international regulatory frameworks including detailed clinical and toxicological studies. Deoxypodophyllotoxin was the only metabolite that was found in all the species and from all localities. Demethylpodophyllotoxin was below the limit of quantitation (<LOQ) in all *Juniperus* species.

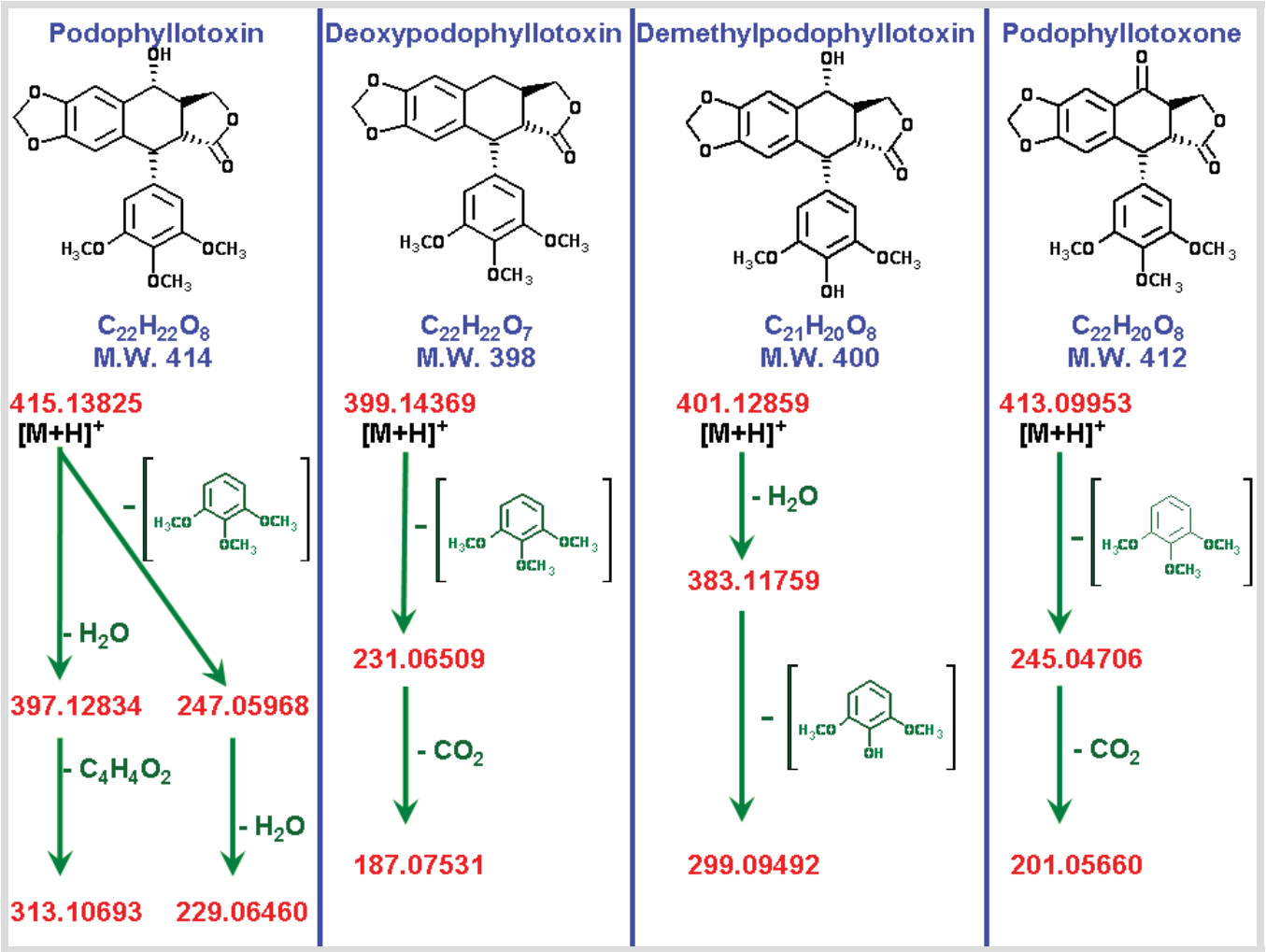

Fig. 69. The MS/MS fragmentation pathway of podophyllotoxin, deoxypodophyllotoxin, demethylpodophyllotoxin, and podophyllotoxone. The high-resolution MS^n precursor and product ions are shown in red color.

MVA of the LC-MS/MS data was carried out to evaluate the individual and holistic phytochemical variability due to differences between categories, namely, the different plant species, the organic and aqueous phases, as well as between the two different genera (Fig. 70). From the MVA, it was evident that the tested compounds were mostly favored in the organic phases, although considerable ratios of podophyllotoxin, deoxypodophyllotoxin, and podophyllotoxone were also found in the aqueous phases in the *Podophyllum* genus. Computation of the individual averages for each category revealed the highest holistic phytochemical load in the organs of *P. hexandrum* (from Pahalgam), followed by *P. hexandrum* (from Gulmarg), and *J. x-media* Pfitzeriana, respectively. It is interesting to note that MVA also revealed *J. x-media* Pfitzeriana as a practically considerable substitute of *P. hexandrum*.

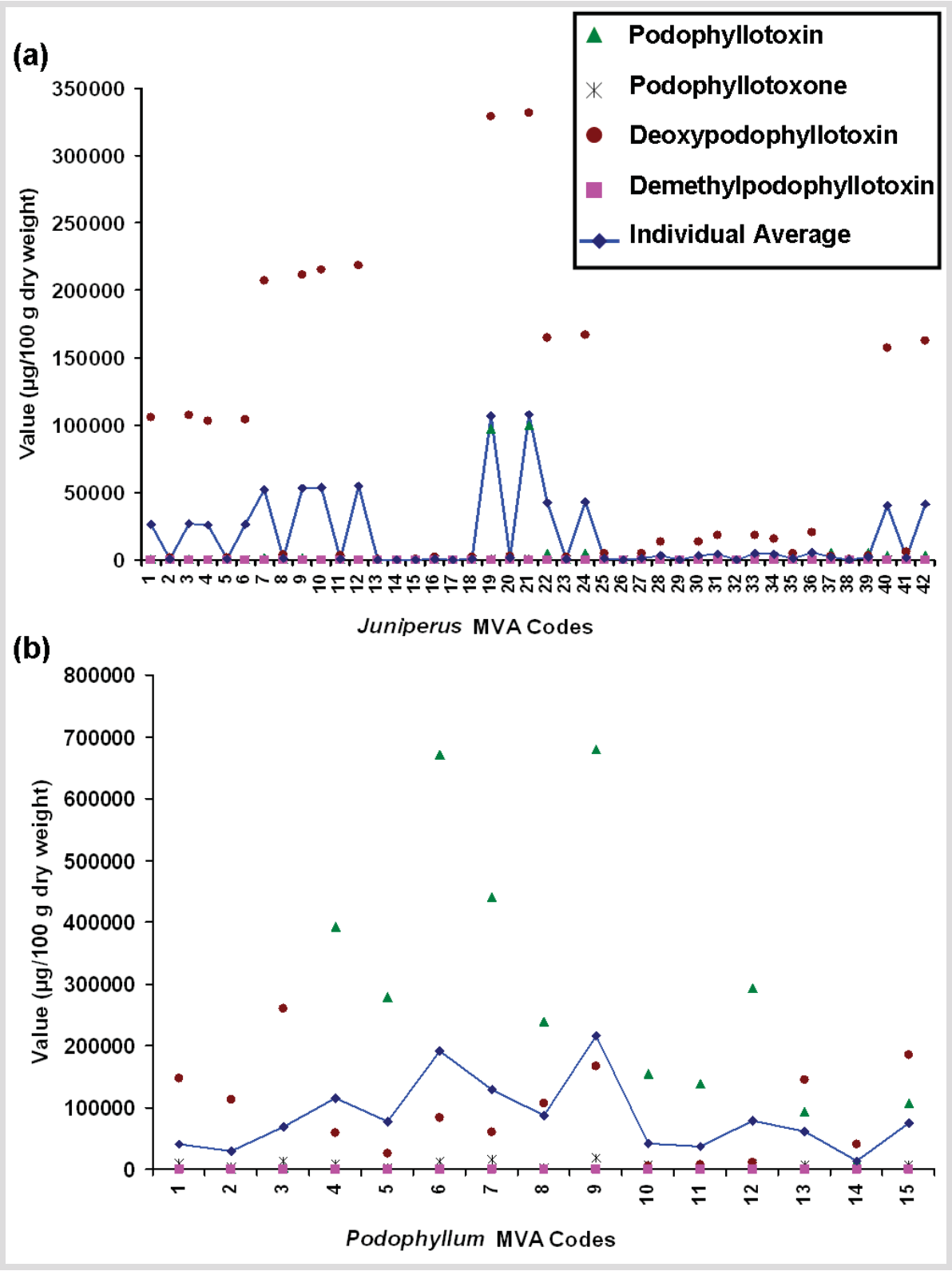

Fig. 70. MVA for evaluating the individual and holistic phytochemical variability due to differences among the different plant species, the organic and aqueous phases, as well as between the two different genera. (a) MVA of *Juniperus* species. (b) MVA of *Podophyllum* species. The MVA codes are detailed in Tables T6 and T7 (Appendix A), respectively.

3.1.2. Multidimensional scaling (MDS)

Kruskal's MDS algorithm based on the Pearson correlation matrix was used to investigate the relationships between the metabolite contents (total) among the investigated *Juniperus* and *Podophyllum* species (Figs. 71-73). The method was executed in a 3-dimensional (3D) module to build a 3D map of the series of phytochemicals under study from the proximities matrix (by dissimilarities) between the categories (Figs. 71a, 72a, and 73a). Furthermore, a 3D surface analysis was performed using the 3D distance in space between the phytochemicals to build the exact map of the phytochemical relativity within about the given symmetry of the 3 axes in 3 different dimensions (Figs. 71c, 72c, and 73c). In order to achieve an optimal representation of the data points in 3D, Kruskal's stress was computed and found to be negligible in all evaluations (5.799×10^{-5} for *Juniperus* species, 2.66×10^{-4} for *Podophyllum* species, and 1.133×10^{-4} for *Juniperus* and *Podophyllum* evaluated together). Moreover, to have an overall idea of the quality of the representation, the Shepard diagram based on Kruskal's stress in 3D was evaluated. The Shepard diagram revealed that the observed dissimilarities and the disparities (distances) were on the same linear curve for each evaluation (Figs. 71b, 72b, and 73b), confirming the reliability of the MDS representation in 3D. The Pearson correlation matrix for *Juniperus* species (Table 12) revealed a significant positive correlation between podophyllotoxin and podophyllotoxone contents (Pearson correlation coefficient, $r = 0.976$, $\alpha \leq 0.05$). However, such a correlation could not be observed among the *P. hexandrum* plants collected from the different natural populations. Nevertheless, a significant negative correlation was revealed between podophyllotoxin and deoxypodophyllotoxin ($r = -0.165$, $\alpha \leq 0.05$), and, podophyllotoxin and demethylpodophyllotoxin ($r = -0.160$, $\alpha \leq 0.05$). Furthermore, the infrageneric relationship between *Juniperus* and *Podophyllum* was evaluated to elucidate whether the infraspecific correlations could be mapped within different genera. A significant positive correlation could be observed between podophyllotoxin and podophyllotoxone ($r = 0.793$, $\alpha \leq 0.05$), suggesting that this pattern could be expected in other genera too that accumulate podophyllotoxin. Interestingly, a positive correlation between podophyllotoxone and demethylpodophyllotoxin ($r = 0.719$, $\alpha \leq 0.05$) was found at the infrageneric level but not at the infraspecific level.

3.1.3. Principal component analysis (PCA)

The reliability of the PCA in 2D was evaluated by computing a Scree Plot in each case using the data variability in the useful dimensions (in this case, up to F4, i.e., 4th dimension) versus the cumulative variability, relative to the eigenvalues (Fig. 74a,c,e). From the Scree Plots, it was revealed that the PCA analyses were reliable in 2D spacing (F1/F2 *Juniperus* = 99.32%, F1/F2 *Podophyllum* = 88.07%, and F1/F2 *Juniperus* and *Podophyllum* = 82.39%).

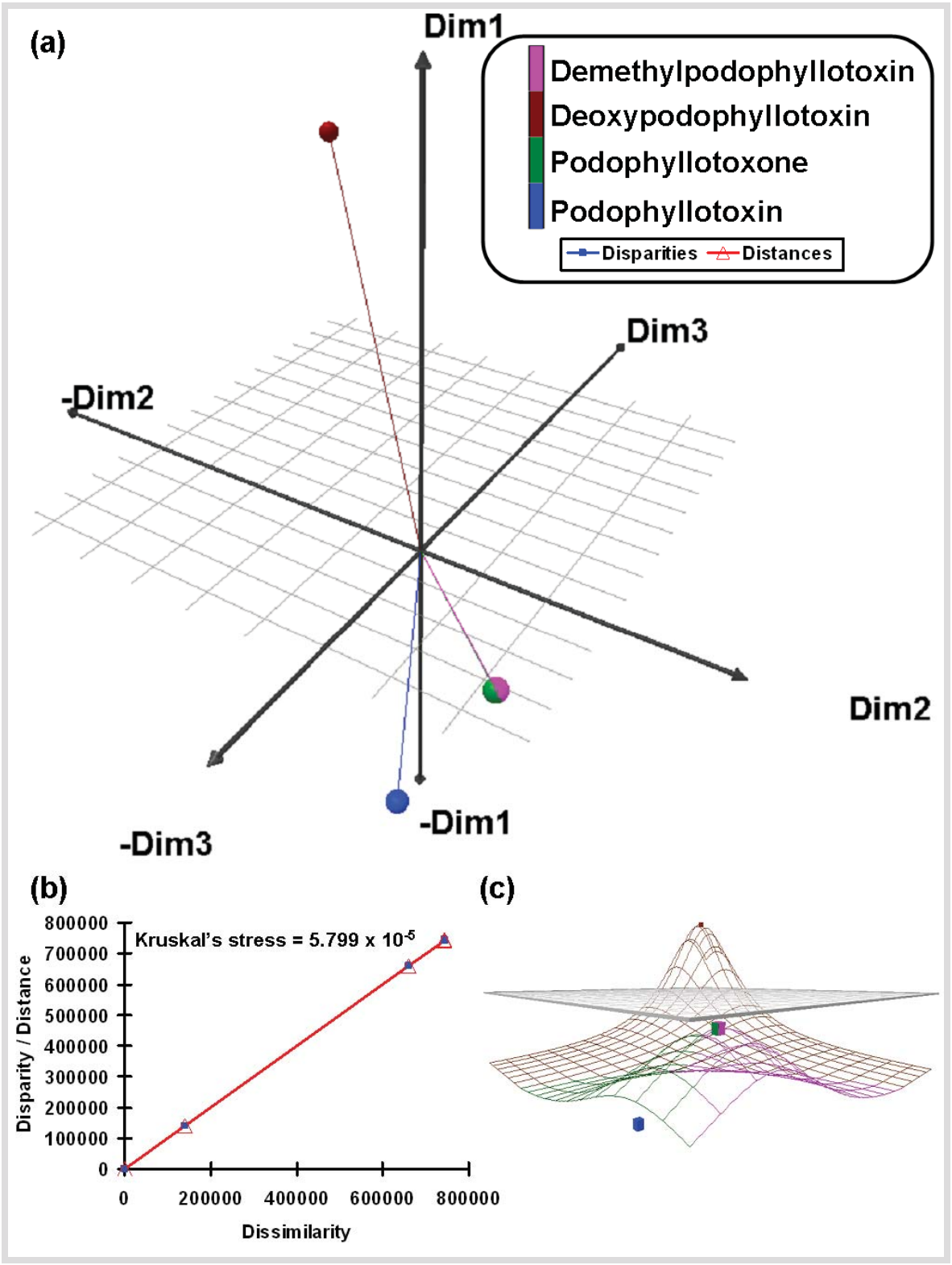

Fig. 71. Kruskal's MDS based on Pearson correlation in *Juniperus* species. (a) 3D MDS map of the four metabolites under study from the proximities matrix (by dissimilarities) between the categories. (b) The Shepard diagram for the MDS analysis in 3D. (c) 3D surface analysis map showing the spatial 3D distance about the given symmetry of the 3 axes in 3 different dimensions.

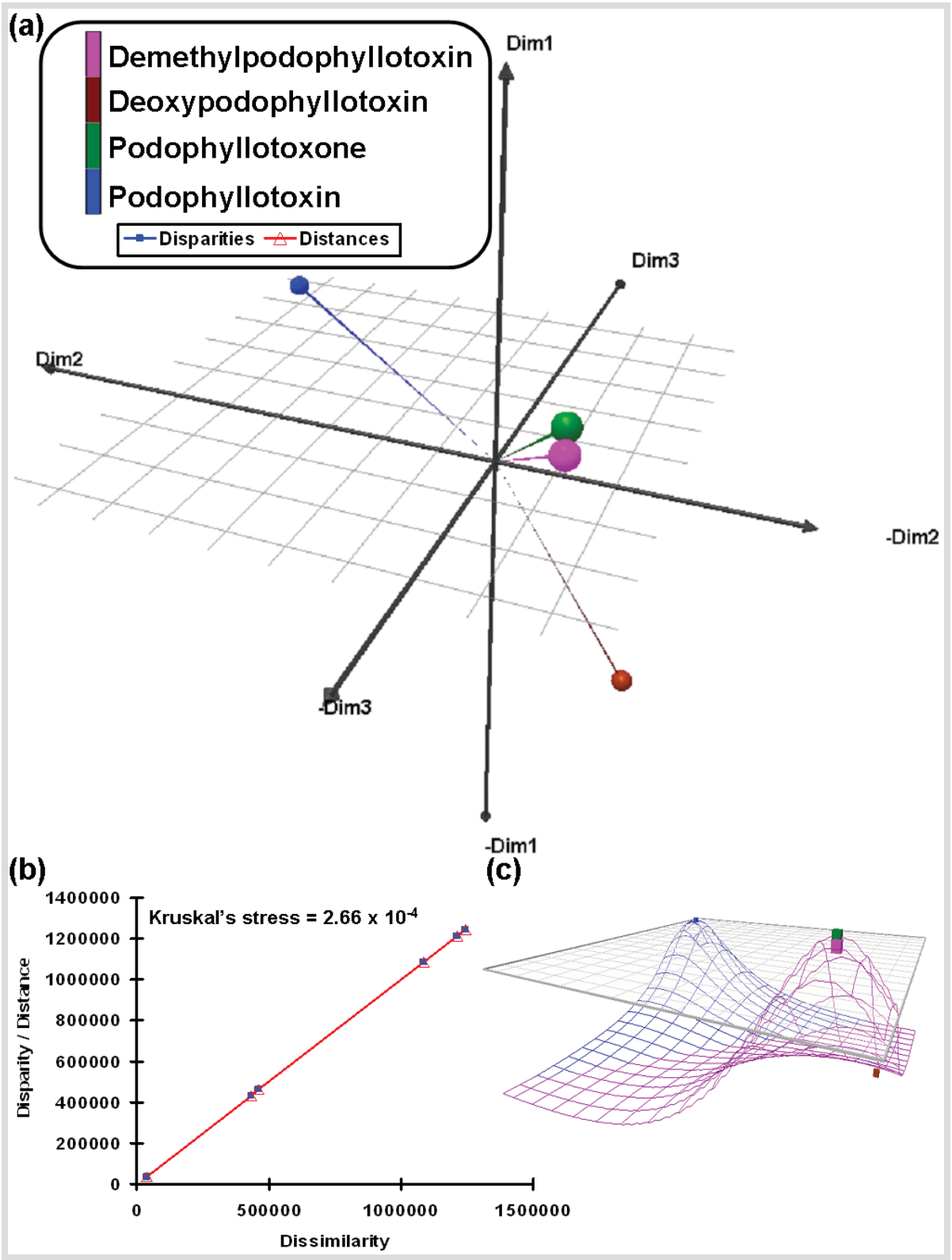

Fig. 72. Kruskal's MDS based on Pearson correlation in *Podophyllum* species. (a) 3D MDS map of the four metabolites under study from the proximities matrix (by dissimilarities) between the categories. (b) The Shepard diagram for the MDS analysis in 3D. (c) 3D surface analysis map showing the spatial 3D distance about the given symmetry of the 3 axes in 3 different dimensions.

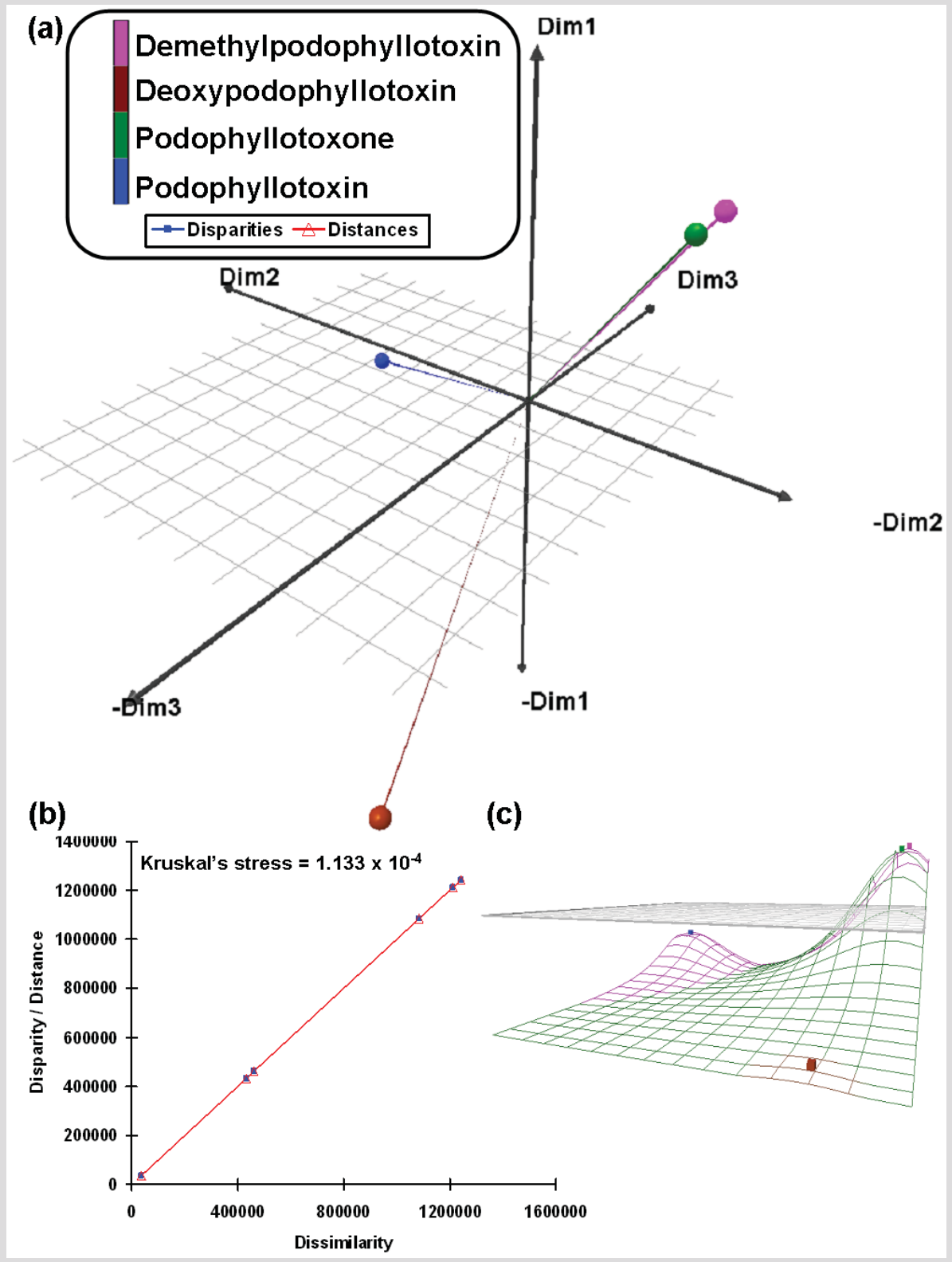

Fig. 73. Kruskal's MDS based on Pearson correlation in *Juniperus* and *Podophyllum* species (infrageneric). (a) 3D MDS map of the four metabolites under study from the proximities matrix (by dissimilarities) between the categories. (b) The Shepard diagram for the MDS analysis in 3D. (c) 3D surface analysis map showing the spatial 3D distance about the given symmetry of the 3 axes in 3 different dimensions.

Table 12. The Pearson correlation matrix depicts the correlations between the four metabolites under study. The significant positive and negative correlations are represented in bold. na, not applicable.

Plant	Variables	Podophyllotoxin	Podophyllotoxone	Deoxypodophyllotoxin	Demethylpodophyllotoxin
***Juniperus* species (infraspecific)**	**Podophyllotoxin**	1	-	-	-
	Podophyllotoxone	**0.976**	1	-	-
	Deoxypodophyllotoxin	0.644	0.575	1	-
	Demethylpodophyllotoxin	na	na	na	Na
***Podophyllum* species (infraspecific)**	**Podophyllotoxin**	1	-	-	-
	Podophyllotoxone	0.587	1	-	-
	Deoxypodophyllotoxin	**-0.165**	0.454	1	-
	Demethylpodophyllotoxin	**-0.160**	0.529	0.640	1
***Juniperus* and *Podophyllum* (infrageneric)**	**Podophyllotoxin**	1	-	-	-
	Podophyllotoxone	**0.793**	1	-	-
	Deoxypodophyllotoxin	0.112	0.239	1	-
	Demethylpodophyllotoxin	0.283	**0.719**	0.299	1

The PCA in each case was represented in the form of a Correlation Circle depicting the projection of the variables in the 2D space. The PCA for *Juniperus* species revealed a significant positive correlation between the podophyllotoxin and podophyllotoxone contents among the studied plants (Fig. 74b), corroborating the MDS. The PCA score plot revealed that *J. x-media* Pfitzeriana was well separated from the rest of the species, similar to what was depicted by LDA (*vide infra*). The PCA for *Podophyllum* species revealed a negative correlation between podophyllotoxin and deoxypodophyllotoxin, as also demethylpodophyllotoxin (Fig. 74d), again ratifying the MDS evaluation. Furthermore, the PCA considering both genera positively correlated podophyllotoxone with both podophyllotoxin and demethylpodophyllotoxin (Fig. 74f). In this case, however, the score plot separated *J. x-media* Pfitzeriana from *P. hexandrum* both from Pahalgam and Gulmarg. The Correlation Circle also depicted an orthonormal projection between podophyllotoxin and deoxypodophyllotoxin. Hence, an infrageneric correlation could not be drawn between these two metabolites.

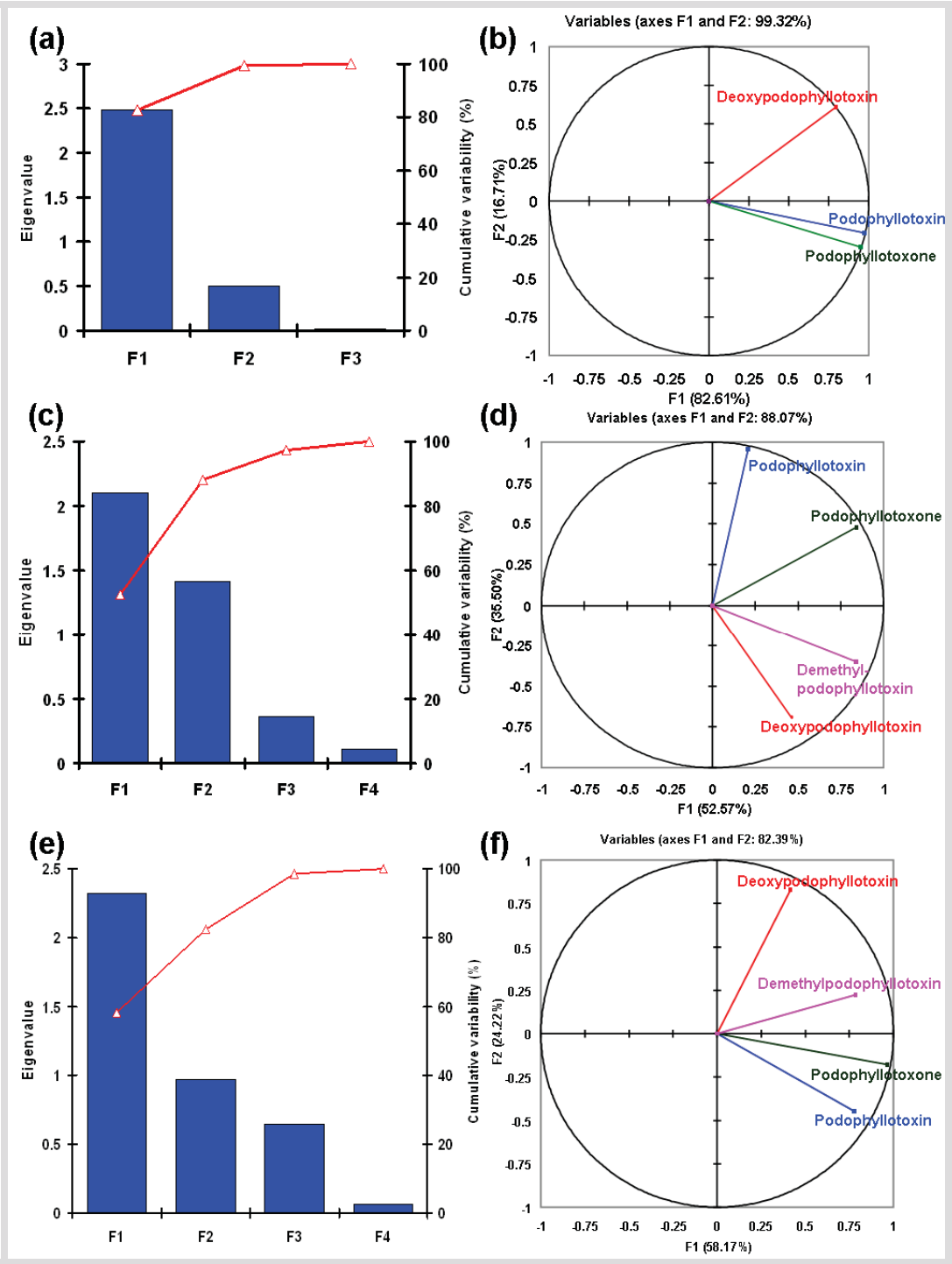

Fig. 74. PCA. (a) The Scree Plot depicting the data variability in the four dimensions versus the cumulative variability, relative to the eigenvalues in *Juniperus*. (b) The PCA Correlation Circle depicting the projection of the variables (phytochemicals) in the 2D space in *Juniperus*. (c) The Scree Plot depicting the data variability in the four dimensions versus the cumulative variability, relative to the eigenvalues in *Podophyllum*. (d) The PCA Correlation Circle depicting the projection of the variables (phytochemicals) in the 2D space in *Podophyllum*. (e) The Scree Plot depicting the data variability in the four dimensions versus cumulative variability, relative to the eigenvalues infragenerically. (f) The PCA Correlation Circle depicting the projection of the variables (phytochemicals) in the 2D space infragenerically.

3.1.4. Linear discriminant analysis (LDA)

In order to evaluate the chemotaxonomic significance (specificity of secondary compound profiles for individual species) of the different plant samples under study and to visualize how the four metabolic constituents allowed discriminating the species, LDA was computed, each for *Juniperus* and *Podophyllum* species. The results were visualized on a 2D map that depicted the degree of separation between the groups (Fig. 75). The LDA projection for *Juniperus* (Fig. 75a) revealed that *J. x-media* Pfitzeriana was well separated from the rest of the species. From the MVA, it was observed that *J. x-media* Pfitzeriana had the highest holistic phytochemical load among the plants of *Juniperus*, and therefore, the LDA projection classified this species as distinct in metabolite spectrum and demarcated from other species. Furthermore, the plants *J. communis* Hibernica and *J. communis* L. Wilseder Berg, *J. squamata* Wilsonii and *J. recurva* (from Sonamarg), and, *J. communis* L. Horstmann and *J. communis* L. Meyer were grouped in close confidence. The rest of the species were tightly-correlated and well separated from the other confidence circles within the projection.

The LDA projection for *Podophyllum* (Fig. 75b) revealed *P. hexandrum* from Pahalgam and Gulmarg were grouped in close confidence and well separated from all the other plants depicted in the projection. This was comparable to the MVA that also revealed a similar load of podophyllotoxin in *P. hexandrum* from these two populations, suggesting that the environmental difference was a non-significant factor in determining the metabolite spectrum in these plants, or that there might not be a significant difference in the environmental conditions in these two locations (during sampling period).

3.1.5. Hierarchical agglomerative cluster analysis (HACA)

For a clearer arrangement, the compounds measured were grouped in a manner that assigned similar behavior using the HACA method by average linkage. Dissimilarity was measured by Euclidean distance using data of all four standard constituents under study, as well as for the different plant samples. The results were visualized by dendrograms (Figs. 76 and 77). The dendrogram obtained by HACA plotting various plant species of *Juniperus* genus versus each of the four phytochemicals under study (Fig. 76a) showed that *J. x-media* Pfitzeriana was well separated from all the other species. This yet again corroborated the distinct metabolic profile of this species as compared to other species of *Juniperus*. HACA also revealed that *J. communis* Hibernica and *J. communis* L. Wilseder Berg, *J. squamata* Wilsonii and *J. recurva* (from Sonamarg), and, *J. communis* L. Horstmann and *J. communis* L. Meyer formed single sub-clusters, respectively. Similarly, the dendrogram obtained by HACA plotting the *P. hexandrum* plants from different natural populations versus each of the four phytochemicals under study (Fig. 76b) showed that *P. hexandrum* from Pahalgam and Gulmarg, and, from Sonamarg and Aru, were closely associated.

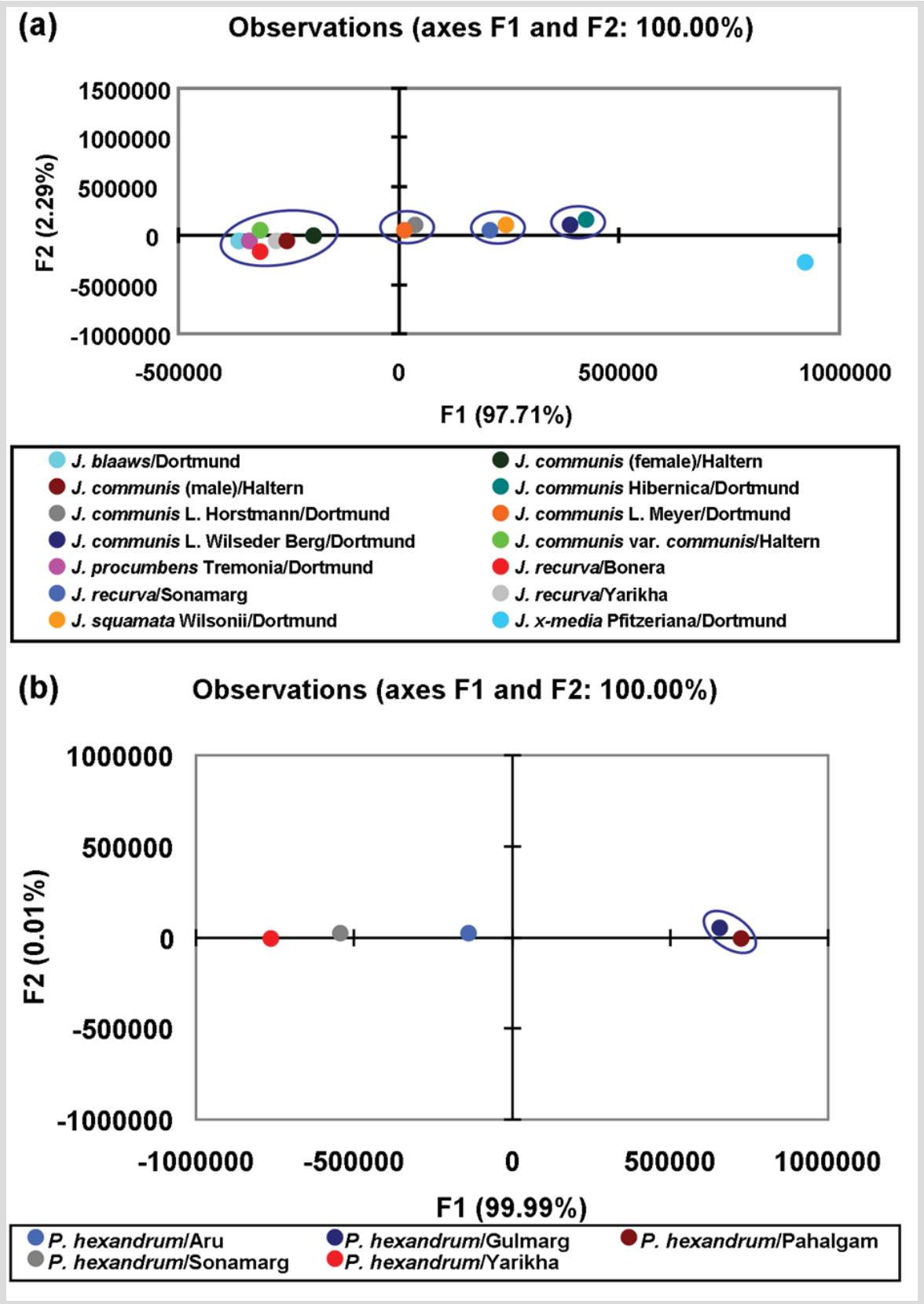

Fig. 75. LDA 2D map. (a) For *Juniperus*. (b) For *Podophyllum*.

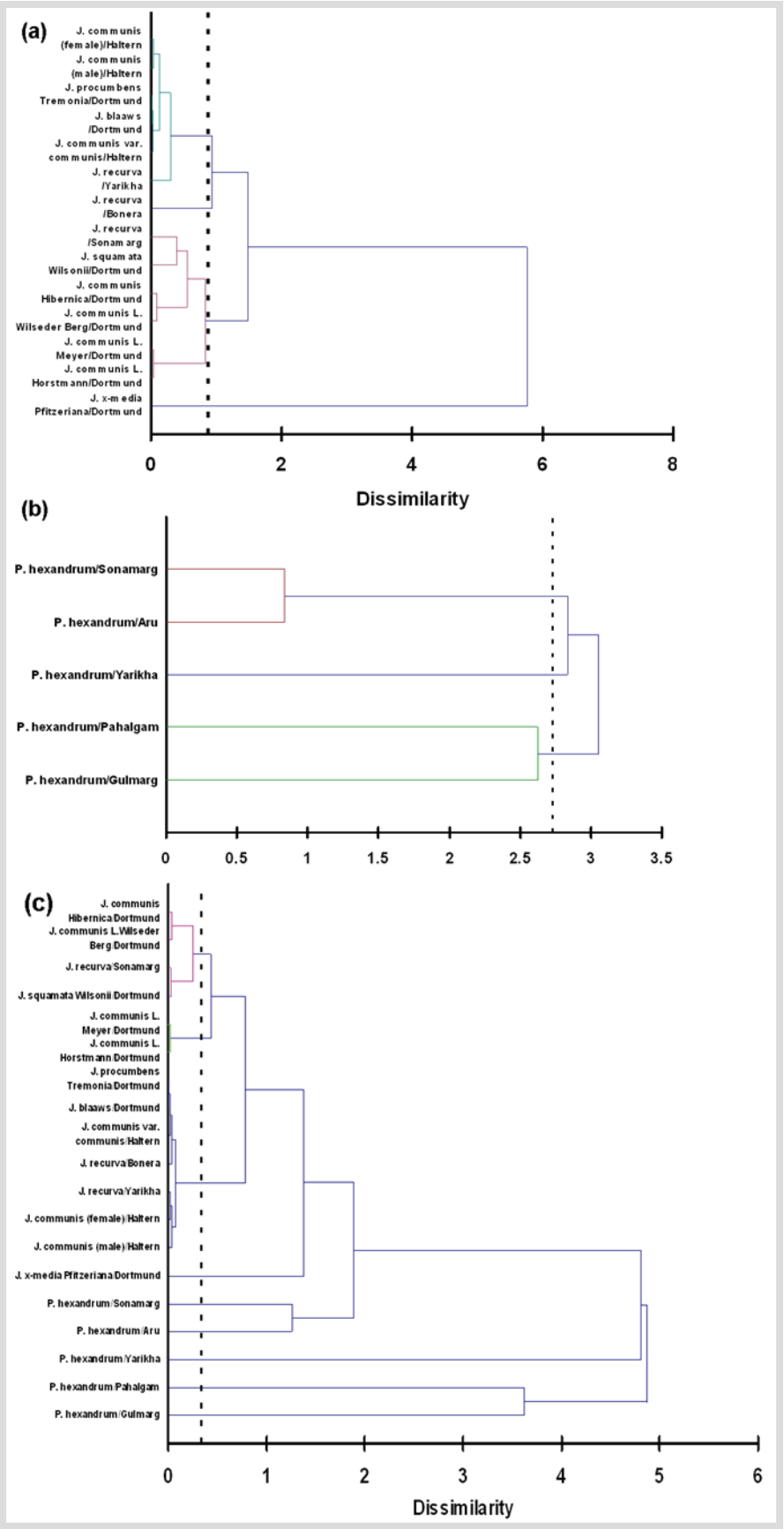

Fig. 76. HACA by average linkage. (a) The dendrogram obtained by HACA plotting the various *Juniperus* plant species under study versus each of the four metabolites under study. (b) The dendrogram obtained by HACA plotting the various *Podophyllum* plant species under study versus each of the four metabolites under study. (c) The dendrogram obtained by HACA plotting the both *Juniperus* and *Podophyllum* species under study versus each of the four metabolites under study.

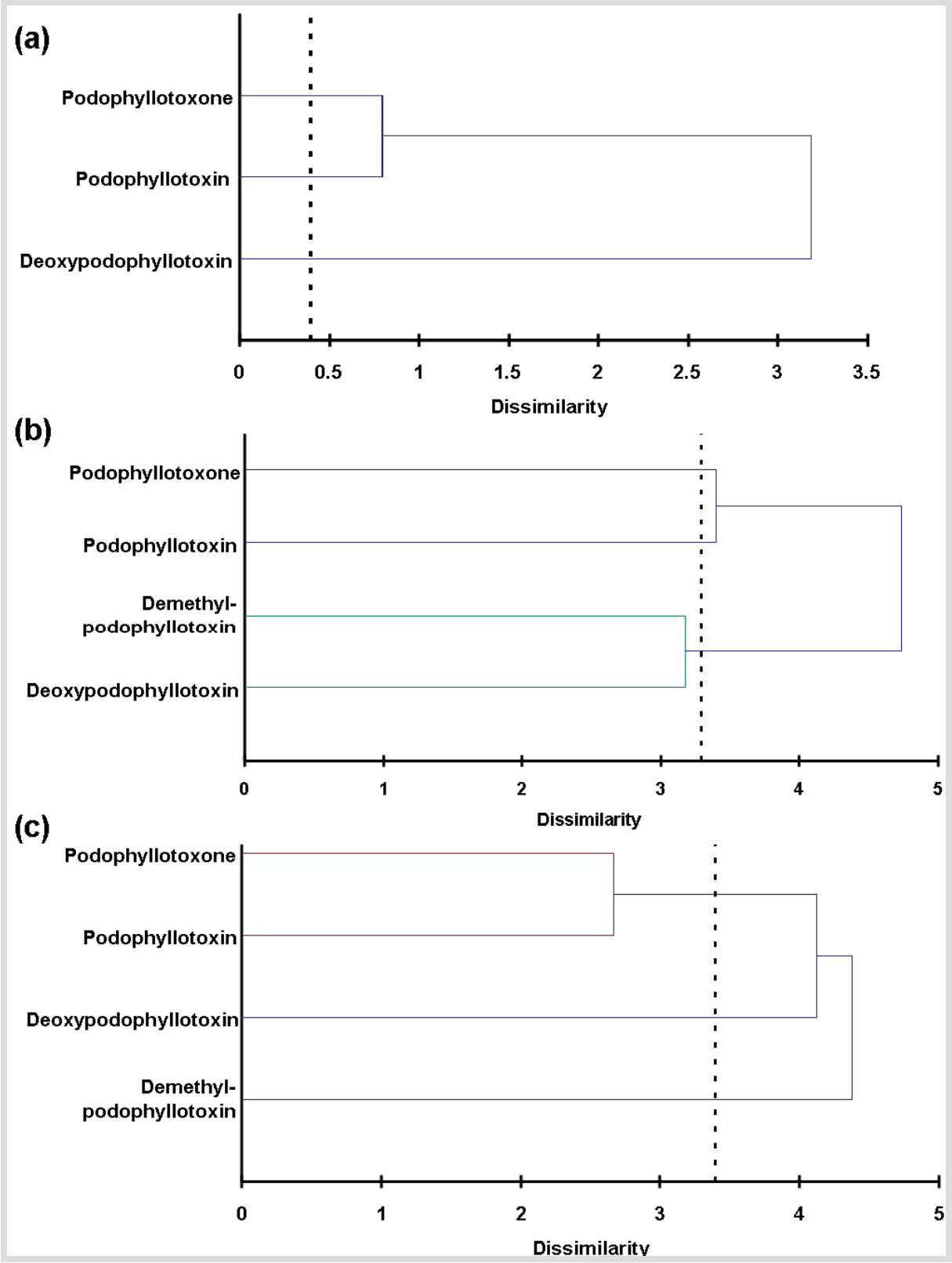

Fig. 77. The dendrogram obtained by HACA plotting the data of all the four metabolites under study versus (a) the *Juniperus* species; (b) the *Podophyllum* species; and (c) both *Juniperus* and *Podophyllum* species together (infrageneric).

Finally, the dendrogram obtained by combining the chemical data of both the genera together (Fig. 76c) revealed that the infrageneric confidence between the two genera was non-significant, although the infraspecific correlations remained visible. The dendrogram obtained by HACA plotting the data of all the four compounds under study versus the plant species (Fig. 77) showed that podophyllotoxin and podophyllotoxone were grouped together, separately from the other components, within both *Juniperus* and *Podophyllum*. This was also reflected at the infrageneric level. Furthermore, a distinct interdependence between deoxypodophyllotoxin and demethylpodophyllotoxin could be observed only in the *Podophyllum* genus.

3.2. Biological characterization of deoxypodophyllotoxin producing endophytic fungus

3.2.1. Isolation and *in vitro* culture of the endophytic fungus

Juniperus and *Podophyllum* species were chosen as the source for isolating the endophytes, since these plants grow mainly in unexplored environments in the forest regions of Europe and high-altitude ranges of South Asia (mainly the Himalayan region) where there is a possibility of mutualistic interactions between different groups of organisms. Earlier studies had indicated that virgin environments favor such interactions (Arnold *et al.*, 2000). Podophyllotoxin, deoxypodophyllotoxin, demethylpodophyllotoxin and related metabolites are not only present in Podophyllaceae, but also in other families. The plant sampling results from Germany and India confirmed the presence of considerable amounts of podophyllotoxin and structural analogues in the host plants and were selected for searching endophytic fungi. Table 13 shows the number of endophytic fungi isolated from various organs of the *Juniperus* and *Podophyllum* plants, which were morphologically different from the strains isolated from unsterilized explants (surface-contaminating fungi). Out of all the endophytes, only one was able to produce deoxypodophyllotoxin (INFU/Jc/KF/6), and was taken up for further studies.

3.2.2. Macroscopic morphological characteristics of the endophytic fungus on agar medium

The fungus produced surficial and submerged hyphae on rich medium like PDA and SA (Fig. 78), however the growth being most prominent on CDA at 25–30°C. The colony on CDA was typically bluish to dull green, and growing rapidly up to 6 mm day^{-1}. The mycelium was colorless and inconspicuous. The colony texture was velutinous. From the reverse side of the Petri plate, the colony was creamy to yellowish in color. Interestingly, the fungus showed good rate of growth even up to 45°C on CDA.

Table 13. The number of endophytic fungi isolated from different organs of the *Juniperus* and *Podophyllum* plants sampled from various locations.

Plant	Location	Organ	Number of isolated endophytic fungi
J. recurva	Yarikha	Twigs	26
J. recurva	Bonera	Twigs	24
J. recurva	Sonamarg	Twigs	33
J. communis L. Horstmann	Dortmund	Twigs	22
J. communis L. Meyer	Dortmund	Twigs	18
J. communis L. Wilseder Berg	Dortmund	Twigs	19
J. communis Hibernica	Dortmund	Twigs	19
J. blaaws	Dortmund	Twigs	14
J. procumbens Tremonia	Dortmund	Twigs	19
J. x-media Pfitzeriana	Dortmund	Twigs	27
J. squamata Wilsonii	Dortmund	Twigs	23
J. communis var. *communis*	Haltern	Twigs	11
J. communis (male cones)	Haltern	Twigs	13
J. communis (female cones)	Haltern	Twigs	9
P. hexandrum	Yarikha	Leaves	16
		Stems	14
P. hexandrum	Gulmarg	Leaves	21
		Stems	15
P. hexandrum	Pahalgam	Leaves	9
		Stems	11
P. hexandrum	Aru	Leaves	16
		Stems	9
P. hexandrum	Sonamarg	Leaves	8
		Stems	7

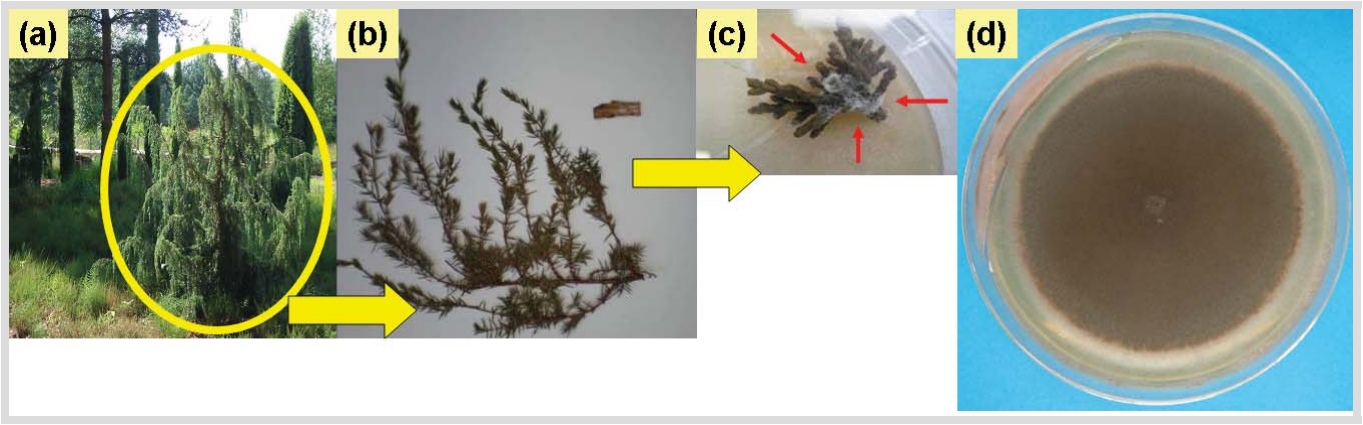

Fig. 78. (a) *J. communis* L. Horstmann plant maintained at botanical gardens, Rombergpark, Dortmund. (b) Twig from where INFU/Jc/KF/6 was isolated. (c) Endophytic mycelia growing out from surface-sterilized *Juniperus* twig on WA supplemented with streptomycin (red arrows). (d) Macroscopic morphology of the endophyte on SA.

3.2.3. Macroscopic morphological characteristics of the endophytic fungus in broth medium

Under shake-flask conditions in SB (Fig. 79), the fungus grew vigorously as small and sticky green to greenish-black pellets. Pellicle formation at the edge of the flask was heavy and sticky. Interestingly, medium or big spherical balls were not formed under the submerged conditions. At the end of 5 days, the spent medium looked more viscous and dark colored than the fresh medium.

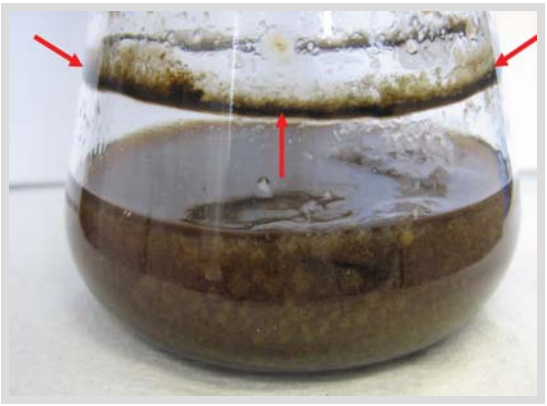

Fig. 79. The macroscopic morphological characteristics of the endophytic fungus in SB. The greenish-black pellets can be seen submerged in the broth. The heavy and sticky pellicle is shown by red colored arrows.

3.2.4. Microscopic morphological characteristics of the endophytic fungus

Microscopic studies of the fungus (Fig. 80) have shown the conidiophores as smooth to finely rough walled, 200–300 µm long, up to 7 µm in diameter, and enlarging gradually into vesicles of 18–20 µm diameter. Metulae were absent; phialides were ampulliform, with a short neck and 7–9 µm long. Conidiation was abundant. The conidia were mostly subglobose-globose to ellipsoidal, 2.5–3 µm in length, echinulate, and adhering in long compact columns.

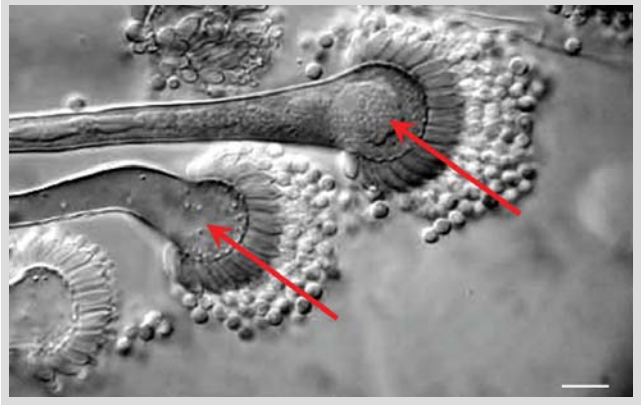

Fig. 80. The microscopic morphological characteristics of the endophytic fungus on SA. The conidia heads are marked by red colored arrows.

3.2.5. Identification and authentication of the endophytic fungus

Molecular analysis of the fungus based on 28S ribosomal DNA partial gene sequencing revealed 97% similarity to *Aspergillus niger* CBS 513.88 contig. An03c0l00 (accession number NW 001594104), 96%

similarity to *A. niger* CBS 513.88 contig. An03c0110 (accession number NW 001594105) and also to other related taxa, e.g., 96% similarity to fungal endophyte isolate 9147 (accession number EF420081). The DNA sequence obtained has been deposited at the EMBL-Bank under accession number FM179606. Since the closest match was at a difference of at least 3% homology, the molecular method was only indicative of the genus of the fungus as *Aspergillus*. The final identification to species level was made using morphological and physiological characteristics in addition to the molecular analysis. Based on the typical microscopic features as detailed above, the fungus has been identified as *Aspergillus fumigatus* Fresenius. The fungal features corroborate the previously published description (Samson *et al.*, 2007). Additionally, the fungal identification has been authenticated by DSMZ. The endophyte has been deposited to DSMZ as *A. fumigatus* Fresenius under the accession number DSM 21023.

3.3. Biochemical characterization of deoxypodophyllotoxin producing endophytic fungus

3.3.1. Structural elucidation of deoxypodophyllotoxin

The detection and elucidation of deoxypodophyllotoxin was done by accurate-mass HPLC-MS^n on the basis of fragmentation pathways as detailed in Fig. 81. The high-resolution MS^2 spectrum of deoxypodophyllotoxin showed the protonated ion at *m/z* 399.14367 with one major fragment ion at *m/z* 231.06500 arising from the elimination of one trimethoxybenzene molecule. MS^3 fragmentation of this fragment ion (Fig. 81d) produced further an ion at *m/z* 187.07528 after elimination of a carbon dioxide molecule. Three more ions at *m/z* 185.05970, *m/z* 157.06481 and *m/z* 129.06982 were observed, showing the loss of a carbon monoxide, formaldehyde and another carbon monoxide molecule, respectively. All measured masses showed a maximal deviation of 1 ppm from the theoretical mass. This fragmentation pathway corroborates not only the previously established report (Wong *et al.*, 2000) but also the deoxypodophyllotoxin obtained from the host *J. communis* plant (Fig. 81a,c).

3.3.2. Growth kinetics of the endophytic fungus

The growth kinetics of the endophyte, under the standardized culture conditions described above, was examined (Fig. 82). Growth commenced immediately on incubation, which exhibited an exponential increase in dry weight of the mycelia up to ninth day (216 h) of fermentation under shake-flask conditions.

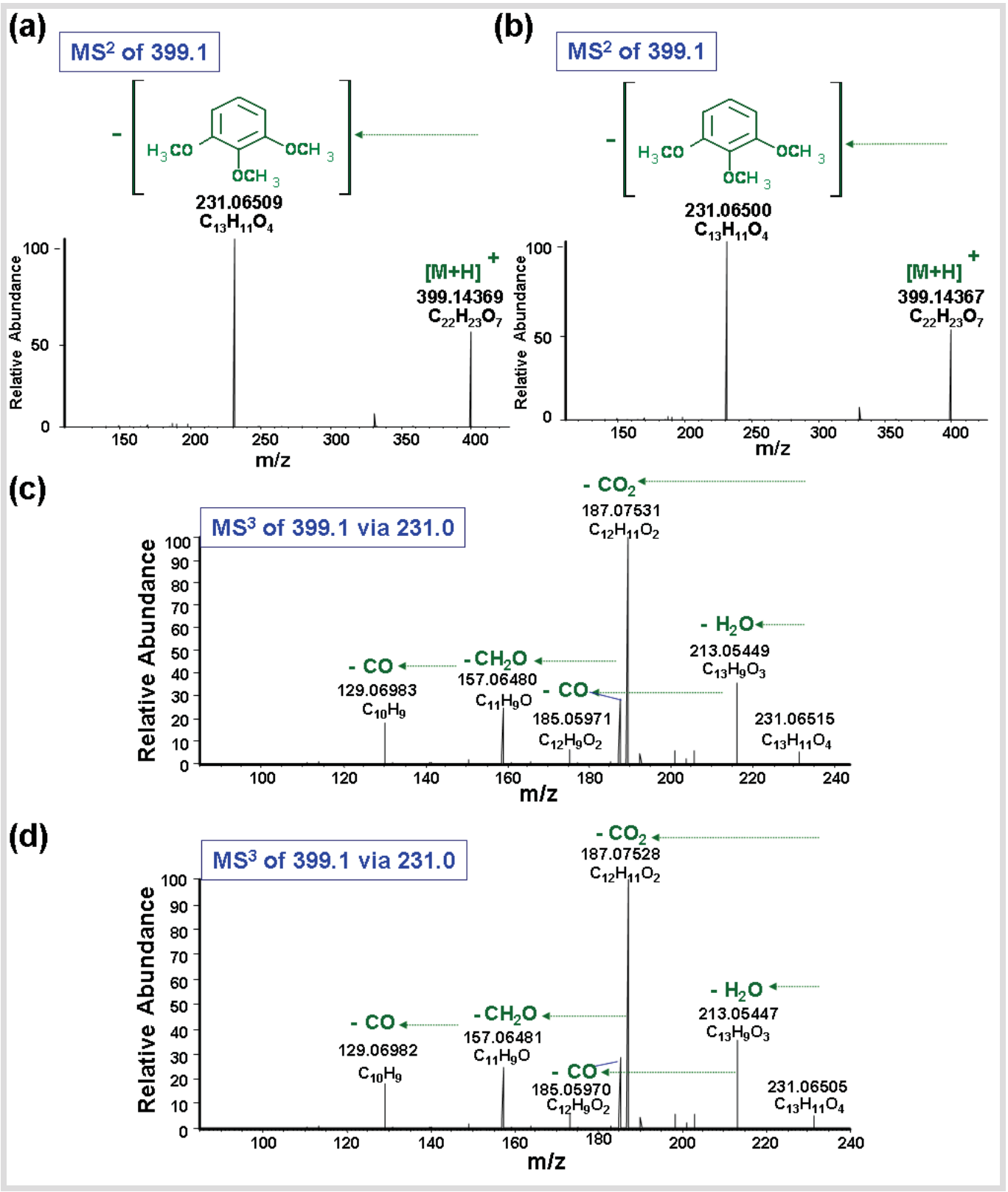

Fig. 81. High-resolution MS^n of deoxypodophyllotoxin from host plant (*J. communis*) and the isolated endophytic fungus. (a) MS^2 from host plant. (b) MS^2 from the endophyte. (c) MS^3 from the host plant. (d) MS^3 from the endophyte.

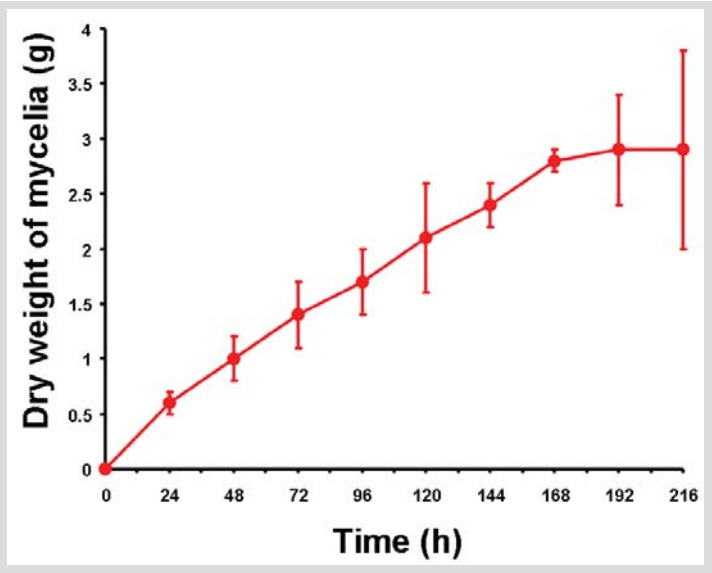

Fig. 82. Growth kinetics of the cultured endophyte.

3.3.3. Production kinetics of the endophytic fungus

In order to study the production kinetics of deoxypodophyllotoxin, the mycelia were collected every 24 h and metabolites were isolated both from the mycelia and spent broth (Fig. 83). The deoxypodophyllotoxin content of the organic extracts of mycelia and broth, collected at periods of regular time intervals, were determined to have an insight into the production kinetics over time. Maximum production of deoxypodophyllotoxin was observed on day 7 (168 h) in terms of µg 100 g^{-1} dry weight of mycelia, although, its formation started as early as 24 h. The deoxypodophyllotoxin content gradually declined after 168 h of incubation.

On the other hand, no deoxypodophyllotoxin was detected in the spent medium (broth) at 24 h. It could be detected only in the later stages (72 h of incubation onwards), which also gradually increased up to day 6 (144 h), and then slowly declined. The maximum yield of deoxypodophyllotoxin was in the range of 4 ± 2 µg 100 g^{-1} dry weight of mycelia and 3 ± 2 µg L^{-1} of spent broth, respectively, after 9 days of fermentation (200 rev min^{-1}) at shake-flask in SB at 28 ± 2°C. Furthermore, the formation of deoxypodophyllotoxin was not observed in inoculated, extracted and processed culture broths at the start of the experiment (0 h). This eliminated the possibility that any deoxypodophyllotoxin had been carried-over from the original plant material source to the fungus via the mycelia (inoculum plugs). This study, thereby, unequivocally established the novel production of deoxypodophyllotoxin by the endophyte.

3.3.4. Reduction of deoxypodophyllotoxin biosynthesis on subculturing

A detailed study of metabolite production was undertaken over generations. In shake-flask incubations

of the endophytic fungus, a substantial decrease in the production of deoxypodophyllotoxin was observed from the first to the second generation, which ceased completely from the third generation onwards. Thus, even though the potential of the endophyte in the indigenous production of deoxypodophyllotoxin was demonstrated, as evidenced by growth and production kinetics, repeated *in vitro* subculturing led to the loss of deoxypodophyllotoxin biosynthesis by the cultured endophyte.

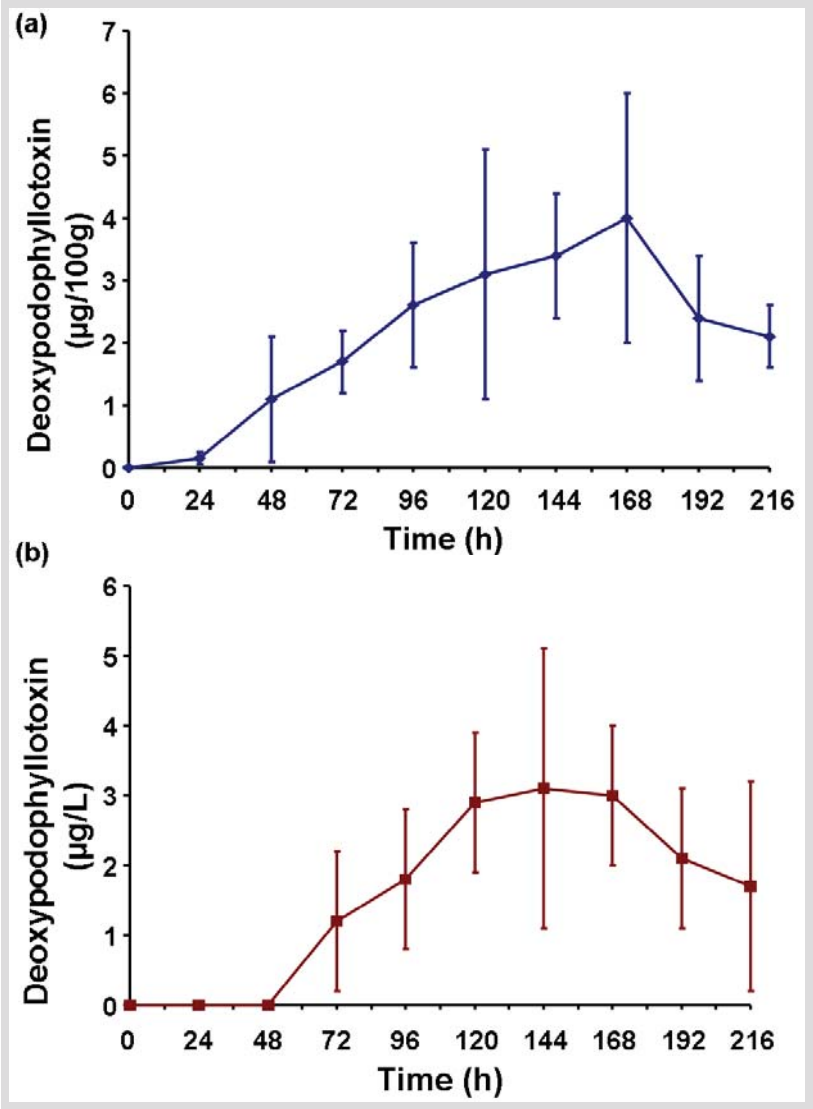

Fig. 83. Production kinetics of the cultured endophyte.
(a) Mycelial extract.
(b) Spent broth.

3.3.5. Antimicrobial activity of fungal deoxypodophyllotoxin

The *in vitro* antimicrobial activities of the crude fungal extracts were tested against a panel of laboratory standard pathogenic control strains, including Gram-positive bacterium *S. aureus* subsp. *aureus* (DSM 799), and Gram negative bacteria *K. pneumoniae* subsp. *ozaenae* (DSM 681), *P. aeruginosa* (DSM 1128), and *E. coli* (DSM 682). Standard podophyllotoxin was run in parallel as a positive reference for comparison. The obtained results are presented in Fig. 84. The antibacterial activity of some of the

synthetic precursors of podophyllotoxin have recently been reported (Nanjundaswamy *et al.*, 2007). Here, the study has been extended to understand the antimicrobial efficacy of deoxypodophyllotoxin (from the endophytic fungal source) in comparison to standard podophyllotoxin against the selected microorganisms. Our results showed considerable activity of standard podophyllotoxin and the fungal metabolite against both Gram-positive and Gram-negative bacteria. The only exception was that of *E. coli*, which was not at all susceptible to either podophyllotoxin or the fungal deoxypodophyllotoxin at the concentrations tested. From the results obtained, it appeared that the antibacterial action of the extracts, and therefore of deoxypodophyllotoxin, was more pronounced on Gram-positive (*S. aureus*) than on Gram-negative bacteria. This corroborates the result of the reference standard (podophyllotoxin) used in parallel, though the action of podophyllotoxin was more pronounced than deoxypodophyllotoxin against all tested bacteria. All the microorganisms were completely unsusceptible to control disks imbued with pure solvent.

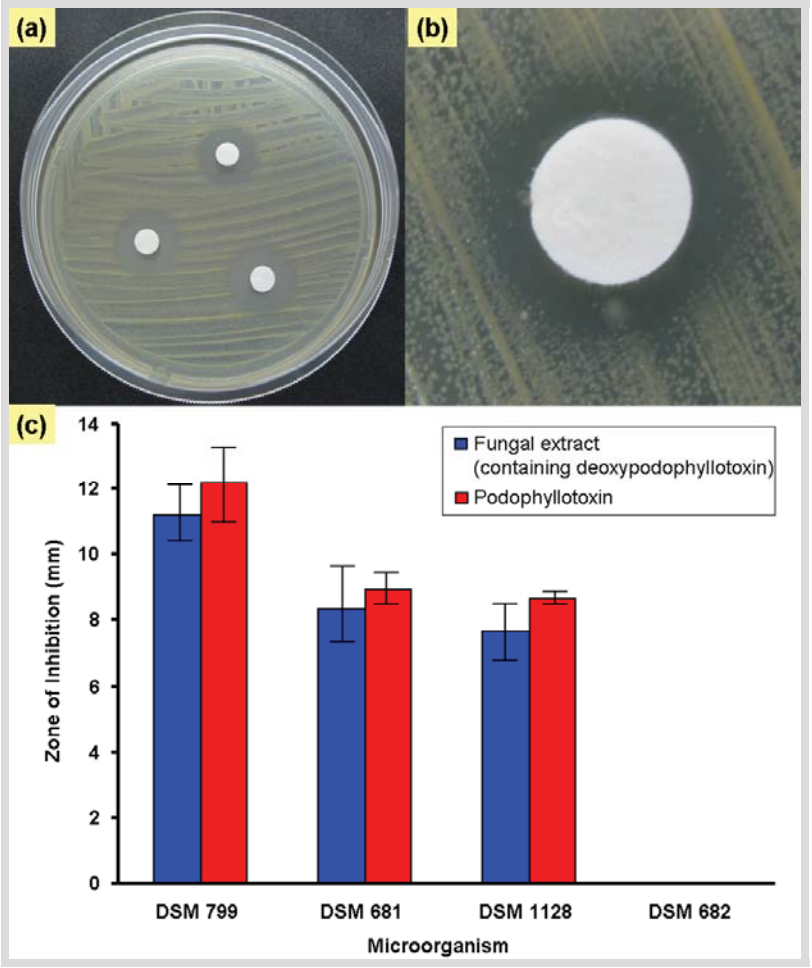

Fig. 84. The antimicrobial activity of crude fungal extracts against different microorganisms, in comparison to standard podophyllotoxin.
(a) Representative Petri plate showing the zone of inhibition (ZOI) against the seeded disc.
(b) Enlarged view of a representative ZOI.
(c) The ZOI represents mean values (± SD) of six experiments, including the diameter of the disc (6.0 mm).

CHAPTER 6:
DISCUSSION

1. Camptothecin (CPT)

1.1. Phytochemical profiling of host plants

The aim of the present study was to evaluate and statistically correlate the distribution of antineoplastic CPT and two important structural analogues, 9-MeO-CPT and 10-OH-CPT. For all the studied plants, it was clear that the phytochemicals were distributed in varying concentrations in the aerial parts of the plants based on the locations from where the plants were sampled. It is well-documented for many plants that the dynamic environmental conditions like temperature, humidity, and soil conditions drastically affect the quantities of phytochemicals in various organs of the same plant species, e.g. the *Hypericum* species (Smelcerovic *et al*., 2006a,b; Smelcerovic and Spiteller, 2006; Smelcerovic *et al*., 2008; Verma *et al*., 2008). The present study ratifies and extends this observation on *C. acuminata*. Furthermore, the combinatorial correlations derived from the different chemometric evaluations revealed novel and significant relationships among the three compounds thereby providing a handle for understanding their synergistic effects and biosynthesis in plants. The results show a correlation in the accumulation of CPT and both 9-MeO-CPT and 10-OH-CPT. This indicates that these substances are produced by the same basic biosynthetic pathway considering the fact that they bear the same backbone skeleton.

Moreover, as evidenced by the SAR studies (Tanizawa *et al*., 1994; Wu *et al*., 1995; Sawada *et al*., 1996; Stehlin *et al*., 1999; Zhou *et al*., 2000; Kehrer *et al*., 2001; Li *et al*., 2006; Huang *et al*., 2007), these three anticancer compounds share the same mode and mechanism of action; thus, it is feasible that they also operate synergistically *in planta* providing chemical-defense. This is yet again evidenced by the significant positive correlation among them irrespective of the sampling location.

It has been established for many plants that extraction employing instant freeze-drying (using liquid nitrogen) of fresh tissues preserves the phytochemical qualities of plants, as opposed to oven drying at high temperature, which greatly affects the phytochemical constituents (Abascal *et al.*, 2005). In *C. acuminata*, oven drying of tissues has been shown to reduce the content and recovery of CPT (Liu *et al.*, 1998). Our results corroborate this observation. In all chemometric evaluations, it was revealed that drying of plant tissues changed the phytochemical profiles of the plants and therefore, the correlations between CPT, 9-MeO-CPT and 10-OH-CPT. Thus, for *C. acuminata*, the results obtained in the form of recovery and inter-correlations among the tested compounds using the fresh tissue extracts were reliable.

Nevertheless, further systematic research is needed to understand the effects of drying under different conditions compared to other preparation methods, including different extraction techniques of fresh plant tissues, to allow a more precise phytochemical profiling of *C. acuminata*.

1.2. Perspectives on the survival-strategies of endophytic *F. solani* against indigenous CPT biosynthesis

Since CPT is highly toxic, its production and detoxification in the plants producing it must be well-coordinated. Both vacuolar sequestration and secretion were initially considered to be the mechanism to avoid the CPT toxicity in plants. However, recent studies have shown that CPT secretion in plants is a passive process depending on the concentration gradient between intracellular and extracellular compartments (Sirikantaramas *et al*., 2007); thus, plants utilize CPT as a mode of chemical defense against pathogen and insect attack (Sirikantaramas *et al*., 2009). Hence, any fungus trying to infect the CPT producing plants will immediately come in contact with the plant CPT, which will kill the fungus right away by targeting its Topo1-DNA complex. It would seem that only those fungi will be able to associate and colonize successfully within the host tissues as 'endophytes' which intrinsically possess the ability to resist the attack of the host CPT after its infection. Our study revealed a number of amino acid residues in the Topo 1 of endophytic *F. solani* capable of preventing the CPT inhibition. These wild-type residues would have been present in the fungal Topo 1 even before it infected the plant and came in contact with the host CPT. This would have been necessary in order to survive the host CPT after initial infection. Therefore, the infecting endophyte, *F. solani*, had to be pre-equipped to resist the CPT toxicity vested by the host *C. acuminata* plant, before evolving towards the biosynthesis of CPT itself as dictated by the *in planta* selection pressures. The interesting observation of wild-type amino acid residues conferring resistance to CPT has also been observed in plants; although *O. japonica* does not produce CPT and its Topo 1 does not contain the critical residues as compared to CPT producing plants, it exhibits partial resistance to CPT *in vivo* (Sirikantaramas *et al*., 2009). This suggests the involvement of yet-unknown wild-type amino acid residues which are responsible for Topo 1 pre-adaptation in *O. japonica*. A close homology of Topo 1 in both the endophytes as well as in the closely relative *F. culmorum* was also found in the present study. Furthermore, the associated endophyte, *A. rigidiuscula*, showed highly similar Topo 1 mainly in the amino acid residues conferring CPT resistance even though it was unable to biosynthesize CPT. This further lends evidence to the fact that only those fungi possessing the necessary CPT resistance features would successfully infect a CPT producing plant, irrespective of their CPT biosynthesis capability.

Sirikantaramas *et al*. (2009) elaborated on the concept of time-dependent target-based resistance features in various species when differentiating the resistance-mediating Topo 1 alterations in CPT producing plants and human CPT resistant cancer cells (CEM/C2). The present study has only revealed some similar alterations in the fungal Topo 1s and not all those observed in the CPT-producing plants and/or CEM/C2 cells. It is possible that some specific mutations are only found in plants (Sirikantaramas *et al*., 2008) because of the much longer evolutionary period of exposure to CPT

in plants than in endophytic fungi. Furthermore, since endophytic *F. solani* is indigenously capable of biosynthesizing CPT, it is compelling that it might develop more and new target-based CPT resistance features in future over evolutionary time. Admittedly, this study dealt with and compared the acquired endophytic Topo 1 structures with previously identified or expected alterations associated with CPT resistance. In addition to the known residues, it is possible that several other wild amino acid residues and alterations might also be evolved in amino acid sequence of the studied endophytic Topo 1s including other mechanisms of CPT resistance.

1.3. Perspectives on the endophytic CPT biosynthesis in relation to the host plant

A plant-fungal cross-species CPT biosynthetic pathway has been elucidated in this study whereby the endophytic fungus utilizes indigenous geraniol 10-hydroxylase, secologanin synthase, and tryptophan decarboxylase to biosynthesize CPT precursors but then requires the host strictosidine synthase to complete the CPT biosynthesis (Fig. 85). The endophyte accumulates 10-hydroxygeraniol from geraniol, using the geraniol 10-hydroxylase enzyme, which in turn is made from IPP and DMAPP via the formation of GPP. This suggests that either the mevalonate (MVA) pathway or the 2-C-methyl-D-erythritol 4-phosphate (MEP) pathway, which have already been studied in many plants and fungi, might be responsible for initially forming IPP and DMAPP (Rohmer, 1999; Rodriguez-Concepcion and Boronat, 2002; Kuzuyama and Seto, 2003; Muntendam *et al*., 2009). Further, the fungal secologanin synthase converts loganin to secologanin; loganin, that is synthesized from 10-hydroxygeraniol via 10-oxogeranial and further irridotrial intermediates, by cyclization and randomization of methyl groups (Uesato *et al.*, 1986). The biosynthetic pathway in the fungal endophyte up to secologanin demonstrates the incorporation of carbon alone; the assimilation of nitrogen occurs via an indole moiety, namely tryptamine. Fungal tryptophan decarboxylase is responsible for the enzymatic conversion of L-tryptophan to tryptamine, channeled through the shikimate pathway (Yamazaki *et al.*, 2004). Since *F. solani* strains from other sources are incapable of CPT biosynthesis, endophytic *F. solani* has *de facto* been subjected to some kind of *in planta* selection pressure to enable the activation of the development of CPT biogenesis.

1.4. ‘Trait-specific endophytic infallibility’ hypothesis

The metabolomics of endophytes are dependent not only on the respective host plants but also on the ecosystem to which the host belongs (Strobel *et al.*, 2004). The host preference and diversity of endophytes in various environmental settings has been the subject of a plethora of investigations. A general consensus has been reached on the population pressure and diversity of endophytes in host plants growing in different ecosystems.

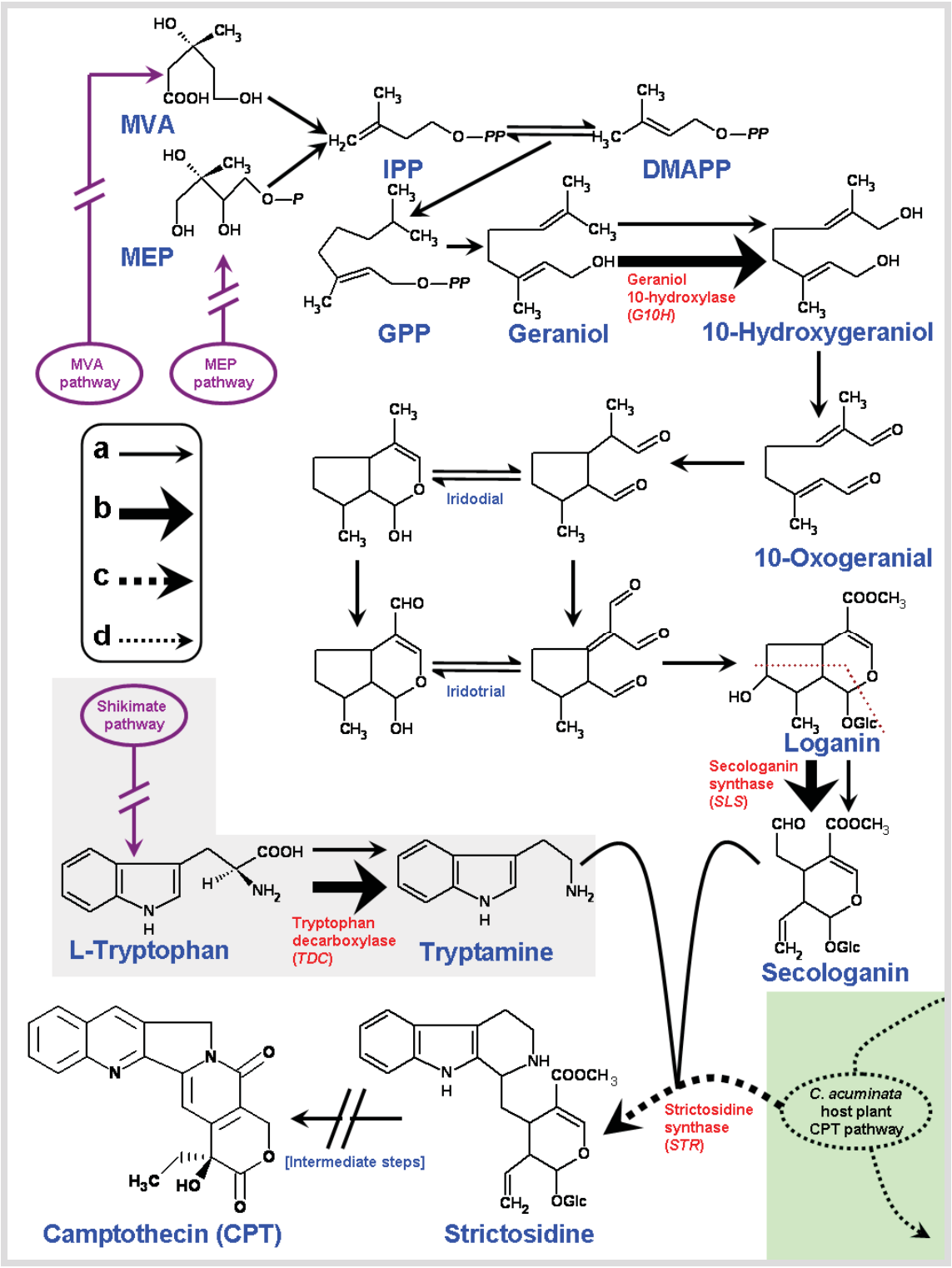

Fig. 85. Schematic representation of the biosynthetic pathway of CPT. (a) The proposed/putative/discovered biosynthetic steps from the literature (as detailed in the text). (b) The biosynthetic steps in endophytic *F. solani* verified/discovered in the present study. (c) The biosynthetic step in endophytic *F. solani* aided *in situ* by the host plant (*C. acuminata*) enzyme (strictosidine synthase, product of *STR*) verified/discovered in the present study. (d) The biosynthetic events occurring indigenously inside the host plant (*C. acuminata*) for the production of plant CPT.

Of particular interest has been the tropical environment; it has been postulated in general and shown in specific cases that tropical environments are the best suited setting for plant-microbe interactions (Arnold *et al*., 2000, 2003; Arnold, 2005, 2008; Rodriguez *et al*., 2009). It has been hypothesized that the optimum setting for these interactions leads to horizontal gene transfer(s) (HGT) or genetic recombination(s), from the plant to its endophytic counterpart or vice versa, that lead to 'novel' endophytes that are capable of acquiring the necessary cellular machinery for accumulating certain metabolites specific to the host plants themselves. The concept of HGT must not, however, be confused with that of the horizontal or vertical transmission of endophytic microorganisms. At present, not much is known regarding the costs and benefits of endophyte infection for plants of different species. However, the ubiquity, abundance, and diversity of the various endophytes strongly suggest that endophytic fungi and host plants may interact in ecologically meaningful ways. In the absence of experimental insights, the theory regarding evolution of symbiosis might prove useful for inferring the general aspects of endophyte-host interactions. In particular, the patterns of symbiont transmission and diversity could be correlated with the chemical diversity characteristics, and can provide a framework for hypotheses regarding the costs and benefits for hosts of an endophyte infection. Further, endophytic fungi could be highly diverse with respect to individual host tissues, host individuals, and host interactions; yet, the plants containing endophytes are overtly asymptomatic. Hence, such gene transfer mechanisms (HGT) could be anticipated for the occurrence of identical natural products in unrelated taxa, viz. the host plant and the invading endophyte (Staniek *et al.*, 2008). Nevertheless, with regard to endophytic microorganisms, one question that this hypothesis does not address is whether HGT and the site of detachment and/or integration in the host and/or recipient genome, respectively, is always a matter of 'chance' or definitive. Added to this is the predicament concerning the expression of a gene or gene cluster in fungal systems acquired from plant systems. For example, in any attempt at isolating and bioprospecting endophytes for host metabolites, it has always been seen that out of a multitude of different endophytes isolated, only one or a few are capable of possessing the potential of indigenously accumulating host-specific metabolites; this of course could be rightly described as a 'genetic serendipity' in the absence of evidence suggesting otherwise. Furthermore, when invoking HGT as a plausible mechanism for a complex secondary metabolite produced by a cascade of biosynthetic steps, the question of all the necessary genes being grouped in a contiguous cluster in the host must be addressed (Staniek *et al.*, 2009). The chance for HGT might also be different in endophytic bacteria than in endophytic fungi.

When assessing endophytic *F. solani* in terms of the above hypothesis, the results showed that the endophyte could produce CPT by means of a cross-species pathway by utilizing the host plant enzyme, strictosidine synthase (coded by the plant *STR*). Therefore, at least one plant gene was not laterally

transferred to the endophytic fungus for it to produce *in planta* CPT. Hence, it is evident that HGT is not the only mechanism by virtue of which endophytes might produce compounds specific to their host plants. In light of the current results and in addition to the current HGT hypothesis, an alternative hypothesis is proposed. It is true that a particular environmental setting, like the tropical setting, greatly influences the interspecies interactions (including plant-microbe and even microbe-microbe) (Arnold *et al.*, 2000, 2003; Arnold, 2005, 2008; Rodriguez *et al.*, 2009). It is probable that this setting might favor the HGT mechanism, but the results of this study demonstrate evidence that a particular endophyte could produce a host metabolite without HGT. The concept of HGT, applied to endophytic microorganisms, centers on the idea that during the course of evolution, an endophyte and a host started co-existing followed then by some gene transfer 'by chance' to provide it with a certain trait. However, considering the fact that fungi themselves are subject to evolution, it is highly feasible that during the co-existence of an endophyte with its host, it underwent an independent evolution to develop its own molecular system (host-microbe co-evolution). This could be due to 'the same' selection pressure, viz., environmental stress, pathogen attack, insect attack, other factors, or a combination of these. This is partly in line with the recently proposed 'xenohormesis' hypothesis (Howitz and Sinclair, 2008), although the subject of the present study has been exclusively endophyte-specific. The tenets of the new proposed hypothesis may be summarized as follows: (a) the evolution of an endophytic fungus to intrinsically accumulate a metabolite that is essentially produced by its host and thus host-specific is subject to an 'identical' selection pressure and organ-specific; (b) this potential is not serendipitous, but dependent on 'both' the host and the microbe genotype-specific features such as genus, species, type of organ, and type of metabolites, simultaneously; and (c) suitable environmental factors such as tropical environments favor the increase in biodiversity and population of the endophytes, thereby exposing a larger number of endophytic traits to a particular *in planta* selection pressure. This concept may be called the 'trait-specific endophytic infallibility' hypothesis based on the differential abilities of endophytes to indigenously accumulate specific metabolites based on their intrinsic traits subjected to specific selection pressures. Thus, this hypothesis could be used to explain the following: (a) difference in the metabolomics of an endophyte and its host; (b) difference in the metabolomics of an endophyte within its host and in axenic cultures, as also suggested by Strobel *et al*. (2004) although in a different perspective; and (c) why only certain specific novel endophytes are capable of producing certain host-specific compounds. Very recently, following our discovery of the above mentioned endophytic fungus, another endophytic fungus also identified as *F. solani* isolated from *Apodytes dimidiata*, has been reported to produce the same three compounds (i.e., CPT, 9-MeO-CPT and 10-OH-CPT) (Shweta *et al.*, 2010), thus ratifying this hypothesis. This hypothesis has been tested not only on the CPT producing endophytic fungus, but also on hypericin and

deoxypodophyllotoxin producing endophytic fungi (*vide infra*). Admittedly, suitable experimental designs should be developed to test this hypothesis further on a case-by-case basis in order to be able to verify or modify it.

1.5. Decrease in biosynthetic potential on subculturing

Even though a number of novel endophytes, capable of indigenously producing various important metabolites, have been isolated and characterized to date, only a few workers have addressed the correlations between the growth and metabolomics of the endophytes in axenic cultures. For instance, Li *et al*. (1998) showed that successive cultures of the endophytic fungus *Periconia* sp., isolated from *Torreya grandifolia*, resulted in the attenuation of Taxol production, although the fungal growth itself was unaffected. With regard to *F. solani*, the production of CPT by the cultured endophyte was substantially reduced on subculturing under *in vitro* axenic conditions. CPT production by the cultured endophyte showed a gradual decrease from the first to second generation followed suddenly by a drastic drop to practically negligible amounts from the third generation. The endophytic fungus carried-over the plant strictosidine synthase enzyme during the isolation procedure, enough to last only up to the second generation subculture, thereby causing the sudden drop in CPT amounts from the third generation. This is a practical possibility owing to the high stability of this enzyme, even on repeated freezing and thawing (Treimer *et al*., 1979). Evaluation of the CPT biosynthetic genes in the seventh generation subculture of the endophytic fungus revealed non-synonymous alterations leading to irreversible dysfunction at the amino acid level rendering the enzymes of the CPT pathway dysfunctional. This was also evidenced by the fact that optimized fermentation conditions and addition of precursors as well as various host plant tissue extracts did not restore the production of CPT, 9-MeO-CPT or 10-OH-CPT. Furthermore, none of the subculture generations demonstrated accumulation of the reactive intermediates revealing that the destabilization of the genes of CPT pathway would have commenced immediately under the *in vitro* axenic conditions due to the lack of *in planta* selection pressures. As expected, the primary structure of the control gene, *Top1*, was not degraded or destabilized over repeated *in vitro* subculturing. This revealed that instability of the CPT biosynthetic genes (secondary metabolism) was not reflected on the primary metabolic processes in the endophytic fungus. Furthermore, the fungal rDNA was still intact in the seventh subculture as in the first parent isolate showing that the functions of the housekeeping genes were not destabilized on repeated subculturing.

1.6. Host affinity and specificity of the endophytic fungus

In vitro cultivated endophytic *F. solani* could be successfully established in *C. acuminata*. This was

independent of the origin, or mode of propagation and growth of the host plants, revealing that the host-affinity and specificity of this endophyte might be only species-specific and not dictated by the *in situ* metabolomic status of the plants. The ability of the endophyte to infect was also completely unrelated to its ability to biosynthesize CPT. The CPT pathway could not be recreated even by restoring the endophyte-host association, although the *in planta* strictosidine synthase was available to the endophytic fungus. None of the intermediates could be found to be accumulated in the recovered endophytes, corroborating the fact that the observed genomic degradation of the CPT-genes was irreversible. Thus, once the biosynthetic potential of the endophyte to produce CPT was impaired, it could not be restored even by providing the original host environment where the endophyte would have evolved the CPT biosynthesis. The genomic degradation was not repaired, even by the *in planta* stimulus such that Koch's postulates were not fulfilled. It is possible that the ability of the endophytic fungus to infect the host and its regulation (i.e., its host affinity and specificity) could be diluted or completely lost on preservation outside the host and on repeated subculturing in axenic conditions.

2. Hypericin

2.1. Phytochemical profiling of host plants

For all the species studied, it was clear that the phytochemicals were accumulated mainly in the aerial parts of the plants, especially the leaves, and the distribution of the metabolites was favored in the organic phases. The combinatorial correlations derived from the different chemometric evaluations revealed new and significant relationships among the different metabolites, thereby providing a handle for understanding their biosynthesis in plants. The results of this study show a correlation in the accumulation of emodin and hypericin/pseudohypericin. This could indicate that the same basic biosynthetic pathway produces these substances. The same could be true for additional polyketides such as quercitrin. Furthermore, the statistical evaluation of analytical data in this study underscores the prospects for close relatives of hitherto pharmaceutically widely used species; in this case, *H. montanum* which is a close relative of *H. perforatum*. *H. montanum* might be an alternative to *H. perforatum* that currently is the most widely used species of *Hypericum* worldwide in phytotherapeutic preparations. Nevertheless, it is worth mentioning that any phytomedicine produced from *H. montanum* would evidently have to pass through the necessary regulatory frameworks including detailed toxicological and clinical studies. The considerable infraspecific variability (in case of *H. maculatum*) suggests the importance of further detailed studies of genotypic variation and environmental factors. Although well known and widely established, *H. perforatum* might not be the optimal resource for high yields of hypericin.

2.2. Perspectives on the endophytic hypericin and emodin biosynthesis: verification of trait-specific endophytic infallibility hypothesis

When assessing endophytic *T. subthermophila* in terms of the trait-specific endophytic infallibility hypothesis, the results showed that the *hyp-1* gene was absent in the genome of the endophyte. Based on experiments on *H. perforatum* cell cultures grown in the dark, it was originally proposed that emodin might be the direct precursor of hypericin in *Hypericum* plants, undergoing direct and specific conversion using the Hyp-1 protein (Bais *et al.*, 2003). The questionable function of Hyp-1 protein was, however, highlighted recently in the work of Michalska *et al*. (2010). These authors were not able to repeat the experiments of Hyp-1 catalyzed conversion of emodin to hypericin as claimed by Bais *et al*. (2003), thus questioning the function of Hyp-1 in plants. A new possibility concerning the final step(s) of the microbial pathway leading to hypericin could be postulated on the basis of the experimental results. Seemingly, both hypericin and emodin could be products of oxidation and dimerization of the precursor emodin anthrone. This would mean that hypericin and emodin are both secondary metabolites of the endophyte. Emodin would not then be the precursor of hypericin that accumulates as an intermediate metabolite, and the pathway would not proceed via protohypericin. This is again emphasized by the lack of dependence of the production of hypericin on light and the absence of protohypericin in all stages of culture. Furthermore, the production of hypericin not only remained independent of the media spiking with emodin, but also emodin was not taken up from the media. The *hyp-1* gene, suggested to encode for the Hyp-1 phenolic coupling protein in plant cell cultures, was absent in the genome of the endophyte. Therefore, it is compelling that there could be some genetic factors responsible for the direct and specific conversion of emodin anthrone to hypericin other than *hyp-1*. This step would then also be light independent. Thus, the biosynthetic pathway in the endophytic fungus is different and/or governed by a different molecular mechanism than the host plant or host cell suspension cultures. Earlier studies in plant systems also revealed the independence of production of hypericin from light, although the amounts varied (Bais *et al.*, 2002). Evidently, the results of the present study support the trait-specific endophytic infallibility hypothesis instead of the HGT hypothesis.

2.3. Regulation of hypericin and emodin production in the endophytic fungus

Hypericin is a peculiar metabolite that exhibits high cytotoxicity upon excitation by irradiation with visible light, a mechanism known as photodynamic activity (Kubin *et al.*, 2005). It has been proposed that the localization, and probably the synthesis, of hypericin in plants occur in specialized structures called the dark glands (Cellarova *et al.*, 1994; Briskin *et al.*, 2000; Onelli *et al.*, 2002). Even though the current understanding of the ultrastructure of the dark glands does not provide sufficient evidence concerning the *in situ* biosynthesis of hypericin in plants, it is evident that the purpose of the localization of this

photodynamic metabolite in the dark glands is to protect it from light and, hence, prevent auto-cytotoxicity. The endophytic fungus *T. subthermophila* does not contain any dark glands or other light-protection structures that are associated with its host plant. This raises the question about the regulation of production of hypericin in the fungus so as to avoid self-damage. On one hand, it might be presumed that this particular endophyte has not developed an independent regulation mechanism for accumulating hypericin. The explanation for this could be that this endophyte has been isolated from the inner stem tissues of the *H. perforatum* plant, where there is complete absence of light, thus protection from the photodynamic effects of hypericin and emodin. This increasingly lends support to the mutual symbiotic association of the host and its endophytic counterpart; the former protecting the latter from light and the latter contributing to the chemical defense of the former. This, however, does not ratify the fact that there is no additional regulatory mechanism within the endophyte itself, since the endophyte continues to accumulate hypericin and emodin under axenic conditions *in vitro*, even after separation from the host. It is well known that the metabolic regulation of an endophytic fungus might be substantially different from that which occurs inside the host plant (Strobel *et al.*, 2004). In this connection, the concept of trait-specific endophytic infallibility is suitable. There is a high probability that this endophyte is able to produce hypericin and emodin independently irrespective of the gene(s) or pathway(s) in its host, since (a) this production has been seen to be light-independent, (b) protohypericin has not been detected, and (c) the *hyp-1* gene has not been found in the endophyte genome. Additional regulation mechanism for hypericin production has been insinuated earlier for *H. perforatum* cell cultures (Bais *et al.*, 2002), but its similarity, if any, to the microbial system remains anecdotal.

2.4. Costs and benefits of endophytic hypericin and emodin biosynthesis to the host plant

It was evident from the growth kinetics of the endophyte that light did not play any role in its growth. Considering the fact that this particular endophyte was isolated from the inner stem tissues of *H. perforatum*, where there is no possibility of illumination, it can be concluded that the survival and growth of the endophyte within the host is unaffected by the lack of light. Furthermore, on the basis of the production patterns of both hypericin and emodin by the cultured endophyte, it would seem that it might demonstrate similar or different metabolomics in the host, independent of light as a factor. Taking note of the fact that novel endophytes might serve as ‘acquired immune systems’ (Arnold *et al.*, 2003) for their respective hosts, the intrinsic defense potential provided by the endophytes *in vivo* is currently a ‘variable’ factor. This is because the potential of the low-biomass endophyte infections to manifest major chemical signatures *in planta* has to be assessed by inexplicably selective and sensitive

measurements. Using the currently available experimental methodologies, it is almost impossible to detect the differences in metabolite amounts with and without endophyte infections. Clearly, this calls for alternative experimental designs that could address such sensitive changes in the metabolite spectra under *in vivo* conditions.

Furthermore, in *Hypericum* species, it has been found that hypericin is produced by the plant as a mode of chemical defense against a variety of specific and nonspecific microbial pathogens, and a number of insect pests (Fields *et al.*, 1990; Guillet *et al.*, 2000). Hypericin is localized (Briskin *et al.*, 2000) and probably also synthesized in the dark glands (Cellarova *et al.*, 1994; Onelli *et al.*, 2002), which are dispersed over all above-ground parts of the plant (flowers, capsules, leaves) but not in the roots (Hölzl and Petersen, 2003). Additionally, the role of hypericin in the *Hypericum* plant defense has been directly demonstrated by its increased production in response to stress. These include *Hypericum*-specific fungal pathogens (Cirak *et al.*, 2005), nonspecific pathogens (Sirvent and Gibson, 2002), chemical elicitors such as mannan (Kirakosyan *et al.*, 2000) and jasmonic acid (Walker *et al.*, 2002), insect pests (Sirvent *et al.*, 2003), and mechanical stress such as cork pieces (Kirakosyan *et al.*, 2001). Therefore, the contribution by the endophytic *T. subthermophila* in producing hypericin and emodin as part of the defensive mechanism of its host (*H. perforatum*) could be a practical possibility. Thus, it would seem that this endophyte could not only contribute to the metabolites in the host tissues but also play an important role in the chemical defense of the host. Admittedly, this particular endophyte was isolated from the stems of the host and not from the leaves and, like many other localized endophytes, is not expected to provide 'systemic' defense to the host plant. Based on these facts, it may be assumed that in the leaves and flower parts, the high number of dark glands, and consequently high amounts of hypericin, is sufficient to provide localized leaf/flower protection, and this endophyte might be only helping in localized stem protection. This is emphasized by the fact that the endophyte does not release hypericin or emodin in the broth in axenic cultures *in vitro*; thus, the same could be expected under *in vivo* conditions, the metabolites not being released into the plant sap.

2.5. Decrease in biosynthetic potential on subculturing

With regard to endophytic *T. subthermophila*, the production of both hypericin and emodin by the cultured endophyte was substantially reduced on storage and subculturing under *in vitro* axenic conditions. This reveals a similar pattern of reduction that was also observed for endophytic *F. solani*. Furthermore, it has been revealed that the addition of emodin to the submerged cultures resulted in the suppression of growth. This lends support to the fact that the growth of the endophyte is inversely related to the production of emodin in axenic cultures. Alternatively, it might also be putatively inferred that there is in fact an additional regulatory mechanism that controls the sub-cellular trafficking of

emodin in the endophyte, although not very similar, from the perspective of the *hyp-1* gene, to what was proposed in the *H. perforatum* cell cultures (Bais *et al.*, 2002).

3. Deoxypodophyllotoxin

3.1. Phytochemical profiling of host plants

The combinatorial correlations derived from the different chemometric evaluations revealed novel and significant relationships among the different metabolites thereby providing a platform for understanding their biosynthesis in plants. Results of the present study showed interesting correlations in the accumulation of podophyllotoxin and important structural analogues. These gave us an idea about the similarity and/or difference between the biosynthetic pathways of the said metabolites and the possible synergistic principles operating *in planta* utilizing them for various purposes including the plant chemical defenses. The significant positive correlations might also be interpreted as a reflection of a plausible similarity in the adaptive co-evolutions, both infraspecific and infrageneric, of biosynthesis of the respective metabolites over evolutionary time. Not only that, the correlations among the phytochemicals can be utilized for further bioprospecting purposes. For example, the positive correlation between podophyllotoxin and podophyllotoxone could be utilized for selecting plants from different wild populations to prospect for either/both of them based on the knowledge of only one compound. Although podophyllotoxone is not commercially available, plant population with high amounts of podophyllotoxin (commercially available) could be directly selected for good yields of podophyllotoxone, based on the positive correlations revealed in this study. This demonstrates the utility of chemometrics in accurate and fast bioprospecting for phytochemical and phylogenetic studies. Furthermore, the chemometric assessment of analytical data in this study highlighted the prospect that close relatives of hitherto pharmaceutically widely used species and even genera could be sources. In this case, it would be *J. x-media* Pfitzeriana as a generic relative of *P. hexandrum*. Moreover, the extensive infraspecific variability (in case of *P. hexandrum*) suggested the value of further meticulous studies of genotypic variation and ecological factors. Although well known and widely established, *P. hexandrum* might not be the only optimal resource for high yields of podophyllotoxin. The close examination of genotypes and taxa, including plant breeding might provide further handle to understand these imminent issues.

There are a number of practical challenges when bioprospecting for potent phytotherapeutic metabolites from nature. For example, the plants were all collected from the natural populations, many of which were in remote locations and difficult to access positions. This led to the problem that there was always due to technical reasons, a gap between the actual sampling and beginning of extraction procedures. This problem is a universal concern when considering sampling of wild populations

irrespective of the genus or species of plants samples which can only be overcome by field labs not available on the sampling sites. For those plants reported in this study to be sampled from tropical climatic conditions (like from India), another practical challenge was the manifestation of fungal infections occurring between the post-harvest and pre-extraction period, because of the natural climatic conditions at the sites of sampling. Therefore, to prevent this, all these samples had to be air-dried at room temperature (25°C) and sealed after harvest before they could be transported to the labs for extraction. Serendipitously for the metabolites reported here, it had previously been shown that podophyllotoxin is unaffected by post-harvest degradation, even at varying temperatures, drying conditions or wear-and-tear (Bedir *et al.*, 2006). Furthermore, the problem of the activation of the enzyme β-glucosidase by re-hydration during the extraction leading to the hydrolization of the glycoside to podophyllotoxin (Canel *et al.*, 2001), was duly addressed in the present study by preventing re-hydration during extraction.

3.2. Perspectives on the endophytic deoxypodophyllotoxin biosynthesis: verification of trait-specific endophytic infallibility hypothesis

The discovery that an endophytic fungus could biosynthesize aryl tetralin lignans, including deoxypodophyllotoxin, has significant implications. It is interesting to note that an endophyte associated with *Juniperus* species could accumulate the same metabolite that is also found in the host, whereas none of the endophytes isolated in parallel from *Podophyllum* species had the same capability. From the genetic standpoint, the production deoxypodophyllotoxin by the cultured fungal endophyte tempts to support the possibility of HGT between *Juniperus* species and its corresponding endophytic organism. However, none of the other endophytes isolated from the same plant, the same species from other locations, or different species and genera containing indigenous podophyllotoxin and/or deoxypodophyllotoxin possessed the biosynthetic potential similar to endophytic *A. fumigatus*. Moreover, although largely unclear, the biosynthesis of deoxypodophyllotoxin is a multi-step cascade process. There is no evidence that all the genes responsible for the complete pathway are grouped together in a contiguous cluster in the host to facilitate the lateral transfer of the complete gene-set for the entire pathway. On the other hand, it could be envisaged that the endophyte might share its pathway with the host plant (as endophytic *F. solani* does for CPT), or the endophyte might have an entirely indigenous pathway for its production (partly similar to endophytic *T. subthermophila* for hypericin and emodin) independent of the host plant. In either case, it would favor the concept of adaptive co-evolution by the endophytic fungus and therefore, the possibility to respect the trait-specific endophytic infallibility hypothesis would seem feasible. Not only that, lignans are believed to act as defense compounds in the plants producing them (Koulman, 2003; Liu *et al.*, 2007), so the production

of these by the endophytic population of those plants possibly demonstrates a probable *in vivo* symbiotic relationship between them.

3.3. Decrease in biosynthetic potential on subculturing

A detailed study of deoxypodophyllotoxin production was undertaken over several subculture generations. In shake-flask incubations of the endophytic fungus, a substantial decrease in the production of deoxypodophyllotoxin was observed from the first to the second generation, which ceased completely from the third generation onwards. Thus, the biosynthetic potential of the endophytic fungus to produce deoxypodophyllotoxin under axenic conditions was lost. Unfortunately, this phenomenon prevented further investigation into the microbial biosynthetic pathway for the production compared to the host plant. Nevertheless, this endophyte possesses potential for further research along the lines of metabolic engineering approaches. This endophyte possessed the capacity to tolerate and resist the inhibition of mitotic spindle formation by deoxypodophyllotoxin (Imbert, 1998; Canel *et al*., 2000; Liu *et al*., 2007) synthesized by itself (intracellular) and by the host plant (intercellular). Therefore, this fungus has indeed developed some form of resistance mechanism against deoxypodophyllotoxin. It can be envisaged that the complete gene-set for the production of deoxypodophyllotoxin (or even podophyllotoxin) could be discovered in plant cell-cultures and then inserted into the endophyte to produce a constant yield in a dependable, reproducible, fast and economic manner by fermentation technology amenable to scale-up. Since the endophyte is already capable of resisting the action of deoxypodophyllotoxin, high levels of this pro-drug could be produced without killing the organism.

CHAPTER 7:
REFERENCES

Abascal, K., Ganora, L., Yarnell, E. (2005). The effect of freeze-drying and its implications for botanical medicine: a review. *Phytother. Res.*, **19**, 655-660.

Aiyama, R., Nagai, H., Nokata, K., Shinohara, C., and Sawada, S. (1988). A camptothecin derivative from *Nothapodytes foetida*. *Phytochemistry*, **27**, 3663–3664.

Amna, T., Puri, S. C., Verma, V., Sharma, J. P., Khajuria, R. K., Musarrat, J., Spiteller, M., and Qazi, G. N. (2006). Bioreactor studies on the endophytic fungus *Entrophospora infrequens* for the production of an anticancer alkaloid camptothecin. *Can. J. Microbiol.*, **52**, 189–196.

Andersen, D. O., Weber, N. D., Wood, S. G., Hughes, B. G., Murray, B. K., and North, J. A. (1991). *In vitro* virucidal activity of selected anthraquinones and anthraquinone derivatives. *Antiviral Res.*, **16**, 185–196.

Aneja, K. R., Jain, P., and Aneja, R. (2008). *A textbook of basic and applied microbiology,* 1st edition. New Age International (P) Ltd. Publishers, New Delhi, India.

Annonymous (1998). *Monographien der Kommission E (Zulassungs- und Aufbereitungskommission am BGA für den humanmed. Bereich, phytotherapeutische Therapierichtung und Stoffgruppe)*. Bundesgesundheitsamt (BGA; German Federal Health Office), Germany. Bundesanzeiger (BAnz), Germany.

Annonymous (2000, 2006a). *Consideration of Proposals for Amendment Of Appendices II: Inclusion of Happy Tree (Camptopheca acuminata Decaisne) in CITES appendix II of convention in accordance with the provisions of Article II, paragraph 2(a). Prop. 11.58*. World Conservation Monitoring Centre, CITES Secretariat/World Conservation Monitoring Centre, Chatelâine-Genève, Switzerland.

Annonymous (2001). *Checklist of CITES species: a reference to the appendices to the Convention on international trade in endangered species of wild fauna and flora*. World Conservation Monitoring Centre, CITES Secretariat/World Conservation Monitoring Centre, Chatelâine-Genève, Switzerland.

Annonymous (2006b). *A field guide to herbal dietary supplements*. Dietary Supplement Information Bureau (DSIB), Sarasota, FL.

Anonymous (2007). *Genomic DNA from Food, Nucleospin 8, Nucleospin 96 (Rev.02)*. Macherey-Nagel, Düren, Germany.

Anonymous (2008). *Genomic DNA from Plant, NucleoSpin Plant II, NucleoSpin Plant II Midi, NucleoSpin Plant II Maxi (Rev. 02)*. Macherey-Nagel, Düren, Germany.

Apostol, I., Brooks, P. D., and Mathews, A. J. (2001). Application of high-precision isotope ratio monitoring mass spectrometry to identify the biosynthetic origins of proteins. *Protein Sci.*, **10**, 1466–1469.

Arisawa, M., Gunasekera, S. P., Cordell, G. A., and Farnsworth, N. R. (1981). Plant anticancer agents XXI. Constituents of *Merrilliodendron megacarpum*. *Planta Med.*, **43**, 404–407.

Arnold, A. E. (2005). Diversity and ecology of fungal endophytes in tropical forests. In Deshmukh, D. (ed.) *Current trends in mycological research*. Oxford & IBH Publishing Co. Pvt. Ltd., New Delhi, India, pp. 49–68.

Arnold, A. E. (2008). Endophytic fungi: hidden components of tropical community ecology. In Schnitzer, S. A., Carson, W. P. (eds.) *Tropical forest community ecology*. Blackwell Scientific, Inc., UK, pp. 254–271.

Arnold, A. E., Maynard, Z., Gilbert, G. S., Coley, P. D., and Kursar, T. A. (2000). Are tropical fungal endophytes hyperdiverse?. *Ecol. Lett.*, **3**, 267–274.

Arnold, A. E., Mejia, L. C., Kyllo, D., Rojas, E. I., Maynard, Z., Robbins, N., and Herre, E. A. (2003). Fungal endophytes limit pathogen damage in a tropical tree. *Proc. Natl. Acad. Sci. U. S. A.*, **100**, 15649–15654.

Ayres, D. C. and Loike, J. D. (1990). *Lignans: chemical, biological and clinical properties*. Cambridge University Press, Cambridge.

Bacon, C. W. and White, J. F. (2000). *Microbial endophytes*. Marcel Deker Inc., New York.

Bacon, C. W., Porter, J. K., Robbins, J. D., and Luttrell, E. J. (1977). *Epichloë typhina* from toxic tall fescue grasses. *Appl. Environ. Microbiol.*, **34**, 576–581.

Bais, H. P., Vepachedu, R., Lawrence, C. B., Stermitz, F. R., and Vivanco, J. M. (2003). Molecular and biochemical characterization of an enzyme responsible for the formation of hypericin in St. John's wort (*Hypericum perforatum* L.). *J. Biol. Chem.*, **278**, 32413–32422.

Bais, H. P., Walker, T. S., McGrew, J. J., and Vivanco, J. M. (2002). Factors affecting growth of cell suspension cultures of *Hypericum perforatum* L. (St. John's wort) and production of hypericin. *In Vitro Cell. Dev. Biol. - Plant*, **38**, 58–65.

Balaram, P. (2010). Chemical synthesis and the synthetic cell. *Curr. Sci.*, **98**, 1415–1416.

Barnard, D. L., Huffman, J. H., Morris, J. L., Wood, S. G., Hughes, B. G., and Sidwell, R. W. (1992). Evaluation of the antiviral activity of anthraquinones, anthrones and anthraquinone derivatives against human cytomegalovirus. *Antiviral Res.*, **17**, 63–77.

Bedir, E., Khan, I., and Moraes, R. M. (2002). Bioprospecting for podophyllotoxin. In Janick, J., Whipkey, A. (eds.) *Trends in new crops and new uses*. ASHS Press, Alexandria, VA, pp. 545–549.

Bedir, E., Tellez, M., Lata, H., Khan, I., Cushman, K. E., and Moraes, R. M. (2006). Post-harvest and scale-up extraction of American mayapple leaves for podophyllotoxin production. *Ind. Crop. Prod.*, **24**, 3–7.

Bendixen, C., Thomsen, B., Alsner, J., and Westergaard, O. (1990). Camptothecin-stabilized topoisomerase I-DNA adducts cause premature termination of transcription. *Biochemistry*, **29**, 5613–5619.

Berghöfer, R. (1987). *Analytik und Isolierung phenolischer Inhaltsstoffe von Hypericum perforatum L. aus Anbau und Vergleich mit anderen Hypericum-Arten*, vol. 106. Dissertationes Botanicae, Verlag J. Cramer, Berlin, Germany.

Bills, J. K., Christensen, M., Powell, M., and Thorn, G. (2004). *Biodiversity of fungi: endophytic Fungi*. Elsevier Academic Press, CA, U.S.A..

Birch, A. J. (1967). Biosynthesis of polyketides and related compounds. *Science*, **156**, 202–206.

Blessing, M., Schmidt, T. C., Dinkel, R., and Hardelein, S. B. (2009). Delineation of multiple chlorinated ethene sources in an industrialized area – a forensic field study using compound-specific isotope analysis. *Environ. Sci. Technol.*, **43**, 2701–2707.

Bodley, A. L., Cumming, J. N., and Shapiro, T. A. (1998). Effects of camptothecin, a topoisomerase I inhibitor, on *Plasmodium falciparum*. *Biochem. Pharmacol.*, **55**, 709–711.

Bonkanka, C. X., Smelcerovic, A., Zühlke, S., Rabanal, R. M., Spiteller, M., and Sanchez-Mateo, C. C. (2008). HPLC-MS analysis and anti-oedematogenic activity of *Hypericum grandifolium* Choisy (Hypericaceae). *Planta Med.*, **74**, 719–725.

Borsche, W. and Niemann, J. (1932). Über Podophyllin. *Justus Liebig's Ann. Chem.*, **494**, 126–142.
Brantner, A., Male, Z., Pepeljnjak, S., and Antoli, A. (1996). Antimicrobial activity of *Paliurus spina-christi* Mill. (Christ's thorn). *J. Ethnopharmacol.*, **52**, 119–122.

Briskin, D. P., Leroy, A., and Gawienowski, M. (2000). Influence of nitrogen on the production of hypericins by St. John's wort. *Plant Physiol. Biochem.*, **38**, 413–420.

Brockmann, H., Falkenhausen, E. H., and Dorlares, A. (1950). Die Konstitution des Hypericins. *Naturwissenschaften*, **37**, 540–540.

Brockmann, H., Haschad, M. N., Maier, K., and Pohl, F. (1939). Über das Hypericin, den photodynamisch wirksamen Farbstoff aus *Hypericum perforatum*. *Naturwissenschaften*, **27**, 550–550.

Brockmann, H., Kluge, F., and Muxfeldt, H. (1957). Totalsynthese des Hypericins. *Chem. Ber.*, **90**, 2302–2318.

Brockmann, H., Pohl, F., Maier, K., and Haschad, M. N. (1942). Über das Hypericin, den photodynamischen Farbstoff des Johanniskrautes (*Hypericum perforatum*). *Ann. Chem.*, **553**, 1–52.

Broomhead, A. J. and Dewick, P. M. (1990a). Aryltetralin lignans from *Linum flavum* and *Linum capitatum*. *Phytochemistry*, **29**, 3839–3844.

Broomhead, A. J. and Dewick, P. M. (1990b). Tumor-inhibitory aryltetralin lignans in *Podophyllum versipelle*, *Diphylleia cymosa* and *Diphylleia grayi*. *Phytochemistry*, **29**, 3831–3837.

Broomhead, A. J., Rahman, M. M., Dewick, P. M., Jackson, D. E., and Lucas, J. A. (1991). Matairesinol as precursor of *Podophyllum* lignans. *Phytochemistry*, **30**, 1489–1492.

Burke, T. G. and Mi, Z. (1993). Preferential binding of the carboxylate form of camptothecin by human serum-albumin. *Anal. Biochem.*, **212**, 285–287.

Buter, B., Orlacchio, C., Soldati, A., and Berger, K. (1998). Significance of genetic and environmental aspects in the field cultivation of *Hypericum perforatum*. *Planta Med.*, **64**, 431–437.

Canel, C., Dayan, F. E., Ganzera, M., Khan, I. A., Rimando, A., Burandt Jr., C. L., and Moraes, R. M. (2001). High yield of podophyllotoxin from leaves of *Podophyllum peltatum* by *in situ* conversion of podophyllotoxin 4-*O*-β-D-glucopyranoside. *Planta Med.*, **67**, 97–99.

Canel, C., Moraes, R. M., Dayan, F. E., and Ferreira, D. (2000). Podophyllotoxin. *Phytochemistry*, **54**, 115–120.

Carpenter, S. and Kraus, G. A. (1991). Photosensitization is required for inactivation of equine infectious anemia virus by hypericin. *Photochem. Photobiol.*, **53**, 169–174.

Carpenter, S., Fehr, M. J., Kraus, G. A., and Petrich, J. W. (1994). Chemiluminescent activation of the antiviral activity of hypericin: a molecular flashlight. *Proc. Natl. Acad. Sci. U. S. A.*, **91**, 12273–12277.

Cavaliere, C., Rea, P., Lynch, M. E., and Blumenthal, M. (2010). Herbal supplement sales rise in all channels in 2009. *HerbalGram (Amer. Bot. Council)*, **86**, 62–65.

Cellarova, E., Daxnerova, Z., Kimakova, K., and Haluskova, J. (1994). The variability of hypericin content in the regenerants of *Hypericum perforatum*. *Acta Biotechnol.*, **14**, 267–274.

Chemler, J. A. and Koffas, M. A. G. (2008). Metabolic engineering for plant natural product biosynthesis in microbes. *Curr. Opin. Biotechnol.*, **19**, 597–605.

Chen, J. J., Chang, Y. L., Teng, C. M., and Chen, I. S. (2000). Anti-platelet aggregation alkaloids and lignans from *Hernandia nymphaeifolia*. *Planta Med.*, **66**, 251–256.

Chen, Z. G., Fujii, I., Ebizuka, Y., and Sankawa, U. (1995). Purification and characterization of emodinanthrone oxygenase from *Aspergillus terreus*. *Phytochemistry*, **38**, 299–305.

Chillemi, G., Fiorani, P., Benedetti, P., and Desideri, A. (2003). Protein concerted motions in the DNA-human topoisomerase I complex. *Nucleic Acids Res.*, **31**, 1525–1535.

Choi, H., Lee, J., Shin, H. J., Lee, B. G., Chang, I., and Hwang, J. S. (2004). Deoxypodophyllotoxin reduces skin pigmentation of brown guinea pigs. *Planta Med.*, **70**, 378–380.

Chomczynski, P. and Sacchi, N. (1987). Single-step method of RNA isolation by acid guanidinium thiocyanate-phenol-chloroform extraction. *Anal. Biochem.*, **162**, 156–159.

Choudhary, D. K., Kaul, B. L., and Khan, S. (1998). Cultivation and conservation of *Podophyllum hexandrum*-an overview. *J. Med. Arom. Plant Sci.*, **20**, 1071–1073.

Chrencik, J. E., Staker, B. L., Burgin, A. B., Pourquier, P., Pommier, Y., Stewart, L., and Redinbo, R. (2004). Mechanisms of camptothecin resistance by human topoisomerase I mutations. *J. Mol. Biol.*, **339**, 773–784.

Cirak, C., Aksoy, H. M., Ayan, A. K., Saglam, B., and Kevseroglu, K. (2005). Enhanced hypericin production in *Hypericum perforatum* and *Hypericum pruinatum* in response to inoculation with two fungal pathogens. *Plant Protect. Sci.*, **41**, 109–114.

Clardy, J. and Walsh, C. (2004). Lessons from natural molecules. *Nature*, **432**, 829–837.

Cockayne, T. O. (1961). *Leechdoms, wortcunning, and starcraft of early England: being a collection of documents, for the most part never before printed, illustrating the history of science in this country before the Norman conquest*, vol. 2. The Holland Press, London.

Cohen, P. A., Hudson, J. B., and Towers, G. H. (1996). Antiviral activities of anthraquinones,

bianthrones and hypericin derivatives from lichens. *Experientia*, **52**, 180–183.

Collu, G., Unver, N., Peltenburg-Looman, A. M. G., van der Heijden, R., Verpoorte, R., and Memelink, J. (2001). Geraniol 10-hydroxylase, a cytochrome P450 enzyme involved in terpenoid indole alkaloid biosynthesis. *FEBS Lett.*, **508**, 215–220.

Cragg, G. M. and Newman, D. J. (2004). A tale of two tumor targets: topoisomerase I and tubulin. The Wall and Wani contribution to cancer chemotherapy. *J. Nat. Prod.*, **67**, 232–244.

Cronquist, A. (1988). *The evolution and classification of flowering plants*. New York Botanical Garden Scientific Publication Department, Bronx, N. Y.

Dai, J. R., Cardellina, J. H., and Boyd, M. R. (1999). 20-*O*-β-glucopyranosyl camptothecin from *Mostuea brunonis*: a potential camptothecin pro-drug with improved solubility. *J. Nat. Prod.*, **62**, 1427–1429.

Davin, L. B., Wang, H. B., Crowell, A. L., Bedgar, D. L., Martin, D. M., Sarkanen, S., and Lewis, N. G. (1997). Stereoselective bimolecular phenoxy radical coupling by an auxiliary (dirigent) protein without an active center. *Science*, **275**, 362–366.

Day, S. H., Chui, N. Y., Won, S. J., and Lin, C. N. (1999). Cytotoxic lignans of *Justicia ciliata*. *J. Nat. Prod.*, **62**, 1056–1058.

de Bary, A. (1866). *Morphologie und Physiologie der Pilze, Flechten, und Myxomyceten. Hofmeister's handbook of physiological botany*, vol. II. Leipzig, Germany.

De Luca, V. and St-Pierre, B. (2000). The cell and developmental biology of alkaloid biosynthesis. *Trends Plant Sci.*, **5**, 168–173.

De Luca, V., Marineau, C., and Brisson, N. (1989). Molecular cloning and analysis of cDNA encoding a plant tryptophan decarboxylase: comparison with animal DOPA decarboxylases. *Proc. Natl. Acad. Sci. U. S. A.*, **86**, 2582–2586.

Decaisne, J. (1873). Caracteres et descriptions de trios genres nouveaus de plantes recueilles en chine par l'abbe a. *David Bull. Soc. Bot. France*, **20**, 155–160.

Degar, S., Lavie, G., and Meruelo, D. (1993). Photodynamic inactivation of radiation leukemia virus produced from hypericin-treated cells. *Virology*, **197**, 796–800.

Degar, S., Prince, A. M., Pascual, D., Lavie, G., Levin, B., Mazur, Y., Lavie, D., Ehrlich, L. S., Carter, C., and Meruelo, D. (1992). Inactivation of the human immunodeficiency virus by hypericin: evidence for photochemical alterations of p24 and a block in uncoating. *AIDS Res. Hum. Retro.*, **8**, 1929–1936.

Delaey, E. M., Obermueller, R., Zupko, I., De Vos, D., Falk, H., and de Witte, P. A. (2001). *In vitro* study of the photocytotoxicity of some hypericin analogs on different cell lines. *Photochem. Photobiol.*, **74**, 164–171.

Dewick, P. M. (1989). *Biosynthesis of lignans: Structure elucidation (part B)*. Series: *Studies in natural products chemistry,* vol. 5. Elsevier, Amsterdam.

Dreyfuss, M. M. and Chapela, I. H. (1994). Potential of fungi in the discovery of novel, low molecular

weight pharmaceuticals. In Gullo, V. P. (ed.) *The discovery of natural product with therapeutic potential*, vol. 26. Butterworth-Heinemann, London, pp. 49-80.

Eagle, H. (1955). Propagation in a fluid medium of a human epidermoid carcinoma, strain KB. *Proc. Soc. Exp. Biol. Med.*, **89**, 362–364.

Ernst, E. (2003). *Hypericum: the genus Hypericum*. Series: *Medicinal and Aromatic Plants - Industrial Profiles.* Taylor and Francis, London, UK.

Eyberger, A. L., Dondapati, R., and Porter, J. R. (2006). Endophyte fungal isolates from *Podophyllum peltatum* produce podophyllotoxin. *J. Nat. Prod.*, **69**, 1121–1124.

Ezra, D., Hess, W. M., and Strobel, G. A. (2004). New endophytic isolates of *Muscodor albus*, a volatile-antibiotic-producing fungus. *Microbiol. - SGM*, **150**, 4023–4031.

Falk, H. (1999). From the photosensitizer hypericin to the photoreceptor stentorin-the chemistry of phenanthroperylene quinones. *Angew Chem. Int. Ed.*, **38**, 3116–3136.

Falk, H. and Schoppel, G. (1991). A synthesis of emodin anthrone. *Monatsh. Chem.*, **122**, 739–744.

Falk, H., Meyer, J., and Oberreiter, M. (1993). A convenient semisynthetic route to hypericin. *Monatsh. Chem.*, **124**, 339–341.

Fan, Y., Weinstein, J. N., Kohn, K. W., Shi, L. M., and Pommier, Y. (1998). Molecular modeling studies of the DNA-topoisomerase I ternary cleavable complex with camptothecin. *J. Med. Chem.*, **41**, 2216–2226.

Fassberg, J. and Stella, V. J. (1992). A kinetic and mechanistic study of the hydrolysis of camptothecin and some analogues. *J. Pharm. Sci.*, **81**, 676–684.

Fehr, M. J., Carpenter, S. L., Wannemuehler, Y., and Petrich, J. W. (1995). Roles of oxygen and photo-induced acidification in the light-dependent antiviral activity of hypocrellin A. *Biochemistry*, **34**, 15845–15848.

Ferlay, J., Autier, P., Boniol, M., Heanue, M., Colombet, M., and Boyle, P. (2007). Estimates of the cancer incidence and mortality in Europe in 2006. *Ann. Oncol.*, **18**, 581–592.

Fields, P. G., Arnason, J. T., and Fulcher, R. G. (1990). The spectral properties of *Hypericum perforatum* leaves: the implications for photoactivated defences. *Can. J. Bot.*, **68**, 1166–1170.

Fiorani, P., Bruselles, A., Falconi, M., Chillemi, G., Desideri, A., and Benedetti, P. (2003). Single mutation in the linker domain confers protein flexibility and camptothecin resistance to human topoisomerase I. *J. Biol. Chem.,* **278**, 43268–43275.

Fisel, J., Gäbler, H., Schwöbel, H., and Trunzler, G. (1966). *Haronga madagascariensis*. Botanik, Pharmakonosie, Chemie und therapeutische Anwendung. *Dtsch. Apoth.*, **106**, 1053–1060.

Fisher, M. (1936). The use of multiple measurements in taxonomic problems. *Ann. Eugenics*, **7**, 179–188.

Flechon, A., Culine, S., and Droz, J. P. (2001). Intensive and timely chemotherapy, the key of success

in testicular cancer. *Crit. Rev. Onco. Hema.*, **37**, 35–46.

Freeman, E. M. (1904). The seed-fungus of *Lolium temulentum*, L., the Darnel. *Phil. Trans. R. Soc. B*, **196**, 1–27.

Fujimori, A., Harker, W. G., Kohlhagen, G., Hoki, Y., and Pommier, Y. (1995). Mutation at the catalytic site of topoisomerase I in CEM/C2, a human leukemia cell line resistant to camptothecin. *Cancer Res.*, **55**, 1339–1346.

Fukamiya, N. and Lee, K. H. (1986). Antitumor agents, 81. Justicidin-A and diphyllin, two cytotoxic principles from *Justicia procumbens*. *J. Nat. Prod.*, **49**, 348–350.

Gao, R., Gao, C. F., Tian, X., Yu, X. Y., Di, X. D., Xiao, H., and Zhang, X. (2004). Insecticidal activity of deoxypodophyllotoxin, isolated from *Juniperus sabina* L, and related lignans against larvae of *Pieris rapae* L. *Pest Manage. Sci.*, **60**, 1131–1136.

Gensler, W. J. and Wang, S. Y. (1954). Synthesis of picropodophyllin. *J. Am. Chem. Soc.*, **76**, 5890–5891.

Gensler, W. J., Samour, C. M., and Wang, S. Y. (1954). Sythesis of a DL-stereoisomer of podophyllic acid. *J. Am. Chem. Soc.*, **76**, 315–316.

Giovanella, B. C., Stehlin, J. S., Wall, M. E., Wani, M. C., Nicholas, A. W., Liu, L. F., Silber, R., and M, P. (1989). DNA topoisomerase I - targeted chemotherapy of human colon cancer in xenografts. *Science*, **246**, 1046–1048.

Glisic, S., Smelcerovic, A., Zühlke, S., Spiteller, M., and Skala, D. (2008). Extraction of hyperforin and adhyperforin from St. John's wort (*Hypericum perforatum* L.) by supercritical carbon dioxide. *J. Supercrit. Fluids*, **45**, 332–337.

Gordaliza, M., Garcia, P. A., del Corral, J. M., Castro, M. A., and Gomez-Zurita, M. A. (2004). Podophyllotoxin: distribution, sources, applications and new cytotoxic derivatives. *Toxicon*, **44**, 441–459.

Gudzic, B. T., Smelcerovic, A., Dordevic, S., Mimica-Dukic, N., and Ristic, M. (2007). Essential oil composition of *Hypericum hirsutum* L. *Flavour Fragr. J.*, **22**, 42–43.

Guerin, P. (1898). Sur la presence d'un champignon dans l'ivraie. *J. Botanique*, **12**, 230–238.

Guillet, G., Podeszfinski, C., Regnault-Roger, C., Arnason, J. T., and Philogene, B. J. R. (2000). Behavioral and biochemical adaptations of generalist and specialist herbivorous insects feeding on *Hypericum perforatum* (Guttiferae). *Environ. Entomol.*, **29**, 135–139.

Gunasekera, S. P., Badawi, M. M., Cordell, G. A., Farnsworth, N. R., and Chitnis, M. (1979). Plant anticancer agents X. Isolation of camptothecin and 9-methoxycamptothecin from *Ervatamia heyneana*. *J. Nat. Prod.*, **42**, 475–477.

Gunatilaka, A. A. L. (2006). Natural products from plant-associated microorganisms: distribution, structural diversity, bioactivity, and implications of their occurrence. *J. Nat. Prod.*, **69**, 509–526.

Gunther, R. T. (1959). *The Greek herbal of Dioscorides*. Hafner Publishing Co., New York.

Häberlein, H., Tschiersch, K. P., Stock, S., and Hölzl, J. (1992). Johanniskraut (*Hypericum perforatum* L.): Nachweis eines weiteren Naphthodianthrons. *Pharm. Ztg. Wiss.*, **5/137**, 169–174.

Hadimani, S. B., Tanpure, R. P., and Bhat, S. V. (1996). Asymmetric total synthesis of (-) podophyllotoxin. *Tetrahedron Lett.*, **37**, 4791–4794.

Hadjur, C., Richard, M. J., Parat, M. O., Jardon, P., and Favier, A. (1996). Photodynamic effects of hypericin on lipid peroxidation and antioxidant status in melanoma cells. *Photochem. Photobiol.*, **64**, 375–381.

Hande, K. R. (1998). Etoposide: Four decades of development of a topoisomerase II inhibitor. *Eur. J. Cancer*, **34**, 1514–1521.

Handley, L. L. and Raven, J. A. (2000). The use of natural abundance of nitrogen isotopes in plant physiology and ecology. *Plant Cell Environ.*, **15**, 965–985.

Hartwell, J. L. and Schrecker, A. W. (1958). Lignans of *Podophyllum*. In Zechmeister, L. (ed.) *Progress in the chemistry of organic natural products*, vol. 15. Springer-Verlag, Wien, pp. 83–166.

Hartwell, J. L., Johnson, J. M., Fitzgerald, D. B., and Belkin, M. (1953). Podophyllotoxin from *Juniperus* species; Savinin. *J. Am. Chem. Soc.*, **75**, 235–236.

Hawksworth, D. L., Kirk, P. M., Sutton, B. C., and Pegler, D. N. (1996). *Ainsworth & Bisby's dictionary of the fungi*. CAB International, Wallingford, Oxford.

Hegnauer, R. (1966). *Chemotaxonomie der Pflanzen*. Springer, Birkhäuser, Basel.

Heron, J. F. (1998). Topotecan: an oncologist's view. *Oncologist*, **3**, 390–402.

Hertweck, C. (2009). The biosynthetic logic of polyketide diversity. *Angew. Chem. Int. Ed.*, **48**, 4688–4716.

Hertzberg, R. P., Busby, R. W., Caranfa, M. J., Holden, K. G., Johnson, R. K., Hecht, S. M., and Kingsbury, W. D. (1990). Irreversible trapping of the DNA-topoisomerase I covalent complex. Affinity labeling of the camptothecin binding site. *J. Biol. Chem.*, **265**, 19287–19295.

Hickey, M. and King, C. (1981). *100 Families of flowering plants,* 2nd ed., Walters, S. M. (ed.). Chembridge University Press, Chembridge.

Hildebrand, M., Waggoner, L. E., Lim, G. E., Sharp, K. H., Ridley, C. P., and Haygood, M. G. (2004). Approaches to identify, clone, and express symbiont bioactive metabolite genes. *Nat. Prod. Rep.*, **21**, 122–142.

Hirsch, G. U. and Braun, U. (1992). *Communities of parasitic microfungi*, vol. 19. Kluwer, Dordrecht.
Holden, J. A., Wall, M. E., and Wani, M C, M. G. (1999). Human DNA topoisomerase I: quantitative analysis of the effects of camptothecin analogs and the benzophenanthridine alkaloids nitidine and 6-ethoxydihydronitidine on DNA topoisomerase I-induced DNA strand breakage. *Arch. Biochem. Biophys.*, **370**, 66–76.

Hölzl, J. and Petersen, M. (2003). Chemical constituents of *Hypericum* ssp. In Ernst, E. (ed.) *Hypericum: the genus Hypericum (Series: Medicinal and Aromatic Plants - Industrial Profiles)*, vol. 31.

Taylor and Francis, London, UK, pp. 77–93.

Hombe Gowda, H. C., Vasudeva, R., Mathachen, G. P., Shaanker, R. U., and Ganeshaiah, K. N. (2002). Breeding types in *Nothapodytes nimmoniana* Graham.: An important medicinal tree. *Curr. Sci.*, **83**, 1077–1078.

Howitz, K. T. and Sinclair, D. A. (2008). Xenohormesis: sensing the chemical cues of other species. *Cell*, **133**, 387–391.

Hsiang, Y. H., Hertzberg, R., Hecht, S., and Liu, L. F. (1985). Camptothecin induces protein-linked DNA breaks via mammalian DNA topoisomerase I. *J. Biol. Chem.*, **260**, 14873–14878.

Huang, M., Gao, H., Chen, Y., Zhu, H., Cai, Y., Zhang, X., Miao, Z., Jiang, H., Zhang, J., Shen, H., Lin, L., Lu, W., and Ding, J. (2007). Chimmitecan, a novel 9-substituted camptothecin, with improved anticancer pharmacologic profiles *in vitro* and *in vivo*. *Clin. Cancer. Res.*, **13**, 1298–1307.

Hudson, J. B., Delaey, E., and de Witte, P. A. (1999). Bromohypericins are potent photoactive antiviral agents. *Photochem. Photobiol.*, **70**, 820–822.

Hudson, J. B., Graham, E. A., and Towers, G. H. (1994). Antiviral assays on phytochemicals: the influence of reaction parameters. *Planta Med.*, **60**, 329–332.

Hudson, J. B., Harris, L., and Towers, G. H. (1993). The importance of light in anti-HIV effect of hypericin. *Antiviral Res.*, **20**, 173–178.

Hudson, J. B., Lopez-Bazzocchi, I., and Towers, G. H. (1991). Antiviral activities of hypericin. *Antiviral Res.*, **15**, 101–112.

Hutchinson, C. R., Heckendorf, A. H., Straughn, J. L., Daddona, P. E., and Cane, D. E. (1979). Biosynthesis of camptothecin. 3. Definition of strictosamide as the penultimate biosynthetic precursor assisted by ^{13}C and ^{2}H NMR spectroscopy. *J. Am. Chem. Soc.*, **101**, 3358–3369.

Ikeda, R., Nagao, T., Okabe, H., Nakano, Y., Matsunaga, H., Katano, M., and Mori, M. (1998). Antiproliferative constituents in umbelliferae plants. III. Constituents in the root and the ground part of *Anthriscus sylvestris* Hoffm. *Chem. Pharm. Bull.*, **46**, 871–874.

Imbert, T. F. (1998). Discovery of podophyllotoxins. *Biochimie*, **80**, 207–222.

Inamori, Y., Kato, Y., Kubo, M., Baba, K., Ishida, T., Nomoto, K., and Kozawa, M. (1985). The biological actions of deoxypodophyllotoxin (anthricin). I. Physiological activities and conformational analysis of deoxypodophyllotoxin. *Chem. Pharm. Bull.*, **33**, 704–709.

Innocenti, G., Puricelli, L., Piacente, S., Caniato, R., Filippini, R., and Cappelletti, E. M. (2002). Patavine, a new arylnaphthalene lignan glycoside from shoot cultures of *Haplophyllum patavinum*. *Chem. Pharm. Bull.*, **50**, 844–846.

Irmler, S., Schröder, G., St-Pierre, B., Crouch, N. P., Hotze, M., Schmidt, J., Strack, D., Matern, U., and Schröder, J. (2000). Indole alkaloid biosynthesis in *Catharanthus roseus*: new enzyme activities and identification of cytochrome P450 CYP72A1 as secologanin synthase. *Plant J.*, **24**, 797–804.

Jackson, D. E. and Dewick, P. M. (1984). Biosynthesis of *Podophyllum* lignans - II. Interconversions of

artyltetralin lignans in *Podophyllum hexandrum*. *Phytochemistry*, **23**, 1037–1042.

Jemal, A., Siegel, R., Ward, E., Hao, Y., Xu, J., Murray, T., and Thun, M. J. (2008). Cancer statistics, 2008. *CA Cancer J. Clin.*, **58**, 71–96.

Jolad, S. D., Wiedhopf, R. M., and Cole, J. R. (1977). Cytotoxic agents from *Bursera morelensis* (Burseraceae): deoxypodophyllotoxin and a new lignan, 5'-desmethoxydeoxypodophyllotoxin. *J. Pharm. Sci.*, **66**, 892–893.

Julsing, M. K., Quax, W. J., and Kayser, O. (2007). The engineering of medicinal plants: prospects and limitations of medicinal plant biotechnology. In Kayser, O., Quax, W. J. (eds.) *Medicinal plant biotechnology. From basic research to industrial applications*. Wiley-VCH Verlag GmbH & Co. KGaA, Weinheim, pp. 3–8.

Julsing, M. K., Vasilev, N. P., Sheneidman-Duhovny, D., Muntendam, R., Woerdenbag, H. J., Quax, W. J., Wolfson, H. J., Ionkova, I., and Kayser, O. (2008). Metabolic stereoselectivity of cytochrome P450 3A4 towards deoxypodophyllotoxin: *In silico* predictions and experimental validation. *Eur. J. Med. Chem.*, **43**, 1171–1179.

Kamil, W. M. and Dewick, P. M. (1986). Biosynthesis of the lignans α- and β- peltatin. *Phytochemistry*, **25**, 2089–2092.

Kamuhabwa, A. R., Agostinis, P. M., D'Hallewin, M. A., Baert, L., and de Witte, P. A. (2001). Cellular photodestruction induced by hypericin in AY-27 rat bladder carcinoma cells. *Photochem. Photobiol.*, **74**, 126–132.

Karppinen, K. and Hohtola, A. (2008). Molecular cloning and tissue-specific expression of two cDNAs encoding polyketide synthases from *Hypericum perforatum*. *J. Plant Physiol.*, **165**, 1079–1086.

Karppinen, K., Hokkanen, J., Mattila, S., Neubauer, P., and Hohtola, A. (2008). Octaketide-producing type III polyketide synthase from *Hypericum perforatum* is expressed in dark glands accumulating hypericins. *FEBS J.*, **275**, 4329–4342.

Kartnig, T., Goebel, I., and Heydel, B. (1996). Production of hypericin, pseudohypericin and flavonoids in cell cultures of various *Hypericum* species and their chemotypes. *Planta Med.*, **62**, 51–53.

Kartnig, T., Gruber, A., and Sauer, H. (1989). Comparative phytochemical investigations of *Hypericum* species. *Planta Med.*, **55**, 215.

Katz, L. and Donadio, S. (1993). Polyketide synthesis: prospects for hybrid antibiotics. *Ann. Rev. Microbiol.*, **47**, 875–912.

Kauh, E. A. and Bjornsti, M. A. (1995). SCT1 mutants suppress the camptothecin sensitivity of yeast-cells expressing wild-type DNA topoisomerase-I. *Proc. Natl. Acad. Sci. U.S.A.*, **92**, 6299–6303.

Kaul, R. (2000). *Johanniskraut*. Wissenschaftliche Verlagsgesellschaft, Stuttgart.

Kayser, O. (2010). Metabolic engineering strategies for the optimization of medicinal and aromatic plants: expectations and realities. In Baricevic, D., Novak, J., Pank, F. (eds.) *ISHS Acta Horticulturae 860. IV. International Symposium on Breeding Research on Medicinal and Aromatic Plants - ISBMAP2009*. International Society for Horticultural Science, Ljubljana, Slovenia, pp. 199–204.

Kayser, O. and Müller, R. H. (2004). A primer on pharmaceutical biotechnology and industrial applications. In Kayser, O., Müller, R. H. (eds.) *Pharmaceutical biotechnology. Drug discovery and clinical applications.* Wiley-VCH Verlag GmbH & Co. KGaA, Weinheim, pp. 3–8.

Keck, J. L. and Berger, J. M. (1999). Enzymes that push DNA around. *Nat. Struct. Biol.*, **6**, 900–902.

Kehrer, D. F. S., Soepenberg, O., Loos, W. J., Verweij, J., and Sparreboom, A. (2001). Modulation of camptothecin analogs in the treatment of cancer: a review. *Anti-Can. Drugs*, **12**, 89–105.

Kennedy, B. V. and Krouse, H. R. (1990). Isotope fractionation by plant and animals: implications for nutrition research. *Can. J. Physiol. Pharmacol.*, **68**, 960–972.

Kerrigan, J. E. and Pilch, D. S. (2001). A structural model for the ternary cleavable complex formed between human topoisomerase I, DNA, and camptothecin. *Biochemistry*, **40**, 9792–9798.

Kim, Y., Kim, S. B., You, Y. J., and Ahn, B. Z. (2002). Deoxypodophyllotoxin; the cytotoxic and antiangiogenic component from *Pulsatilla koreana*. *Planta Med.*, **68**, 271–274.

King, J. (1857). Discovery of podophyllin. *Coll. J. M. Sci.*, **2**, 557–559.

Kirakosyan, A., Hayashi, H., Inoue, K., Charchoglyan, A., and Vardapetyan, H. (2000). Stimulation of the production of hypericins by mannan in *Hypericum perforatum* shoot cultures. *Phytochemistry*, **53**, 345–348.

Kirakosyan, A., Hayashi, H., Inoue, K., Charchoglyan, A., Vardapetyan, H., and Yammoto, H. (2001). The effect of cork pieces on pseudohypericin production in cells of *Hypericum perforatum* shoots. *Russ. J. Plant Physiol.*, **48**, 816–819.

Kitanov, G. M. (2001). Hypericin and pseudohypericin in some *Hypericum* species. *Biochem. Syst. Ecol.*, **29**, 171–178.

Konuklugil, B. (1996a). Aryltetralin lignans from genus *Linum*. *Fitoterapia*, **LXVII**, 379–381.

Konuklugil, B. (1996b). Investigation of podophyllotoxin in some plants in Lamiaceae using HPLC. *J. Fac. Pharm. Ankara.*, **25**, 23–27.

Kosuth, J., Katkovcinova, Z., Olexova, P., and Cellarova, E. (2007). Expression of the *hyp-1* gene in early stages of development of *Hypericum perforatum* L. *Plant Cell Rep.*, **26**, 211–217.

Koulman, A. (2003). *Podophyllotoxin: a study of the biosynthesis, evolution, function and use of podophyllotoxin and related lignans*. Phd thesis, Rijksuniversiteit Groningen, The Netherlands.

Koulman, A. and Konuklugil, B. (2004). Lignan profile of *Linum meletonis*. *Biochem. Syst. Ecol.*, **32**, 91–93.

Koulman, A., Beekman, A. C., Pras, N., and Quax, W. J. (2003). The bioconversion process of deoxypodophyllotoxin with *Linum flavum* cell cultures. *Planta Med.*, **69**, 739–744.

Kour, A., Shawl, A. S., Rehman, S., Sultan, P., Qazi, P. H., Suden, P., Khajuria, R. K., and Verma, V. (2008). Isolation and identification of an endophytic strain of *Fusarium oxysporum* producing podophyllotoxin from *Juniperus recurva*. *World J. Microbiol. Biotechnol.*, **24**, 1115–1121.

Kozawa, M., Baba, K., Matsuyama, Y., Kido, T., Sakai, M., and Takemoto, M. (1982). Components of the root of *Anthriscus sylvestris* Hoffm. II. Insecticidal activity. *Chem. Pharm. Bull.*, **30**, 2885–2888.

Kozawa, M., Morita, N., and Hata, K. (1978). Structure of anthriscusin, a new phenylpropanoid ester from the roots of *Anthriscus sylvestris* Hoffm. *Chem. Pharm. Bull.*, **26**, 1337–1338.

Kraus, G. A., Melekhov, A., Carpenter, S., Wannemuhler, Y., and Petrich, J. (2000). Phenanthrenequinone antiretroviral agents. *Bioorg. Med. Chem. Lett.*, **10**, 9–11.

Kruskal, J. B. (1964). Non-metric multidimensional scaling: a numerical method. *Psychometrika*, **29**, 115–129.

Kubin, A., Wierrani, F., Burner, U., Alth, G., and Grunberger, W. (2005). Hypericin - the facts about a controversial agent. *Curr. Pharm. Des.*, **11**, 233–253.

Kuhnt, M., Rimpler, H., and Henrich, M. (1994). Lignans and other compounds from the mixed Indian medicinal plant *Hyptis verticillata*. *Phytochemistry*, **36**, 485–489.

Kumar, K. R. and Ved, D. K. (2000). *100 Red listed medicinal plants of conservation concern in southern India*. Foundation for Revitalisation of Local Health Traditions (FRLHT), Bangalore, India.

Kupchan, S. M., Hemingway, J. C., and Knox, J. R. (1965). Tumor inhibitors VII. Podophyllotoxin, the active principle of *Juniperus virginiana*. *J. Pharm. Sci.*, **54**, 659–660.

Kusari, S., Prabhakaran, D., Lamshöft, M., and Spiteller, M. (2009). *In vitro* residual anti-bacterial activity of difloxacin, sarafloxacin and their photoproducts after photolysis in water. *Environ. Pollut.*, **157**, 2722–2730.

Kutchan, T. M. (1989). Expression of enzymatically active cloned strictosidine synthase from the higher plant *Rauvolfia serpentina* in *Escherichia coli*. *FEBS Lett.*, **257**, 127–130.

Kutchan, T. M. (1995). Alkaloid biosynthesis -the basis for metabolic engineering of medicinal plants. *Plant Cell*, **7**, 1059–1070.

Kutchan, T. M., Bock, A., and Dittrich, H. (1994). Heterologous expression of the plant proteins strictosidine synthase and berberine bridge enzyme in insect cell culture. *Phytochemistry*, **35**, 353–360.

Kutchan, T. M., Hampp, N., Lottspeich, F., Beyreuther, K., and Zenk, M. H. (1988). The cDNA clone for strictosidine synthase from *Rauvolfia serpentina*. DNA sequence determination and expression in *Escherichia coli*. *FEBS Lett.*, **237**, 40–44.

Kuzuyama, T. and Seto, H. (2003). Diversity of the biosynthesis of isoprene units. *Nat. Prod. Rep.*, **20**, 171–183.

Laco, G. S., Collins, J. R., Luke, B. T., Kroth, H., Sayer, J. M., Jerina, D. M., and Pommier, Y. (2002). Human topoisomerase I inhibition: docking camptothecin and derivatives into a structure-based active site model. *Biochemistry*, **41**, 1428–1435.

Lam, K. S. (2007). New aspects of natural products in drug discovery. *Trends Microbiol.*, **15**, 279–289.

Lamari, F. N. and Cordopatis, P. (2008). Exploring the potential of natural products in cancer treatment.

In Missailidis, S. (ed.) *Anticancer therapeutics*. Wiley-Blackwell, John Wiley & Sons Ltd., UK, pp. 3–16.

Lanen, S. G. V. and Shen, B. (2006). Microbial genomics for the improvement of natural product discovery. *Curr. Opin. Microbiol.*, **9**, 252–260.

Larsson, S. (2007). The "new" chemosystematics: phylogeny and phytochemistry. *Phytochemistry*, **68**, 2904–2908.

Lasasso, C., Cretaio, E., Palle, K., Pattarello, L., Bjornsti, M. A., and Benedetti, P. (2007). Alterations in linker flexibility suppress DNA topoisomerase I mutant-induced cell lethality. *J. Biol. Chem.,* **282**, 9855-9864.

Lavie, G., Mazur, Y., Lavie, D., Prince, A. M., Pascual, D., Liebes, L., Levin, B., and Meruelo, D. (1995). Hypericin as an inactivator of infectious viruses in blood components. *Transfusion*, **35**, 392–400.

Lavie, G., Valentine, F., Levin, B., Mazur, Y., Gallo, G., Lavie, D., Weiner, D., and Meruelo, D. (1989). Studies of the mechanisms of action of the antiretroviral agents hypericin and pseudohypericin. *Proc. Natl. Acad. Sci. U. S. A.*, **86**, 5963–5967.

Lee, S. H., Son, M. J., Ju, H. K., Lin, C. X., Moon, T. C., Choi, H. G., Son, J. K., and Chang, H. W. (2004). Dual inhibition of cyclooxygenases-2 and 5-lipoxygenase by deoxypodophyllotoxin in mouse bone marrow-derived mast cells. *Biol. Pharm. Bull.*, **27**, 786–788.

Lenard, J., Rabson, A., and Vanderoef, R. (1993). Photodynamic inactivation of infectivity of human immunodeficiency virus and other enveloped viruses using hypericin and Rose Bengal: inhibition of syncytia formation. *Proc. Natl. Acad. Sci. U. S. A.*, **90**, 158–162.

Li, J. Y., Sidhu, R. S., Ford, E. J., Long, D. M., Hess, W. M., and Strobel, G. A. (1998). The induction of Taxol production in the endophytic fungus-*Periconia sp.* from *Torreya grandifolia*. *J. Ind. Microbiol. Biotechnol.*, **20**, 259–264.

Li, Q. Y., Zu, Y. G., Shi, R. Z., and Yao, L. P. (2006). Review camptothecin: current perspectives. *Curr. Med. Chem.*, **13**, 2021–2039.

Li, S., Yi, Y., Wang, Y., Zhang, Z., and Beasley, R. S. (2002). Camptothecin accumulation and variations in *Camptotheca*. *Planta Med.*, **68**, 1010–1016.

Li, S., Zhang, Z., Cain, A., Wang, B., Long, M., and Taylor, J. (2005). Antifungal activity of camptothecin, trifolin, and hyperoside isolated from *Camptotheca acuminata*. *J. Agric. Food Chem.*, **53**, 32–37.

Lin, C. X., Lee, E., Jin, M. H., Yook, J., Quan, Z., Ha, K., Moon, T. C., Kim, M. J., Kim, K. J., Lee, S. H., and Chang, H. W. (2006). Deoxypodophyllotoxin (DPD) inhibits eosinophil recrument into the airway and Th2 cytokine expression in an ova-induced lung inflammation. *Planta Med.*, **72**, 786–791.

Lin, C. X., Son, M. J., Ju, H. K., Moon, T. C., Lee, E., Kim, S. H., Kim, M. J., Son, J. K., Lee, S. H., and Chang, H. W. (2004). Deoxypodophyllotoxin, a naturally occurring lignan, inhibits the passive cutaneous anaphylaxis reaction. *Planta Med.*, **70**, 474–476.

Linnaeus, C. (1753). *Species Plantarum: exhibentes plantas rite cognitas, ad genera relatas, cum differentiis specificis, nominibus trivialibus, synonymis selectis, locis natalibus, secundum systema*

sexuale digestas, vol. 1. Laurentius Salvius, Sweden.

Liu, K., Ding, X., Deng, B., and Chen, W. (2010). 10-Hydroxycamptothecin produced by a new endophytic *Xylaria sp*., M20, from *Camptotheca acuminata*. *Biotechnol. Lett.*, **32**, 689–693.

Liu, Y. Q., Yang, L., and Tian, X. (2007). Podophyllotoxin: current perspectives. *Curr. Bioact. Compd.*, **3**, 37–66.

Liu, Z., Carpenter, S. B., and Constantin, R. J. (1997). Camptothecin production in *Camptotheca acuminata* seedlings in response to shading and flooding. *Can. J. Bot.*, **75**, 368–373.

Liu, Z., Carpenter, S. B., Bourgeois, W. J., Yu, Y., Constantin, R. J., Falcon, M. J., and Adams, J. C. (1998). Variations in the secondary metabolite camptothecin in relation to tissue age and season in *Camptotheca acuminata*. *Tree Physiol.*, **18**, 265–270.

Lodge, D. J., Fisher, P. J., and Sutton, B. C. (1996). Endophytic fungi of *Manilkara bidentata* leaves in Puerto Rico. *Mycologia*, **88**, 733–738.

Lopez-Bazzocchi, I., Hudson, J. B., and Towers, G. H. (1991). Antiviral activity of the photoactive plant pigment hypericin. *Photochem. Photobiol.*, **54**, 95–98.

Lopez-Meyer, M. and Nessler, C. L. (1997). Tryptophan decarboxylase is encoded by two autonomously regulated genes in *Camptotheca acuminata* which are differentially expressed during development and stress. *Plant J.*, **11**, 1167–1175.

Lopez-Meyer, M., Nessler, C. L., and McKnight, T. D. (1994). Sites of accumulation of the antitumor alkaloid camptothecin in *Camptotheca acuminata*. *Planta Med.*, **60**, 558–560.

Lorence, A. and Nessler, C. L. (2004). Camptothecin, over four decades of surprising findings. *Phytochemistry*, **65**, 2735–2749.

Maggi, F., Ferretti, G., Pocceschi, N., Meneghini, L., and Ricciutelli, M. (2004). Morphological, histochemical and phytochemical investigation of the genus *Hypericum* of the central Italy. *Fitoterapia*, **75**, 702–711.

Maresh, J. J., Giddings, L. A., Friedrich, A., Loris, E. A., Panjikar, S., Trout, B. L., Stöckigt, J., Peters, B., and O'Connor, S. E. (2008). Strictosidine synthase: mechanism of a Pictet-Spengler catalyzing enzyme. *J. Am. Chem. Soc.*, **130**, 710–723.

Martinez, B., Kasper, S., Ruhrmann, S., and Moller, H. J. (1993). *Hypericum* in the treatment of seasonal affective disorders. *Nervenheilkunde*, **36**, 103–108.

Mascaux, C., Paesmans, M., Berghmans, T., Branle, F., Lafitte, J. J., Lemaitre, F., Meert, A. P., Vermylen, P., and Sculier, J. P. (2000). A systematic review of the role of etoposide and cisplatin in the chemotherapy of small cell lung cancer with methodology assessment and meta-analysis. *Lung Cancer*, **30**, 23–26.

Masuda, T., Oyama, Y., Yonemori, S., Takeda, Y., Yamazaki, Y., Mizuguchi, S., Nakata, M., Tanaka, T., Chikahisa, L., Inaba, Y., and Okada, Y. (2002). Flow cytometric estimation on cytotoxic activity of leaf extracts from seashore plants in subtropical Japan: isolation, quantification and cytotoxic action of (-)-deoxypodophyllotoxin. *Phytother. Res.*, **16**, 353–358.

Mazur, Y., Bock, H., and Lavie, D. (1992). *Preparation of hypericin*. *U. S. Patent 5,120,412.*

McKnight, T. D., Bergey, D. R., Burnett, R. J., and Nessler, C. L. (1991). Expression of enzymatically active and correctly targeted strictosidine synthase in transgenic tobacco plants. *Planta*, **185**, 148–152.

McKnight, T. D., Roessner, C. A., Devagupta, R., Scott, A. I., and Nessler, C. L. (1990). Nucleotide sequence of a cDNA encoding the vacuolar protein strictosidine synthase from *Catharanthus roseus*. *Nucleic Acids Res.*, **18**, 4939.

Meier, B. (2003). Herbal medicinal products of St. John's wort: manufacturing and quality control. In Ernst, E. (ed.) *Hypericum: the genus Hypericum (Series: Medicinal and Aromatic Plants - Industrial Profiles)*. Taylor and Francis, London, UK, pp. 106–136.

Michalska K., Fernandes H., Sikorski M., and Jaskolski M. (2010). Crystal structure of Hyp-1, a St. John's wort protein implicated in the biosynthesis of hypericin. *J. Struct. Biol.,* **169**, 161-171.

Middel, O., Woerdenbag, H. J., Van Uden, W., Van Oeveren, A., Jansen, J. F. G. A., Feringa, B. L., Konings, A. W. T., Pras, N., and Kellogg, R. M. (1995). Synthesis and cytotoxicity of novel lignans. *J. Med. Chem.*, **38**, 2112–2117.

Mittermeier, R. A., Myers, N., Gil, P. R., and Mittermeier, C. G. (1999). *Hotspots: Earth's biologically richest and most endangered ecoregions*. CEMEX Conservation International, Washington, DC.

Moertel, C. G., Schutt, A. J., Reitemeier, R. J., and Hahn, R. G. (1972). Phase II study of camptothecin (NSC-100880) in treatment of advanced gastrointestinal cancer. *Cancer Chemother. Rep.*, **56**, 95.

Mohagheghzadeh, A., Schmidt, T. J., and Alfermann, A. W. (2002). Arylnaphthalene lignans from *in vitro* cultures of *Linum austriacum*. *J. Nat. Prod.*, **65**, 69–71.

Moraleda, G., Wu, T. T., Jilbert, A. R., Aldrich, C. E., Condreay, L. D., Larsen, S. H., Tang, J. C., Colacino, J. M., and Mason, W. S. (1993). Inhibition of duck hepatitis B virus replication by hypericin. *Antiviral Res.*, **20**, 235–247.

Muntendam, R., Melillo, E., Ryden, A., and Kayser, O. (2009). Perspectives and limits of engineering the isoprenoid metabolism in heterologous hosts. *Appl. Microbiol. Biotechnol.*, **84**, 1003–1019.

Muranaka, T., Miyata, M., Ito, K., and Tachibana, S. (1998). Production of podophyllotoxin in *Juniperus chinensis* callus cultures treated with oligosaccharides and a biogenetic precursor. *Phytochemistry*, **49**, 491–496.

Nahrstedt, A. and Butterweck, V. (1997). Biologically active and other chemical constituents of the herb of *Hypericum perforatum* L. *Pharmacopsychiatry*, **30**, 129–134.

Namdeo, A. G., Sharma, A., and Mahadik, K. R. (2008). Some observations on *Nothapodytes foetida*: an overview. *Pharmacogn. Rev.*, **2**, 110–115.

Nanjundaswamy, N., Satish, S., Rai, K. M. L., Shashikanth, S., and Raveesha, K. A. (2007). Antibacterial activity of synthetic precursors of podophyllotoxin. *Int. J. Biomed. Sci.*, **3**, 113–116.

Navarro, E., Alonso, S. J., Trujillo, J. M., Jorge, E., and Pérez, C. (2001). General behavior, toxicity, and cytotoxic activity of elenoside, a lignan from *Justicia hyssopifolia*. *J. Nat. Prod.*, **64**, 134–135.

Needleman, S. B. and Wunsch, C. D. (1970). A general method applicable to the search for similarities in the amino acid sequence of two proteins. *J. Mol. Biol.*, **48**, 443–453.

Noé, W., Mollenschott, C., and Berlin, J. (1984). Tryptophan decarboxylase from *Catharanthus roseus* cell suspension cultures: purification, molecular and kinetic data of the homogenous protein. *Plant Mol. Biol.*, **3**, 281–288.

O'Connor, S. E. and Maresh, J. J. (2005). Chemistry and biology of monoterpene indole alkaloid biosynthesis. *Nat. Prod. Rep.*, **23**, 532–547.

O'Leary, J. and Muggia, F. M. (1998). Camptothecins: a review of their development and schedules of administration. *Eur. J. Cancer*, **34**, 1500–1508.

Oberlies, N. H. and Kroll, D. J. (2004). Camptothecin and Taxol: historic achievements in natural product research. *J. Nat. Prod.*, **67**, 129–135.

Onelli, E., Rivetta, A., Giorgi, A., Bignami, M., Cocucci, M., and Patrignani, G. (2002). Ultrastructural studies on the developing secretory nodules of *Hypericum perforatum*. *Flora*, **197**, 92–102.

Pantazis, P., Han, Z., Chatterjee, D., and Wyche, J. (1999). Water-insoluble camptothecin analogues as potential antiviral drugs. *J. Biomed. Sci.*, **6**, 1–7.

Park, J., English, D. S., Wannermuehler, Y., Carpenter, S., and Petrich, J. W. (1998). The role of oxygen in the antiviral activity of hypericin and hypocrellin. *Photochem. Photobiol.*, **68**, 593–597.

Partida-Martinez, L. P. and Hertweck, C. (2005). Pathogenic fungus harbours endosymbiotic bacteria for toxin production. *Nature*, **437**, 884–888.

Petcher, T. J., Weber, H. P., Kuhn, M., and von Wartburg, A. (1973). Crystal structure and absolute configuration of 2'-bromopodophyllotoxin-0.5 ethyl acetate. *J. Chem. Soc.*, **Perkin Trans. 2**, 288–292.

Petersen, M. and Alfermann, A. W. (2001). The production of cytotoxic lignans by plant cell cultures. *Appl. Microbiol. Biotechnol.*, **55**, 135–142.

Pirozynski, K. A. and Hawksworth, D. L. (1988). *Coevolution of fungi with plants and animals*. Academic Press, London.

Podwyssotzki, V. (1881). The active constituent of podophyllin. *Pharm. J. Trans.*, **12**, 217–218.

Podwyssotzki, V. (1882). On the active constituents of podophyllin. *Am. J. Pharm.*, **12**, 102–115.

Podwyssotzki, V. (1884). Pharmakologische Studien über *Podophyllum peltatum*. *Naunyn. Schmied Arch. Exp. Path. Phar.*, **13**, 29–52.

Pommier, Y. (2006). Topoisomerase I inhibitors: camptothecins and beyond. *Nat. Rev. Cancer*, **6**, 789–802.

Pommier, Y. (2009). DNA topoisomerase I inhibitors: chemistry, biology, and interfacial inhibition. *Chem. Rev.*, **109**, 2894–2902.

Pommier, Y., Kohlhagen, G., Kohn, K. W., Leteurtre, F., Wani, M. C., and Wall, M. E. (1995).

Interaction of an alkylating camptothecin derivative with a DNA base at topoisomerase I-DNA cleavage sites. *Proc. Natl. Acad. Sci. U. S. A.*, **92**, 8861–8865.

Potmesil, M. and Pinedo, H. M. (1995). *Camptothecins: new anticancer agents*. CRC Press: Boca Raton.

Preston, T. (1992). The measurement of stable isotope natural abundance variation. *Plant Cell Environ.*, **15**, 1091–1097.

Priel, E., Showalter, S. D., and G, B. D. (1991). Inhibition of human immunodeficiency virus (HIV-1) replication *in vitro* by noncytotoxic doses of camptothecin, a topoisomerase I inhibitor. *AIDS Res. Hum. Retro.*, **7**, 65–72.

Prince, A. M., Pascual, D., Meruelo, D., Liebes, L., Mazur, Y., Dubovi, E., Mandel, M., and Lavie, G. (2000). Strategies for evaluation of enveloped virus inactivation in red cell concentrates using hypericin. *Photochem. Photobiol.*, **71**, 188–195.

Puri, S. C., Nazir, A., Chawla, R., Arora, R., Riyaz-ul Hasan, S., Amna, T., Ahmed, B., Verma, V., Singh, S., Sagar, R., Sharma, A., Kumar, R., Sharma, R. K., and Qazi, G. N. (2006). The endophytic fungus *Trametes hirsuta* as a novel alternative source of podophyllotoxin and related aryl tetralin lignans. *J. Biotechnol.*, **122**, 494–510.

Puri, S. C., Verma, V., Amna, T., Qazi, G. N., and Spiteller, M. (2005). An endophytic fungus from *Nothapodytes foetida* that produces camptothecin. *J. Nat. Prod.*, **68**, 1717–1719.

Radulovic, N., Stankov-Jovanovic, V., Stojanovic, G., Smelcerovic, A., Spiteller, M., and Asakawa, Y. (2007). Screening of *in vitro* antimicrobial and antioxidant activity of nine *Hypericum* species from the Balkans. *Food Chem.*, **103**, 15–21.

Raffa, R. B. (1998). Screen of receptor and uptake-site activity of hypericin component of St. John's wort reveals sigma receptor binding. *Life Sci.*, **62**, 265–270.

Rai, L. K., Prasad, P., and Sharma, E. (2000). Conservation threats to some important medicinal plants of the Sikkim Himalaya. *Biol. Cons.*, **93**, 27–33.

Rajasekhar, D., Subbaraju, G. V., Ravikumar, K., and Chandramohan, K. (1998). *Justicia* lignans V. Three new β-apolignans from *Justicia neesii* Ramamoorthy. *Tetrahedron*, **54**, 13227–13236.

Ramesha, B. T., Amna, T., Ravikanth, G., Gunaga, R. P., Vasudeva, R., Ganeshaiah, K. N., Shaanker, R. U., Khajuria, R. K., Puri, S. C., and Qazi, G. N. (2008). Prospecting for camptothecines from *Nothapodytes nimmoniana* in the Western Ghats, south India: identification of high-yielding sources of camptothecin and new families of camptothecines. *J. Chromatogr. Sci.*, **46**, 362–368.

Rasheed, Z. A. and Rubin, E. H. (2003). Mechanisms of resistance to topoisomerase I-targeting drugs. *Oncogene*, **22**, 7296–7304.

Raskin, I., Ribnicky, D. M., Komarnytsky, S., Ilic, N., Poulev, A., Borisjuk, N., Brinker, A., Moreno, D. A., Ripoll, C., Yakoby, N., O'Neal, J. M., Cornwell, T., Pastor, I., and B, F. (2002). Plants and human health in the twenty-first century. *Trends Biotechnol.*, **20**, 522–531.

Razinkov, S. P., Yerofeyeva, L. N., Khovrina, M. P., and Lazarev, A. I. (1989). Validation of the use of

Hypericum perforatum medicamentous form with a prolonged action to treat patients with maxillary sinusitis. *Zh. Ushn. Nos. Gorl. Bolezn.*, **49**, 43–46.

Redinbo, M. R., Stewart, L., Kuhn, P., Champoux, J. J., and Hol, W. G. (1998). Crystal structures of human topoisomerase I in covalent and noncovalent complexes with DNA. *Science*, **279**, 1504–1513.

Rehman, S., Shawl, A. S., Kour, A., Andrabi, R., Sudan, P., Sultan, P., Verma, V., and Qazi, G. N. (2008). An endophytic *Neurospora sp*. from *Nothapodytes foetida* producing camptothecin. *Appl. Biochem. Microbiol.*, **44**, 203–209.

Robson, N. K. B. (1977). Studies in the genus *Hypericum* L. (Guttiferae) 1. Infrageneric classification. *Bull. Br. Mus. Nat. Hist. (Botany)*, **5**, 293–355.

Robson, N. K. B. (1981). Studies in the genus *Hypericum* L. (Guttiferae). 2. Characters of the genus. *Bull. Br. Mus. Nat. Hist. (Botany)*, **8**, 55–226.

Robson, N. K. B. and Strid, A. (1986). *Hypericum* L. In Strid, A. (ed.) *Mountain flora of Greece*, vol. 1. Cambrige University Press, NY, pp. 594–608.

Rodriguez, R. J., White, J. F. J., Arnold, A. E., and Redman, R. S. (2009). Fungal endophytes: diversity and functional roles. *New Phytol.*, **182**, 314–330.

Rodriguez-Concepcion, M. and Boronat, A. (2002). Elucidation of methyl-erythritol phosphate pathway for isoprenoid biosynthesis in bacteria and plastids. A metabolic milestone achieved through genomics. *Plant Physiol.*, **130**, 1079–1089.

Roessner, C. A., Devagupta, R., Hasan, M., Williams, H. J., and Scott, A. I. (1992). Purification of an indole biosynthetic enzyme, strictosidine synthase, from a recombinant strain of *Escherichia coli*. *Protein Expression Purif.*, **3**, 295–300.

Rohmer, M. (1999). A mevalonate-independent route to isopentenyl diphosphate. In Cane, D. E. (ed.) *Comprehensive natural product chemistry*, vol. 2. Elsevier Science Ltd., Amsterdam, pp. 45–67.

Rothenberg, M. L. (1997). Topoisomerase I inhibitors: review and update. *Ann. Oncol.*, **8**, 837–855.

Saito, K., Sudo, H., Yamazaki, M., Koseki-Nakamura, M., Kitajima, M., Takayama, H., and Aimi, N. (2001). Feasible production of camptothecin by hairy root culture of *Ophiorrhiza pumila*. *Plant Cell Rep.*, **20**, 267–271.

Sali, A. and Blundell, T. L. (1993). Comparative modeling by satisfaction of spatial restraints. *J. Mol. Biol.*, **234**, 779–815.

Samson, R. A., Hong, S., Peterson, S. W., Frisvad, J. C., and Varga, J. (2007). Polyphasic taxonomy of *Aspergillus* section *Fumigati* and its teleomorph *Neosartorya*. *Stud. Mycol.*, **59**, 147–203.

San Feliciano, A., Del Corral, J. M. M., Gordaliza, M., and Castro, M. A. (1989a). Acetylated lignans from *Juniperus sabinai*. *Phytochemistry*, **28**, 659–660.

San Feliciano, A., Medarde, M., Lopez, J. L., Puebla, P., Del Corral, J. M. M., and Barrero, A. F. (1989b). Lignans from *Juniperus thurifera*. *Phytochemistry*, **28**, 2863–2866.

Sánchez, S. (2005). Ecology and industrial microbiology. Microbial diversity - the bright and promising future of microbial manufacturing. *Curr. Opin. Microbiol.*, **8**, 229–233.

Sankar-Thomas, Y. D. (2010). *In vitro culture of Camptotheca acuminata (Decaisne) in Temporary Immersion System (TIS): growth, development and production of secondary metabolites*. Phd thesis, Universität Hamburg, Germany.

Sawada, S., Yokokura, T., and Miyasaka, T. (1995). Synthesis and antitumor activity of A-ring or E-lactone modified water-soluble prodrugs of 20(S)-camptothecin, including development of irinotecan hydrochloride trihydrate (CPT-11). *Curr. Pharm. Des.*, **1**, 113–132.

Sawada, S., Yokokura, T., and Miyasaka, T. (1996). Synthesis of CPT-11 (irinotecan hydrochloride trihydrate). *Ann. NY. Acad. Sci.*, **803**, 13–28.

Schardl, C. L., Leuchtmann, A., and Spiering, M. J. (2004). Symbioses of grasses with seedborne fungal endophytes. *Ann. Rev. Plant Biol.*, **55**, 315–340.

Schilcher, H. (1997). *Phytotherapy in paediatrics - handbook for physicians and pharmacists*. Medpharm Scientific Publishers, Berlin, Germany.

Sconocchia, S. (1983). Scribonius largus compositions. In Hansen, G. C. (ed.) *Bibliotheca Scriptorum Graecorum et Romanorum Teubneriana (B.G. Teubner)*. Verlagsgesellschaft, Leipzig, Germany, pp. 76–77.

Sheriha, G. M. and Rapoport, H. (1976). Biosynthesis of *Camptotheca acuminata* alkaloids. *Phytochemistry*, **15**, 505–508.

Shweta, S., Zühlke, S., Ramesha, B. T., Priti, V., Kumar, P. M., Ravikanth, G., Spiteller, M., Vasudeva, R., and Shaanker, R. U. (2010). Endophytic fungal strains of *Fusarium solani*, from *Apodytes dimidiata* E. Mey. ex Arn (Icacinaceae) produce camptothecin, 10-hydroxycamptothecin and 9-methoxycamptothecin. *Phytochemistry*, **71**, 117–122.

Sirikantaramas, S., Sudo, H., Asano, T., Yamazaki, M., and Saito, K. (2007). Transport of camptothecin in hairy roots of *Ophiorrhiza pumila*. *Phytochemistry*, **68**, 2881–2886.

Sirikantaramas, S., Yamazaki, M., and Saito, K. (2008). Mutations in topoisomerase I as a self-resistance mechanism coevolved with the production of the anticancer alkaloid camptothecin in plants. *Proc. Natl. Acad. Sci. U. S. A.*, **105**, 6782–6786.

Sirikantaramas, S., Yamazaki, M., and Saito, K. (2009). A survival strategy: the coevolution of the camptothecin biosynthetic pathway and self-resistance mechanism. *Phytochemistry*, **70**, 1894–1898.

Sirvent, T. and Gibson, D. (2002). Induction of hypericins and hyperforin in *Hypericum perforatum* L. in response to biotic and chemical elicitors. *Physiol. Mol. Plant Pathol.*, **60**, 311–320.

Sirvent, T., Stuart, B., and Gibson, D. M. (2003). Induction of hypericins and hyperforins in *Hypericum perforatum* in response to damage by herbivores. *J. Chem. Ecol.*, **29**, 2667–2681.

Slichenmyer, W. J., Rowinsky, E. K., Donehower, R. C., and Kaufmann, S. H. (1993). The current status of camptothecin analogues as antitumor agents. *J. Natl. Cancer. Inst.*, **85**, 271–291.

Smelcerovic, A. and Spiteller, M. (2006). Phytochemical analysis of nine *Hypericum* L. species from Serbia and F. Y. R. Macedonia. *Pharmazie*, **61**, 251–252.

Smelcerovic, A., Lepojevic, Z., and Djordjevic, S. (2004). Sub- and supercritical CO_2-extraction of *Hypericum perforatum* L. *Chem. Eng. Technol.*, **27**, 1327–1329.

Smelcerovic, A., Spiteller, M., and Zühlke, S. (2006a). Comparison of methods for the exhaustive extraction of hypericins, flavonoids, and hyperforin from *Hypericum perforatum* L. *J. Agric. Food Chem.*, **54**, 2750–2753.

Smelcerovic, A., Spiteller, M., Ligon, A. P., Smelcerovic, Z., and Raabe, N. (2007). Essential oil composition of *Hypericum* L. species from southeastern Serbia and their chemotaxonomy. *Biochem. Syst. Ecol.*, **35**, 99–113.

Smelcerovic, A., Verma, V., Spiteller, M., Ahmad, S. M., Puri, S. C., and Qazi, G. N. (2006b). Phytochemical analysis and genetic characterization of six *Hypericum* species from Serbia. *Phytochemistry*, **67**, 171–177.

Smelcerovic, A., Zühlke, S., Spiteller, M., Raabe, N., and Özen, T. (2008). Phenolic constituents of 17 *Hypericum* species from Turkey. *Biochem. Syst. Ecol.*, **36**, 316–319.

Smith, T. F. and Waterman, M. S. (1981). Identification of common molecular subsequences. *J. Mol. Biol.*, **147**, 195–197.

Spiteller, M., Özen, T., Smelcerovic, A., Zühlke, S., and Mimica-Dukic, N. (2008). Phenolic constituents and *in vitro* antioxidant activity of the flowers of *Hypericum venustum*. *Fitoterapia*, **79**, 191–193.

Stähblin, H. (1973). Activity of a new glycosidic lignan derivative (VP 16-213) related to podophyllotoxin in experimental tumors. *Eur. J. Cancer*, **9**, 215–221.

Stähelin, H. F. and von Wartburg, A. (1991). The chemical and biological route from podophyllotoxin glucoside to etoposide: Ninth Cain Memorial Award Lecture. *Cancer Res.*, **51**, 5–15.

Staker, B. L., Feese, M. D., Cushman, M., Pommier, Y., Zembower, D., Stewart, L., and Burgin, A. B. (2005). Structures of three classes of anticancer agents bound to the human topoisomerase I-DNA covalent complex. *J. Med. Chem.*, **48**, 2336–2345.

Staniek, A., Woerdenbag, H. J., and Kayser, O. (2008). Endophytes: exploiting biodiversity for the improvement of natural product-based drug discovery. *J. Plant Interact.*, **3**, 75–93.

Staniek, A., Woerdenbag, H. J., and Kayser, O. (2009). *Taxomyces andreanae*: a presumed paclitaxel producer demystified?. *Planta Med.*, **75**, 1561–1566.

Staunton, J. and Weissman, K. J. (2001). Polyketide biosynthesis: a millennium review. *Nat. Prod. Rep.*, **18**, 380–416.

Stehlin, J. S., Giovanella, B. C., Natelson, E. A., De Ipolyi, P. D., Coil, D., Davis, B., Wolk, D., Wallace, P., and Trojacek, A. (1999). A study of 9-nitrocamptothecin (RFS-2000) in patients with advanced pancreatic cancer. *Int. J. Oncol.*, **14**, 821–831.

Stevenson, N. R. and Lenard, J. (1993). Antiretroviral activities of hypericin and Rose Bengal:

photodynamic effects on friend leukemia virus infection of mice. *Antiviral Res.*, **21**, 119–127.

Stierle, A., Strobel, G. A., and Stierle, D. (1993). Taxol and taxane production by *Taxomyces andreanae*, an endophytic fungus of Pacific yew. *Science*, **260**, 214–216.

Stöckigt, J. and Ruppert, M. (1999). Strictosidine - the biosynthetic key to monoterpenoid indole alkaloids. In Barton, S. D., Nakanishi, K., Meth-Cohn, O. (eds.) *Comprehensive natural products chemistry*, vol. 4. Pergamon, Oxford, pp. 109–138.

Stöckigt, J. and Zenk, M. H. (1977). Strictosidine (isovincoside): the key intermediate in the biosynthesis of monoterpenoid indole alkaloids. *J. Chem. Soc., Chem. Commun.*, **-**, 646–648.

Stone, J. K., Bacon, C. W., and White, J. F. (2000). *An overview of endophytic microbes: endophytism defined*. Marcel Dekker Inc., New York.

Strobel, G. A. and Daisy, B. (2003). Bioprospecting for microbial endophytes and their natural products. *Microbiol. Mol. Biol. Rev.*, **67**, 491–502.

Strobel, G. A. and Long, D. M. (1998). Endophytic microbes embody pharmaceutical potential. *ASM News*, **64**, 263–268.

Strobel, G. A., Daisy, B., Castillo, U., and Harper, J. (2004). Natural products from endophytic microorganisms. *J. Nat. Prod.*, **67**, 257–268.

Strobel, G. A., Kluck, K., Hess, W. M., Sears, J., and Erza, D Vargas, P. N. (2007). *Muscodor albus* E-6, an endophyte of *Guazuma ulmifolia* making volatile antibiotics: isolation, characterization and experimental establishment in the host plant. *Microbiol. - SGM*, **153**, 2613–2620.

Sudo, K., Konno, K., Shigeta, S., and Yokota, T. (1998). Inhibitory effects of podophyllotoxin derivatives on *Herpes simplex* virus replication. *Antivir. Chem. Chemother.*, **9**, 263–267.

Sukul, P., Lamshöft, M., Kusari, S., Zühlke, S., and Spiteller, M. (2009). Metabolism and excretion kinetics of ^{14}C-labeled and non-labeled difloxacin in pigs after oral administration, and antimicrobial activity of manure containing difloxacin and its metabolites. *Environ. Res.*, **109**, 225–231.

Sung, C. K., Kimura, T., But, P. P. H., and Guo, J. X. (1998). *International Collation of Traditional and Folk Medicine: Northeast Asia, Part III. A project of UNESCO*, vol. 3. World Scientific Publishing Co. Pte. Ltd., Singapore.

Suryanarayanana, T. S., Thirunavukkarasub, N., Govindarajulub, M. B., Sassec, F., Jansend, R., and Murali, T. S. (2009). Fungal endophytes and bioprospecting. *Fungal Biol. Rev.*, **23**, 9–19.

Tafur, S., Nelson, J. D., DeLong, D. C., and Svoboda, G. H. (1976). Antiviral components of *Ophiorrhiza mungos* isolation of camptothecin and 10-methoxycamptothecin. *Lloydia*, **39**, 261–262.

Takeuchi, S., Dobashi, K., Fujimoto, S., Tanaka, K., Suzuki, M., Terashima, Y., Hasumi, K., Akiya, K., Negishi, Y., and Tayama, T. (1991). A late phase II study of CPT-11 on uterine cervical cancer and ovarian cancer. Research groups of CPT-11 in gynecologic cancers. *Gan To Kagaku Ryoho*, **18**, 1681–1689.

Tammaro, F. and Xepapadakis, G. (1986). Plants used in phytotherapy, cosmetics and dyeing in the

Pramanda district (Epirus, north-west Greece). *J. Ethnopharmacol.*, **16**, 167–174.

Tang, J., Colacino, J. M., Larsen, S. H., and Spitzer, W. (1990). Virucidal activity of hypericin against enveloped and nonenveloped DNA and RNA viruses. *Antiviral Res.*, **13**, 313–325.

Tanizawa, A., Fujimori, A., Fujimori, Y., and Pommier, Y. (1994). Comparison of topoisomerase I inhibition, DNA damage, and cytotoxicity of camptothecin derivatives presently in clinical trials. *J. Natl. Cancer Inst.*, **86**, 836–842.

Tekelova, D., Repcak, M., Zemkova, E., and Toth, J. (2000). Quantitative changes of dianthrones, hyperforin and flavonoids content in the flower ontogenesis of *Hypericum perforatum*. *Planta Med.*, **66**, 778–780.

Thomson, R. H. (1957). *Naturally occurring quinones*. Butterworths Scientific Publications, London, UK.
Tobin, G. J., Ennis, W. H., Clanton, D. J., and Gonda, M. A. (1996). Inhibition of bovine immunodeficiency virus by anti-HIV-1 compounds in a cell culture based assay. *Antiviral Res.*, **33**, 21–31.

Torck, M. and Pinkas, M. (1996). Camptothecin and derivatives: a new class of antitumor agents. *J. Pharm. Belg.*, **51**, 200–207.

Treimer, J. F., Zenk, M. H. (1979). Purification and properties of strictosidine synthase, the key enzyme in indole alkaloid formation. *Eur. J. Biochem.,* **101**, 225-233.

Tsurutani, J., Nitta, T., Hirashima, T., Komiya, T., Uejima, H., Tada, H., Syunichi, N., Tohda, A., Fukuoka, M., and Nakagawa, K. (2002). Point mutations in the topoisomerase I gene in patients with non-small cell lung cancer treated with irinotecan. *Lung Cancer*, **35**, 299–304.

Uesato, S., Kanomi, S., Iida, A., Inouye, H., and Zenk, M. H. (1986). Mechanism for iridane skeleton formation in the biosynthesis of secologanin and indole alkaloids in *Lonicera tatarica*, *Catharanthus roseus* and suspension cultures of *Rauwolfia serpentina*. *Phytochemistry*, **25**, 839–842.

Uma Shaanker, R., Ramesha, B. T., Ravikanth, G., Gunaga, R. P., Vasudeva, R., and Ganeshaiah, K. N. (2008). Chemical profiling of *Nothapodytes nimmoniana* for camptothecin, an important anticancer alkaloid: towards the development of a sustainable production system. In Ramawat, K. G., Merillon, J. M. (eds.) *Bioactive molecules and medicinal plants*. Springer-Verlag, Berlin and Heidelberg, pp. 197–213.

Umek, A., Kreft, S., Karting, T., and Heydel, B. (1999). Quantitative phytochemical analyses of six *Hypericum* species growing in Slovenia. *Planta Med.*, **65**, 388–390.

Urasaki, Y., Laco, G., Takebayashi, Y., Bailly, C., Kohlhagen, G., and Pommier, Y. (2001). Use of camptothecin-resistant mammalian cell lines to evaluate the role of topoisomerase I in the antiproliferative activity of the indolocarbazole, NB-506, and its topoisomerase I binding site. *Cancer Res.*, **61**, 504–508.

Utsumi, T., Okuma, M., Kanno, T., Yasuda, T., Kobuchi, H., Horton, A. A., and Utsumi, K. (1995). Light-dependent inhibition of protein kinase C and superoxide generation of neutrophils by hypericin, an antiretroviral agent. *Arch. Biochem. Biophys.*, **316**, 493–497.

van der Merwe, M. and Bjornsti, M. A. (2008). Mutation of Gly^{721} alters DNA topoisomerase I active site

architecture and sensitivity to camptothecin. *J. Biol. Chem.*, **283**, 3305–3315.

Van Uden, W., Bos, J. A., Boeke, G. M., Woerdenbag, H. J., and Pras, N. (1997). The large scale isolation of deoxypodophyllotoxin from rhizomes of *Anthriscus sylvestris* followed by its bioconversion into 5-methoxypodophyllotoxin β-D-glucoside by cell cultures of *Linum flavum*. *J. Nat. Prod.*, **60**, 401–403.

Van Uden, W., Bouma, A. S., Bracht Waker, J. F., Middel, O., Wichers, H. J., De Waard, P., Woerdenbag, H. J., Kellogg, R. M., and Pras, N. (1995). The production of podophyllotoxin and its 5-methoxy derivative through bioconversion of cyclodextrin-complexed desoxypodophyllotoxin by plant cell cultures. *Plant Cell Tiss. Org. Cult.*, **42**, 73–79.

Verma, V., Smelcerovic, A., Zühlke, S., Hussain, M. A., Ahmad, S. M., Ziebach, T., Qazi, G. N., and Spiteller, M. (2008). Phenolic constituents and genetic profile of *Hypericum perforatum* L. from India. *Biochem. Syst. Ecol.*, **36**, 201–206.

Walker, T. S., Hars, B. P., and Jorge, M. V. (2002). Jasmonic acid-induced hypericin producion in cell suspension cultures of *Hypericum perforatum* L. (St. John's wort). *Phytochemistry*, **60**, 289–293.

Wall, M. E. (1993). Camptothecin and Taxol. In Lednicer, D. (ed.) *Chronicles of drug discovery*, vol. 3. American Chemical Society, Washington, D.C., pp. 327–348.

Wall, M. E., Wani, M. C., Cook, C. E., Palmer, K. H., Mcphail, A. T., and Sim, G. A. (1966). Plant antitumor agents. I. The isolation and structure of camptothecin, a novel alkaloidal leukemia and tumor inhibitor from *Camptotheca acuminata*. *J. Am. Chem. Soc.*, **88**, 3888–3890.

Wang, J. C. (1996). DNA topoisomerase. *Annu. Rev. Biochem.*, **65**, 635–692.

Watase, I., Sudo, H., Yamazaki, M., and Saito, K. (2004). Regeneration of transformed *Ophiorrhiza pumila* plants producing camptothecin. *Plant Biotechnol.*, **21**, 337–342.

White, T. J., Bruns, T., Lee, S., and Taylor, J. W. (1990). Amplification and direct sequencing of fungal ribosomal RNA genes for phylogenetics. In Innis, M. A., Gelfand, D. H., Sninsky, J. J., White, T. J. (eds.) *PCR protocols: a guide to methods and applications*. Academic Press, San Diego, CA, pp. 315–322.

Wichtl, M. (1986). *Hypericum perforatum* L. Das Johanniskraut. *Zeitschrift Phytother.*, **3**, 87–90.

Wickramaratne, D. B. M., Mar, W., Chai, H., Castillo, J. J., Farnsworth, N. R., Soejarto, D. D., Cordell, G. A., Pezzuto, J. M., and Kinghorn, A. D. (1995). Cytotoxic constituents of *Bursera permollis*. *Planta Med.*, **61**, 80–81.

Wikler, M. A. (2006). *Performance Standards for Antimicrobial Disk Susceptibility Tests; Approved Standard - Ninth Edition (M2-A9)*. CLSI (Clinical and Laboratory Standards Institute), Wayne, PA.

Wink, M. (2003). Evolution of secondary metabolites from an ecological and molecular phylogenetic perspective. *Phytochemistry*, **64**, 3–19.

Witterland, A. H., Koks, C. H., and Beijnen, J. H. (1996). Etoposide phosphate, the water soluble prodrug of etoposide. *Pharm. World Sci.*, **18**, 163–170.

Wong, S. K., Tsui, S. K., Kwan, S. Y., L, S. X., and C, L. R. (2000). Identification and characterization of *Podophyllum emodi* by API-LC/MS/MS. *J. Mass Spectrom.*, **35**, 1246–1251.

Woo, M. H., Vance, J. R., Marcos, A. R., Bailly, C., and Bjornsti, M. A. (2002). Active site mutations in DNA topoisomerase I distinguish the cytotoxic activities of camptothecin and the indolocarbazole, rebeccamycin. *J. Biol. Chem.*, **277**, 3813–3822.

Wu, T. S., Leu, Y. L., Hsu, H. C., Ou, L. F., Chen, C. C., Chen, C. F., Ou, J. C., and Wu, Y. C. (1995). Constituents and cytotoxic principles of *Nothapodytes foetida*. *Phytochemistry*, **39**, 383–385.

Xu, Y. and Lu, C. (2005). Raman spectroscopic study on structure of human immunodeficiency virus (HIV) and hypericin-induced photosensitive damage of HIV. *Sci. China C Life Sci.*, **48**, 117–132.

Yamamoto, M., Katano, N., Ooi, A., and Inoue, K. (2000). Secologanin synthase which catalyzes the oxidative cleavage of loganin into secologanin is a cytochrome P450. *Phytochemistry*, **53**, 7–12.

Yamazaki, Y., Kitajima, M., Arita, M., Takayama, H., Sudo, H., Yamazaki, M., Aimi, N., and Saito, K. (2004). Biosynthesis of camptothecin. *In silico* and *in vivo* tracer study from [1-^{13}C]glucose. *Plant Physiol.*, **134**, 161–170.

Yamazaki, Y., Urano, A., Sudo, H., Kitajima, M., Takayama, H., Yamazaki, M., Aimi, N., and Saito, K. (2003). Metabolite profiling of alkaloids and strictosidine synthase activity in camptothecin producing plants. *Phytochemistry*, **62**, 461–470.

Yan, X. F., Wang, Y., Yu, T., Zhang, Y. H., and Dai, S. J. (2003). Variation in camptothecin content in *Camptotheca acuminata* leaves. *Bot. Bull. Acad. Sin.*, **44**, 99–105.

Yazaki, K. and Okada, T. (1994). *Hypericum erectum* Thunb. (St. John's wort): *in vitro* culture and the production of procyanidins. In Bajaj, Y. P. S. (ed.) *Biotechnology in Agriculture and Forestry. Medicinal and Aromatic Plants VI*, vol. 26. Springer-Verlag, Berlin, pp. 167–178.

Yu, P., Wang, L., and Chen, Z. (1991). A new podophyllotoxin-type lignan from *Dysosma versipellis* var. *tomentosa*. *J. Nat. Prod.*, **54**, 1422–1424.

Zaichikova, S. G., Grinkevich, N. I., and Barabanov, E. I. (1985). Healing properties and determination of the upper parameters of toxicity of *Hypericum* herb. *Farmatsiya*, **34**, 62–64.

Zhang, H. W., Song, Y. C., and Tan, R. X. (2006). Biology and chemistry of endophytes. *Nat. Prod. Rep.*, **23**, 753–771.

Zhao, H. and Chen, W. (2008). Chemical biotechnology: microbial solutions to global change. *Curr. Opin. Biotechnol.*, **19**, 541–543.

Zhou, B. N., Hoch, J. M., Johnson, R. K., Mattern, M. R., Eng, W. K., Ma, J., Hecht, S. M., Newman, D. J., and Kingston, D. G. I. (2000). Use of compare analysis to discover new natural product drugs: isolation of camptothecin and 9-methoxycamptothecin from a new source. *J. Nat. Prod.*, **63**, 1273–1276.

Zobayed, S. M. A., Afreen, F., Goto, E., and Kozai, T. (2006). Plant-environment interactions: accumulation of hypericin in dark glands of *Hypericum perforatum*. *Ann. Bot.*, **98**, 793–804.

APPENDIX A

Table T1. Compositions of different basic liquid media, liquid media supplemented with different carbon and nitrogen sources, and with trace minerals **(A1-A23)**, monotonic carbon-only media **(B1-B5)**, monotonic nitrogen-only media **(C1-C4)**, basic liquid media supplemented with some putative precursors without and with additional supplements **(D1-D4)**, and basic liquid media spiked with various forms of host (*C. acuminata*) intact tissues and tissue aqueous extracts **(E1-E7)** used in attempting to reverse the observed phenomena of attenuation of CPT production by the cultured endophytic *F. solani* (INFU/Ca/KF/3/VII) by the classical approach of optimization. The observed attenuation could not be reversed or stopped under any condition. All the host tissues were surface-sterilized by the established method (refer to **Materials and Methods**) before using. *****The basic media names have been used based on their composition. ******The pH values were adjusted and/or noted down before autoclaving the media.

Media Code	Media Name*	pH**	Media Composition (g/L)
A1	POTATO DEXTROSE BROTH	5.6	Potato Starch: 4 g Dextrose: 20 g
A2	POTATO DEXTROSE BROTH Modified/Supplemented	5.6	Potato Starch: 4 g Dextrose: 20 g Magnesium sulfate: 0.5 g Potassium dihydrogen orthophosphate: 1.0 g
A3	SABOURAUD DEXTROSE BROTH	5.6	Enzymatic digest of casein: 10 g Dextrose: 40 g
A4	SABOURAUD DEXTROSE BROTH Modified/Supplemented	5.6	Enzymatic digest of casein: 10 g Dextrose: 40 g Magnesium sulfate: 0.5 g Potassium dihydrogen orthophosphate: 1.0 g
A5	MALT EXTRACT BROTH	7.0	Malt extract: 20 g Glucose: 20 g Peptone: 1.0 g
A6	MALT EXTRACT BROTH Modified/Supplemented	5.4	Malt extract: 30 g Peptone: 5.0 g
A7	MALT SUCROSE BROTH	7.0	Malt extract: 20 g Sucrose: 200 g
A8	MALT SALT BROTH	7.0	Malt extract: 100 g Sodium chloride: 100 g
A9	YEAST MALT EXTRACT BROTH	7.0	Malt extract: 10 g Yeast extract: 4.0 g Magnesium sulfate: 0.5 g Potassium hydrogen phosphate: 0.5 g
A10	YEAST MALT EXTRACT DEXTROSE BROTH	7.0	Malt extract: 10 g Yeast extract: 4.0 g Dextrose: 4 g
A11	YEAST BEEF EXTRACT BROTH	7.2	Yeast extract: 1.0 g Beef extract: 1.08 g Peptone: 2.0 g Glucose: 10 g Ferrous sulfate: 0.001 g
A12	GLUCOSE YEAST BROTH	7.0	Glucose: 20 g Peptone: 5.0 g Yeast extract: 2.0 g
A13	CZAPEK DOX BROTH	7.0	Sucrose: 30 g Ferrous sulfate: 0.01 g

			Magnesium sulfate: 0.5 g Potassium chloride: 0.5 g Potassium phosphate dibasic: 1.0 g Sodium nitrate: 3.0 g
A14	CZAPEK DOX BROTH Modified/Supplemented	7.0	Dextrose: 30 g Ammonium oxalate: 3.0 g Potassium hydrogen phosphate: 1.0 g Magnesium sulfate: 0.5 g Potassium chloride: 0.5 g Ferric sulfate: 0.05 g
A15	CZAPEK DOX BROTH Modified/Supplemented	7.0	Dextrose: 30 g Urea: 3.0 g Potassium hydrogen phosphate: 1.0 g Magnesium sulfate: 0.5 g Potassium chloride: 0.5 g Ferric sulfate: 0.05 g
A16	CZAPEK DOX BROTH Modified/Supplemented	7.0	Sucrose: 30 g Urea: 3.0 g Ammonium oxalate: 3.0 g Potassium hydrogen phosphate: 1.0 g Magnesium sulfate: 0.5 g Potassium chloride: 0.5 g Ferric sulfate: 0.05 g
A17	UREA BROTH	6.8	Urea: 20 g Yeast extract: 0.1 g Dipotassium hydrogen phosphate: 9.5 g Potassium dihydrogen phosphate: 9.1 g Phenol red: 0.01 g
A18	GOOSE AND TSCHESSCH BROTH	7.0	Peptone: 2.0 g Glucose: 10 g Magnesium sulfate: 0.5 g Potassium hydrogen phosphate: 0.5 g
A19	LEONINE BROTH	7.2	Peptone: 0.625 g Maltose: 6.25 g Malt extract: 6.25 g Potassium hydrogen phosphate: 1.25 g Magnesium sulfate: 0.625 g
A20	BIANCHI BROTH	7.0	Starch: 0.2 g Glucose: 0.2 g Sucrose: 0.2 g Potassium hydrogen phosphate: 1.0 g Potassium nitrate: 1.0 g Magnesium sulfate: 0.55 g Potassium chloride: 0.5 g
A21	BRILA BROTH	7.2	Peptone: 10 g Lactose: 10 g Ox bile: 20 g Brilliant green: 0.0133 g
A22	CORN MEAL BROTH	6.0	Corn meal infusion: 2 g
A23	POTATO CARROT BROTH	5.6	Potato Starch: 4 g Boiled carrot extract: 20 g

B1	GLUCOSE BROTH	7.0	Glucose: 25 g
B2	SUCROSE BROTH	7.0	Sucrose: 25 g
B3	FRUCTOSE BROTH	7.0	Fructose: 25 g
B4	DEXTROSE BROTH	7.0	Dextrose: 25 g
B5	STARCH BROTH	7.0	Starch: 25 g
C1	MALT EXTRACT BROTH	7.0	Malt extract: 25 g
C2	YEAST EXTRACT BROTH	7.0	Yeast extract: 25 g
C3	BEEF EXTRACT BROTH	7.0	Beef extract: 25 g
C4	PEPTONE BROTH	7.0	Peptone: 25 g
D1	POTATO DEXTROSE BROTH Spiked with Tryptamine	5.6	Potato Starch: 4 g Dextrose: 20 g Tryptamine: 0.0045 g
D2	POTATO DEXTROSE BROTH Spiked with Peptone and Tryptamine	5.6	Potato Starch: 4 g Dextrose: 20 g Peptone: 10 g
D3	POTATO DEXTROSE BROTH Spiked with Indole	5.6	Potato Starch: 4 g Dextrose: 20 g Indole: 0.0035 g
D4	POTATO DEXTROSE BROTH Spiked with Peptone and Indole	5.6	Potato Starch: 4 g Dextrose: 20 g Peptone: 10 g Indole: 0.0035 g
E1	POTATO DEXTROSE BROTH Spiked with fresh *C. acuminata* leaves	5.6	Potato Starch: 4 g Dextrose: 20 g Fresh surface-sterilized *C. acuminata* leaves: 5 g; 5 cm × 5 cm dimension
E2	POTATO DEXTROSE BROTH Spiked with dry *C. acuminata* leaves	5.6	Potato Starch: 4 g Dextrose: 20 g Dry surface-sterilized *C. acuminata* leaves: 5 g; 5 cm × 5 cm dimension
E3	POTATO DEXTROSE BROTH Spiked with fresh *C. acuminata* stems	5.6	Potato Starch: 4 g Dextrose: 20 g Fresh surface-sterilized *C. acuminata* stems: 5 g; 5 cm × 2 cm dimension
E4	POTATO DEXTROSE BROTH Spiked with dry *C. acuminata* stems	5.6	Potato Starch: 4 g Dextrose: 20 g Dry surface-sterilized *C. acuminata* stems: 5 g; 5 cm × 2 cm dimension
E5	POTATO DEXTROSE BROTH Spiked with fresh *C. acuminata* leaves aqueous extract	5.6	Potato Starch: 4 g Dextrose: 20 g Fresh surface-sterilized *C. acuminata* leaves aqueous extract: 5 g
E6	POTATO DEXTROSE BROTH Spiked with fresh *C. acuminata* stems aqueous extract	5.6	Potato Starch: 4 g Dextrose: 20 g Fresh surface-sterilized *C. acuminata* stems aqueous extract: 5 g
E7	POTATO DEXTROSE BROTH Spiked with fresh *C. acuminata* leaves and stems aqueous extract	5.6	Potato Starch: 4 g Dextrose: 20 g Fresh surface-sterilized *C. acuminata* leaves + stem (1:1 *w/w*) aqueous extract: 5 g

Table T2. The various optimized PCR conditions employed for the present study.

PCR number	Reaction volume	Total volume	Annealing temperature	Number of cycles	Elongation
1	2 µL 10 µM forward primer 2 µL 10 µM reverse primer 10 µL 5x PCR buffer 5 µL 10 mM dNTPs 0.5 µL purified DNA template solution 29.3 µL ddH_2O 1 µL Firepol polymerase 0.2 µL Pfu polymerase	50 µL	57°C	40	1 min
2	2 µL 10 µM forward primer 2 µL 10 µM reverse primer 10 µL 5x PCR buffer 5 µL 10 mM dNTPs 2 µL purified DNA template solution 27.8 µL ddH_2O 1 µL Firepol polymerase 0.2 µL Pfu polymerase	50 µL	55°C	50	1 min
3	2 µL 10 µM forward primer 2 µL 10 µM reverse primer 10 µL 5x PCR buffer 5 µL 10 mM dNTPs 2 µL purified DNA template solution 27.8 µL ddH_2O 1 µL Firepol polymerase 0.2 µL Pfu polymerase	50 µL	58°C	50	1 min

Table T3. The phytochemical compositions of different aerial tissues (fresh and dried in parallel) in organic, aqueous and total (organic and aqueous) phases of the studied *Camptotheca* species. 10-OH-CPT, 10-hydroxycamptothecin; 9-MeO-CPT, 9-methoxycamptothecin; L, leaf; S, stem; d, dry; f, fresh; A, aqueous; O, organic; T, total content (organic + aqueous); n.q., less than the limit of quantitation (< LOQ).

Plant Codes	MVA Codes	10-OH-CPT (ng/mL)	CPT (ng/mL)	9-MeO-CPT (ng/mL)
Mp36/L/d/A	**1**	60	207	26
Mp36/L/d/O	**2**	76	785	193
Mp36/L/d/T	**3**	136	993	219
Mp36/L/f/A	**4**	n.q.	n.q.	n.q.
Mp36/L/f/O	**5**	864	3700	1048
Mp36/L/f/T	**6**	864	3700	1048
Mp36/S/d/A	**7**	702	3419	716
Mp36/S/d/O	**8**	284	2106	438
Mp36/S/d/T	**9**	985	5525	1153
Mp36/S/f/A	**10**	n.q.	27	n.q.
Mp36/S/f/O	**11**	507	2934	753
Mp36/S/f/T	**12**	507	2961	753
Lp4/L/d/A	**13**	n.q.	141	n.q.
Lp4/L/d/O	**14**	96	887	185
Lp4/L/d/T	**15**	96	1028	185
Lp4/L/f/A	**16**	n.q.	20	n.q.
Lp4/L/f/O	**17**	118	6046	575
Lp4/L/f/T	**18**	118	6065	575
Lp4/S/d/A	**19**	n.q.	45	n.q.
Lp4/S/d/O	**20**	n.q.	393	38
Lp4/S/d/T	**21**	n.q.	438	38
Lp4/S/f/A	**22**	n.q.	n.q.	n.q.
Lp4/S/f/O	**23**	n.q.	755	107
Lp4/S/f/T	**24**	n.q.	755	107
Bp81/L/d/A	**25**	n.q.	n.q.	n.q.
Bp81/L/d/O	**26**	243	7411	608
Bp81/L/d/T	**27**	243	7411	608
Bp81/L/f/A	**28**	n.q.	n.q.	n.q.
Bp81/L/f/O	**29**	698	7352	886
Bp81/L/f/T	**30**	698	7352	886
Bp81/S/d/A	**31**	212	986	77
Bp81/S/d/O	**32**	257	2381	250
Bp81/S/d/T	**33**	470	3367	326
Bp81/S/f/A	**34**	n.q.	22	n.q.
Bp81/S/f/O	**35**	470	6364	669
Bp81/S/f/T	**36**	470	6386	669
Bp81seed/L/d/A	**37**	n.q.	52	n.q.
Bp81seed/L/d/O	**38**	65	1308	296
Bp81seed/L/d/T	**39**	65	1360	296
Bp81seed/L/f/A	**40**	n.q.	13	n.q.
Bp81seed/L/f/O	**41**	536	7671	984

Bp81seed/L/f/T	**42**	536	7684	984
Bp81seed/S/d/A	**43**	302	1164	103
Bp81seed/S/d/O	**44**	427	3337	382
Bp81seed/S/d/T	**45**	730	4501	485
Bp81seed/S/f/A	**46**	n.q.	10	n.q.
Bp81seed/S/f/O	**47**	395	3592	320
Bp81seed/S/f/T	**48**	395	3602	320
Bay/L/d/A	**49**	222	182	n.q.
Bay/L/d/O	**50**	704	2271	584
Bay/L/d/T	**51**	926	2453	584
Bay/L/f/A	**52**	n.q.	38	n.q.
Bay/L/f/O	**53**	4537	11858	3090
Bay/L/f/T	**54**	4537	11896	3090
Bay/S/d/A	**55**	59	76	n.q.
Bay/S/d/O	**56**	560	3697	667
Bay/S/d/T	**57**	619	3772	667
Bay/S/f/A	**58**	n.q.	n.q.	n.q.
Bay/S/f/O	**59**	557	6868	1211
Bay/S/f/T	**60**	557	6868	1211
Fre/L/d/A	**61**	n.q.	28	n.q.
Fre/L/d/O	**62**	120	1827	374
Fre/L/d/T	**63**	120	1854	374
Fre/L/f/A	**64**	n.q.	n.q.	n.q.
Fre/L/f/O	**65**	159	5232	940
Fre/L/f/T	**66**	159	5232	940
Fre/S/d/A	**67**	10	83	n.q.
Fre/S/d/O	**68**	378	2751	322
Fre/S/d/T	**69**	388	2834	322
Fre/S/f/A	**70**	n.q.	n.q.	n.q.
Fre/S/f/O	**71**	86	449	86
Fre/S/f/T	**72**	86	449	86
Hal/L/d/A	**73**	n.q.	n.q.	n.q.
Hal/L/d/O	**74**	339	5417	1488
Hal/L/d/T	**75**	339	5417	1488
Hal/L/f/A	**76**	n.q.	n.q.	n.q.
Hal/L/f/O	**77**	3237	12429	5633
Hal/L/f/T	**78**	3237	12429	5633
Hal/S/d/A	**79**	41	431	93
Hal/S/d/O	**80**	707	4359	1478
Hal/S/d/T	**81**	748	4790	1570
Hal/S/f/A	**82**	n.q.	n.q.	n.q.
Hal/S/f/O	**83**	2844	13285	5570
Hal/S/f/T	**84**	2844	13285	5570
Ham/L/d/A	**85**	n.q.	n.q.	n.q.
Ham/L/d/O	**86**	330	6219	1239
Ham/L/d/T	**87**	330	6219	1239
Ham/L/f/A	**88**	n.q.	n.q.	n.q.
Ham/L/f/O	**89**	1248	10356	2195

Ham/L/f/T	**90**	1248	10356	2195
Ham/S/d/A	**91**	n.q.	382	122
Ham/S/d/O	**92**	70	1218	476
Ham/S/d/T	**93**	70	1600	598
Ham/S/f/A	**94**	n.q.	n.q.	n.q.
Ham/S/f/O	**95**	524	2118	1576
Ham/S/f/T	**96**	524	2118	1576
Mai/L/d/A	**97**	n.q.	1170	110
Mai/L/d/O	**98**	63	4432	603
Mai/L/d/T	**99**	63	5602	713
Mai/L/f/A	**100**	n.q.	134	n.q.
Mai/L/f/O	**101**	380	13887	2885
Mai/L/f/T	**102**	380	14021	2885
Mai/S/d/A	**103**	n.q.	506	49
Mai/S/d/O	**104**	151	3558	652
Mai/S/d/T	**105**	151	4063	702
Mai/S/f/A	**106**	n.q.	203	25
Mai/S/f/O	**107**	1906	10424	2534
Mai/S/f/T	**108**	1906	10627	2559
Stu/L/d/A	**109**	n.q.	n.q.	n.q.
Stu/L/d/O	**110**	196	3872	419
Stu/L/d/T	**111**	196	3872	419
Stu/L/f/A	**112**	n.q.	n.q.	n.q.
Stu/L/f/O	**113**	947	6868	970
Stu/L/f/T	**114**	947	6868	970
Stu/S/d/A	**115**	64	63	n.q.
Stu/S/d/O	**116**	1122	6603	991
Stu/S/d/T	**117**	1186	6667	991
Stu/S/f/A	**118**	n.q.	39	n.q.
Stu/S/f/O	**119**	978	4291	630
Stu/S/f/T	**120**	978	4330	630
INFU/Ca/L/d/A	**121**	n.q.	n.q.	n.q.
INFU/Ca/L/d/O	**122**	343	5528	1572
INFU/Ca/L/d/T	**123**	343	5528	1572
INFU/Ca/L/f/A	**124**	n.q.	n.q.	n.q.
INFU/Ca/L/f/O	**125**	3561	13021	5819
INFU/Ca/L/f/T	**126**	3561	13021	5819
INFU/Ca/S/d/A	**127**	56	587	118
INFU/Ca/S/d/O	**128**	867	5209	1532
INFU/Ca/S/d/T	**129**	923	5796	1650
INFU/Ca/S/f/A	**130**	n.q.	n.q.	n.q.
INFU/Ca/S/f/O	**131**	4789	14568	6755
INFU/Ca/S/f/T	**132**	4789	14568	6755
LOQ	**-**	**20.0**	**10.0**	**10.0**

Table T4. Detailed information on the templates and PCR conditions employed/elaborated in the present study, as detailed in the text. *The PCR method numbers are referred to from the Table 4.

Template	Primers used for	Direction	PCR method used* (ref. Table T2)	Product obtained
INFU/Ca/KF/3/I	*G10H*	Full-length/F	**1**	Yes
INFU/Ca/KF/3/I		Full-length/R	**1**	
INFU/Ca/KF/3/I	*SLS*	Full-length/F	**1**	Yes
INFU/Ca/KF/3/I		Full-length/R	**1**	
INFU/Ca/KF/3/I	*TDC*	Full-length/F	**1**	Yes
INFU/Ca/KF/3/I		Full-length/R	**1**	
INFU/Ca/KF/3/I	*STR*	Full-length/F	**1, 2, 3**	No
INFU/Ca/KF/3/I		Full-length/R	**1, 2, 3**	
INFU/Ca/KF/3/VII	*G10H*	Full-length/F	**1**	Yes
INFU/Ca/KF/3/VII		Full-length/R	**1**	
INFU/Ca/KF/3/VII	*SLS*	Full-length/F	**1**	Yes
INFU/Ca/KF/3/VII		Full-length/R	**1**	
INFU/Ca/KF/3/VII	*TDC*	Full-length/F	**1**	Yes
INFU/Ca/KF/3/VII		Full-length/R	**1**	
INFU/Ca/KF/3/VII	*STR*	Full-length/F	**1, 2, 3**	No
INFU/Ca/KF/3/VII		Full-length/R	**1, 2, 3**	
C. acuminata	*STR*	Full-length/F	**3**	Yes
C. acuminata		Full-length/R	**3**	

Table T5. The phytochemical compositions of the leaves, stems and roots in organic, aqueous and total (organic and aqueous) phases of the studied *Hypericum* species. All values more than 0.9 were justified to the nearest whole number. [L]leaf; [R]root; [S]stem; [A]aqueous; [O]organic; [T]total content (organic + aqueous); n.d., less than the limit of detection (< LOD); n.q., less than the limit of quantitation (< LOQ).

Plant Voucher Number	Emodin (µg/g)	Rutin (µg/g)	Hyperoside (µg/g)	Quercetin (µg/g)	Quercitrin (µg/g)	Pseudohypericin (µg/g)	Hyperforin (µg/g)	Hypericin (µg/g)
112^{L-A}	n.d.	65	123	65	n.q.	n.d.	n.d.	n.d.
112^{L-O}	1	456	372	229	378	538	6224	158
112^{L-T}	**1**	**521**	**495**	**294**	**378**	**538**	**6224**	**158**
112^{R-A}	n.d.	n.d.	n.d.	n.d.	n.q.	n.d.	43	n.d.
112^{R-O}	n.d.	n.d.	n.d.	n.d.	n.q.	n.d.	1345	n.d.
112^{R-T}	**n.d.**	**n.d.**	**n.d.**	**n.d.**	**n.q.**	**n.d.**	**1388**	**n.d.**
112^{S-A}	n.d.	n.d.	31	n.d.	n.q.	n.d.	n.d.	n.d.
112^{S-O}	n.d.	241	209	n.d.	n.q.	n.d.	314	n.d.
112^{S-T}	**n.d.**	**241**	**240**	**n.d.**	**n.q.**	**n.d.**	**314**	**n.d.**
3900^{L-A}	n.d.	n.d.	349	65	n.q.	26	n.d.	n.d.
3900^{L-O}	0.8	62	1275	146	631	604	4	107
3900^{L-T}	**0.8**	**62**	**1624**	**211**	**631**	**630**	**4**	**107**
3900^{R-A}	n.d.	n.d.	n.d.	n.d.	n.q.	n.d.	n.d.	n.d.
3900^{R-O}	n.d.	n.d.	20	n.d.	n.q.	n.d.	3	n.d.
3900^{R-T}	**n.d.**	**n.d.**	**20**	**n.d.**	**n.q.**	**n.d.**	**3**	**n.d.**
3900^{S-A}	n.d.	n.d.	218	n.d.	n.q.	n.d.	n.d.	n.d.
3900^{S-O}	n.d.	n.d.	1020	8	n.q.	35	n.d.	n.d.
3900^{S-T}	**n.d.**	**n.d.**	**1238**	**8**	**n.q.**	**35**	**n.d.**	**n.d.**
3901^{L-A}	n.d.	632	345	91	n.q.	n.d.	39	n.d.
3901^{L-O}	0.1	1884	936	189	n.q.	279	1695	61
3901^{L-T}	**0.1**	**2516**	**1281**	**280**	**n.q.**	**279**	**1734**	**61**
3901^{R-A}	n.d.	n.d.	n.d.	n.d.	n.q.	n.d.	n.d.	n.d.
3901^{R-O}	n.q.	n.d.	10	n.d.	n.q.	n.d.	23	n.d.
3901^{R-T}	**n.q.**	**n.d.**	**10**	**n.d.**	**n.q.**	**n.d.**	**23**	**n.d.**
3901^{S-A}	n.d.	n.d.	27	n.d.	n.q.	n.d.	n.d.	n.d.
3901^{S-O}	n.d.	156	123	14	n.q.	16	60	n.d.
3901^{S-T}	**n.d.**	**156**	**150**	**14**	**n.q.**	**16**	**60**	**n.d.**
3902^{L-A}	n.d.	n.d.	895	7	n.q.	n.d.	n.d.	n.d.
3902^{L-O}	0.2	164	3132	22	411	283	n.d.	27
3902^{L-T}	**0.2**	**164**	**4027**	**29**	**411**	**283**	**n.d.**	**27**
3902^{R-A}	n.d.	n.d.	14	n.d.	n.q.	n.d.	n.d.	n.d.
3902^{R-O}	n.d.	n.d.	30	n.d.	n.q.	n.d.	n.d.	n.d.
3902^{R-T}	**n.d.**	**n.d.**	**44**	**n.d.**	**n.q.**	**n.d.**	**n.d.**	**n.d.**
3902^{S-A}	n.d.	n.d.	67	n.d.	n.q.	n.d.	n.d.	n.d.
3902^{S-O}	n.q.	n.d.	261	n.d.	n.q.	42	n.d.	n.d.
3902^{S-T}	**n.q.**	**n.d.**	**328**	**n.d.**	**n.q.**	**42**	**n.d.**	**n.d.**

3907^{L-A}	n.d.	665	225	56	n.q.	n.d.	31	n.d.
3907^{L-O}	0.3	2662	1201	219	282	318	2418	84
3907^{L-T}	**0.3**	**3327**	**1426**	**275**	**282**	**318**	**2449**	**84**
3907^{R-A}	n.d.	n.d.	n.d.	n.d.	n.q.	n.d.	n.d.	n.d.
3907^{R-O}	n.d.	n.d.	15	n.d.	n.q.	n.d.	266	n.q.
3907^{R-T}	**n.d.**	**n.d.**	**15**	**n.d.**	**n.q.**	**n.d.**	**266**	**n.q.**
3907^{S-A}	n.d.	93	35	n.d.	n.q.	n.d.	3	n.d.
3907^{S-O}	n.d.	310	107	10	n.q.	17	378	3
3907^{S-T}	**n.d.**	**403**	**142**	**10**	**n.q.**	**17**	**381**	**3**
3903^{L-A}	n.d.	n.d.	652	27	n.q.	12.5	n.d.	n.d.
3903^{L-O}	2	172	2125	73	628	785	n.d.	251
3903^{L-T}	**2**	**172**	**2777**	**100**	**628**	**797**	**n.d.**	**251**
3903^{R-A}	n.d.	n.d.	15	n.d.	n.q.	n.d.	n.d.	n.d.
3903^{R-O}	n.d.	n.d.	43	n.d.	n.q.	n.d.	n.d.	n.d.
3903^{R-T}	**n.d.**	**n.d.**	**58**	**n.d.**	**n.q.**	**n.d.**	**n.d.**	**n.d.**
3903^{S-A}	n.d.	n.d.	267	n.d.	n.q.	n.d.	n.d.	n.d.
3903^{S-O}	n.d.	123	1137	n.d.	n.q.	32	n.d.	n.d.
3903^{S-T}	**n.d.**	**123**	**1404**	**n.d.**	**n.q.**	**32**	**n.d.**	**n.d.**
3908^{L-A}	n.d.	n.d.	396	34	n.q.	n.d.	n.d.	n.d.
3908^{L-O}	2	n.d.	1226	93	700	137	n.d.	87
3908^{L-T}	**2**	**n.d.**	**1622**	**127**	**700**	**137**	**n.d.**	**87**
3908^{R-A}	n.d.	n.d.	9	n.d.	n.q.	n.d.	n.d.	n.d.
3908^{R-O}	n.d.	n.d.	18	n.d.	n.q.	n.d.	n.d.	n.d.
3908^{R-T}	**n.d.**	**n.d.**	**27**	**n.d.**	**n.q.**	**n.d.**	**n.d.**	**n.d.**
3908^{S-A}	n.d.	n.d.	103	n.d.	n.q.	n.d.	n.d.	n.d.
3908^{S-O}	n.d.	n.d.	430	8	n.q.	20	n.d.	n.d.
3908^{S-T}	**n.d.**	**n.d.**	**533**	**8**	**n.q.**	**20**	**n.d.**	**n.d.**
3913^{L-A}	n.d.	n.d.	236	34	n.q.	n.d.	n.d.	n.d.
3913^{L-O}	0.3	n.d.	997	108	388	71	3	29
3913^{L-T}	**0.3**	**n.d.**	**1233**	**142**	**388**	**71**	**3**	**29**
3913^{R-A}	n.d.	n.d.	10	n.d.	n.q.	n.d.	n.d.	n.d.
3913^{R-O}	n.d.	n.d.	20	13	n.q.	n.d.	n.d.	n.d.
3913^{R-T}	**n.d.**	**n.d.**	**30**	**13**	**n.q.**	**n.d.**	**n.d.**	**n.d.**
3913^{S-A}	n.d.	n.d.	76	n.d.	n.q.	n.d.	n.d.	n.d.
3913^{S-O}	n.d.	n.d.	356	6	n.q.	10	n.d.	n.d.
3913^{S-T}	**n.d.**	**n.d.**	**432**	**6**	**n.q.**	**10**	**n.d.**	**n.d.**
LOD	**0.03**	**20.0**	**5.0**	**2.0**	**20.0**	**3.0**	**1.0**	**1.0**
LOQ	**0.1**	**50.0**	**15.0**	**6.0**	**100.0**	**10.0**	**3.0**	**3.0**

Table T6. The phytochemical compositions of the organic, aqueous, and total (organic and aqueous) phases of the studied *Juniperus* species. MVA, multivariate analysis; [A]aqueous; [O]organic; [T]total (aqueous + organic); n.q., less than the limit of quantitation (<LOQ). LOQ (podophyllotoxin, deoxypodophyllotoxin, podophyllotoxone) was 0.2 µg/mL; LOQ (demethylpodophyllotoxin) was 0.05 µg/mL.

PLANT SAMPLES	MVA Codes	Podophyllotoxin (µg/100 g dry weight)	Podophyllotoxone (µg/100 g dry weight)	Deoxypodophyllotoxin (µg/100 g dry weight)	Demethylpodophyllotoxin (µg/100 g dry weight)
J. communis L. Horstmann[Dortmund/O]	**1**	600	n.q.	105600	n.q.
J. communis L. Horstmann[Dortmund/A]	**2**	n.q.	n.q.	1600	n.q.
J. communis L. Horstmann[Dortmund/T]	**3**	600	n.q.	107200	n.q.
J. communis L. Meyer[Dortmund/O]	**4**	n.q.	2	103000	n.q.
J. communis L. Meyer[Dortmund/A]	**5**	n.q.	2	1500	n.q.
J. communis L. Meyer[Dortmund/T]	**6**	n.q.	4	104500	n.q.
J. communis L.Wilseder Berg[Dortmund/O]	**7**	1500	3	207000	n.q.
J. communis L.Wilseder Berg[Dortmund/A]	**8**	n.q.	n.q.	3900	n.q.
J. communis L.Wilseder Berg[Dortmund/T]	**9**	1500	3	210900	n.q.
J. communis Hibernica[Dortmund/O]	**10**	n.q.	1	215000	n.q.
J. communis Hibernica[Dortmund/A]	**11**	n.q.	n.q.	3000	n.q.
J. communis Hibernica[Dortmund/T]	**12**	n.q.	1	218000	n.q.
J. blaaws[Dortmund/O]	**13**	n.q.	n.q.	400	n.q.
J. blaaws[Dortmund/A]	**14**	n.q.	2	100	n.q.
J. blaaws[Dortmund/T]	**15**	n.q.	2	500	n.q.
J. procumbens Tremonia[Dortmund/O]	**16**	n.q.	1	2000	n.q.
J. procumbens Tremonia[Dortmund/A]	**17**	n.q.	1	50	n.q.
J. procumbens Tremonia[Dortmund/T]	**18**	n.q.	2	2050	n.q.
J. x-media Pfitzeriana[Dortmund/O]	**19**	97000	552	329000	n.q.
J. x-media Pfitzeriana[Dortmund/A]	**20**	3000	3	2500	n.q.
J. x-media Pfitzeriana[Dortmund/T]	**21**	100000	555	331500	n.q.
J. squamata Wilsonii[Dortmund/O]	**22**	4700	1	165000	n.q.
J. squamata Wilsonii[Dortmund/A]	**23**	n.q.	1	2000	n.q.
J. squamata Wilsonii[Dortmund/T]	**24**	4700	2	167000	n.q.
J. communis var. *communis*[Haltern/O]	**25**	n.q.	n.q.	5000	n.q.
J. communis var. *communis*[Haltern/A]	**26**	n.q.	n.q.	100	n.q.
J. communis var. *communis*[Haltern/T]	**27**	n.q.	n.q.	5100	n.q.
J. communis (male)[Haltern/O]	**28**	n.q.	n.q.	13000	n.q.
J. communis (male)[Haltern/A]	**29**	n.q.	n.q.	200	n.q.
J. communis (male)[Haltern/T]	**30**	n.q.	n.q.	13200	n.q.
J. communis (female)[Haltern/O]	**31**	n.q.	n.q.	18000	n.q.

J. communis (female)$^{Haltern/A}$	**32**	n.q.	n.q.	200	n.q.
J. communis (female)$^{Haltern/T}$	**33**	n.q.	n.q.	18200	n.q.
J. recurva$^{Yarikha/O}$	**34**	800	33	15000	n.q.
J. recurva$^{Yarikha/A}$	**35**	n.q.	6	5000	n.q.
J. recurva$^{Yarikha/T}$	**36**	800	39	20000	n.q.
J. recurva$^{Bonera/O}$	**37**	6000	135	3000	n.q.
J. recurva$^{Bonera/A}$	**38**	n.q.	6	300	n.q.
J. recurva$^{Bonera/T}$	**39**	6000	141	3300	n.q.
J. recurva$^{Sonamarg/O}$	**40**	3000	57	157000	n.q.
J. recurva$^{Sonamarg/A}$	**41**	n.q.	3	6000	n.q.
J. recurva$^{Sonamarg/T}$	**42**	3000	60	163000	n.q.

Table T7. The phytochemical compositions of the organic, aqueous, and total (organic and aqueous) phases of the studied *Podophyllum* species. MVA, multivariate analysis; [A]aqueous; [O]organic; [T]total (aqueous + organic); n.q., less than the limit of quantitation (<LOQ). LOQ (podophyllotoxin, deoxypodophyllotoxin, podophyllotoxone) was 0.2 µg/mL; LOQ (demethylpodophyllotoxin) was 0.05 µg/mL.

PLANT SAMPLES	MVA Codes	Podophyllotoxin (µg/100 g dry weight)	Podophyllotoxone (µg/100 g dry weight)	Deoxypodophyllotoxin (µg/100 g dry weight)	Demethylpodophyllotoxin (µg/100 g dry weight)
P. hexandrum$^{Yarikha/O}$	**1**	2400	9000	147000	270
P. hexandrum$^{Yarikha/A}$	**2**	n.q.	4000	113000	60
P. hexandrum$^{Yarikha/T}$	**3**	2400	13000	260000	330
P. hexandrum$^{Gulmarg/O}$	**4**	393000	9000	58000	100
P. hexandrum$^{Gulmarg/A}$	**5**	279000	3000	25000	n.q.
P. hexandrum$^{Gulmarg/T}$	**6**	672000	12000	83000	100
P. hexandrum$^{Pahalgam/O}$	**7**	441000	16000	60000	80
P. hexandrum$^{Pahalgam/A}$	**8**	239000	3000	106000	n.q.
P. hexandrum$^{Pahalgam/T}$	**9**	680000	19000	166000	80
P. hexandrum$^{Aru/O}$	**10**	155000	7000	4000	40
P. hexandrum$^{Aru/A}$	**11**	138000	2000	7000	n.q.
P. hexandrum$^{Aru/T}$	**12**	293000	9000	11000	40
P. hexandrum$^{Sonamarg/O}$	**13**	93000	7000	145000	30
P. hexandrum$^{Sonamarg/A}$	**14**	14000	1000	40000	n.q.
P. hexandrum$^{Sonamarg/T}$	**15**	107000	8000	185000	30

APPENDIX B

List of abbreviations

$[(CH_3)_2SiO]_6$	Polydimethylcyclosiloxane
°C	Degree Celsius
10-MeO-CPT	10-Methoxycamptothecin
10-OH-CPT	10-Hydroxycamptothecin
2D	Two dimensional
3D	Three dimensional
9-MeO-CPT	9-Methoxycamptothecin
9-OH-CPT	9-Hydroxycamptothecin
Å	Angstrom
A.D.	*Anno Domini*
ACP	Acyl carrier protein
AIDS	Acquired immune deficiency (or immunodeficiency) syndrome
Ala or A	Alanine
approx.	Approximately
Arg or R	Arginine
Asn or N	Asparagine
AUs	Arbitrary units
BIV	Bovine immunodeficiency virus
BLAST	Basic Local Alignment Search Tool
BVDV	Bovine viral diarrhea virus
$CaCl_2$	Calcuim chloride
cat. no.	Catalogue number
CD_3OD	Deuterated methanol
CDA	Czapek-dextrose agar
$CDCl_3$	Deuterated chloroform
cDNA	Complementary deoxyribonucleic acid
CFU	Colony forming units
$CHCl_3$	Chloroform
CID	Collision induced dissociation
CITES	Convention for International Trade in Endangered Species
CLSI	Clinical and Laboratory Standards Institute
CO_2	Carbon dioxide gas
CoA	Coenzyme A
COX	Cyclooxygenase
CPT	Camptothecin
CSCI	Compound-specific carbon isotope
CSNI	Compound-specific nitrogen isotope
ddH_2O	Double distilled water
DF	Dilution factor
DHBV	Duck hepatitis B virus
DI	Deionized water
DMAPP	Dimethylallyl diphosphate
DMSO	Dimethyl sulfoxide
DNA	Deoxyribonucleic acid
dNTP	Deoxyribonucleotide triphosphate
DSMZ	German Collection of Microorganisms and Cell Cultures (*Deutsche Sammlung von Mikroorganismen und Zellkulturen GmbH*), Braunschweig, Germany
EC number	Enzyme Commission number
EDTA	Ethylenediamine-tetraacetic acid

EIAV	Equine infectious anemia virus
EMBL	European Molecular Biology Laboratory
eV	Electron volt
FBS	Fetal bovine serum
FDA	U. S. Federal Food and Drug Administration
FDM	Food, Drug, and Mass Market
FLV	Friend leukemia virus
FS	Fractional survival
g	Gram
g^{-1}	Per gram
G10H	Geraniol 10-hydroxylase
gDNA	Genomic deoxyribonucleic acid
Glu or E	Glutamic acid
Gly or G	Glycine
GPP	Geranyl diphosphate
h	Hour
h^{-1}	Per hour
H_2O	Water
HACA	Hierarchical agglomerative cluster analysis
HCl	Hydrogen chloride (or hydrochloric acid; in solution)
HCMV	Human cytomegalovirus
HGT	Horizontal gene transfer(s)
His or H	Histidine
HIV	Human immunodeficiency virus
HP-IRMS	High-precision isotope-ratio mass spectrometry
HPLC	High performance (or pressure) liquid chromatography
HR-MS or HRMS	High resolution-mass spectrometry
HSA	Human serum albumin
HSV	*Herpes simplex* virus
Hz	Hertz
Ile or I	Isoleucine
IPP	Isopentenyl diphosphate
IRI	Information Resources Inc. (U.S.)
ITS	Internal Transcript Spacer
IU	International units
K_2O	Potassium oxide
KCl	Potassium chloride
kHz	Kilohertz
kV	Kilovolts
L	Liter
L^{-1}	Per liter
LC	Liquid chromatography
LC-ESI-HRMS^n	Liquid chromatography-electrospray ionization-high-resolution-tandem mass spectrometry
LC-MS	Liquid chromatography-mass spectrometry
LDA	Linear discriminant analysis
LOD	Limit of detection
LOQ	Limit of quantitation
LOX	Lipoxygenase
LSU	Large subunit
Lys or K	Lysine
m/z	Mass-to-charge ratio

MAO	Monoamine oxidase
MCMV	Murine cytomegalovirus
MDS	Multidimensional scaling
MEA	Malt extract agar
MeOH	Methanol
MEP	2-C-Methyl-D-erythritol-4-phosphate
mg	Milligram
mg^{-1}	Per milligram
MgO	Magnesium oxide
min	Minute
min^{-1}	Per minute
mL	Milliliter
mL^{-1}	Per milliliter
mm	Millimeter
mM	Millimolar
mm^{-1}	Per millimeter
Mo-MuLV	Moloney murine leukemia virus
MRM	Multiple reaction monitoring
MS	Mass spectrometer
MVA	Mevalonate or Multivariate analysis
N_2	Nitrogen gas
NA	Nutrient agar
NaCl	Sodium chloride
NB	Nutrient broth
NCBI	U. S. National Center for Biotechnology Information
ng	Nanogram
NH_4Ac	Ammonium acetate
NMR	Nuclear magnetic resonance
OKS	Octaketide synthase
ORF	Open reading frame
Orn	Ornithine
P_2O_5	Phosphorous pentoxide
Para-3	Para-influenza virus type 3
PBS	Phosphate buffered saline
PCA	Passive cutaneous anaphylaxis or principal component analysis
PCR	Polymerase chain reaction
PDA	Potato dextrose agar
pg	Picogram
Phe or F	Phenylalanine
PKS	Polyketide synthase
ppm	Parts per million
PR\LR	Pinoresinol–lariciresinol reductase
r	Pearson correlation coefficient
RadLV	Radiation leukemia virus
rDNA	Ribosomal deoxyribonulceic acid
rev	Revolution(s)
RNA	Ribonucleic acid
ROS	Reactive oxygen species
rpm	Revolutions per minute
RPMI-1640	Roswell Park Memorial Institute culture media 1640
rRNA	Ribosomal ribonucleic acid
RSD	Relative standard deviation

RT-PCR	Reverse transcriptase-polymerase chain reaction
s	Second
s^{-1}	Per second
SA	Sabouraud dextrose agar
SAD	Seasonal affective disorder
SAR	Structure-activity relationship(s)
SB	Sabouraud dextrose broth
SD	Secoisolariciresinol dehydrogenase
SD	Standard deviation
SEM	Scanning electron microscope
Ser or S	Serine
SIM	Single ion monitoring
SLS	Secologanin synthase
SRM	Single (or selected) reaction monitoring
STR	Strictosidine synthase
SV	Sindbis virus
TAE	Tris-acetate-EDTA
TDC	Tryptophan decarboxylase
THP-1	Human acute monocytic leukemia cells
TIA	Terpenoid indole alkaloid
TIC	Total ion current (or chromatogram)
Topo 1	Topoisomerase I
Topo 2	Topoisomerase II
t_R	Retention time
Trp or W	Tryptophan
Tyr or Y	Tyrosine
U	Enzyme unit
U.S. or U.S.A.	United States of America
US$	United States dollar
UV	Ultraviolet
UV/VIS or UV-VIS	Ultraviolet/visible
V	Volt
v/v	Volume to volume
VIS	Visible
viz.	*Videlicet*
VSV	Vesicular stomatitis virus
VV	Vaccinia virus
W	Watt
WA	Water agar
WHO	World Health Organization
ZOI	Zone of inhibition
µL	Microliter
μL^{-1}	Per microliter
µm	Micrometer
µM	Micromolar
μm^{-1}	Per micrometer

List of figures

List of tables